The Effects of Energetic Substrate Manipulation on Myocardial Metabolism and Cardiac Function

WILLIAM DONALD WATSON

St Anne's College

University of Oxford



A thesis submitted in partial fulfilment of the requirements for the degree of

Doctor of Philosophy in Medical Sciences

Declaration

This thesis is entirely my own work unless otherwise indicated. It has not been submitted, either wholly or substantially, for another degree at this university, or for a degree at any other institution. I have acknowledged assistance from colleagues and collaborators where relevant.

The word count, not including references, abstract and front matter is 41,218.

Table of Contents

1 Chapter 1: Introduction 1
1.1 Introduction: A brief history of cardiac metabolic manipulation in heart failure..... 1
1.2 Heart Failure 5
1.2.1 Definition and Epidemiology 5
1.2.2 Current Concepts of Treatment 6
1.3 Myocardial Energy Use and Oxygen Consumption 9
1.4 Myocardial Energy Production 13
1.4.1 Myocardial Energy Substrate Metabolism 13
1.4.2 Energy of Synthesis of ATP 21
1.4.3 Energy of Hydrolysis of ATP 23
1.4.4 Phosphotransfer 25
1.4.5 Linking Increased Demand to Increased Supply 27
1.4.6 Substrate Metabolism at Higher Workloads 30
1.5 Energetic Changes in Heart Failure 32
1.5.1 ATP and Heart Failure in vivo 32
1.5.2 Substrate Metabolism in the Failing Heart 33
1.5.3 Mitochondrial Dysfunction in Heart Failure 37
1.5.4 Substrate Selection at Stress in the Failing Heart 38
1.6 Altering Substrate Metabolism as a Potential Treatment for Heart Failure 38
1.6.1 Increasing glucose/pyruvate metabolism 39
1.6.2 Increasing fatty acid metabolism 41
1.6.3 Increasing Ketone Body Metabolism 47
1.6.4 Therapeutic Approaches Targeting Metabolism in Heart Failure 47
1.7 Current Gaps in Evidence 53
1.7.1 Conflicting data 53
1.7.2 Focus on Glucose as a Therapeutic Target 53
1.7.3 Lack of Data on Substrate Flexibility During Changing Metabolic Conditions 54
1.7.4 Lack of Data on Substrate Metabolism at Stress in the Failing Heart 54
1.8 Aims of the Thesis 55
1.8.1 To compare and contrast the effects of changes to glucose and fat metabolism in the healthy and failing heart. 55
1.8.2 To examine the effects of changes to fat and glucose metabolism on stress performance in the healthy and failing heart 56

1.8.3 To examine the effects of vasodilator stress on the healthy heart and the dependence upon phosphocreatine reserves to resist stressors 56
2 Chapter 2: Methods 58
2.1 Substrate Manipulation 58
2.1.1 Free Fatty Acid Elevation with Intralipid 58
2.1.2 Glucose Uptake Elevation with Euglycaemic Clamp 58
2.1.3 Reduction of Circulating Free Fatty Acids with Nicotinic Acid Receptor Agonists 59
2.2 Stressor Agents 59
2.2.1 Dobutamine 59
2.2.2 Glyceryl Trinitrate (GTN) 60
2.2.3 Monitoring 60
2.3 Magnetic Resonance 61
2.3.1 ^{1}H Imaging for Cardiac Volumes and Function 61
2.3.2 ^{31}P 3D Chemical Shift Imaging for Spectroscopy 62
2.3.3 Assessment of Creatine Kinase first order rate constant through Triple Repetition Saturation Transfer (TRIST) 66
2.4 Invasive Arteriovenous and Haemodynamic Measurements 75
2.4.1 Measurement 76
2.4.2 Analysis 77
2.5 Methods used in Animal Experiments 80
2.5.1 Animal Handling 80
2.5.2 Acipimox 81
2.5.3 MRI/MRS 82
2.5.4 Langendorff Perfusion 84
2.6 Statistical Techniques 85
2.7 Ethics Overview 86
2.7.1 Human Research: Nicotinic Acid 86
2.7.2 Human Studies: Substrate Selection 86
2.7.3 Human Studies: Vasodilator 86
2.8 Anthropometric and biochemical measurements 87
2.9 Blood Samples 87
3 Chapter 3: The Effects of Nicotinic Acid on Cardiac Metabolism and Function 88
3.1 Introduction 88
3.1.1 Myocardial Metabolism 88
3.1.2 Nicotinic Acid 89
3.1.3 Intralipid 89

3.1.4 Rationale 90
3.2 Methods 91
3.2.1 Human Experiment 91
3.2.2 Animal Experiment 93
3.3 Results 95
3.3.1 Baseline Characteristics of Human Study Participants 95
3.3.2 Effects of Fatty Acid Elevation with Intralipid in Human Subjects 96
3.3.3 Effects of Fatty Acid lowering with Nicotinic acid in Human Subjects 100
3.3.4 Pooled Data and Correlations in Human Subjects 103
3.3.5 Whole Animal Experiment 107
3.3.6 Perfusion Experiment 115
3.4 Discussion 117
3.4.1 Effects of Intralipid on the Fasted Human Heart 117
3.4.2 Effects of Nicotinic Acid on the Fasted Human Heart 118
3.4.3 Animal Hyperpolarized [1-^{13}C]Pyruvate Magnetic Resonance Spectroscopy 119
3.4.4 Cardiac Contractility in Healthy Rats 122
3.4.5 31P Magnetic Resonance Spectroscopy and Contractility in Langendorff perfused hearts given nicotinic acid receptor agonists 122
3.4.6 Possible Mechanisms of Nicotinic Acid induced Ventricular Impairment 122
3.5 Conclusions 125
4 Chapter 4: The Effects of Substrate Manipulation at Rest in Normal Hearts and in Heart Failure 126
4.1 Introduction 126
4.2 Methods 128
4.2.1 Recruitment 128
4.2.2 Inclusion and Exclusion Criteria 129
4.2.3 Substrate Manipulation 132
4.2.4 CMR study and protocol 133
4.2.5 Invasive Study 137
4.3 Results 139
4.3.1 Healthy Volunteers 139
4.3.2 Heart Failure 150
4.3.3 Comparisons between Healthy Volunteers and Heart Failure Patients and Pooled Data 163
4.3.4 Invasive Data 166
4.4 Discussion 181

4.4.1 The Failing Heart Demonstrates Substrate Flexibility....181
4.4.2 Intralipid Increases Contractility in both Healthy and Failing Hearts....182
4.4.3 Myocardial Oxygen Delivery Does Not Limit Substrate Oxidation at Rest.183
4.4.4 There is no energetic benefit from euglycaemic clamp over Intralipid infusion in heart failure....184
4.4.5 Energetics Limit Contractility in the Failing Heart, but not the Healthy Heart 185
4.4.6 There is a greater degree of uncoupling of substrate uptake from oxidative metabolism with Intralipid than with glucose....186
4.5 Limitations....188
4.5.1 Different methods between invasive and noninvasive arms....188
4.5.2 Supraphysiological levels of circulating free fatty acids....189
4.5.3 Metabolic Fates and Other Metabolites....190
4.5.4 Discordant Invasive and Noninvasive Measures....191
4.6 Summary....191
5 Chapter 5: The Effects of Substrate Manipulation at Stress in Normal Hearts and in Heart Failure....192
5.1 Introduction....192
5.2 Methods....193
5.2.1 CMR....193
5.2.2 Invasive Protocol....193
5.3 Results....194
5.3.1 Healthy Volunteers....194
5.3.2 Heart Failure Volunteers....208
5.3.3 Invasive Data....221
5.4 Discussion....238
5.4.1 The failing heart retains flexibility to take up different substrates under stress 238
5.4.2 In the Healthy Heart, Substrate Metabolised does not impact Stress Cardiac Work 241
5.4.3 In The Failing Heart, there is no Change in Cardiac Work during Dobutamine Stress but Cardiac Work remains higher with Intralipid Infusion....242
5.4.4 There is no Significant Change in Oxygen Consumption in the Failing Heart during Rapid Pacing....243
5.5 Limitations....244
5.5.1 Metabolic Fates....244
5.5.2 Rapid pacing and dobutamine may not be equivalent....244
5.5.3 Venous Sampling in the CMR Experiment....245

6 Chapter 6: The Effect of Vasodilator Stress on Cardiac Function and Energetics 246
6.1 Introduction and Rationale 246
6.1.1 Myocardial Energy Use 246
6.1.2 Vasodilators and Venodilators 246
6.1.3 Effects of GTN on Myocardial Oxygen Consumption and Oxidative Phosphorylation 251
6.1.4 Experimental Rationale 251
6.2 Methods 252
6.2.1 CMR Protocol 252
6.3 Results 254
6.3.1 Participant Characteristics 254
6.3.2 Ventricular volumes and haemodynamics 255
6.3.3 ^{31}P Spectroscopy 258
6.3.4 Correlations 260
6.4 Discussion 262
6.4.1 Effect of Nitrate on Energy Metabolism 262
6.4.2 Calculated Cardiac Work and Energy Demand 262
6.4.3 Flexibility in Myocardial Energy Delivery Protects Against Vasodilator Stress 263
6.5 Limitations 265
6.5.1 Other Physiological Effects of Nitric Oxide 265
6.5.2 Cohort Containing Mixed Athletic Ability / Body Morphology 265
7 Summary and Future Directions 266
8 Reference 271

Abstract

The healthy human heart uses fat and glucose as its predominant metabolic substrates, approximately in a ratio of 70% to 30%. In heart failure, substrate oxidation is decreased as is ATP production. Free fatty acid uptake and oxidation is reduced, while glucose uptake and glycolysis are increased, although pyruvate oxidation falls. This thesis set out to establish the links between myocardial substrate metabolism and function in the healthy and the failing human heart, at rest and at stress.

In chapter 3, an inhibitor of lipolysis, nicotinic acid, is compared to a lipid infusion in normal human subjects and in rats. While the lipid infusion increases cardiac contractility, a decline in both contractility and PCr/ATP ratio is shown with the nicotinic acid. This is revealed to result from inhibition in lipolysis combined with reduction in glucose stimulated insulin secretion, hence the heart is starved of energetic substrate, revealing metabolism's importance and close link to contractile function.

In chapters 4 and 5, lipid infusion is further shown in the failing human heart to increase contractility and PCr/ATP ratio at rest as well as increasing maximum available cardiac work. It is demonstrated that the failing heart displays substrate flexibility with an ability to take up higher amounts of free fatty acids when their availability is increased and increase their uptake during rapid pacing stress. In addition, the failing heart is not shown to be oxygen starved and oxygen consumption increases during the lipid infusion without deleterious consequence.

In chapter 6, in normal human subjects, vasodilator stress with glyceryl trinitrate is shown to greatly increase myocardial ATP demand while inhibiting mitochondrial ATP production, creating a mismatch between supply and demand and resulting in a fall in PCr/ATP ratio.

A higher baseline PCr/ATP is shown to be protective against stress induced changes, confirming the importance of PCr/ATP as a target for interventions.

Together, these data show myocardial metabolism is an important target for heart failure therapeutics and that it may be manipulated via increasing availability of free fatty acids.

Publications

Some ideas, data and figures have appeared previously in the following publications:

Nicotinic acid receptor agonists impair myocardial contractility by energy starvation.

Watson WD, Timm KN, Lewis AJ, Miller JJJ, Emmanuel Y, Clarke K, Neubauer S, Tyler DJ, Rider OJ (2020). Journal of the Federation of American Societies for Experimental Biology, 34(11), 14878-14891.

Use of cardiac magnetic resonance to detect changes in metabolism in heart failure.

William D. Watson, Jack J. J. Miller, Andrew Lewis, Stefan Neubauer, Damian Tyler, Oliver J. Rider, Ladislav Valkovič. (2020). Cardiovascular Diagnosis and Therapy, in press.

Acknowledgements

The British Heart Foundation for funding this work and providing support throughout.

The patients and volunteers who took part.

Dr Peregrine Green for working together on almost every experiment.

My supervisors: Professor Oliver Rider, Professor Neil Herring and Professor Stefan Neubauer.

Spectroscopy: Dr Mark Peterzan, Dr Ladislav Valkovic, Professor Chris Rodgers and Dr Will Clarke

Animal experiments: Dr Kerstin Timm, Dr Jack Miller

Researchers: Dr Jennifer Rayner, Dr Moritz Hundertmark, Dr Andrew Apps, Dr Rebecca Chamley, Dr Andrew Lewis

Radiographers: Jane Francis, Rebecca Mills, Joana Leal-Pelado, Raj Soundarajan, Cassandra Baker

Research nurses: Roser Farras-Araya, Judith Delos Santos, Cathy Krasopoulos, Claudia Nunes, Harriet Nixon, Nancy Panopoulou

Patient Administration: Karen Whatley, Ella May

Rebecca Gower: for forbearance and love

List of Figures

Page 7 ***Figure 1.1****: Frank-Starling curves in the healthy and failing hearts*

Page 11 ***Figure 1.2****: Total blue shaded area is the pressure-volume area (PVA), whereas the dark blue shaded area is the pressure-volume loop.*

Page 14 ***Figure 1.3****: Overview of substrate uptake and metabolism within myocytes.*

Page 24 ***Figure 1.4****: Linking impaired ΔG_{ATP} to functional impairment in vivo.*

Page 25 ***Figure 1.5****: Conception of ΔG_{ATP} as a column of water.*

Page 27 ***Figure 1.6****: Direct channelling and facilitated diffusion.*

Page 29 ***Figure 1.7****: Phosphotransfer acts as an energy shuttle in the forward direction but also as a signalling system in reverse: changes in ATP and ADP concentration at sites of use are fed back to the mitochondrion to alter rate of ATP synthesis.*

Page 61 ***Figure 2.1****: Left and right ventricular contours in Circle CVI 42.*

Page 63 ***Figure 2.2****: Positioning of the CSI grid in 2-chamber (left), 4-chamber (centre) and short-axis (right) orientations*

Page 64 ***Figure 2.3****: Positioning of centre frequency (red line) relative to other spectral peaks*

Page 66 ***Figure 2.4****: Example of a spectral fit from the in-house Matlab analysis package*

Page 69 ***Figure 2.5****: Positioning of the 1-D CSI grid with voxels oriented parallel to the coil and chest wall.*

Page 70 ***Figure 2.6****: positioning of the centre frequency between PCr and γ-ATP peaks*

Page 71 ***Figure 2.7****: Spectra from corresponding voxels in the matlab package.*

Page 72 ***Figure 2.8****: Spectra from the same volunteer, processed with the analysis tool*

Page 74 ***Figure 2.9****: The four spectra generated as part of the TRiST experiment*

Page 76 ***Figure 2.10****: Example positioning of catheters and wires during the invasive procedure*

Page 78 ***Figure 2.11****: Segmental volumes and pressure tracings over time*

Page 79 ***Figure 2.12****: Doppler flow wire analysis.*

Page 80 ***Figure 2.13****: Coronary Angiography with measurement of the left main stem coronary artery diameter.*

Page 81 ***Figure 2.14****: Pilot data demonstrating levels of glucose and free fatty acids*

Page 82 ***Figure 2.15****: Oxford Instruments Alpha system used to generate hyperpolarised [1-^{13}C]pyruvate*

Page 83 ***Figure 2.16****: Labelled ^{13}C spectrum*

Page 85 ***Figure 2.17****: Langendorff perfusion apparatus*

Page 91 ***Figure 3.1****: Overview of study methods.*

Page 99 ***Figure 3.2****: Summary graphs of free fatty acids (FFA), glucose, beta-hydroxybutyrate, PCr/ATP ratio, left ventricular (LV) ejection fraction and circumferential strain before and during Intralipid infusion*

Page 102 ***Figure 3.3:*** *Summary graphs of free fatty acids (FFA), glucose, beta-hydroxybutyrate, PCr/ATP ratio, left ventricular (LV) ejection fraction and circumferential strain before and following nicotinic acid administration*

Page 103 ***Figure 3.4:*** *Correlations of β-hydroxybutyrate with free fatty acids and glucose (upper panels) and correlations of free fatty acids with measures of contractility (lower panels) in data pooled from both arms of the study*

Page 104 ***Figure 3.5:*** *Significant correlations in the nicotinic acid arm of the experiment.*

Page 105 ***Figure 3.6:*** *Significant correlations in the Intralipid arm of the experiment.*

Page 106 ***Figure 3.7*** *Changes in serum free fatty acids correlated with changes in β-hydroxybutyrate (BOHB), ejection fraction (EF) and global circumferential strain (GCS).*

Page 108 ***Figure 3.8****: Circulating Metabolites in the animal experiment*

Page 111 ***Figure 3.9:*** *Measures of contractility in animal data. Cardiac Index is cardiac output indexed to body mass in grams*

Page 113 ***Figure 3.10:*** *Hyperpolarized [1-^{13}C]pyruvate MRS*

Page 114 ***Figure 3.11****, correlations between Hyperpolarized [1-^{13}C]pyruvate MRS, free fatty acids, glucose and cardiac index.*

Page 116 ***Figure 3.12****: Rate Pressure Product and PCr/ATP ratio in the Langendorff perfused hearts given acipimox or controls perfused with Krebs buffer only.*

Page 133 ***Figure 4.1****: Summary diagram of CMR study*

Page 137 ***Figure 4.2****: Invasive study summary diagram*

Page 141 ***Figure 4.3****: Circulating venous metabolites 1hr after Acipimox, Insulin+Glucose infusion or Intralipid infusion.*

Page 143 ***Figure 4.4****: Left ventricular volumes and function in healthy volunteers*

Page 145 ***Figure 4.5:*** *Healthy Volunteer Right Ventricular Volumes and Function during substrate manipulation*

Page 147 ***Figure 4.6:*** *Healthy Volunteer Haemodynamics and calculated cardiac work during substrate manipulation*

Page 149 ***Figure 4.7****: Normal Heart* ^{31}*P MRS data for PCr/ATP, CK* k_f *and CK Flux during the different substrate altering interventions*

Page 153 ***Figure 4.8:*** *Venous metabolites and Insulin 1 hour after substrate altering intervention in the heart failure group*

Page 155 ***Figure 4.9:*** *The effect of substrate manipulation on left ventricular volumes and function in the heart failure cohort*

Page 159 ***Figure 4.10****: The effect of substrate manipulation on right ventricular volumes and function in the heart failure cohort*

Page 161 ***Figure 4.11:*** *Haemodynamics and calculated cardiac work during substrate manipulation in heart failure*

Page 161 ***Figure 4.12:*** *Heart failure cohort* ^{31}*P MRS data for PCr/ATP, CK* k_f *and CK Flux during the different substrate altering interventions*

Page 162 ***Figure 4.13:*** *Correlations between PCr/ATP and resting measures of left ventricular contractility in the heart failure cohort during substrate manipulation.*

Page 163 ***Figure 4.14****: PCr/ATP comparison between healthy and heart failure groups receiving insulin-glucose and Intralipid infusions. Mean for each group is displayed.*

Page 164 ***Figure 4.15****: Creatine kinase measurement comparison between healthy and heart failure groups receiving Intralipid and insulin-glucose infusions.*

Page 165 ***Figure 4.16****: differences in rate pressure product and cardiac work by arms of the experiment.*

Page 168 ***Figure 4.17:*** *Left mainstem arterial metabolite concentrations during substrate manipulation in the invasive study*

Page 169 ***Figure 4.18****: Correlations between resting arterial coronary sinus bloods in invasive studies and venous bloods at baseline in CMR studies on participants in both parts of the study.*

Page 170 ***Figure 4.19:*** *Arteriovenous differences in oxygen content and extraction during substrate manipulation*

Page 171 ***Figure 4.20****: Arteriovenous metabolites in heart failure during substrate manipulation in the invasive study*

Page 173 ***Figure 4.21:*** *Proportion of ATP production by substrate, during resting intrinsic rhythm*

Page 174 ***Figure 4.22:*** *Correlations between arterial metabolites and substrate uptake.*

Page 175 ***Figure 4.23:*** *MVO2 compared to total oxygen required to fully oxidise all metabolites*

Page 177 ***Figure 4.24****: The effect of Substrate modulation on Invasive measures of resting contractility in intrinsic rhythm in patients with heart failure with reduced ejection fraction*

Page 179 ***Figure 4.25****: Invasive measures of contractility during biventricular paced rhythm*

Page 180 ***Figure 4.26:*** *Correlation between oxygen consumption (MVO2) and cardiac work during substrate manipulation in HFrEF in intrinsic rhythm*

Page 191 ***Figure 4.27****: Unusually shaped pressure-volume loop recorded in intrinsic rhythm.*

Page 195 ***Figure 5.1****: Circulating metabolites at stress in healthy volunteers (venous blood taken immediately following dobutamine infusion)*

Page 197 ***Figure 5.2****: Changes in venous metabolites in healthy volunteers between rest and stress*

Page 200 ***Figure 5.3****: Haemodynamics and Cardiac Work in Healthy Volunteers*

Page 203 ***Figure 5.4****: CMR volumes during dobutamine stress in healthy volunteers*

Page 204 ***Figure 5.5****: Changes in CMR volumes between rest and stress in healthy volunteers*

Page 205 ***Figure 5.6****: Correlations between PCr/ATP at rest and measures of contractility and haemodynamics.*

Page 207 ***Figure 5.7****: Rest and stress Creatine Kinase First Order Rate Constant (Ck_{kf}), PCr/ATP ratio and CK flux.*

Page 210 ***Figure 5.8****: Venous metabolites at stress in heart failure volunteers*

Page 211 ***Figure 5.9****: Venous metabolites at rest and stress in heart failure volunteers*

Page 213 ***Figure 5.10****: Stress Contractility in Heart Failure Volunteers*

Page 214 ***Figure 5.11****: Rest and Stress Contractility in Heart Failure Volunteers*

Page 216 ***Figure 5.12****: Haemodynamics in heart failure volunteers during CMR stress*

Page 217 ***Figure 5.13****: Rest and Stress Haemodynamics in heart failure volunteers*

Page 219 ***Figure 5.14****: Stress 31P Creatine Kinase First Order Rate Constant, PCr/ATP ratio and flux, with comparison to rest values in Heart Failure*

Page 220 ***Figure 5.15****: Correlations between resting PCr/ATP and stress haemodynamics in heart failure*

Page 222 ***Figure 5.16****: Left mainstem arterial metabolite concentrations during rapid atrial pacing and substrate manipulation, during the invasive study, in the HFrEF group.*

Page 224 ***Figure 5.17****: Arteriovenous metabolite uptake during rapid atrial pacing and substrate manipulation, during the invasive study, in the HFrEF group*

Page 226 ***Figure 5.18****: Rest and Stress comparison of cardiac arteriovenous metabolite uptake in patients with HFrEF*

Page 228 ***Figure 5.19****: ATP generation per substrate as proportion of the total.*

Page 229 ***Figure 5.20****: Arteriovenous oxygen extraction at stress in patients with HFrEF*

Page 230 ***Figure 5.21****: Oxygen consumption at stress compared to that at rest (intrinsic rhythm compared to rapid atrial pacing).*

Page 231 ***Figure 5.22****: Calculated oxygen uptake (based on the complete oxidation of each substrate taken up) compared to measured oxygen uptake (MVO2).*

Page 233 ***Figure 5.23****: Invasive Measures of Contractility during rapid pacing in HFrEF*

Page 234 ***Figure 5.24****: Rest (intrinsic rhythm) and Stress (rapid atrial pacing) invasive measures of contractility in HFrEF*

Page 236 ***Figure 5.25****: Measures of Contractility during Rapid Biventricular Pacing in HFrEF patients*

Page 237 ***Figure 5.26****: Comparison of slow biventricular pacing (rest) and rapid biventricular pacing (stress) in cardiac contractility.*

Page 247 ***Figure 6.1****: Changes in pressure-volume loops with afterload change*

Page 248 ***Figure 6.2****: Changes in pressure-volume loops with preload change*

Page 249 ***Figure 6.3****: Changes in pressure-volume loops with preload and afterload changes*

Page 250 ***Figure 6.4****: Changes in pressure-volume loops with preload and afterload changes and inotropy*

Page 253 ***Figure 6.5****: Study diagram*

Page 255 ***Figure 6.6****: Haemodynamic changes before and during GTN infusion*

Page 257 ***Figure 6.7****: Volume changes before and during GTN infusion.*

Page 259 ***Figure 6.8****: 31P Spectroscopic Measurements before and during GTN infusion in the vasodilator experiment*

Page 260 ***Figure 6.9****: Baseline PCr/ATP ratio compared to change in stroke volume before and during vasoplegic stress*

Page 261 ***Figure 6.10****: Creatine kinase first order rate constant correlated with rate pressure product at rest and during vasoplegic stress (GTN)*

List of Tables

Page 73 ***Table 2.1****: TRiST and StreST acquisition parameters*

Page 95 ***Table 3.1****: Baseline characteristics of 9 participants (mean ± standard deviation)*

Page 98 ***Table 3.2****: Changes in circulating metabolites, haemodynamics, myocardial energetics and ventricular systolic function with Intralipid infusion*

Page 101 ***Table 3.3****: Changes in circulating metabolites, haemodynamics, myocardial energetics and ventricular systolic function following nicotinic acid.*

Page 107 ***Table 3.4:*** *Baseline weights of rats in the animal experiment by group*

Page 109 ***Table 3.5****: Animal Circulating Metabolites.*

Page 110 ***Table 3.6:*** *Animal Left Ventricular Contractility Data*

Page 112 ***Table 3.7****: Hyperpolarized [1-^{13}C]pyruvate MRS by metabolite and study arm of animal.*

Page 139 ***Table 4.1****: Baseline Characteristics of the healthy volunteers*

Page 140 ***Table 4.2:*** *Circulating venous metabolites 1hr after Acipimox, Insulin+Glucose infusion or Intralipid infusion.*

Page 142 ***Table 4.3****: Left ventricular volumes and function in healthy volunteers*

Page 144 ***Table 4.4:*** *Healthy Volunteer Right Ventricular Contractility and Volumes during substrate manipulation*

Page 146 ***Table 4.5:*** *Healthy Volunteer Haemodynamics and calculated cardiac work during substrate manipulation*

Page 148 ***Table 4.6****: Normal Heart ^{31}P MRS data for PCr/ATP, CK k_f and CK Flux during the different substrate altering interventions*

Page 150 ***Table 4.7.*** *Baseline data for the Heart Failure cohort*

Page 151 ***Table 4.8:*** *Drug therapy in heart failure cohort*

Page 152 ***Table 4.9****: Venous Circulating Metabolites one hour into infusion in the heart failure group*

Page 154 ***Table 4.10:*** *The effect of substrate manipulation on left ventricular volumes and function in the heart failure cohort*

Page 156 ***Table 4.11:*** *The effect of substrate manipulation on right ventricular volumes and function in the heart failure cohort.*

Page 158 ***Table 4.12:*** *Haemodynamics and calculated cardiac work during substrate manipulation in heart failure*

Page 160 ***Table 4.13:*** *Heart failure cohort ^{31}P MRS data for PCr/ATP, CK k_f and CK Flux during the different substrate altering interventions*

Page 160 ***Table 4.14:*** *Heart failure cohort ^{31}P MRS data for PCr/ATP, CK k_f and CK Flux during the different substrate altering interventions*

Page 166 ***Table 4.15:*** *Baseline Data for the Invasive subgroup*

Page 166 ***Table 4.16****: Medical therapy in the invasive group*

Page 167 ***Table 4.17:*** *Left mainstem arterial metabolite concentrations in HFrEF during substrate manipulation in the invasive study*

Page 170 ***Table 4.18:*** *Arteriovenous differences in oxygen content and extraction during substrate manipulation*

Page 171 ***Table 4.19:*** *Arteriovenous metabolite uptake in HFrEF during substrate manipulation in the invasive study*

Page 172 ***Table 4.20:*** *ATP produced per metabolite as a percentage of total ATP production in HFrEF during substrate manipulation in the invasive study*

Page 176 ***Table 4.21****: Invasive measures of contractility in intrinsic rhythm*

Page 178 ***Table 4.22****: Invasive measures of contractility during biventricular paced rhythm*

Page 198 ***Table 5.1****: Circulating metabolites at stress in healthy volunteers (venous blood taken immediately following dobutamine infusion)*

Page 196 ***Table 5.2****: Change from baseline to stress in venous blood in healthy volunteers*

Page 199 ***Table 5.3****: Haemodynamics and Cardiac Work in healthy volunteers during dobutamine stress*

Page 202 ***Table 5.4****: Left Ventricular Volumes and Contractility At Rest and During Stress*

Page 206 ***Table 5.5****: Stress Creatine Kinase First Order Rate Constant (Ck $_{kf}$)*

Page 209 ***Table 5.6****: Venous metabolites at stress in heart failure volunteers*

Page 212 ***Table 5.7****: Volumes During Stress in Heart Failure Volunteers*

Page 215 ***Table 5.8****: Rest and Stress Haemodynamics and Cardiac Work in Volunteers with Heart Failure*

Page 218 ***Table 5.9****: Stress Creatine Kinase First Order Rate Constant in Heart Failure at stress*

Page 221 ***Table 5.10****: Left mainstem arterial metabolite concentrations during rapid atrial pacing and substrate manipulation, during the invasive study, in the HFrEF group.*

Page 223 ***Table 5.11****: Arteriovenous metabolite uptake during rapid atrial pacing and substrate manipulation, during the invasive study, in the HFrEF group.*

Page 225 ***Table 5.12****: Rest and Stress comparison of cardiac arteriovenous metabolite uptake in patients with HFrEF*

Page 227 ***Table 5.13****: ATP produced per metabolite as a percentage of total ATP production during stress*

Page 227 ***Table 5.14****: Comparison between rest and stress of proportional ATP production by substrate*

Page 229 ***Table 5.15****: Cardiac arteriovenous oxygen difference and extraction in HFrEF, during rapid atrial pacing, and substrate manipulation*

Page 232 ***Table 5.16****: Invasive measures of contractility during rapid atrial pacing in HFrEF, and the change from intrinsic rhythm (rest) to rapid pacing (stress)*

Page 235 ***Table 5.17****: Cardiac contractility during rapid biventricular pacing and compared between slow and rapid biventricular pacing in patients with HFrEF*

Page 254 ***Table 6.1****: Participant characteristics for study volunteers for the vasodilator experiment.*

Page 255 ***Table 6.2****: 5-minute averaged haemodynamic values collected during GTN infusion.*

Page 256 ***Table 6.3****: Left and right ventricular volumes before and during GTN infusion.*

Page 258 ***Table 6.4****: Spectroscopic values before and during GTN infusion.*

List of Abbreviations

1D-CSI: 1-dimensional Chemical Shift Imaging

^{1}H: Proton

^{31}P: 31-phosphorus

AAA: Abdominal Aortic Aneurysm

ACE: Angiotensin Converting Enzyme

ACT: Activated Coagulation Time

ADP: Adenosine Diphosphate

ALAT: Alanine Aminotransferase

AMP: Adenosine Monophosphate

AMPK: Adenosine Monophosphate Kinase

APV: Average Peak Velocity

ARB: Angiotensin Receptor Blocker

ARNI: Angiotensin Receptor blocker – Neprilysin Inhibitor

ATGL: Adipose Triglyceride Lipase/desnutrin

ATP: Adenosine Triphosphate

BDH1: Beta-hydoxybutyrate Dehydrogenase 1

BiV: Biventricular pacing

BOHB: Beta hydroxybutyrate

BMI: Body Mass Index

BNP: Brain-type Natriuretic Peptide

cAMP: Cyclic Adenosine Monophosphate

CK: Creatine Kinase

CKk_f: Creatine Kinase First Order Rate Constant

CMR: Cardiac Magnetic Resonance

CoA: Coenzyme A

CPO: Cardiac Power Output

CRT: Cardiac Resynchronisation Therapy

CSI: Chemical Shift Imaging

CPT1/2: Carnitine Palmitoyl Transferase 1 / 2

CW: Cardiac Work

DAG: Di-acyl Glycerol

DANTE: Delays Alternating with Nutation for Tailored Excitation

ECG: Electrocardiogram

EDPVR: End Diastolic Pressure Volume Relationship

EDV: End Diastolic Volume

EF: Ejection Fraction

ERR: Estrogen Related Receptor

ESC: European Society of Cardiology

ESPVR: End Systolic Pressure Volume Relationship

ESV: End Systolic Volume

FAD: Flavin Adenine Dinucleotide

FAT: Fatty Acid Translocase

FFA: Free Fatty Acid(s)

FOV: Field Of View

G-6-P: Glucose-6-phosphate

GCS: Global Circumferential Strain

GIK: Glucose Insulin Potassium infusion

GLUT: Glucose Transporter

GTN: Glyceryl Trinitrate

HBP: Hexosamine Biosynthetic Pathway

HIF: Hypoxia Inducible Factor

HFrEF: Heart Failure with Reduced Ejection Fraction

HFmrEF: Heart Failure with Mid Range Ejection Fraction

HFpEF: Heart Failure with Preserved Ejection Fraction

LAD: Left Anterior Descending coronary artery

LDH: Lactate Dehydrogenase

LV: Left Ventricle

LVAD: Left Ventricular Assist Device

LVEDP: Left Ventricular End Diastolic Pressure

LVEF: Left Ventricular Ejection Fraction

MACE: Major Adverse Cardiovascular Event(s)

MAP: Mean Arterial Pressure

MCT: Monocarboxylate Transporter

MEE: Mechanical External Efficiency

MI: Myocardial Infarction

MPC: Mitochondrial Pyruvate Carrier

MR: Magnetic Resonance

MRS: Magnetic Resonance Spectroscopy

MRI: Magnetic Resonance Imaging

MVO_2: Myocardial Oxygen Consumption

NAD: Nicotinamide Adenine Dinucleotide

NEFA: Non-Esterified Fatty Acids

NMR: Nuclear Magnetic Resonance

NYHA: New York Heart Association

OCMR: Oxford Centre for clinical Magnetic Resonance research

PCr: Phosphocreatine

PDK: Pyruvate Dehydrogenase Kinase

PGC: PPAR-gamma coactivator

Pi: Inorganic Phosphate

PPA: Phenyl-Phosphoric Acid

PPAR: Peroxisome proliferator activated receptor

PPM: Parts Per Million

PDH: Pyruvate Dehydrogenase

PET: Positron Emission Tomography

PFK: Phosphofructokinase

PV Loop: Pressure-Volume Loop

PVA: Pressure-Volume Area

RPP: Rate Pressure Product

RF: Radiofrequency

ROS: Reactive Oxygen Species

RV: Right Ventricle

SAR: Specific Absorption Rate

SCOT: Succinyl-CoA:3-Oxoacid-CoA-Transferase

SERCA: Sarcoplasm-Endoplasmic Reticulum Calcium ATPase

SNR: Signal to Noise Ratio

SSFP: Steady State Free Precession

StreST: Stress Saturation Transfer

SV: Stroke Volume

SW: Stroke Work

TAG: Tri Acyl Glycerol

TCA: Tricarboxylic Acid Cycle

TE: Excitation Time

TPN: Total Parenteral Nutrition

TR: Repetition Time

TRIST: Triple Repetition Saturation Transfer

UCP: Uncoupling Protein

VLDL: Very Low Density Lipoprotein

$\Delta G'_{ATP\ hydrolysis}$: Free Energy of ATP hydrolysis

1 Chapter 1: Introduction

1.1 Introduction: A brief history of cardiac metabolic manipulation in heart failure

Cardiac metabolism and its links to myocardial dysfunction have been a topic of research for a hundred years or more.

In 1932 the Canadian Jonathan Campbell Meakins, extrapolating from work done on skeletal muscle and drawing on his experiences in Edinburgh with insulin, published the first paper to consider substrate and energy metabolism in the myocardium[1]. He proposed a cycle where the breakdown of glycogen to lactic acid generated 'phosphagen' to drive contraction, proposed several situations (oxygen deficiency, pH changes, insulin deficiency in diabetes) where this cycle was disrupted and speculated that glycogen depletion could drive impairment of cardiac function in apparently structurally normal hearts. Tinsley Harrison made similar assertions in his 1935 textbook 'Failure of the Circulation': oxygen deficiency, insulin deficiency and defective glycogen metabolism could drive cardiac failure.

Over the next two to three decades, the Krebs cycle was discovered[2] (earning Krebs and Lippman the 1953 Nobel Prize in physiology) and both histological and cardiac catheter studies demonstrated that fatty acids, ketones, glucose, lactate and pyruvate all formed substrates for heart muscle[3], with the idea that heart failure could in many situations have a biochemical basis persisting.

Metabolic modulation for cardiac disease has an even longer history, a Dr Goulston describing giving cane sugar to a series of patients with angina or heart failure with empirically good effect after watching the effects of perfusing a heart with dextrose in 1911[4].

However, the first serious usage was of a potassium-insulin-glucose infusion on a series of patients in 1962, where it was observed to reverse some of the ECG changes in acute ischaemia, putatively via changes in potsssium ion homeostasis[5]. In 1970, Lionel Opie published an editorial suggesting 'the glucose hypothesis': that increasing blood glucose may benefit ischaemic myocardium by increasing both aerobic and anaerobic glycolysis and decreasing circulating free fatty acids[6], which informed the direction of research in this sector. The idea of using insulin-glucose to increase glycolysis showed promise in reducing infarct size in animals[7, 8] and was shown to reduce mortality in a post-MI population[9].

In the late 1980s dichloroacetate, an activator of pyruvate dehydrogenase, the entry point into oxidation of glucose, was discovered to stimulate glucose metabolism and inhibit fatty acid metabolism, hence was tested in coronary artery disease where it was shown to increase stroke volume and increase myocardial efficiency while increasing glucose and lactate uptake[10]. However, dichloroacetate has a narrow therapeutic window, short half life and toxic side effects[11], hence attention turned to other approaches.

The Randle cycle had been discovered in the mid-1980s[12]; also known as the glucose-fatty acid cycle, this provided a mechanism by which fatty acid metabolism would inhibit glucose metabolism and vice-versa. This provided the idea that inhibiting fatty acid metabolism could activate PDH and provide benefits for cardiac metabolism. Several drugs have been shown to be successful in ischaemic heart disease in this regard: carnitine palmitoyltransferase (CPT-1) inhibitors were first shown to be successful using Etomoxir in animal models in 1988[13] and the 3-ketoacylCoA thiolase (3-KAT) inhibitors such as trimetazadine and ranolazine had been found to increase pyruvate dehydrogenase activity[14] and showed promise in reducing angina symptoms[15].

In the early 2000s, the application of theories of switching substrate metabolism started to be expanded from ischaemia and applied to heart failure[16]; the predominant cause of which is ischaemic heart disease. There was existing evidence that contractile function was increased when metabolising glucose and lactate compared to free fatty acids for a given rate of oxygen consumption[17, 18], hence altering substrate was postulated as a treatment, based on the assumption that oxygen delivery was limited. The possibility that changing substrate could result in improvements in redox state[19, 20], energy of ATP hydrolysis[19-21] and calcium transients[21] had been recognised, but along with suggestions that fatty acids promote mitochondrial uncoupling (directly or via PPARα)[22] and other toxic effects such as opening of the mitochondrial permeability transition pore, leading to increased apoptosis[23]. Intra-coronary infusion of pyruvate increased cardiac index[24] and improved diastolic function [25] in non-ischaemic cardiomyopathy and alternate day infusions of glucose-insulin improved EF and reduced BNP in patients with ischaemic cardiomyopathy, with improvement sustained after a month[26]. A small study infusing dicholoacetate for 30 minutes had shown increases in stroke volume with decreases in myocardial oxygen consumption in a mixed population of ten heart failure patients (7 with ischaemic cardiomyopathy, 3 non-ischaemic).[27] While the evidence seemed to come in the most part from ischaemic cardiomyopathy, increasing PDH flux seemed an attractive approach to treatment.

Could inhibiting fatty acid metabolism also provide benefits in heart failure? Mechanistic studies in animals had shown promise (e.g. ranolazine in a multi-infarct canine model of heart failure[28]) and a study in 47 elderly patients with chronic stable angina and reduced left ventricular (LV) function showed a 7% absolute increase in left ventricular ejection fraction with trimetazidine[29]. Despite several further studies (reviewed in detail below); the fatty acid oxidation inhibition and activation of glucose oxidation, at least in HFrEF, has never fully

delivered on the theoretical benefits and has increasingly fallen by the wayside as a therapeutic option, being superseded by successful strategies based around renin-angiotensin-aldosterone inhibition, neprilysin inhibition and beta blockade.

While the putative benefits of increased glucose oxidation seem clear in ischaemia, the case is not so certain in heart failure where ischaemia is not always the driving force. The greater ATP per mole of substrate oxidised from fatty acids may be beneficial and the two have not been experimentally compared previously.

The key aims of this thesis are to compare the benefits of glucose compared to fatty acid metabolism in heart failure and investigate their translational potential for novel therapeutics. I will review the existing evidence, describe the biochemical advantages of the metabolism of the different substrates and outline experimental evidence of substrate manipulation affecting the biochemistry and function of the heart.

1.2 Heart Failure

1.2.1 Definition and Epidemiology

Heart failure is given the following definition in the European Society of Cardiology guidelines[30]:

> *"Heart failure is a clinical syndrome characterised by symptoms of breathlessness, ankle swelling and fatigue with clinical signs of fluid overload (elevated jugular venous pressure, pulmonary crackles and peripheral oedema) caused by a structural and/or functional cardiac abnormality resulting in a reduced cardiac output and/or elevated intracardiac pressures at rest or during stress."*

The prevalence of heart failure is approximately 1-2% in the Western world, rising with age[31]. Prognosis is poor, with a 1-year survival of 80-90% and a 5-year survival of 50-60%[32].

Historically, heart failure has been categorised depending upon the left ventricular ejection fraction: there has been some debate about the use of this classification[33] but it remains the most accessible and easiest to use. Patients with ejection fraction of less than or equal to 40% are termed "heart failure with reduced ejection fraction" (HFrEF) and occupy a traditional group of heart failure due to systolic dysfunction and remodelling with cavity dilation[34]. Patients with ejection fraction of greater than 50% occupy a group termed "heart failure with preserved ejection fraction" (HFpEF) which represents a mixture of aetiologies and mechanisms[35] including diastolic dysfunction and chronotropic incompetence. On the other hand, patients with ejection fraction 40-50% are termed "heart failure with mid-range

ejection fraction" (HFmrEF) and form an intermediate group[30]. In the UK, the majority of patients (64%) had HFrEF[36].

Within HFrEF, the majority (around 60%[37]) of patients have an ischaemic cause, however a significant proportion have non-ischaemic cardiomyopathy, including genetic causes, toxic damage (increasingly from cancer therapies), inflammatory (post viral myocarditis) or infiltrative causes (such as amyloidosis, sarcoidosis, Fabry's disease or haemochromatosis)[30].

1.2.2 Current Concepts of Treatment

The usual neuronohumoral responses to a reduction in forward blood flow will cause activation of the natriuretic peptide-renin-angiotensin-aldosterone axis (promoting retention of fluid as well as vasoconstriction) and activation of the sympathetic nervous system (causing vasoconstriction as well as cardiac inotropy and chronotropy)[38].

In a healthy heart, the additional circulating volume increases preload and thereby stroke volume via the Starling effect, however the paradigm is different in the failing heart.

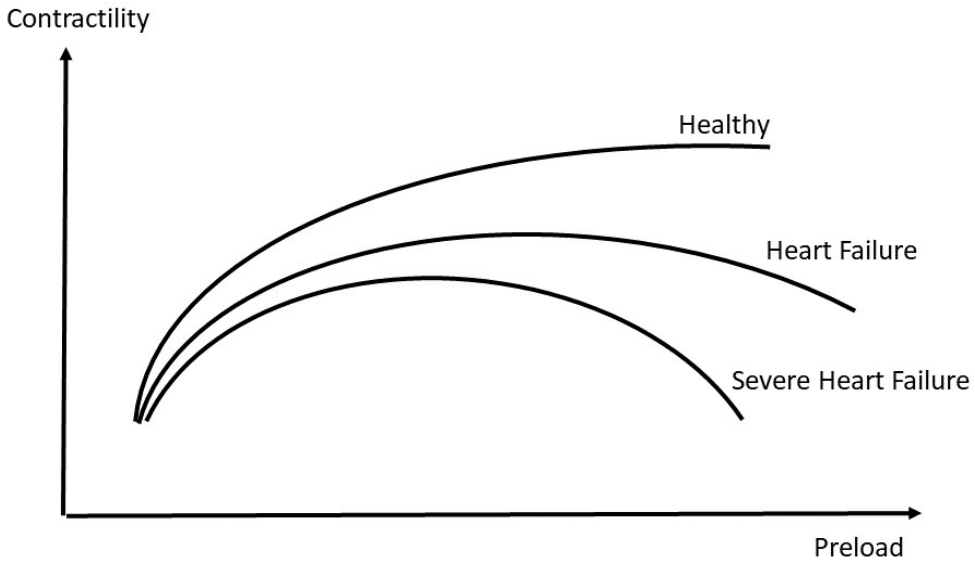

Figure 1.1: Frank-Starling curves in the healthy and failing hearts

As preload increases in the failing heart, the Frank-Starling curve flattens and then dips as Laplace's law dominates, tension increases and the energy required for contraction increases. Likewise, while an increased systemic vascular resistance may elevate arterial blood pressure, a higher afterload will also increase energy requirements (see section 1.3 page 9). Therefore, vasodilation and diuresis formed the cornerstone of heart failure treatment: reducing the energetic demand. Discoveries in the 1990s of the value of ACE inhibition and beta blockade paved the way for the discovery of neprilysin inhibition in 2014[39].

Nonetheless, the focus remains on optimising the heart's function by reducing the demands placed upon it. No therapy exists which increases the contractility of the myocardium while conferring long term beneficial effects on mortality, although digoxin and omecamtiv mecarbil have been shown to have beneficial effects on hospitalisation[40, 41]. The majority of drugs which increase contractility do so at the expense of exacerbating the mismatch between cardiac work and mitochondrial ATP generation, depleting energy stores and

resulting in generation of reactive oxygen species[42] as well as dysfunctional calcium handling, promoting ventricular arrhythmias. Inotropic drugs have only ever shown neutral or deleterious effects on mortality long term effects in clinical trials[43] and while they support contractility in the short term, on withdrawal of these drugs those variables worsen dramatically, suggesting these therapies accelerate ventricular deterioration[44]. A therapy which can increase the ATP output of cardiac mitochondria and, therefore, the capacity of the heart to do work is therefore desirable.

1.3 Myocardial Energy Use and Oxygen Consumption

The heart's energetic requirements (and therefore the myocardial oxygen consumption or MVO_2) will depend on the force, duration and frequency of contraction. They can be modelled as cardiac stroke work, also known as ventricular stroke work or simply stroke work (SW)[45]:

Stroke work = stroke volume x (arterial pressure during systole – LV end diastolic pressure)

In this case, the mean arterial pressure (MAP) represents the average afterload during systole and the left ventricular end diastolic pressure (LVEDP) the preload. This is often simplified by considering LVEDP to be equal to right atrial pressure or even by considering it to have a negligible contribution and discounting it completely.

Stroke work = stroke volume x mean arterial pressure

The total work done in a minute, therefore (the cardiac work, CW) is the stroke work multiplied by the number of beats per minute:

Cardiac work = stroke work x heart rate

Or, calculated another way:

Cardiac work = mean arterial pressure x cardiac output

Which can be converted into an approximation of the cardiac power output in watts (Cardiac Power Output, CPO) by dividing by 451[46].

Additionally, rate pressure product (RPP) has been shown to correlate well with oxygen demand[47]:

Rate Pressure Product = Systolic Blood Pressure x Heart Rate

Therefore by varying heart rate, stroke volume or systolic blood pressure, the energy requirements will change. Extrapolating from this, we can assume that by manipulating afterload and stroke volume, we can alter the energetic demand of the heart: this is the basis for maximizing the capacities of the heart by reducing afterload with vasodilator therapies.

These, of course are an oversimplification, for numerous reasons:

- The work done by the right ventricle and the atria are discounted (although it is possible to separately calculate left and right ventricular cardiac work).
- Calculating the mechanical work of the ventricle would require continuous measurement of the force generated and the curvature of the wall of the left ventricle. This would be extremely difficult even under experimental conditions. Hence pressure is substituted for force and we do not properly account for how chamber size can influence wall stress.
- Other energetic demands on the myocardium, termed 'internal' cardiac work: mechanical ones such as creating elastic compression which is released in diastole as the ventricle relaxes or biochemical processes such as the movement of ions to facilitate electrical signalling to co-ordinate the myocardium.

A more accurate but more experimentally intensive method is to extrapolate cardiac work from a pressure-volume loop. In a series of experiments throughout the 1980s, Suga and colleagues demonstrated that myocardial oxygen consumption correlated with the pressure-volume area: an area bounded by the end-systolic pressure volume relationship, the end diastolic pressure volume relationship and the systolic limb of the pressure-volume loop[48-50], see figure 1.2.

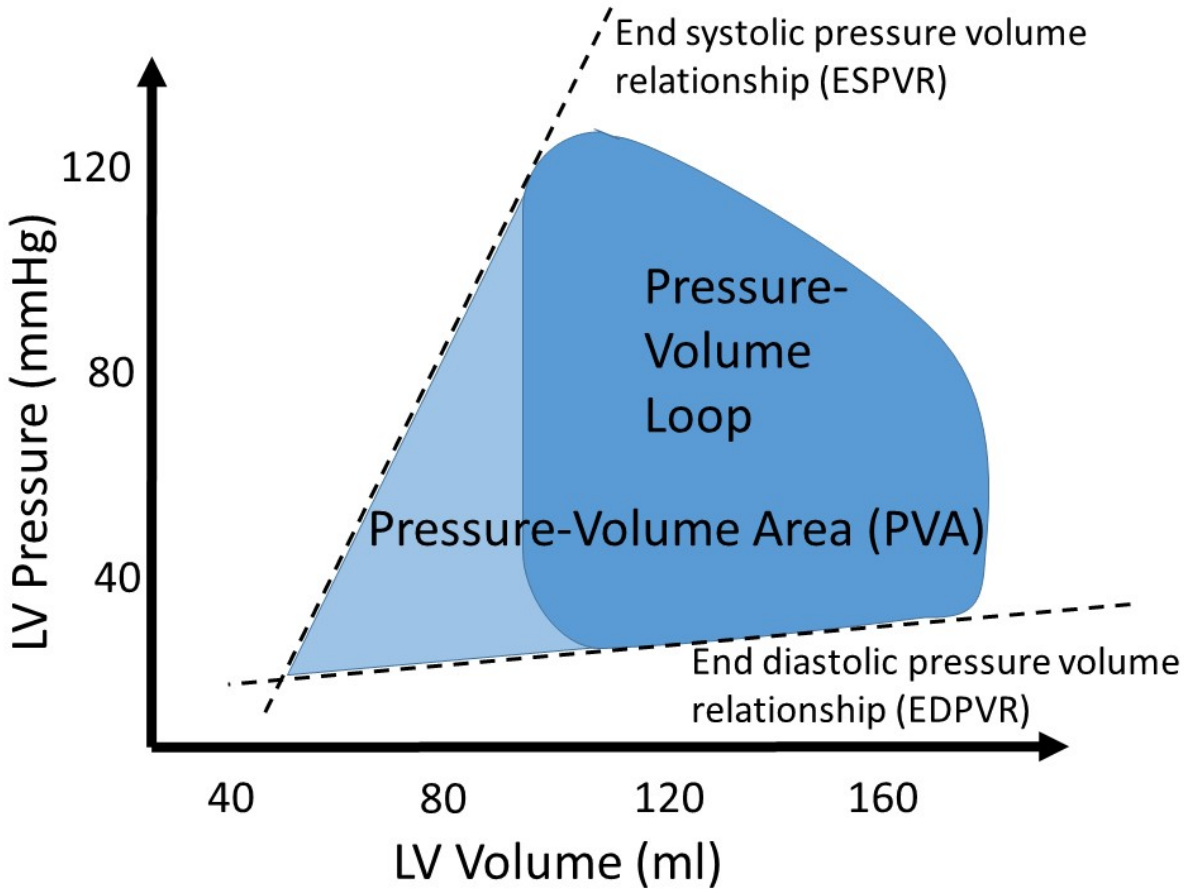

Figure 1.2*: Total blue shaded area is the pressure-volume area (PVA), whereas the dark blue shaded area is the pressure-volume loop.*

However, they discovered that the correlation between PVA and MVO_2 was linear in a given inotropic state, it would vary with loading conditions[49] or exposure to inotropes[50].

Increasing inotropy with catecholamines carries with it a greater oxygen requirement (MVO_2) than increasing the cardiac output by filling the heart to increase stroke volume via Frank-Starling forces[17, 50-52], owing to an increase in the load-independent oxygen consumption (i.e. the proportion of energy wasted and not converted into contractile energy[53]). More simply put, the relative increase in MVO2 per unit of work done is greater with catecholaminergic stimulation. These differences can be reflected in mechanical

efficiency (or mechanical external efficiency, MEE – so called as it discounts internal cardiac work), calculated thus:

$$MEE = \frac{\text{Mean Arterial Pressure x Stroke Volume x Heart Rate x } 1.33 \text{ x } 10^{-4}}{\text{Myocardial oxygen uptake x Left Ventricular Myocardial Mass x } 20}$$

This brings us to a more fundamental flaw with all the above models of cardiac energy: that they assume pressure and volume have a linear effect on myocardial energy (and MVO_2) when fundamental laws of physics show us this is not the case. Myocyte tension is the primary determinant of oxygen consumption per cell, with the magnitude of tension correlating with ATP hydrolysis rates. Laplace's law states that, for a curved vessel, wall tension is proportional to the product of pressure and the vessel's radius. If one is to roughly model the area of the ventricle as a sphere, as volume is equal to $4/3\pi r^3$, then tension will be proportional to pressure multiplied by the cube root of volume. Therefore, a given increase in pressure will create greater tension increase (and therefore greater energy requirement) than the corresponding increase in volume. The counter, whereby if available energy is the limiting factor, then a reduction in pressure may yield a proportionally greater volume increase.

We can surmise that these techniques for estimating MVO2 are not without their flaws, however when used correctly, they provide a useful and easily calculated surrogate and a helpful way to model energetic requirements. Myocardial oxygen uptake is conventionally measured invasively (via paired arteriovenous oxygen measurements), noninvasively by measuring isotope kinetics of inhaled ^{15}O-O_2 or kinetics of ^{11}C labelled acetate on PET, the latter being technically easier and therefore more frequently used.

1.4 Myocardial Energy Production

The heart takes up and oxidises a mixture of fat, glucose and other substrates to produce adenosine triphosphate (ATP) from adenosine diphosphate (ADP): energy is stored in phosphate bonds from which it may be released by ATPases at sites of use: principally in the heart the actin-myosin ATPase which provides energy for contraction.

1.4.1 Myocardial Energy Substrate Metabolism

Upstream of ATP utilisation, all cardiac ATP is generated from the oxidation of metabolic substrates: either fat, sugar, ketone bodies or lactate. The normal heart in the resting state can exhibit remarkable flexibility, allowing the natural fluctuations in substrate supply that occur with fasting (increased fatty acid availability) and feeding (increased glucose availability and insulin activity) to be accommodated. Typically, the heart receives the majority of energy from oxidation of fat and a much smaller proportion from oxidation of glucose[54]. Also, the quantities of each substrate metabolised will depend upon demand for ATP within the myocardium, with exercise[55], pressure overload or ischaemia[56] causing a shift to glucose, e.g. via activation of AMPK[57].

Largely, energy metabolism can be broken down into three crucial steps:

1. The uptake of substrate into the cell.

2. The oxidation of substrate within mitochondria and entry into the Krebs cycle to generate reducing agents and thereafter a proton gradient via the electron transport chain.

3. The generation of ATP from ADP using this proton gradient.

While this process may seem straightforward, it is important to recognise that substrate taken up is not necessarily oxidised and may be shunted into other pathways. Likewise, the proton gradient may be dissipated, lost as heat energy rather than producing chemical energy in the form of ATP. The relationships between these steps differs not just by substrate but also by conditions within the myocyte such as mechanical load, electrolyte gradients or other external factors.

An overview of substrate uptake and metabolism is given in figure 1.3.

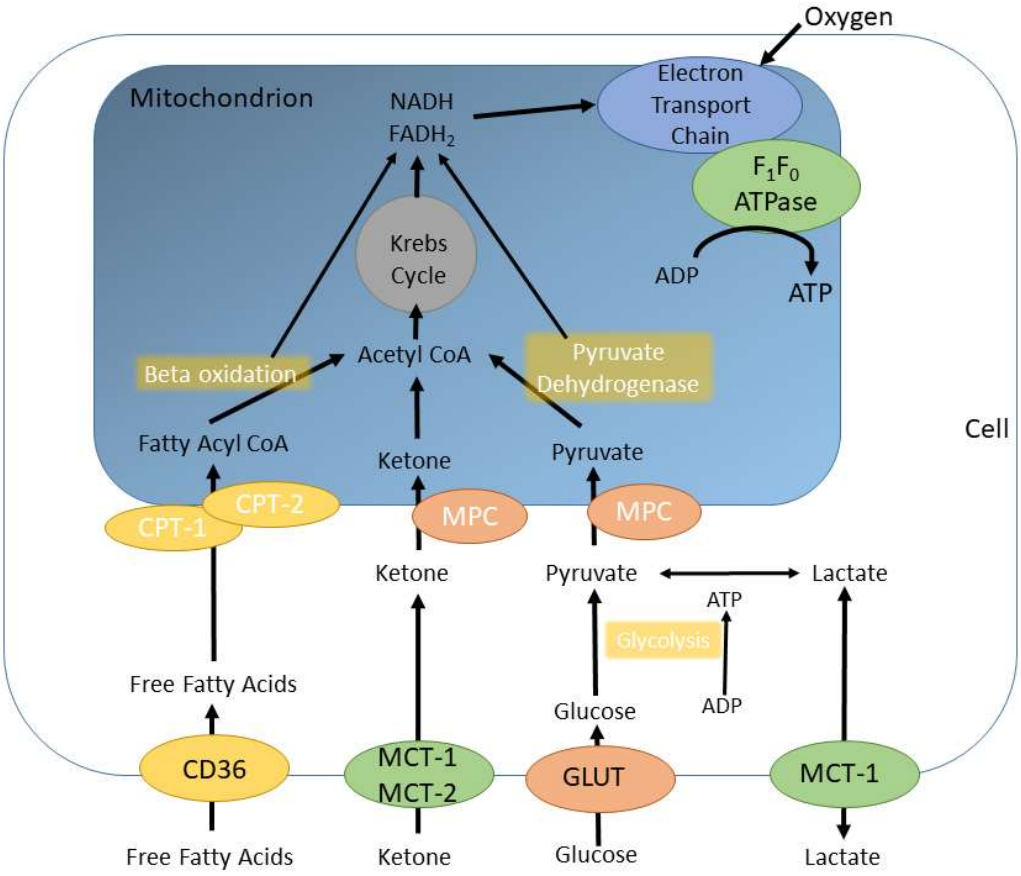

Figure 1.3*: Overview of substrate uptake and metabolism within myocytes. CPT, Carnitine Palmitoyl Transferase; GLUT, Glucose Transporter; MCT, Monocarboxylate Transporter; MPC, Mitochondrial Pyruvate Carrier*

1.4.1.1 Tricarboxylic Acid Cycle

Also known as the TCA, citric acid cycle (CAC) or Krebs cycle (after its discoverer), this key pathway represents the final common end pathway for substrate metabolism. Substrates are metabolised to acetyl-CoA, then this enters the cycle, being oxidised in a stepwise fashion into carbon dioxide and water. In the process, nicotinamide adenine dinucleotide (NAD+) is reduced to NADH and Flavin adenine dinucleotide (FAD) is reduced to $FADH_2$. These reducing agents donate electrons to the electron transport chain, creating a proton gradient across the inner mitochondrial membrane, in turn driving F_1F_0 ATPase to convert ADP to ATP. Electron transport is discussed further in 1.4.2 page 21.

1.4.1.2 Lipid Metabolism in the Normal Heart

There are three principal steps for fatty acid utilisation: transport across the cell membrane into the cytosol, transport across the mitochondrial membrane and then oxidation once inside the mitochondria.

Lipids are supplied to the heart in the form of free fatty acids (also called nonesterified fatty acids, NEFA) bound to albumin and fatty acids released by hydrolysis by lipoprotein lipase from tri-acylglycerol (TAG) from chylomicrons or very low density lipoproteins (VLDL)[58]. The main fatty acids encountered are oleate (C18), palmitate (C16) and linoleate (C18) and uptake is predominantly determined by the concentration of these substrates in the plasma[59]; hence is affected by metabolic states that elevate plasma free fatty acids (catecholamine release due to sympathetic nervous system activation[60] or metabolic conditions such as obesity and diabetes[61]).

Fatty acids may cross the cell membrane by translocation through the lipid bilayer, however adsorption into the outer leaflet is promoted by fatty acid translocase (FAT or CD36) and desorption from the inner leaflet promoted by the cytoplasmic fatty acid binding protein (FABPc; H-FABPc in the case of myocytes). Once inside the cell, fatty acids are esterified to form fatty acyl-CoA by the enzyme acyl CoA synthetase (ACSL1); this Acyl CoA having diverse fates not limited to providing metabolic substrate but also forming a store of TAG and from this, di-acylgylcerol (DAG), ceramides or membrane lipids[62].

Short or medium chain fatty acids may enter the mitochondrion directly but long chain acyl-CoA (C16 or C18 fatty acids, the commonest) requires carnitine palmitolytransferase (CPT1 on the outer membrane and CPT2 on the inner membrane) to enter.

Once inside the mitochondrion, acyl-CoA undergoes beta-oxidation, producing acetyl CoA to enter the Krebs cycle and NADH and $FADH_2$, which pass to the electron transport chain.

1.4.1.2.1 Regulation

Transport forms a key regulatory step, CPT1 being inhibited by malonyl CoA (a marker of excess acetyl CoA and hence a negative feedback system), while peroxisome proliferator activated receptors (PPARs) and estrogen related receptors (ERRs) regulate fatty acid oxidation on the transcriptional level, their activities in turn enhanced by PPAR-γ coactivator-1 (PGC-1)[63]. TAG itself is a ligand for PPAR activation, hence the amount of TAG stored within the myocyte has a feed-forward effect on fatty acid oxidation, either directly[64] or via SIRT1[65].

Three forms of PPAR are expressed in cardiomyocytes: PPARα and PPARβ/δ (which are more abundant) and PPARγ[66]. PPARα upregulates fatty acid oxidation[67], while PPARβ/δ

also increases myocardial glucose utilisation[68]. There are three ERRs, α, β and γ, with α and γ the dominant isoforms[69], activating fatty acid uptake as well as perioxisomal and mitochondrial oxidation of fatty acids, partly via PPARα activation[70]. PGC-1α is activated by various stimuli including stress, fasting, β-adrenergic stimulation and exercise[66] but also by various signalling pathways including AMPK, Calcium and SIRT1.

1.4.1.3 Glucose Metabolism in the Normal Heart

Glucose is taken into the cell via insulin independent (GLUT-1) and insulin sensitive (GLUT-4) transporters and converted via glycolysis to pyruvate. GLUT-4 transporters are held within cytosolic vesicles and translocate to the cell membrane in response to insulin, ischaemia or increased work[71].

Glucose is phosphorylated by hexokinase to glucose-6-phosphate, preventing it from leaving the cell. G-6-P has a number of roles; it may be converted to glycogen for storage, enter glycolysis to form pyruvate for oxidative metabolism or enter metabolic pathways such as the pentose phosphate pathway (producing NADPH for redox regulation or ribose 5-phosphate, a DNA precursor) or the hexosamine biosynthetic pathway (forming UDP-N-acetylglucosamine, a donor for glycosylation). Following glycolysis to pyruvate, this enters the mitochondrion via the mitochondrial pyruvate carrier (MPC) and is then oxidised by pyruvate dehydrogenase (PDH) to form acetyl CoA (commonly referred to as glucose oxidation). Alternatively, pyruvate may also enter the TCA cycle directly via carboxylation to oxaloacetate or malate.

The hexosamine biosynthetic pathway (HBP) converts glucose into uridine diphosphate -β-N-acetylglucosamine (UDP-GlcNAc), a monosaccharide donor for protein glycosylation

(termed O-GlcNAcylation), a pathway with multiple regulatory roles: for instance, AMPK dampens O-GlcNAc signalling by inhibiting the rate-limiting step of HBP, which has been shown to reduce cardiac hypertrophy[72].

1.4.1.3.1 Regulation

PDH is highly regulated, inhibited by acetyl CoA in a feedback circuit and NADH from beta oxidation as well as pyruvate dehydrogenase kinase (PDK), an enzyme which phosphorylates and inhibits PDH. HIF-1α stimulates glycolysis during stress to adapt to an oxygen limited environment but also represses glucose oxidation by activating PDK[73].

Insulin stimulates glucose uptake, glycolysis and oxidation (directly or indirectly): stimulating the translocation of GLUT-4 to the cell membrane[74] and activating hexokinase[75] and glycogen synthetase. Indirectly, insulin causes a fall in circulating free fatty acid levels and thereby releasing fatty acid inhibition of PDH, indirectly increasing glucose oxidation[76].

Glycogen synthesis and storage and regulated by the concentration of G-6-P and the activity of glycogen synthetase, itself activated by insulin[77], while glycogenolysis is activated by Calcium concentrations and Protein Kinase A (and hence, by cAMP), therefore beta-adrenergic stimulation and increased cardiac work[78]. Hyperglycaemia and hyperinsulinaemia prior to cardiac surgery resulted in an increase in myocardial glycogen[79], while exercise[80] or ischaemia[81] would deplete myocardial glycogen.

1.4.1.4 The Randle Cycle

Glucose and fatty acid metabolism cross-regulate each other via the Randle cycle, whereby fatty acid metabolism inhibits glucose oxidation (via inhibition of Pyruvate dehydrogenase, Phosphofructokinase-1 and GLUT-4), principally by an increase in mitochondrial [acetyl-CoA]/[CoA] and [NADH]/[NAD+], inhibiting PDH activity and efflux of citrate into the cytosol, which inhibits PFK-1[82]. Glucose oxidation inhibits fatty acid metabolism via enhancing acetyl CoA carboxylase and accumulated Acetyl CoA being converted to Malonyl CoA leading to inhibition of CPT-1[82]. This helps auto-regulate substrate preference depending on available metabolites.

1.4.1.5 Ketone Metabolism in the Normal Heart

β-hydroxybutyrate (βOHB or BOHB) and acetoacetate are the primary ketone bodies that circulate in the blood and can be metabolised[83]. Synthesis occurs in the liver when there is elevated fatty acid availability (e.g. fasting) and circulating ketones enter cardiomyocytes via MCT-1, then being transported into the mitochondrial matrix where they are oxidised. βOHB is oxidised into acetoacetate by βOHB dehydrogenase (BDH1). Acetoacetate and succinyl-CoA are converted to acetoacetyl-CoA by succinyl-CoA:3-oxoacid-CoA-transferase (SCOT), which is converted to acetyl-CoA by acetyl-CoA acetyltransferase[84]. Regulation is not well understood[85].

1.4.1.6 Amino Acid Metabolism in the Normal Heart

Amino acids, in addition to providing substrate to build proteins, can also provide TCA cycle intermediates (see anaplerosis) or energetic substrate, although provides <2% of ATP production in the healthy heart[54]. Branched chain amino acid (BCAA) oxidation is the best characterised source of amino acid oxidation in the heart. Amino acids are transaminated to the corresponding branched chain α-keto-acid (BCKA) by mitochondrial branched chain amino-transferase (BCATm). Next, there is oxidative decarboxylation of the BCKA by branched chain α-keto acid dehydrogenase (BCKDH), either generating acetyl-CoA for the TCA cycle or succinyl-CoA for anaplerosis[86]. BCKDH is inhibited by phosphorylation by BCKDH kinase (BDK) or activated by protein phosphatase C2m (PPC2m).

1.4.1.7 Lactate Metabolism in the Normal Heart

Even under high workload, the healthy heart is a net consumer of lactate[87], only producing it where there is glycolysis during impaired pyruvate oxidation, e.g. during ischaemia or in diabetes[78]. Lactate transport across the cell membrane in either direction is facilitated by monocarboxylic acid transporter-1 (MCT-1). Lactate is produced from pyruvate by lacatate dehydrogenase (LDH), regenerating NAD+ from NADH and maintaining glycolytic flux in anaerobic glycolysis or where oxygen is abundant, LDH catalyses the reverse reaction.

1.4.1.8 Anaplerosis

The Krebs cycle intermediates citrate and succinate continuously efflux from the mitochondria into the cytosol (cataplerosis), so for the cycle to function properly they must

be present in sufficient quantities. Therefore, fat and glucose (and to a lesser extent amino acids) are drawn into anaplerotic pathways to replenish these intermediates[88]. Pyruvate produces oxaloacetate which reacts with acetyl-CoA to form citrate (pyruvate carboxylation) and odd-chain fatty acids also serve an important role in this process as a provider of propionyl- CoA to form Succinyl CoA. Glutamine may replenish alpha-ketoglutarate and the purine nucleotide cycle fumarate. The process can also run in reverse (pyruvate decarboxylation) with malate being converted into pyruvate[89]. Citrate efflux appears to be important for signalling, as it varies depending on substrate metabolized and has regulatory roles in glucose metabolism (inhibiting phosphofructokinase) and long chain fatty acid utilization (inhibiting carnitine palmitoyl transferase-1)[90]. In health, citrate efflux from the mitochondria seems to sit at around 20% of pyruvate carboxylation, and given it acts to regulate glycolysis, this suggests a role in metabolic signal transduction between mitochondria and cytosol[89].

1.4.2 Energy of Synthesis of ATP

ATP synthesis occurs when electrons are transferred to oxygen, driven by a proton gradient across the inner mitochondrial membrane. The reducing agents NADH and $FADH_2$ formed from glycolysis, fatty acid oxidation and the tricarboxylic acid cycle donate electrons to the electron transport chain (ETC) complexes, driving hydrogen ions out across the inner mitochondrial membrane. This creates a hydrogen ion gradient, which drives the F_1F_o ATP-ase: the passage of ions through this complex catalysing ADP and Pi into ATP. The larger the electrical gradient produced by pumping hydrogen ions across the membrane, the greater the energy of synthesis of ATP[91].

However, $FADH_2$ enters the electron transport chain at complex II[92] – a lower energy level than NADH. Therefore, a change in the relative supply of different reducing agents (NADH or $FADH_2$) will influence the mitochondrial proton electrochemical gradient and as such the $\Delta G'_{ATP\ synthesis.}$ Hence, the free energy of ATP production is not identical for all substrates. [82, 93, 94].

β-oxidation of fat produces $FADH_2$ and NADH in a 1:2 ratio while glucose and ketone body oxidation produce FADH2 and NADH in a 1:4 ratio and therefore produce a larger energy of synthesis. This can be seen when the normal heart is perfused with increasing concentrations of free fatty acids, this results in an additional oxygen cost of between 25% and 48% for the same work output when compared to glucose and insulin infusion [95]. At rest, where fat is abundantly available and myocardial ATP demand is not high it can act as the main source of fuel for ATP production, however where demand increases, this efficiency may be a limiting factor.

In addition to a more favourable FADH2:NADH ratio, Ketone causes other changes in the electron transport chain that lead to a greater energy of synthesis. When metabolising ketone, there is increased reduction of CoEnzyme Q, increasing the potential between between ETC sites I and site III[96]: therefore an increase in the difference between sites I and IV, making more energy available for the synthesis of ATP, and hence an increase in the $\Delta G'$ of ATP hydrolysis[83, 92]. Measured experimentally, hydraulic efficiency of the rat heart increased 28% when it was perfused with ketones over glucose[92] and isolated dog hearts showed increased PCr/ATP ratios and falls in ADP when perfused with ketone[97].

Put simply, the substrate metabolised will determine the heart's maximal energy of synthesis – which in turn will determine the maximal energy of hydrolysis and, therefore, function.

1.4.3 Energy of Hydrolysis of ATP

The free energy released from hydrolysis of ATP, ΔG_{ATP}, provides a chemical driving force for ATP-requiring reactions within the cell, its magnitude being proportional to the ratio between ATP and ADP concentrations:

The free energy of ATP hydrolysis ($\Delta G'_{ATP\ hydrolysis}$) can be calculated from the equation [98]

$$\Delta G' = \Delta G° - RT\ \ell n\ \frac{[ADP][Pi]}{[ATP]}$$

Where $\Delta G°$ is the standard free energy change of ATP hydrolysis (-30.5 kJ/mol under standard conditions, where each substrate and product is present at concentration 1mmol/L, standard temperature and pH 7), R is the gas constant (8.3 J/mol.K) and T is the temperature in kelvin. It is expressed as a negative value, with 'more negative' describing 'more power'. To summarise this, free energy of ATP hydrolysis will increase (become more negative) when ATP concentration increases relative to that of ADP and decrease (become less negative) when ADP concentration rises but may also be affected by the pH and temperature of the cell. The myocyte has numerous mechanisms to maintain ΔG_{ATP} at a steady state by coupling production to consumption, however disease states can cause disruption of these processes and a reduction of free energy, disrupting ATP dependent processes[99].

The ATPase enzymes catalysing different reactions require different values of free energy, and the difference between the free energy requirement for the enzyme and the available free energy from ATP hydrolysis adjacent to the enzyme can be considered the available driving force or energy reserve for the reaction[99]. Experimentally, when ATP delivery falls in perfused hearts given iodoacetamide to inhibit creatine kinase activity, supply cannot keep

up with demand and ADP concentrations increase due to workload, resulting in a fall in ΔG_{ATP}. In this experiment, peak contractility was measured at ΔG_{ATP} of -52 to -53 kg/mol, equivalent to the free energy of the sarcoplasm-endoplasmic reticulum calcium ATPase (SERCA) and suggesting a link between energy of synthesis and cardiac performance[100]. Indeed, SERCA has the highest free energy requirement of any myocardial ATPase and its activity has been shown to be closely tied to ΔG_{ATP}[101]. Rises in ADP inhibit the myosin ATPase and their concentration correlates with elevated LV end-diastolic pressure suggesting a link to diastolic dysfunction[102]. This is visualised in figure 1.4.

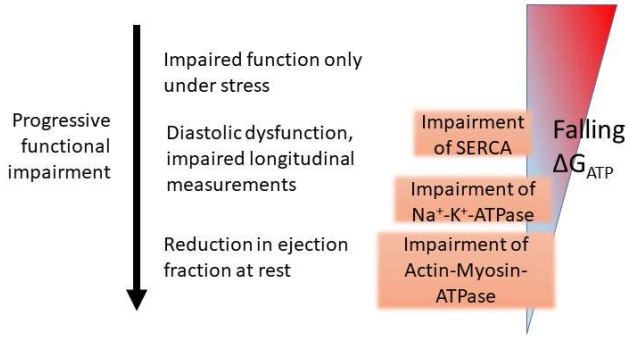

***Figure 1.4**: Linking impaired ΔG_{ATP} to functional impairment in vivo.*

The system can be conceptualized as a cylinder of water with ΔG_{ATP} as the height of the column (figure 1.5) and enzymes represented as pipes at different heights of the column. When the height of water drops below the minimum requirement for an enzyme, there is no flow, exactly as an enzyme will cease to function when ΔG_{ATP} drops below required levels. A column with greater height of water is not only sufficient to run the process but also has energy reserve should the height be depleted, as a ΔG_{ATP} above what is required for cellular functions gives a myocyte 'headroom' for ΔG_{ATP} to fall but still maintain activity [99].

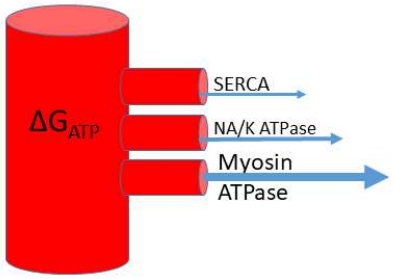

***Figure 1.5**: Conception of ΔG_{ATP} as a column of water.*

Anything that effects this driving force will affect the ability of the heart to do work.

1.4.4 Phosphotransfer

ATP's gamma phosphoryl group is transferred to creatine by the enzyme creatine kinase (CK), forming phosphocreatine, in the following equation:

$$PCr^{2-} + MgADP^{-} + H+ \rightleftharpoons Cr + MgATP^{2-}$$

Phosphocreatine diffuses to sites of ATP use, where creatine kinase transfers phosphate back to ADP to form ATP. Through this mechanism, phosphocreatine forms the prime temporal and spatial energy reserve within the myocyte: a pool of high energy phosphate which can buffer short term peaks in demand and also bridges the gap between sites of ATP synthesis and sites of its use. At baseline, the ratio of phosphocreatine to ATP is around 2:1.

ATP is synthesized principally in the mitochondria. The large size and relative polarity of ATP and ADP limits the distance they can rapidly diffuse and creates a requirement for a large concentration gradient for diffusion to occur, so it is advantageous to transfer phosphate to a substance which can move more easily within the myocyte, in order to get to where it is required. Accumulation of end products (ADP and Pi) adjacent to ATPases

would inhibit their function and accumulation of ATP at the mitochondria would inhibit oxidative phosphorylation, so there is also a need to ensure constant turnover [103].

Different isoforms of CK exist at the mitochondria (CK_{Mito}) and myofibrils (CK_{MB}), creating 'microdomains': production of phosphocreatine favoured at the mitochondria and the reverse reaction favoured at sites of use. The equilibria of these reactions are strongly biased to favour the formation of ATP, to the extent that cellular ATP, ADP and Pi concentrations will remain constant except in extreme circumstances[104]. The concentration of Phosphocreatine (and as such the ratio of Phosphocreatine to Creatine) may fluctuate [105] as a short-term buffer (over seconds) in order to maintain ATP concentration and therefore free energy of hydrolysis.

Around 80% of myocardial high-energy phosphate production is carried by this creatine kinase transfer system, with 15% via adenylate kinase and the remainder via glycolysis[106]. Adenylate kinase catalyses the reaction $2ADP \rightleftharpoons ATP + AMP$. This reaction becomes more important during ischaemia and has the knock-on effect of producing AMP, activating AMPK which is discussed in more detail in section 1.4.6 page 30.

A more recent idea, direct channelling, suggests enzymatic networks exist to transfer phosphate via a series of coupled reactions in near equilibrium which allow the propagation of a wave of concentration changes across the cell more rapidly than could occur via diffusion and with very small concentration gradients[107]. It is likely that a combination of the direct channelling and facilitated diffusion co-exist within the cell (figure 1.6).

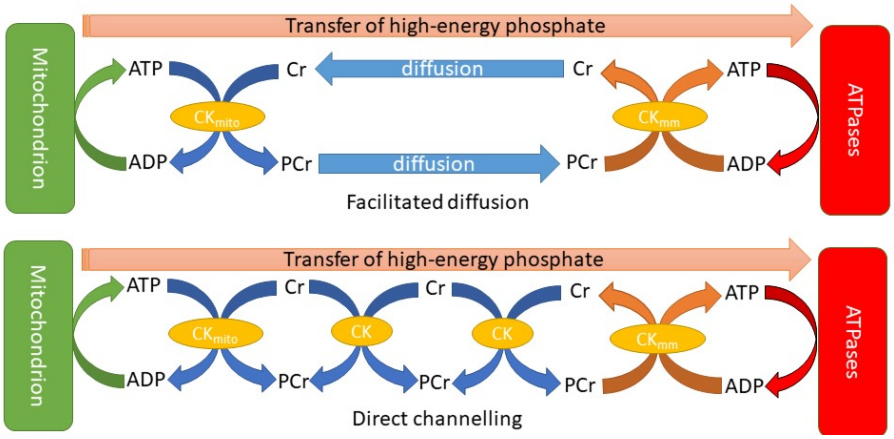

***Figure 1.6**: Direct channelling and facilitated diffusion.*

In a healthy system, changes in ADP and creatine around the mitochondria will stimulate oxidative phosphorylation to rise to meet demand, rapidly correcting any deficit. If the free energy of synthesis is unable to rise to meet this demand, a rise in concentration of ADP and Pi would occur at the mitochondria, shifting the equilibrium, with a fall in Phosphocreatine concentration and rise in free creatine concentration causing a rise in ADP at sites of use, bringing about a reduced energy of hydrolysis and ultimately limiting the contractile function.

Therefore, anything reducing energy of synthesis will have an impact on energy of hydrolysis and, eventually, cardiac function.

1.4.5 Linking Increased Demand to Increased Supply

The heart has a remarkable ability to match ATP synthesis to hydrolysis with cardiac oxygen consumption, increasing proportionately with workload but intracellular ATP concentrations and ΔG_{ATP} remaining constant[108]. In the healthy heart, PCr/ATP remains constant under moderate stress[109 110], suggesting that at these workloads there is sufficient

ability to increase substrate metabolism, oxidative phosphorylation and phosphotransfer rates to meet the increased ATP demand. When studied in the rat heart with magnetic resonance techniques, at varying workload ATP remains constant while ATP synthesis and transfer rose to meet the demand[111]. Multiple processes (Calcium levels, AMP signalling, coupled reactions) interact to produce this balance [57].

Calcium acts as a master regulator: increased cytosolic calcium is the signal to promote contraction (using up ATP) but it also enters mitochondria, stimulating an increase in Krebs cycle reactions (several of the enzymes are Calcium dependent), increasing mitochondrial ATP production in a fashion that matches the increased ATP requirement [112].

Increased ATPase activity alters ATP/ADP balance at sites of use, with the phosphotransfer mechanism now acting as a feedback system to change this balance within the mitochondria or other sensitive areas (figure 1.7). An increase in reaction substrates at the mitochondrion (ADP and Pi) increases the rate of oxidative phosphorylation[107, 113], which in turn leads to a change in flux through the Krebs cycle and a decrease in Krebs cycle intermediates and other reactants. For instance, a fall in Acetyl CoA leads to an increase in fatty acid transport, while a fall in Citrate stimulates glycolysis [57, 114].

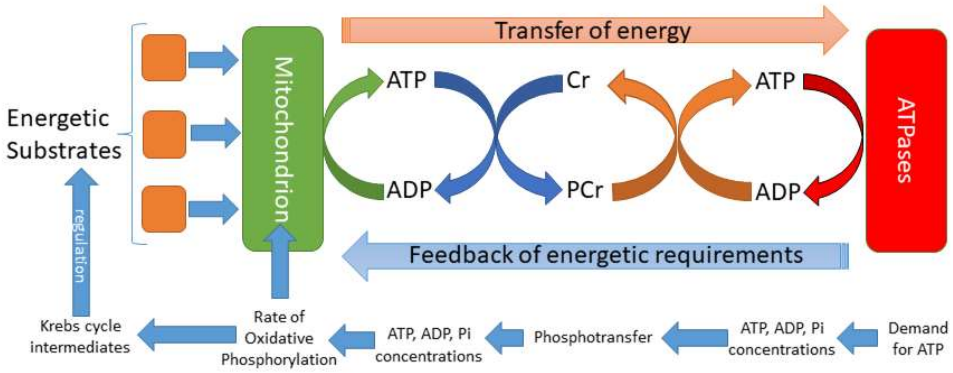

Figure 1.7*: Phosphotransfer acts as an energy shuttle in the forward direction but also as a signalling system in reverse: changes in ATP and ADP concentration at sites of use are fed back to the mitochondrion to alter rate of ATP synthesis.*

AMPK (AMP-activated protein kinase) promotes ATP production during higher workloads or oxidative stress, being activated by an increase in AMP (produced by adenylate kinase converting 2 ADP into an ATP and AMP when ADP levels rise)[115]. AMPK turns on ATP-generating fatty acid oxidation and glycolysis via various pathways (activating Acetyl-CoA carboxylase and Phosphofructokinase and recruiting GLUT-4 to the plasma membrane)[82]. This can override the Randle cycle during high demand in order to maximise the use of both fatty acids and glucose. Inorganic phosphate (P_i) will also stimulate glycogenolysis and anaerobic glycolysis (at the level of phosphofructokinase).

Finally, the redox state of the $NADH/NAD^+$ and $FADH_2/FAD$ couplets are important regulators of dehydrogenases involved in fatty acid beta-oxidation, glucose oxidation and TCA cycle activity[66].

1.4.6 Substrate Metabolism at Higher Workloads

As work increases, there is feedback via the phosphocreatine transfer system which increases the rate of TCA cycle flux and hence changes the ratio of Acetyl-CoA to CoA, in turn increasing the activity of 3-ketoacyl-CoA thiolase and PDH[66]. Increased workload decreases malonyl-CoA which increases fatty acid oxidation[55]. Hypoxia inducible factor (HIF-1) increases glycolysis while inhibiting pyruvate oxidation, in order to reduce oxygen demand[73].

β-adrenergic agonists cause increased intracellular Calcium concentrations and cAMP synthesis via β1 and β2 receptors, resulting in increased glucose uptake, PFK and PDH flux[116]: releasing the Randle cycle mediated brake on glucose metabolism[117] so both are metabolised and overall oxidation increases, predominantly of glucose[118]. However, catecholamines are known to stimulate lipolysis via β3 receptors, with mobilisation of lipid from adipocytes[60, 119], which would be expected to increase circulating levels of free fatty acids and hence myocardial fat uptake. In addition, perfusion of isolated myocytes with adrenaline was shown to reduce malonyl-CoA content[120], which would in turn promote beta-oxidation of free fatty acids.

Animal studies have been conflicting in this regard. Isolated working rat hearts show an increase in carbohydrate metabolism during higher workloads[118, 121] with minimal or lesser change in fat oxidation[122], while larger mammals (swine) increased fatty acid uptake during dobutamine infusion[123]. Labelling or uptake studies are also inadequate to assess the flux into or out of TAG stores within myocytes as a source of fat for beta-oxidation[124].

Invasive human studies are limited in number. In the adult human heart there is a linear increase in glucose uptake (and lactate production) with increased workload during atrial

pacing,[87] and also an increase in fat uptake and oxidation[125]. In human athletes (who may handle substrate differently), glucose and fatty acid uptake and oxidation both rose during exertion, however glucose rose to a greater extent than fatty acids[126] – i.e. the relative proportion of fatty acids as substrate declined.

Taking a modelling based approach to the interacting pathways in metabolism can provide some more answers[57]. At lower workloads, the NADH and mitochondrial acetyl-CoA from β-oxidation inhibit PDH while citrate is exported from the mitochondrion and inhibits cytosolic PFK[127]. However, medium and higher workloads are limited by the requirement for a low NADH/NAD+ ratio for flux through glyceraldehyde phosphate dehydrogenase, with the transfer of reducing agents into the mitochondria the rate limiting step[128]: fatty acid oxidation is free from such limitations.

1.5 Energetic Changes in Heart Failure

1.5.1 ATP and Heart Failure in vivo

ATP and phosphocreatine concentrations are lower in the failing human heart[129-132], however the phosphocreatine falls to a greater extent, giving rise to a reduced ratio between Phosphocreatine and ATP (the PCr/ATP ratio). This can be measured in vivo via ^{31}Phosphorus magnetic resonance spectroscopy, (^{31}P MRS) an important tool to assay the energy state within the myocardium noninvasively.

In long term heart failure, the total creatine pool is diminished in part due to downregulation of the creatine transporter [133]. It may be this is protective against a fall in the concentration of phosphocreatine, as this maintains the ratio of phosphocreatine to creatine and prevents this translating to a decrease in the ATP/ADP ratio and a reduced ΔG_{ATP} via a shift in the equilibrium [134]. Therefore, the reduced PCr/ATP ratio seen in chronic heart failure may not directly link to a change in ΔG_{ATP}. Hence the rationale behind assessing other components of the creatine kinase system: estimating creatine kinase pseudo first order rate constant with saturation transfer experiments, combined with an estimation of phosphocreatine concentration via the PCr/ATP ratio provides a non-invasive assay of the flux of ATP through the creatine kinase system[135]. Absolute quantification of the different components of the creatine kinase system is possible but challenging; by using proton spectroscopy the total creatine pool size can be estimated and from this the concentrations of ADP and hence ΔG_{ATP}, although to date this has only been performed in animals[136]. Compare these metabolite changes over the long term to stress experiments where the PCr/ATP ratio is measured before and during an increase in cardiac workload in

the same individual: here the creatine pool size is constant and hence PCr/ATP will track ΔG_{ATP} more directly.

PCr/ATP is reduced even in subclinical cardiac dysfunction [137-140], predicts mortality in dilated cardiomyopathy[141] and, interestingly, in heart failure with preserved ejection fraction it is correlated with the degree of diastolic impairment[142], drawing a parallel with the linear relationship seen between left ventricular end diastolic pressure and ADP concentration in perfused rat hearts[143].

Phosphotransfer, too, is impaired in heart failure, with activity of creatine kinase and other enzymes having reduced activity in biopsy[100] or when measured non-invasively via ^{31}P magnetic resonance spectroscopy saturation transfer techniques (where it is a predictor of mortality)[144]. In mice with heart failure, declining creatine kinase activity paralleled the fall in ejection fraction as the condition progressed[145]. This may be a more sensitive marker than PCr/ATP ratio, as it represents the actual transfer of high-energy phosphate through the system [146].

1.5.2 Substrate Metabolism in the Failing Heart

Many studies on myocardial metabolism often conflict with each other, owing to different models of heart failure, different stages of the disease or whether substrate uptake or oxidation are measured. Studies of the resting heart in advanced heart failure (dilated cardiomyopathy in humans or experimentally induced heart failure in animal models) show that both fatty acid and glucose uptake and utilisation are reduced. [138, 147-150] However, fat uptake is reduced to a greater extent than glucose so a relative 'substrate switch' towards glucose is frequently described [151] and the heart loses its flexibility, becoming more reliant on

glycolysis as a source of energy[85]. Energy substrates are increasingly drawn into biosynthetic pathways as heart failure progresses[63].

Pressure overload hypertrophy[152, 153] and ischaemia[154] consistently cause a switch in substrate preference towards glucose. As there is an energetic advantage of oxidising glucose when compared to fatty acids[155, 156], this switch is argued to be an adaptive change by the failing heart to limit the progressive decline in ATP production enforced by the reduction in total substrate uptake and metabolism.

Heart failure is also accompanied by many other changes which alter the efficiency of the excitation-contraction coupling (e.g. changes in channel expression, Calcium handling, β-adrenoreceptor signalling and alterations in contractile and cytoskeletal proteins[157]).

1.5.2.1 Fat Metabolism in Heart Failure

Most studies show fatty acid uptake and oxidation are reduced across a variety of heart failure models as well as in human studies[147, 150, 158]. In biopsies taken from explanted hearts prior to heart transplant, mRNA encoding enzymes involved in beta oxidation (e.g. acyl-CoA dehydrogenase) were downregulated[159]; while reduced expression of fatty acid transporters is seen in animal models of heart failure and correlates with the reduction in ejection fraction[160]. Reduced PPAR expression and activity is the chief culprit[161], with PPARα-alpha downregulated[162] alongside PGC1-α[163].

Reduced lipid oxidation is also associated with cardiomyopathy in animal models, e.g. cardiac specific knockouts of PPARγ[164] or lipoprotein lipase[165].

Much less is known about the changes to anabolic or regulatory pathways of cardiac lipid metabolism in heart failure. TAG turnover is reduced, which may have further effects on lipid metabolism given its role as a PPAR activator[63], however the mechanisms behind this are undefined[124].

1.5.2.2 Glucose Metabolism in Heart Failure

A decrease in glucose oxidation accompanies severe systolic heart failure, with myocardial glucose oxidation declining to a greater extent than glucose uptake and glycolysis in heart failure[85]. Biopsies from LVAD recipients demonstrate an accumulation of pyruvate and lactate without an increase in tricarboxylic acid cycle intermediates indicating glycolysis outstripping glucose oxidation [166] and animal studies show PDH flux unchanged despite this increased glycolysis[153]. Glucose is diverted into anaplerotic reactions to maintain the TCA cycle[167], bypassing energy-producing reactions[153], possibly to facilitate hypertrophic growth in response to pressure or volume load (e.g. aspartate production[167]) but also consuming NADPH required for TAG synthesis[168]. In a porcine pacing model of heart failure, PDH flux monitored by ^{13}-Carbon magnetic resonance spectroscopy was maintained until late in the disease process, where it accompanied a transition into left ventricular dilation[138].

There are multiple causes for the changes in glucose metabolism. Transcriptional analyses have shown a reduction in mRNA for GLUT transporters and PDK[169]. Activation of PDK4 by reduced PPAR expression will inactivate PDH but not glycolysis[170], perhaps accounting for the disconnect between glycolysis and oxidation seen.

Insulin resistance is well known to occur in human heart failure[171]: insulin increases GLUT4 translocation to allow glucose entry and increases glycolysis, so its absence impairs glucose

metabolism. In a mouse model of pressure overload, GLUT4 expression and insulin sensitivity both decreased as the heart started to transition from diastolic dysfunction to overt systolic failure[149]. Additionally, hyperacetylation occurs in mitochondrial proteins of the failing heart[172], which has been shown to reduce PDH activity[173]. Long-term beta adrenoreceptor stimulation has been shown to induce insulin resistance[174] and it is possible beta blockers have a beneficial effect on metabolism by reversing this change.

Alterations in regulation of the hexosamine biosynthetic pathway result in increased substrate flux[175], causing O-GlcNAcylation of proteins such as those involved in calcium handling and resulting in further interference with calcium flux in the failing heart[176].

1.5.2.3 Ketone Bodies

A shift towards using ketone has been observed in animal experimental models of heart failure[177] and from metabolite data in biopsies taken from human heart transplant or ventricular assist device recipients[178], while arteriovenous metabolite studies have shown increased reliance on ketone[54]. However, invasive catheter studies have failed to find a difference between arterial and venous cardiac ketone content in heart failure patients[179], possibly because circulating ketone levels (and therefore availability to the heart) remain low.

Ketones' acetyl CoA production competes with that of fatty acids and glucose for Krebs cycle intermediates, so predominant ketone metabolism will reduce that of the other substrates[180]. When ketones are the only metabolic substrate, contractile function gradually declines as substrates for anaplerosis are not provided[181]. On the other hand, SCOT knock-out mice (unable to metabolise myocardial ketone) developed increased anaplerosis, mitochondrial ultrastructure abnormalities and were less protected against remodelling[182],

while overexpression of BDH1 (the first enzyme in the ketone body oxidation pathway) attenuated remodelling in pressure overload[183].

1.5.2.4 Amino Acids

Branched chain amino acids accumulate in failing myocardium, without fulfilling their anaplerotic roles in replacing TCA intermediates[184]. Further, they may suppress glucose oxidation by inhibiting PDH[185].

1.5.3 Mitochondrial Dysfunction in Heart Failure

Mitochondria have roles far beyond that of a simple 'power plant' and are involved in redox balance, biosynthesis, ROS signalling, inflammation, cell growth and ion homeostasis[186]. Impaired mitochondrial biogenesis and mitochondrial dysfunction are prominent features of heart failure[148] and hence all these roles are dysregulated, not simply ATP generation.

Mitochondria are a major site of reactive oxygen species (ROS), which are produced under normal physiological conditions but are protected from damage by mitochondrial anti-oxidant systems such as super-oxide dismutase (SOD), glutathione peroxidase and peroxiredoxins 3 and 5[187]. ROS release is increased in heart failure[188] and inactivation of antioxidants is associated with a reduction in cardiac function[189]. Also, dysregulated calcium signalling (key for stimulating mitochondrial activity) in heart failure is linked to cellular dysfunction via ROS generation/scavenging[190]. Calcium overload can trigger mitochondria-induced cell death via activating the mitochondrial permeability pore[191].

1.5.4 Substrate Selection at Stress in the Failing Heart

Relatively little is known about substrate selection under acute stressors in the failing heart, with few studies. The mechanisms behind changes seen are multifactorial and overlapping with those which impair metabolism in the resting heart, for instance insulin resistance[192]. Calcium uptake by mitochondria is reduced, with the 'master signal' no longer being transduced into the mitochondria and the link between contraction and energy production being broken[193]. Failure of ADP or AMP uptake by the mitochondria and impaired phosphotransfer may prevent proper transduction of energetic demand: failing to feed back a fall in ATP and rises in ADP or Pi which remain compartmentalised around sites of use [194].

Invasive catheter studies employing arteriovenous sampling have shown significantly blunted increases in glucose and fatty acid uptake during rapid pacing stress, remaining similar to the resting state or only slightly increasing[147, 195]. Fat oxidation was shown to increase more markedly in patients with cardiomyopathy and impaired glucose tolerance (who had the very little increase in glucose uptake) compared to those with cardiomyopathy and normal glucose tolerance, the increased fat uptake apparently partially compensating for blunted glucose uptake[195].

1.6 Altering Substrate Metabolism as a Potential Treatment for Heart Failure

Despite decades of research highlighting ineffective energy metabolism in heart failure, effective therapies for improving the energy supply of the heart are lacking. Much of the

evidence and the paradigms draw upon ischaemia, where oxygen is limited and the metabolic adaptations are not necessarily the same as those seen in heart failure[23, 196].

1.6.1 Increasing glucose/pyruvate metabolism

The failing heart is acknowledged to be insulin resistant and shows downregulated glucose oxidation, hence increasing glucose oxidation seems an attractive strategy[197]. Stimulating pyruvate oxidation by PDH would seem to have a dual benefit, not only increasing the usage of a more oxygen-efficient fuel, but also reducing the anaplerotic flux of glucose metabolism.

Intra-coronary pyruvate infusion increased cardiac index[24] and improved diastolic function[25] in non-ischaemic cardiomyopathy but its rapid breakdown in peripheral blood causing osmolar changes limits its utility. Glucose-insulin infusion is a slightly more practical approach to increasing glucose uptake, and alternate day infusions improved LVEF and reduced BNP in patients with heart failure with reduced ejection fraction, with improvement sustained after a month[26] and were shown to acutely lower Nt-pro-BNP[198]. This more medium term improvement may be explained by an increase in myocardial glycogen stores, as patients given a preoperative glucose-insulin-potasssium infusion were found to have higher myocardial glycogen content at surgery and fewer postoperative arrhythmias[79]. Dichloroacetate increases PDH flux, and has been shown to improve cardiac function in the pressure overloaded and post-ischaemic rat heart[199, 200], improves contractile reserve associated with increased PDH activity in porcine heart failure[201]; while in small-scale human studies has shown modest benefit in coronary artery disease[202], but in HFrEF both improvement[27] and no change have been observed[203].

1.6.1.1 Oxygen Efficiency

Glucose is a more oxygen-efficient substrate, with a P:O ratio of 2.58 compared to 2.33 for palmitate[85] Oxygen efficiency carries the advantage of allowing higher levels of ATP generation, hence where there is ischaemia, there would be clear benefit from favouring glucose oxidation.

1.6.1.2 Energy of Synthesis

Glucose metabolism also generates a higher energy of synthesis of ATP (as discussed in section 1.4.3 page 23). In heart failure, where ΔG_{ATP} is lower[96], there may be benefit from oxidising this energetically favourable fuel.

1.6.1.3 Glucose Metabolism and the close link with Diastolic Function

Activity of glycolytic and glycogenolytic enzymes are associated with the sarcoplasmic reticulum[204], suggesting[78] that glycolytically derived ATP is preferentially used for calcium re-uptake into the sarcoplasmic reticulum, as inhibition of glycolysis results in impaired relaxation[205]. This makes modulation of glycolysis an attractive target for improving diastolic dysfunction and indeed the GLP-1 agonist liraglutide normalised pyruvate dehydrogenase flux and reversed impaired PCr/ATP and diastolic dysfunction in a diet induced obesity model in rodents [206].

1.6.1.4 Inhibition of fatty acid metabolism to increase glucose metabolism

There has been much interest in using the Randle cycle to promote glucose metabolism by supressing fatty acid metabolism[196]. By inhibiting fatty acid metabolism, glucose oxidation is increased[207] and fatty acid-induced oxygen wastage is reduced[23]. Inhibitors of fatty acid oxidation such as trimetazidine[208] or ranolazine[209] or inhibitors of fatty acid transport such as perhexiline[210] or etoxomir[211] have been shown in small studies to produce modest improvements in systolic function [212] and myocardial energetics[213] in chronic ischaemic HFrEF.

1.6.2 Increasing fatty acid metabolism

Increasing fatty acid metabolism has received far less attention as a pathway for heart failure therapy. In non-ischaemic cardiomyopathies, where oxygen supply is not limiting to the same degree as ischaemic cardiomyopathies, the putative oxygen sparing effect of enhanced glucose metabolism may not be as beneficial. The advantage of fatty acid oxidation is that it yields 3.5 times more ATP per mole than oxidising glucose[155, 156].

It has also been suggested that the Randle cycle may not function normally in heart failure[63, 161] as fat oxidation is downregulated in heart failure already, therefore therapies which inhibit fat metabolism are likely to have less effect on glucose oxidation.

In animal models, cardiac-specific deletion of acetyl CoA carboxylase 2 promoted fatty acid metabolism, preventing systolic dysfunction in aortic constriction[214] and preventing diastolic dysfunction during angiotensin infusion[215], while fat diets have been shown to attenuate ventricular remodelling[216]. Blocking fat uptake via the knock out of CD36 worsened the

outcome of aortic constriction[217]. The chain length of lipid is likely to be important: where pressure overload failure was induced, perfusing the heart with oleate (C18) preserved the triglyceride pool turnover, compared to palmitate (C16), which reduced turnover and showed a ~25% lower contractility than oleate[218]. However, in a study in patients with chronically stunned or hibernating ischaemic myocardium, there were no changes during insulin-glucose or fatty acid infusions[219].

1.6.2.1 Oxygen Inefficiency

Fat is a less oxygen-efficient substrate, with a P:O ratio of 2.33 compared to 2.58 for glucose[85]. Based on this a switch to exclusively using glucose would be calculated to save 11-13% of the myocardial oxygen use[23], however perfusing hearts with progressively higher concentrations of fat increases oxygen uptake disproportionately. In the isolated perfused rat heart, doubling free fatty acids in the perfusate from a physiological level (0.4-0.6mmol/L) to 0.8-1.2mmol/L increased oxygen uptake by 33%[220] and in anaesthetised pigs, there was a 48% difference in MVO_2 between glucose-insulin-potassium infusion and Intralipid-heparin infusion, where the ratio of free fatty acid : glucose derived ATP was 0.26:1 with Glucose-Insulin-Potassium (GIK) and 23.5:1 with Intralipid-heparin[18].

1.6.2.2 Uncoupling Proteins

One proposed explanation for this oxygen inefficiency is an uncoupling effect of high circulating free fatty acid levels. Uncoupling refers to a loss of the linkage between mitochondrial respiration and the generation of ATP: protons "leak" across the inner mitochondrial membrane, dissipating the proton gradient required for F_1F_0 ATPase to

generate ATP[221]. The uncoupling proteins (UCPs) are present in the inner mitochondrial membrane and allow the proton gradient to dissipate[221], although it is becoming increasingly apparent that they have additional functions[222], UCP2 having been shown to transport 4-carbon metabolites out of mitochondria[223]. Fatty acids are known to activate UCPs[224] and increased UCP expression in the heart is associated with diabetes, fasting and increased fatty acid mobilisation from adipose tissue[225].

However, UCPs have been proposed to have protective actions, including reducing the production of reactive oxygen species[226]. UCP3 knock-out mice compared to wild type developed larger infarcts following left coronary artery occlusion and did not benefit from ischaemic preconditioning[227]. It is therefore reasonable to question the previous assertions (e.g. in Essop & Opie[23]) that free fatty acid induced expression of UCPs has deleterious effects on the myocardium.

1.6.2.3 Lipotoxicity

A potential drawback of increased myocardial fatty acid uptake is lipotoxicity, where lipid metabolism is uncoupled from uptake and lipid is diverted into toxic metabolites, which accumulate within the myocyte. This is seen in obesity and diabetes, where it is associated with impaired contractile function[228] and has been found in human heart failure, where it is reduced following LVAD therapy[229]. In animal models such as long-chain acyl-CoA synthetase 1 over-expression where palmitate uptake is doubled, myocardial ceramide and diacylglycerol content was increased and there was increased mitochondrial reactive oxygen species generation and mitochondrial dysfunction[230].

When adipose triglyceride lipase/desnutrin (ATGL, responsible for hydrolysing lipid droplets of triglyceride) is knocked out in mice, there is lipid accumulation accompanied by severe cardiomyopathy[231]. Accumulation of medium chain acyl carnitines[232] and saturated long chain fatty acids are also associated with toxicity[233].

It has been suggested that accumulation of ceramide may cause cardiotoxicity through mitochondrial dysfunction and oxidative stress, although the pathway has not been fully elucidated[63, 234, 235], and it is unclear if the accumulation of ceramide is secondary to dysfunctional fatty acid metabolism in heart failure rather than a causative factor itself[63], although activation of ceramidase has been shown to have beneficial effects[236]. Where PPARγ overexpression is crossed with PPARα deficiency, both fatty acid oxidation and myocardial lipid droplet size increased, as did myocardial DAG and ceramide; however myocardial function was preserved[237]. It seems likely that lipotoxicity may result as an interaction from the specific types of cardiac lipid present, their compartmentalisation within the myocyte and the specific cause of heart failure present[58].

1.6.2.4 PPAR agonists: Fibrates and Glitazones

Fibrate drugs activate PPAR-alpha, which would seem a logical target, however studies in heart failure have yet to take place. A meta-analysis of cardiac outcomes in fibrate trials showed an overall beneficial effect, however this was neutral for new-onset heart failure[238]. In the ATGL knock-out mouse (which accumulates myocardial lipid accompanied by cardiac dysfunction), treatment with a PPARα agonist corrected the cardiac dysfunction and restored normal life expectancy[239]. Nontheless, PPARα null mice were protected against diabetes induced cardiac hypertrophy, while over-expression worsened the phenotype[240].

Glitazones are activators of PPAR-gamma, however large scale clinical trials have reported fluid retention and increases in plasma volume with peripheral oedema in 2-5% patients, leading to their contra-indication in heart failure[241]. The mechanism is unclear but thought to relate to changes in endothelial cell permeability[242] and renal sodium handling, resulting in retention of salt and water[243]. This is disappointing, as they have beneficial myocardial effects in isolation, including reducing ischaemia-reperfusion injury[244], although while pioglitazone was shown to improve diastolic function in diabetics this was not associated with changes in myocardial metabolism[245].

Although a specific activator is not yet available for PPAR β / δ [246], it may have a role to play. Overexpression induced gene expression associated with fatty acid oxidation, although did not lead to fatty acid accumulation or cardiac dysfunction[68], possibly as it did not induce CD36 expression and so did not greatly increase fatty acid uptake. This was protective against pressure overload in a mouse model[247].

1.6.2.5 Intralipid

This compound is worthy of special mention. It is a lipid emulsion derived from soy bean oil consisting primarily of polyunsaturated long-chain fatty acids: linoleic acid (C18), oleic acid (C18), palmitic acid (C16) and α-linolenic acid (C18) and was developed for use as a base for total parenteral nutrition (TPN).

There have been multiple studies where Intralipid has been used as a 'rescue' for drug related cardiac depression and it is an accepted therapy in UK Adult Life Support guidelines for lignocaine overdose. This follows a chance observation in 1998 showing that intravenous lipid increased the dose of bupivacaine required to produce asystole in rats, with the authors hypothesizing that the lipid may act as a 'sink' and sequester the lipid soluble

drug (a theory that continues to gain popular traction)[248]. Roughly a decade later, the first case reports of successful resuscitation in patients with local anaesthetic induced asystole following Intralipid[249]. Further animal experimental models followed, however the evidence for the clinical use of lipid 'rescue' from poisoning remains weak, with evidence solely based on animal studies and individual case reports[250]. This has not stopped further animal models and human case reports of Intralipid being used for resuscitation from poisoning of many other lipophilic drugs such as verapamil, diltiazem, amlodipine, quetiapine and sertraline, haloperidol, lamotrigine, olanzapine, propranolol, atenolol, nevibolol, doxepin, dosulepin, imipramine, amitriptyline, glyosphate herbicide, flecainide, venlafaxine and moxidectin[251]. Multiple mechanisms are hypothesized, all with varied evidence. It is unclear whether lipid concentrations within the blood reach sufficient quantities to properly sink local anaesthetic[252]. Relevant to this thesis, the metabolic properties do appear important to the effect on toxicity, with inhibition of fatty acid oxidation preventing any beneficial effect on bupivacaine induced toxicity[253].

Elevating fatty acids with infusions such as Intralipid has been shown to cause changes in blood pressure[254], altering vascular resistance (overall increasing total systemic vascular resistance[254] but also causing vasodilation in peripheral vessels[255, 256]) and exert a positive inotropic effect[257]. Sympathetic nervous system activation[258] and increased intracellular calcium release[259] via GPR40[260] have been implicated, while Intralipid has been shown to modulate sensitivity to nitric oxide and cause its overproduction[261, 262]. A beneficial metabolic effect from increased fat metabolism has been proposed, but never proven[263].

There is evidence to suggest that lipid infusion is beneficial following myocardial infarction. In a rat model of myocardial infarction (coronary artery ligation), Intralipid 20% infusion administered 5 minutes prior to reperfusion reduced infarct size by ~70% as well as

improving contractility[264], something also seen in perfused hearts[265]. Inhibition of the prosurvival PI3K-AKT pathway abolished the protective effects and inhibition of ERK had a partial effect (although neither inhibitor altered myocardial contractility) while Intralipid was shown to significantly increase the threshold for mitochondrial permeability transition pore opening, leading the authors to conclude that Intralipid activated the reperfusion-injury-salvage-kinase (RISK) pathway. The effect does not seem confined to cardiac tissues, with Intralipid improving oxygenation following rat lung transplantation[266]. Human data is very limited: there was no difference in troponin release following cardiac surgery following preconditioning with Intralipid[267].

1.6.3 Increasing Ketone Body Metabolism

Ketones not only provide a freely diffusible source of Acetyl-CoA, (as MCT-1 activity is not limited by insulin resistance), but also an energetic advantage in mitochondrial redox. This potentially provides an alternative source of ATP production which is more energetically favourable that fatty acid metabolism, is not down regulated in heart failure, and as such is a potential therapeutic target. Ketone infusion has been shown to improve cardiac output and ejection fraction while improving MVO2 in patients with HFrEF[268] and may prove a promising approach for treatment.

1.6.4 Therapeutic Approaches Targeting Metabolism in Heart Failure

1.6.4.1 Pyruvate Dehydrogenase Kinase Inhibitors

Examples: Dichloroacetate

1.6.4.1.1 Mechanism / Preclinical studies

Dichloroacetate causes rapid inhibition of PDK activity [269], increasing PDH flux. It improves diastolic function in a rodent model of diabetes [270].

1.6.4.1.2 Clinical trials

Dichloroacetate improves cardiac oxygen efficiency and left ventricular function in humans with heart failure[27]. The potential for clinical translation of dichloroacetate is limited by a narrow therapeutic window and toxicity.

1.6.4.2 Carnitine Palmitoyl Transferase (CPT1) inhibitors

Examples: Etomoxir, Perhexiline

1.6.4.2.1 Mechanism / Preclinical studies

Inhibition of fatty acid metabolism which promotes glucose metabolism via the Randle cycle[271].

1.6.4.2.2 Clinical trials

A 10-patient study (9 of whom had non-ischaemic cardiomyopathy) taking etoxomir over three months showed improvements in stress cardiac output and wedge pressures, although few differences in resting parameters[272].

Perhexiline improved VO2max, quality of life, PCr/ATP ratio and ejection fraction compared to placebo in HFrEF, however the study is of poor quality with unequally matched placebo and intervention groups[210] while Perhexiline brought about small

improvements in VO2max, NYHA status and PCr/ATP ratio in hypertrophic cardiomyopathy[273].

These drugs have a narrow therapeutic window and the etoxomir study was stopped owing to liver toxicity[274].

1.6.4.3 3-ketoacyl CoA Thiolase (3-KAT) Inhibitors

Examples: Trimetazidine, Ranolazine

1.6.4.3.1 Mechanism/Preclinical Studies

3-KAT is an enzyme vital for beta-oxidation, converting acetyl-CoA to acetoacetyl-CoA, inhibition of 3-KAT results in a switch of substrate preference from fatty acid to glucose oxidation[208]. Interestingly, however, when tested on rat heart homogenates, only ranolazine inhibited beta-oxidation, with trimetazidine having no effect[275].

1.6.4.3.2 Clinical trials

Trimetazadine has been shown in several small studies to improve both left ventricular systolic and diastolic function in ischaemic cardiomyopathy[276-278], exercise capacity in ischaemic heart disease[279] and prognosis[280] in patients with predominantly ischaemic cardiomyopathy. The evidence is weaker outside of ischaemia, with the main study in non-ischaemic cardiomyopathy showing no changes in ejection fraction, exercise capacity or quality of life[281], although meta-analysis of all heart failure trials with trimetazidine showed improvements in LVEF in non-ischaemic patients[282].

Ranolazine improved ejection fraction in a mixed heart failure group[283] and functional class and 6-minute walk as well as diastolic parameters in a small study of HFpEF patients[284].

1.6.4.4 Glucagon-Like Peptide-1 (GLP-1) analogues

Examples: Liraglutide, Exenatide

1.6.4.4.1 Mechanism/Preclinical Studies

Increase pyruvate dehydrogenase flux and reversed impaired PCr/ATP diastolic dysfunction in a diet induced obesity model in rodents [206].

1.6.4.4.2 Clinical trials

Small series of 12 inpatients with NYHA III/IV heart failure undergoing 5-week infusion of GLP-1 showed improvements in both EF and performance during exercise (VO2max and 6-minute walk distance) [285], however, other studies have been neutral[286, 287] and longer term administration of the GLP-1 agonist liraglutide has been shown to not improve mortality or hospital readmission rate in patients admitted to hospital with decompensated heart failure[288].

1.6.4.5 Sodium-Glucose Linked Transporter 2 (SGLT2) inhibitors

Examples: Dapagiflozin, Empaglifozin

1.6.4.5.1 Mechanism/Preclinical Studies

The mechanism has not been fully elucidated, as SGLT-2 is not expressed in the heart and there are suggestions that these drugs inhibit the sodium-hydrogen exchanger-1 (NHE-1)[289]. It has been hypothesized the beneficial cardiac effects are brought about by the drug elevating blood ketone, putatively via urinary glucose loss causing a shift in substrate metabolism towards fat and ketone[290, 291]. A single dose improved cardiac energy status in

diabetic mice [292] and increased glucose and ketone metabolism in rats with heart failure post MI[293].

1.6.4.5.2 Clinical trials

In a landmark trial, Dapagiflozin was shown to reduce the risk of heart failure progression and death from cardiovascular causes[294].

1.6.4.6 Co-enzyme Q10

Examples: Q-symbio, MitoQ10

1.6.4.6.1 Mechanism/Preclinical Studies

Co-enzyme Q10 is a lipid-soluble electron carrier important in the electron transport chain with antioxidant effects. Decreased levels have been seen in myocardium and plasma in heart failure[295].

1.6.4.6.2 Clinical trials

In the Q-symbio study, co-enzyme Q10 supplements reduced a composite MACE rate in patients with moderate to severe heart failure and improved symptoms[296].

1.6.4.7 Elamipretide

1.6.4.7.1 Mechanism/Preclinical Studies

Elampretide binds to cardiolipin, a phospholipid on the inner mitochondrial membrane important for cristae formation. It inhibits cytochrome C peroxidase activity and reduces

ROS[297]. Treatment in dogs with ischaemic cardiomyopathy improved ATP synthesis and ejection fraction as well as decreasing nt-pro-BNP[298].

No clinical trials have been undertaken as yet.

1.7 Current Gaps in Evidence

1.7.1 Conflicting data

As illustrated above, there are many conflicting studies in substrate metabolism in heart failure. The literature relies upon animal studies, extrapolation from other conditions (hypertensive heart disease, diabetes or obesity related cardiac dysfunction) and a mix of ischaemic and non-ischaemic cardiomyopathies in humans. Small animal models tend to have myocardial metabolism which is more dependent upon carbohydrate than in humans, diabetes and obesity have different metabolic profiles of insulin resistance and fat accumulation not necessarily applicable to systolic heart failure and ischaemia presents its own challenges in terms of limitations of oxygen supply. In addition, animal heart failure models are not treated with the range of proven therapeutics that human subjects are to look for an incremental benefit of further agents.

Where human studies have been undertaken, these are usually in patients who are fasted or under general anaesthetic (conditions where fatty acid uptake will predominate) and these may not represent the full spectrum of substrate metabolism as human beings feed and fast throughout the day, giving rise to dogmatic views about myocardial inflexibility.

Metabolism is a complex and interrelated network and hence the need to test theories on a whole body level in a homogenous patient population is necessary.

1.7.2 Focus on Glucose as a Therapeutic Target

Perhaps related to the above, as summarised in section 1.1 page 1, the idea that increased glucose metabolism (and the corollary, downregulated fatty acid metabolism) may be

beneficial has grown from a putative therapy for ischaemia to be a potential treatment for heart failure. This is dependent upon myocardial oxygen supply being limiting and the idea that increased myocardial lipid has toxic effects; reasonable conclusions in the 1990s but ones which now require re-examination: we now know lipid related uncoupling may have positive effects[226] and while lipid accumulation may lead to the production of toxic intermediates, activation of PPAR and increased lipid oxidation may have beneficial effects.

1.7.3 Lack of Data on Substrate Flexibility During Changing Metabolic Conditions

Due to the limitations of performing interventional procedures on humans who may require sedation or general anaesthetic, many studies in human subjects are performed following an overnight fast[54, 147], hence study myocardial substrate metabolism in a state where circulating free fatty acids are high and insulin is low. A fed state where insulin is elevated and glucose uptake would be promoted has not been studied in comparison to this fasted state.

1.7.4 Lack of Data on Substrate Metabolism at Stress in the Failing Heart

The majority of patients with heart failure are comfortable at rest but only experience symptoms on exertion[36], hence there is a rationale for preferentially targeting stress metabolism. Few studies have looked at this directly and none have examined substrate manipulation in this setting.

1.8 Aims of the Thesis

1.8.1 To compare and contrast the effects of changes to glucose and fat metabolism in the healthy and failing heart.

In chapter 3, I look at the effects of increased (with lipid infusion) compared to reduced (with nicotinic acid receptor agonism) fat metabolism in the healthy human heart to evaluate the abilities of the healthy heart to deal with switches between substrate, then investigating the underlying mechanisms of these changes in an animal model, shining a light on how fat and glucose compete and counter-regulate and how it is possible to effect contractility by starving the myocardium of substrate. ^{31}Phosphorus spectroscopy is used in healthy human volunteers to examine the changes in phosphocreatine pool while hyperpolarised pyruvate ^{13}Carbon spectroscopy is used to examine the changes to pyruvate metabolism in the animal study.

In chapter 4, I look at the relative differences in contractility and ATP metabolism in vivo in healthy and failing human hearts with increased glucose uptake (with euglycaemic clamp) and increased fat availability (with lipid infusion). Again, phosphorus-31 spectroscopy is used to examine phosphocreatine changes, with saturation transfer spectroscopy used to demonstrate changes in ATP flux through creatine kinase. Here, the conflicting effects of ATP demand and supply in different substrate conditions are examined.

I then use an invasive approach with paired arteriovenous sampling to examine substrate uptake and oxygen consumption in the failing human heart with increased glucose uptake and increased fat availability.

1.8.2 To examine the effects of changes to fat and glucose metabolism on stress performance in the healthy and failing heart

In chapter 5, I examine the changes in contractility and ATP metabolism *in vivo* in healthy and failing human hearts during dobutamine stress, comparing increased glucose uptake to increased fat availability. Again, phosphorus-31 spectroscopy is used. An invasive approach with rapid pacing stress is then used to examine substrate and oxygen uptake in the failing heart under increased glucose uptake or increased fat availability. The focus in particular is whether the maximal performance and energetic reserves of the failing heart can be altered.

1.8.3 To examine the effects of vasodilator stress on the healthy heart and the dependence upon phosphocreatine reserves to resist stressors

In chapter 6, the vasodilator glyceryl trinitrate is used to deprive the healthy human heart of preload and the energetic response to this type of stress and the body's reaction to it is examined. I use phosphorus-31 spectroscopy with saturation transfer to show the effects on ATP synthesis and transfer during this different form of stress. The focus here is on understanding the relationship between ATP metabolism and the heart's ability to incrementally increase work under stress, underlining the importance of myocardial energy metabolism and the maximal energy output of the heart. The aim of this chapter is to make a robust link between myocardial metabolism and response to stressors, consider the role of constant stress in heart failure progression and how metabolism is therefore a viable target for heart failure therapeutics.

2 Chapter 2: Methods

2.1 Substrate Manipulation

2.1.1 Free Fatty Acid Elevation with Intralipid

To elevate free fatty acids, 20% Intralipid™ (Fresenius Kabi, UK) was infused intravenously at 60 ml/h. In CMR experiments, unfractionated heparin (Monoparin, CP Pharmaceuticals, UK) is concomitantly infused at 0.4 U/kg/h, whereas in invasive experiments, heparin is administered intravenously as a bolus (100 U/kg) with further boluses to maintain ACT (activated coagulation time) around 250 secs whilst instrumentation of the arterial/left ventricular side is performed.

2.1.2 Glucose Uptake Elevation with Euglycaemic Clamp

A protocol was used modified from the technique of DeFronzo[299].

A 22G or larger cannula was sited in two large veins (ideally antecubital fossae) and three-way taps attached, with one used for sampling and one used for infusion of insulin and glucose. A point of care testing device (Freestyle Optimum Neo, Abbott Diabetes, UK) was used to measure blood sugar from venous samples. A baseline sample was taken prior to commencing the infusion.

Insulin (Actrapid™, Novo, Denmark) was infused at 20 mU/m^2/min following a loading regime (63.8 mU/m^2/min for 1 minute, 56.8 mU/m^2/min for 1 minute, 50.6 mU/m^2/min for 1 minute, 45.1 mU/m^2/min for 1 minute, 40.1 mU/m^2/min for 1 minute, 35.7 mU/m^2/min for 1 minute, 31.8 mU/m^2/min for 1 minute, 28.4 mU/m^2/min for 1 minute,

25.2 mU/m^2/min for 1 minute, 22.5 mU/m^2/min for 1 minute, then 20 mU/m^2/min). At minute 10, a single venous blood sugar measurement was taken and then thereafter every 5 minutes. An infusion of 20% glucose was started at minute 4, at a rate of 2 mg/kg/min then from minute 15 the rate was titrated based on the difference between the measured and baseline blood sugar readings.

2.1.3 Reduction of Circulating Free Fatty Acids with Nicotinic Acid Receptor Agonists

2.1.3.1 Acipimox

A single 250 mg dose of the nicotinic acid receptor agonist acipimox was administered (Olbetam®, Pfizer, UK) with 0.9% saline was infused at a rate of 60ml/h via a peripheral vein.

2.1.3.2 Nicotinic Acid

A single 400 mg dose of nicotinic acid (Niaspan®, Abbot, UK) was administered orally.

2.2 Stressor Agents

2.2.1 Dobutamine

Dobutamine (Hameln pharma, UK) was drawn up neat from pre-filled 250 mg in 50 ml ampoules and infused at a rate according to body weight. A baseline heart rate and blood pressure were recorded prior to commencing the infusion at a rate of 5 mcg/kg/min. The

infusion was then adjusted against heart rate at 2-minute intervals until a target of 65% predicted maximum heart rate for age was achieved. Blood pressure was recorded non-invasively every 4 minutes via an arm cuff.

2.2.2 Glyceryl Trinitrate (GTN)

Glyceryl trinitrate (Hameln pharma, UK) was drawn up neat from pre-filled 50 mg in 50 ml ampoules. A baseline heart rate and blood pressure were recorded and the infusion was commenced at a rate of 3 ml/h and titrated in 5 minute intervals against mean arterial blood pressure, with a target 15 mmHg fall in mean arterial pressure. Heart rate was monitored continuously throughout.

2.2.3 Monitoring

Participants were monitored non-invasively with a pulse oximeter and blood pressure cuff via a MR200 MRI safe monitoring system (MR Devices, UK).

2.3 Magnetic Resonance

2.3.1 ^{1}H Imaging for Cardiac Volumes and Function

Unless otherwise specified, scans were performed supine in a Siemens Tim Trio 3T system. A 24 channel spine matrix and 6 channel body matrix were used (excepting in the GTN experiments where the 6 channel body matrix was used without the spine matrix).

The following steady state free precession (SSFP) parameters were used by default: slice thickness 8 mm, gap 2 mm, retrospective gating, TE 1.5 ms, TR 46 ms, flip-angle 50°, field-of-view (FOV) 400 mm, matrix size 256 in frequency encode direction, although in some cases FOV was decreased to reduce duration or prospective gating was used in arrhythmia. Volumes were acquired in end-expiration breath-hold. Contouring at end-systole and end-diastole was performed using cvi42 version 5.10.1 (Circle Cardiovascular Imaging Inc, Calgary, Alberta, Canada), shown in figure 2.1.

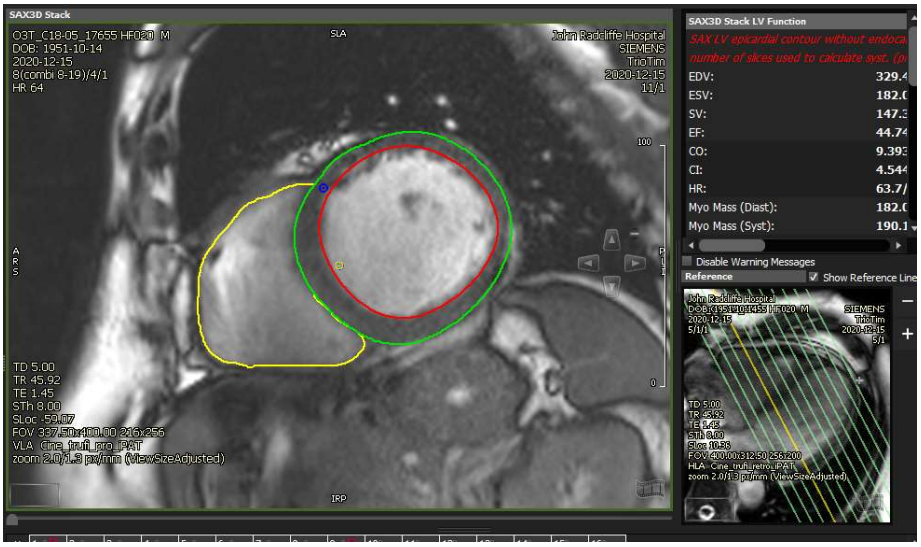

***Figure 2.1**: Left and right ventricular contours in Circle CVI 42.*

2.3.2 ^{31}P 3D Chemical Shift Imaging for Spectroscopy

All human scans were performed on a Siemens 3T Tim Trio system (Erlangen, Germany). A Siemens 1.5T Heart/Liver ^{31}P coil was modified to produce a working coil: it consisted of a large outer element (26 x 28 cm) which acts as ^{1}H transmit-receive and ^{31}P transmit, with a smaller loop/butterfly receive pair (12 x 15 cm loop and 23 x 12 cm butterfly) which receives ^{31}P signal.

Subjects would lie prone with their left ventricle positioned over the centre of the coil at the magnet iso-center. Proton localisers were used to position the subject correctly. Ten free induction decay inversion recovery (IR-FID) curves (1 ms hard inversion) with increasing inversion delay (100 – 3000 ms) are acquired, along with locations of phenylphosphonic acid (PPA) fiducial and codliver oil phantoms.

Pilot images were taken to position the CSI matrix. Piloting was performed in vertical long axis (VLA), horizontal long axis (HLA) and short axis planes, where a stack of 20 slices was obtained. Fast low-angle shot (FLASH) images were used: slice thickness 10 mm, TR 7 ms, TE 3.37 ms, FOV 400 x 340 mm.

A 3D acquisition-weighted chemical shift imaging (CSI) was used: acquisition matrix size 16 x 16 x 8, FOV 240 x 240 x 200 mm, 10 averages at the centre of k-space, 1690 total acquisitions, voxel size 5.6ml. The grid was oriented to place voxels in the interventricular septum, as per figure 2.2. Two saturation bands were placed over the skeletal muscle in the chest wall and one over the liver in order to minimise signal contamination.

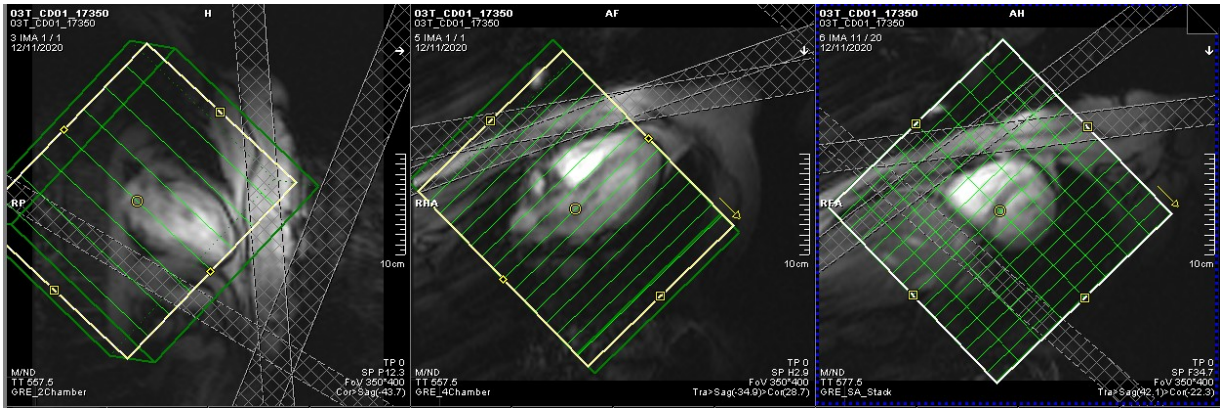

Figure 2.2*: Positioning of the CSI grid in 2-chamber (left), 4-chamber (centre) and short-axis (right) orientations. Note the green CSI grid is oriented with voxels positioned along the septum in long axis (centre panel) and are in the mid septum in short axis (right panel). Saturation bands (grey cross-hatched areas) are positioned over skeletal muscle and liver. Images taken from a healthy volunteer at 3.0 Tesla.*

The acquisition was non-gated with TR around 910-1010 ms depending upon SAR. The echo time was reduced to a minimum (TE = 0.3 ms) using the ultra-short echo time (UTE-CSI) technique to maximise acquired signal and reduce first order phase effects (therefore reducing artefact). The optimised RF pulse (duration 2.4 ms) was centred between γ and α peaks (usually by subtracting 250 Hz from the observed phosphocreatine frequency) to ensure uniform excitation[300], as per figure 2.3.

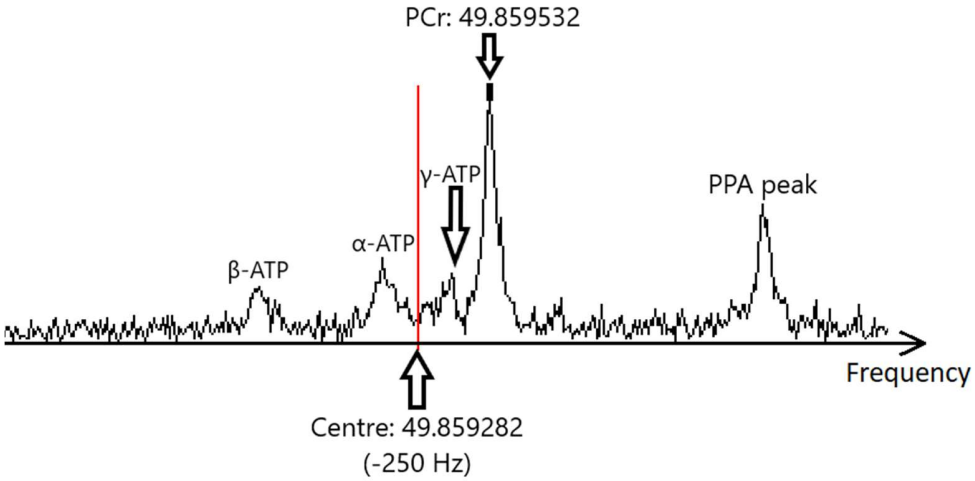

Figure 2.3*: Positioning of centre frequency (red line) relative to other spectral peaks. It sits between alpha and gamma ATP-peaks by subtracting 250Hz from the phosphocreatine (PCr) peak. Example unlocalised spectrum used for frequency setting from a healthy volunteer at 3.0 Tesla.*

Nuclear Overhauser enhancement (NOE) was used to increase SNR in acquired spectra: five pulses, length 2.5 ms, inter-pulse delay 80.5 ms, pulse voltage 222.5 V and average flip angle 150°.

2.3.2.1 Analysis

The basal septal voxel was selected for analysis: this was the only user-dependent part of the process, the rest being fully automated. In-house Matlab software determined the flip angle for the selected voxel by co-registering the short axis images with the spectral data. Flip angle variation due to coil loading effects was calculated by the use of acquired inversion recovery data and the localizer containing the locations of codliver oil capsules in fixed positions in the coil.

Pre-processing (baseline correction) was undertaken before fitting spectral peaks using the AMARES (advanced method of accurate, robust and efficient spectroscopic fitting) method. Peaks for phosphocreatine, α, β, γ - ATP, 2,3-diphosphoglycerate and phosphodiesters were fitted using prior knowledge of relative peak frequencies, J-coupling constants for ATP, relative peak amplitudes, relative phases and assumed Lorentzian lineshapes along with acquisition parameters (central frequency, bandwidth, TR and calculated flip angles at various depths). Peak areas were corrected for RF partial saturation effects using the recorded excitation flip angle, T_1 values (PCr 3.8s, γ-ATP 2.4s, α-ATP 2.5s, β-ATP 2.7s, 2,3-DPG 1.39s, PDE 1.11s) and spectral overlap with the NADH peak. The value of the ATP peak was corrected for blood contamination by subtracting 11% of the DPG peak area[300].

PCr/ATP ratio was calculated using the average of the three ATP peaks. The quality of spectral fit was assessed using the coefficient of variation in the coefficient of variation in the measured PCr/ATP ratio, based on Cramer-Rao lower bounds (an indicator of signal to noise ratio in the sample) and standard error propagation formulae. Samples with a greater than 20% coefficient of variation were excluded.

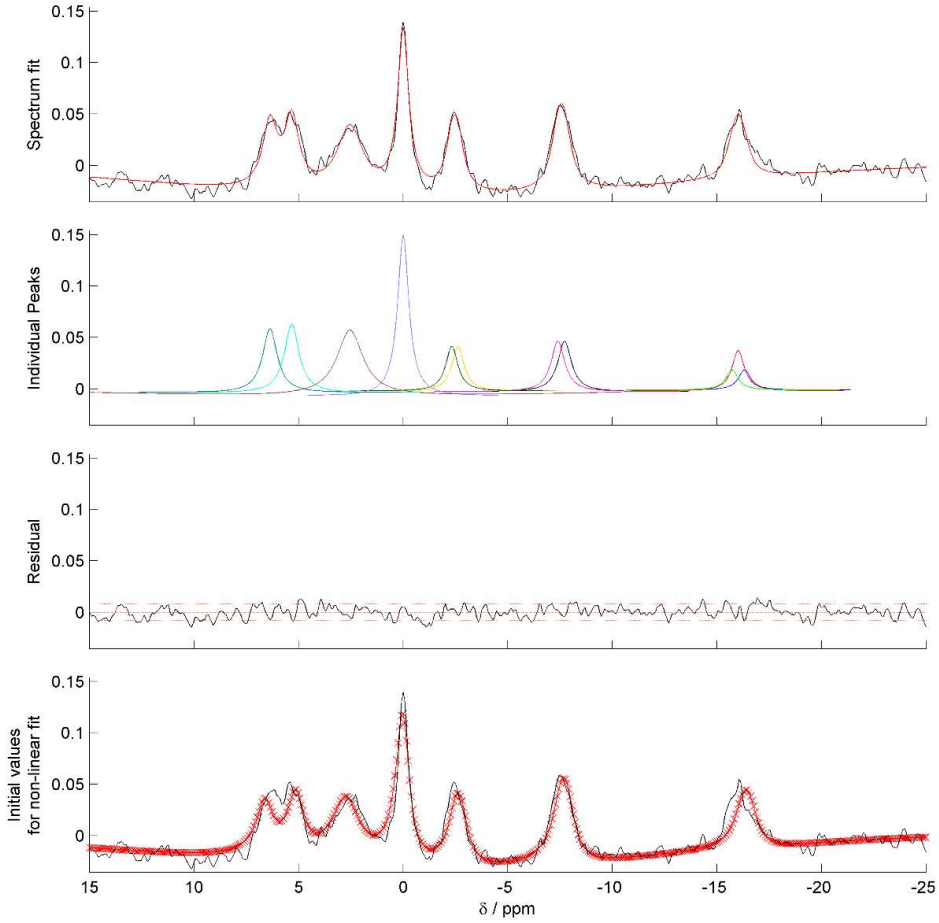

Figure 2.4: Example of a spectral fit from the in-house Matlab analysis package

2.3.3 Assessment of Creatine Kinase first order rate constant through Triple Repetition Saturation Transfer (TRIST)

2.3.3.1 Principles

The creatine kinase equilibrium reaction is thus:

$$MgADP^{-} + PCr^{2-} + H^{+} <_{k-1}^{k1}> MgATP^{2-} + Cr$$

Which can hence be simplified to a two site exchange:

$$PCr <_{kr}^{kf}> \gamma ATP$$

Where k_f and k_r are the unidirectional pseudo-first-order rate constants. The forward (ATP producing) direction is k_f and the reverse (PCr-producing direction) is k_r. Forward flux can be calculated as [PCr] x k_f and reverse flux as [PCr] x k_r.

Very simply, in a saturation transfer experiment, the γ-ATP peak is saturated and the fall in the height of the PCr peak is observed. The two metabolites are separated by 2.47 parts per million, or 123Hz at 3.0 Tesla. As the saturated phosphate from γ-ATP has been transferred to Creatine to form phosphocreatine, the degree of saturation of the PCr peak allows us to work out the rate of the reaction. This is something of an oversimplification as it does not take into account the compartmentalization of PCr and ATP within cells as discussed in the introduction, nonetheless it has proven to be a useful technique in the investigation of CK flux in heart disease.

k_f is calculated as follows:

$$kf = \frac{1}{T1'PCr} \cdot \left(\frac{M'PCr}{M0,PCr}\right)$$

Where $M'_{0,PCr}$ is the magnetization of PCr during $^{\gamma}$-ATP saturation, $M_{0,PCr}$ is the magnetization of PCr without $^{\gamma}$-ATP saturation and $T'_{1,PCr}$ is the apparent T_1 of PCr during $^{\gamma}$-ATP saturation.

Four saturation transfer techniques for measuring k_f in the human heart have been developed:

1. Four angle saturation transfer (FAST) at 1.5T[301]

2. Triple repetition saturation transfer (TRiST) at 3T[302, 303]

3. Two repetition time saturation transfer (TwiST) at 3T[304]

4. Bloch-Siegert four-angle saturation transfer at 7T[305]

In this work, the second implementation (TRiST) is used, adapted from the original protocol to suit the Pulsteq coils and Siemens 3T Tim Trio available in OCMR[306]. The acquisition has four acquisition steps (a short TR sequence with no gamma saturation, a short TR sequence with gamma saturation, a long TR sequence with gamma saturation and a short TR sequence with a 'control' saturation pulse falling down field of PCr), taking around 60 minutes in total. An extension (stress saturation transfer or StreST) allows an additional measurement of k_f to be made during a stressor, taking only 18 minutes.

2.3.3.2 Implementation in OCMR

The subject is positioned in the Siemens Tim Trio 3 tesla scanner supine with the ^{31}P loop coil positioned over the left ventricle at the isocentre of the scanner. Axial and sagittal proton localisers were used to confirm coil position over the LV, helped by a phantom positioned in the centre of the coil.

As the bandwidth of the Trist acquisitions themselves is narrow (200Hz), specifying the center frequency and saturation offset for γ-ATP is crucial to the technique's success. To scout for these frequencies, a 1D-CSI sequence is run prior to the main TRiST acquisition. 16 phase encode steps for depth, TR 330ms, TE 2.3ms, flip angle 35°, 125 averages.

The 1D-CSI matrix (200 x 200 x 160 mm) is oriented with voxels parallel to the chest wall, fully covering the heart and centred on the centre point of the receive coil. A 25mm saturation band is placed across skeletal muscle and the adjust volume (200 x 200 x 80 mm)

oriented over the centre of the heart as per figure 2.5. The most apical unambiguously cardiac voxel (i.e. not contaminated by skeletal muscle) is chosen as the voxel of interest.

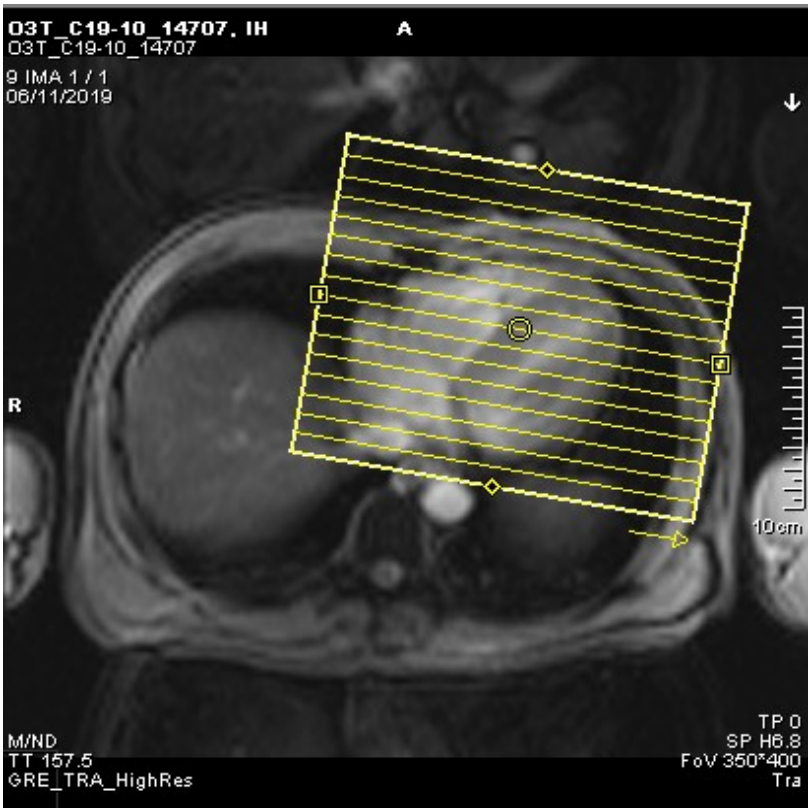

Figure 2.5*: Positioning of the 1-D CSI grid with voxels oriented parallel to the coil and chest wall.*

The centre frequency should be exactly halfway between the PCr and γ-ATP; where the γ-ATP peak is difficult to find, the centre is set by subtracting 70Hz from the PCr peak as per figure 2.6.

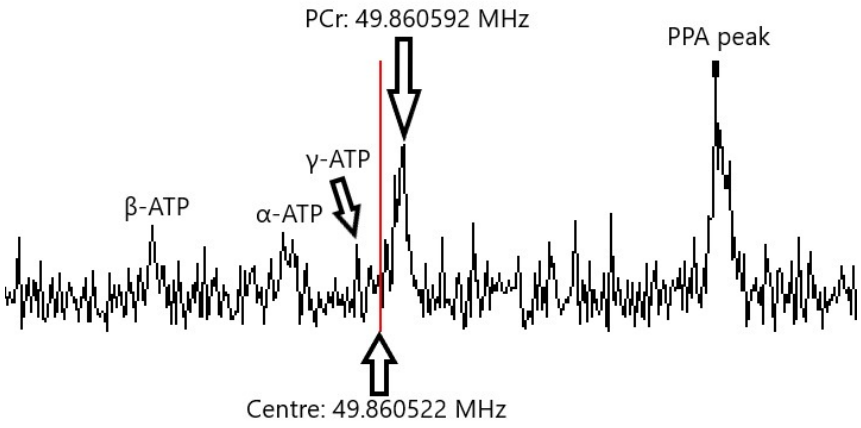

Figure 2.6*: positioning of the centre frequency between PCr and γ-ATP peaks (or by subtracting 70Hz from the PCr peak when γ-ATP is hard to find). Unlocalised spectrum acquired at 3.0T from a healthy volunteer; note the reduced SNR compared to that acquired for the CSI sequence.*

Once acquired, this is analysed in a dedicated tool based on a Matlab implementation to generate the centre and offset frequencies (shown in figure 2.7). The gamma saturation offset is the number of hertz to deduct from the centre frequency to saturate gamma while the control offset is calculated to saturate on the positive side of the PCr peak, the same distance away from it as the gamma saturation.

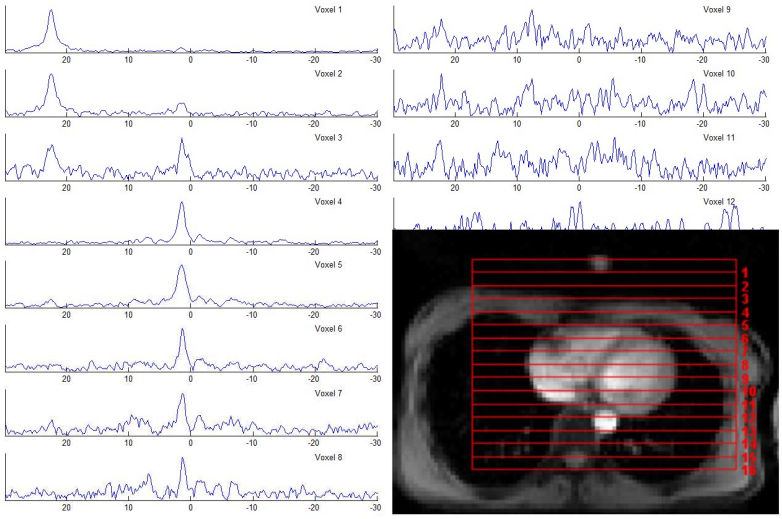

Figure 2.7*: Spectra from corresponding voxels in the matlab package. In Voxels 1 and 2, the spectra are dominated by the PPA fiducial peak at +20PPM. In Voxels 4 and 5, spectra from skeletal muscle are recorded. Voxel 6 contains a mixture of skeletal muscle and cardiac spectra. Voxels 7, 8 and 9 contain cardiac spectra. As voxel 7 is the most apical unambiguously cardiac voxel, it is chosen as the voxel of interest. Spectra taken from a healthy volunteer at 3.0 Tesla.*

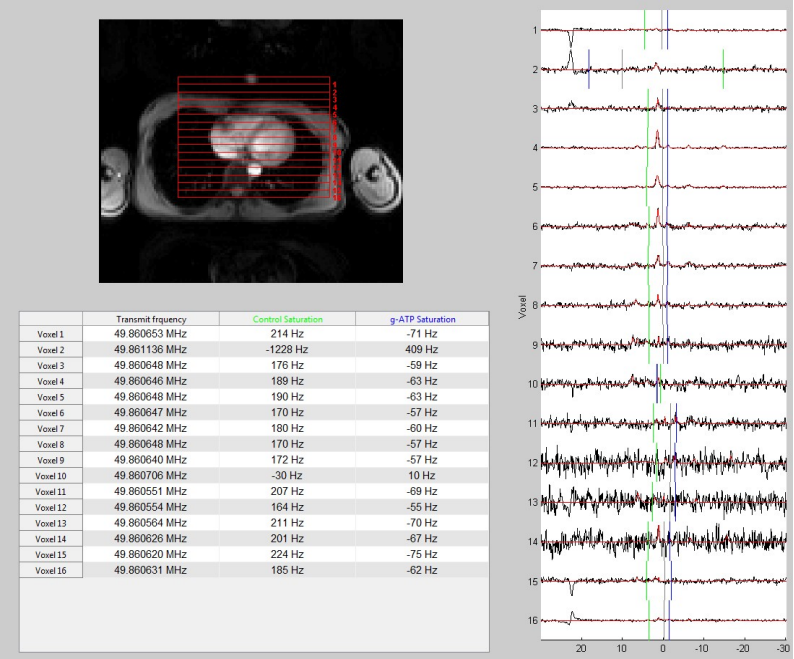

***Figure 2.8**: Spectra from the same volunteer, processed with the analysis tool. On each spectrum, a blue line shows the position of γ-ATP, a grey line the centre frequency (halfway between PCr and γ-ATP) and a green line the position for the control saturation. As the SNR falls beyond voxel 9, peaks cannot be reliably distinguished.*

The offline tool will give these values for all 16 voxels and typically those for the voxel with is both unambiguously cardiac and closest to the coil are chosen. Observationally, there are slight differences between skeletal muscle PCr resonance and that in the heart (of around 30 Hz), hence there are advantages to using a specific cardiac voxel rather than an unlocalised (whole body) spectrum.

The TRiST and StreST acquisition parameters are laid out in table 2.1.

Sequence	TR (s)	Selective saturation	Averages	Duration (min)	Measured parameters
1	15	None	2	9	$M_{0,PCr}$
2	1.5	$^{\gamma}$ATP	18	11	$M'_{1.5s,PCr}$
3	9.5	$^{\gamma}$ATP	8	21	$M'_{9.5s,PCr}$
4	15	Control	2	9	M^{Ctrl}_{PCr}
StreST 1	15	Control	2	9	M^{Ctrl}_{PCr}
StreST 2	15	$^{\gamma}$ATP	2	9	$M'_{15s,PCr}$

Table 2.1: TRiST and StreST acquisition parameters

TRiST uses frequency-cycled adiabatic half-passage (AHP) pulses to achieve 90° excitation irrespective of B_1 transmit strength (i.e., irrespective of distance from the coil), providing the adiabatic threshold is reached. In general, voltage of 210-220 V were used, depending on coil. Saturation is achieved with a modified Delays Alternating with Nutation for Tailored Excitation (DANTE) pulse train (duration 0.1 ms, inter-pulse delay 0.25 ms) with the maximum possible allowed voltage within SAR to achieve saturation (around 30-40 V). The small amount of off-target saturation ("spill-over" across adjacent frequencies) is accounted for by the control saturation sequence. Incomplete γ-ATP saturation would result in under-estimation of k_f, so the transmit voltage for the DANTE train was maximized within the confines of SAR (typically 30-40V). Example spectra are shown in figure 2.9.

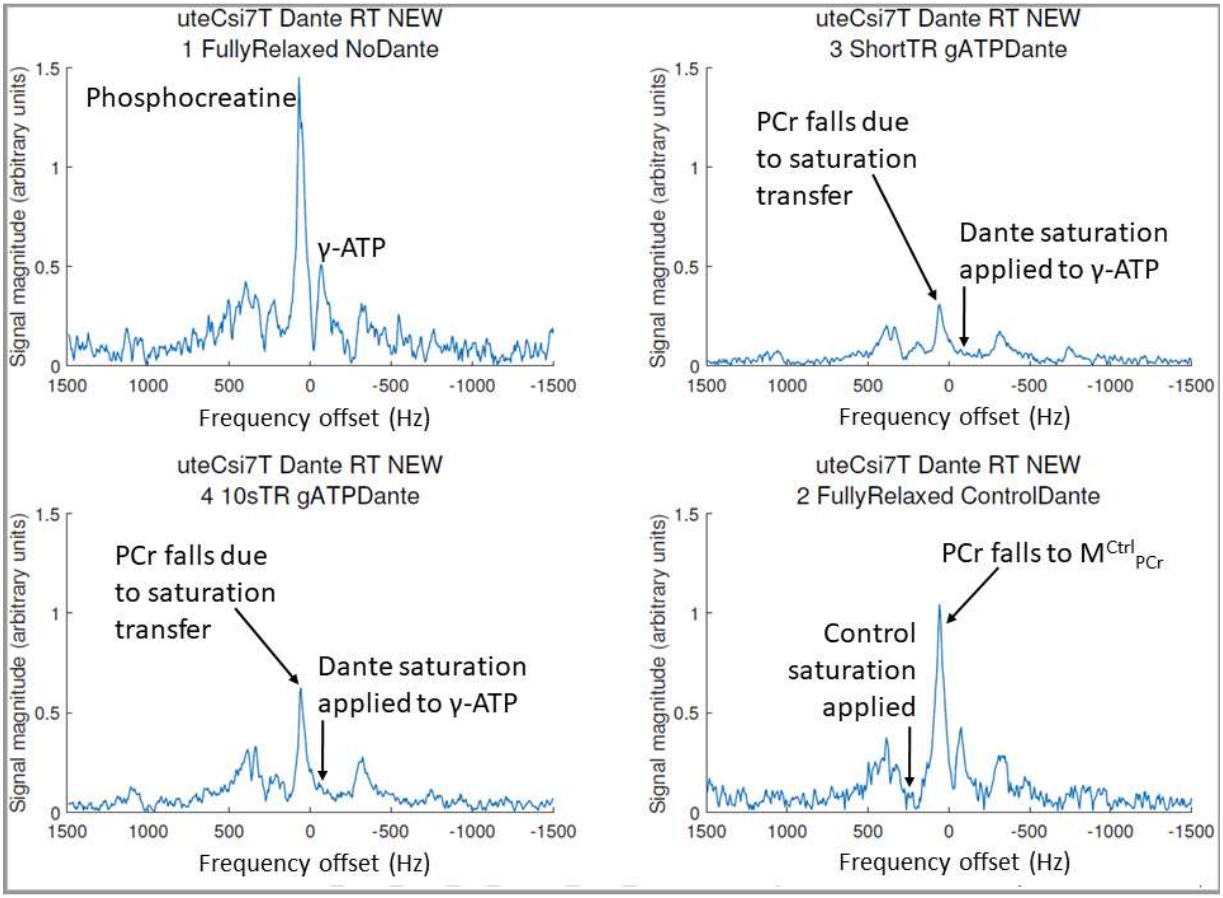

***Figure 2.9**: The four spectra generated as part of the TRiST experiment. Taken from a healthy volunteer at 3.0 Tesla. PCr, phosphocreatine.*

Steps 2 and 3 allow the calculation of $T'_{1,PCr}$ using a two-TR partial saturation method using a lookup table for the ratio $M'_{9.5s,PCr} : M'_{1.5s,PCr}$.

M^{Ctrl}_{PCr} is substituted for $M_{0,PCr}$.

$M'_{0,PCr}$ is calculated as:

$$M'0, PCr = \frac{M'1.5s, PCr}{1 - e^{-1.5s}/T'1}$$

And then k_f is calculated as:

$$kf = \frac{1}{T1'PCr} \cdot \left(\frac{M'0, PCr}{MCtrl\ 0, PCr}\right)$$

Within the StreST sequences, it is assumed that T1 remains constant and new values from the additional two sequences are substituted in.

2.4 Invasive Arteriovenous and Haemodynamic Measurements

All measurements were taken during a scheduled cardiac resynchronisation therapy (CRT) pacemaker or defibrillator implantation. The disposition is demonstrated in figure 2.10.

Following implantation of all pacing leads, the catheter to the coronary sinus (typically a Worley CS guide catheter, Merit Medical, UK) was left in situ and used for aspiration of blood samples. Arterial access is established radially (6Fr) and femorally (8Fr). An appropriate guide catheter (typically Launcher Extra Back-Up (EBU), Medtronic, Minneapolis, USA) is passed to the left main coronary artery from the radial route and an angiogram undertaken to measure the width of the left main coronary artery.

A Volcano Flowire® Doppler guidewire (Phillips, NL) is then positioned to record flow velocity in the left main coronary artery (or if this is not possible, the left anterior descending artery), with data recorded on a Volcano Combomab® system (Philips, NL). From the femoral route, an Inca conductance (or pressure-volume, PV) catheter was passed to the left ventricular apex (Leycom, NL) and connected to a dedicated Inca analysis station (Leycom, NL).

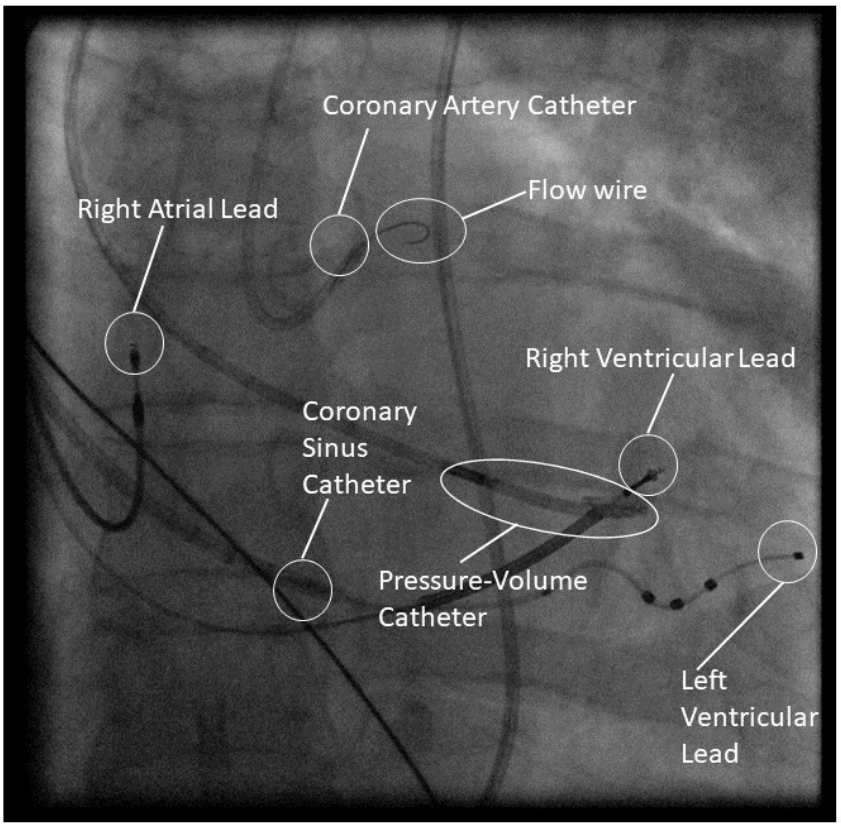

Figure 2.10*: Example positioning of catheters and wires during the invasive procedure (anteroposterior projection).*

2.4.1 Measurement

Measurements where recorded from the Volcano Flowire and the Inca conductance catheter for one minute. After this minute had elapsed, serum, plasma and blood gas samples were drawn simultaneously from the coronary artery and coronary sinus catheters. Where pacing parameters were changed prior to a measurement, a minute was allowed to elapse prior to recording.

2.4.2 Analysis

Serum and plasma bloods were immediately spun down then frozen at -80°C. They were thawed for analysis in Oxford University Hospitals laboratories. Blood gas samples were analysed at point of care on a clinical blood gas analyser (Seca, USA).

Conductance catheter data was analysed using commercial software provided by the manufacturer (Leycom, NL), see figure 2.11. A 10Hz filter was applied to recordings, volumes were calibrated using baseline CMR data (or echo data if CMR was unavailable) and pressure was adjusted to correct for any offset recorded at the time of catheter withdrawal from the femoral artery Any catheter segments within the aorta were discarded from the final volume calculations. Final measurements were averaged from 30 representative consecutive beats in each recording. In the case of ectopy, the ectopic beat and the preceding and following beats were discarded from the recording.

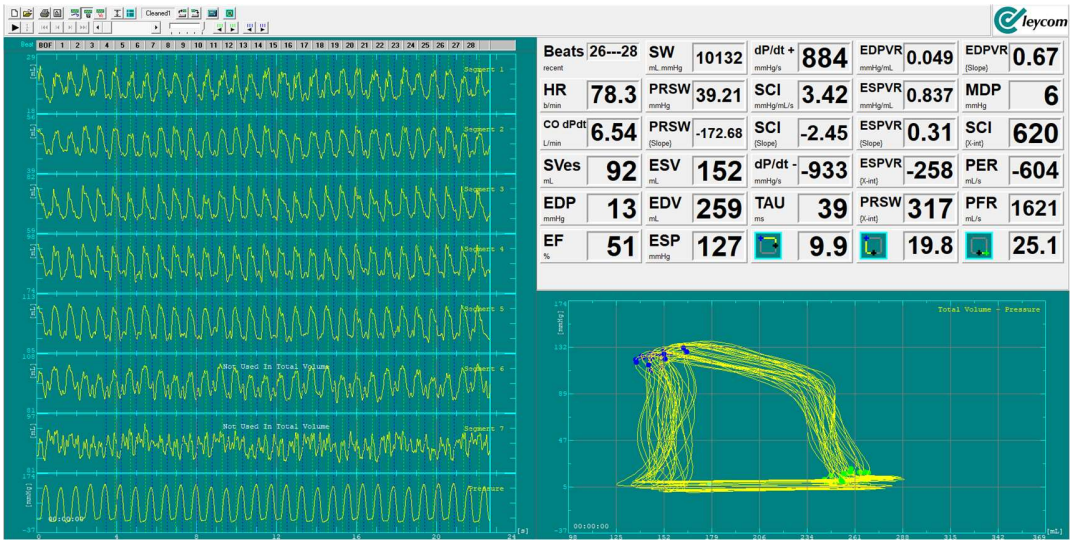

***Figure 2.11**: Segmental volumes and pressure tracings over time (left), derived values (upper right) and pressure-volume loops (lower right) from the CD Leycom analysis software.*

Flowire data was analysed using commercial software provided by the manufacturer (Combomap Version 1.9, Philips, NL), figure 2.12. The doppler recording of velocity was auto-contoured by the software to provide an average peak velocity (APV – cm/s) for each heartbeat, which was then averaged over 10 representative beats, again with ectopics and their succeeding and preceding beats excluded.

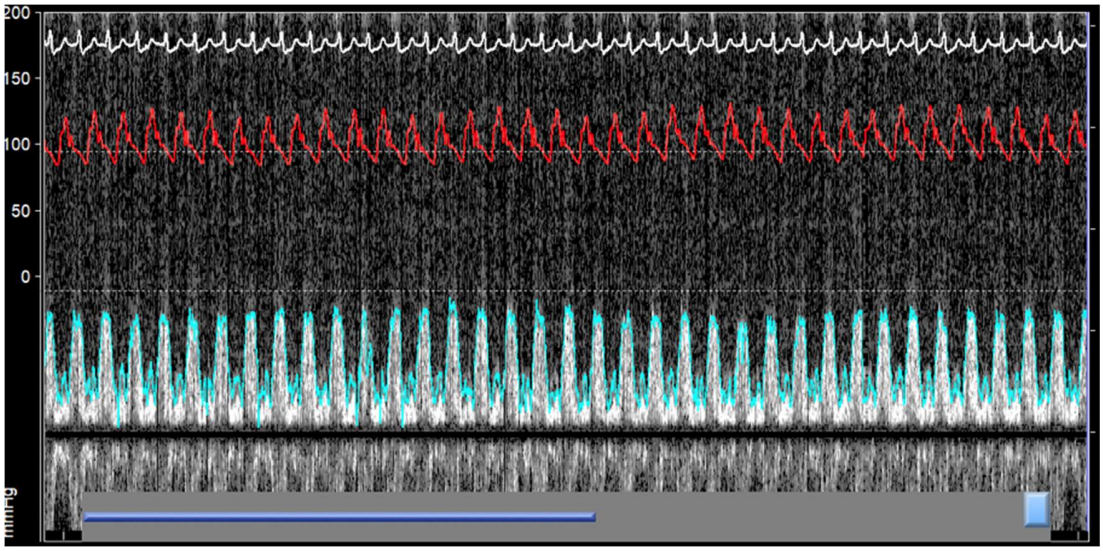

Figure 2.12*: Doppler flow wire analysis. Upper panel: ECG. Middle: aortic pressure. Centre panel: coronary flow (with blue tracing around the flow integral).*

Flow volume was then calculated as APV multiplied by cross-sectional area of the left main coronary artery/LAD (calculated from the average of 2 orthogonal diameters measured on angiogram, see figure 2.13).

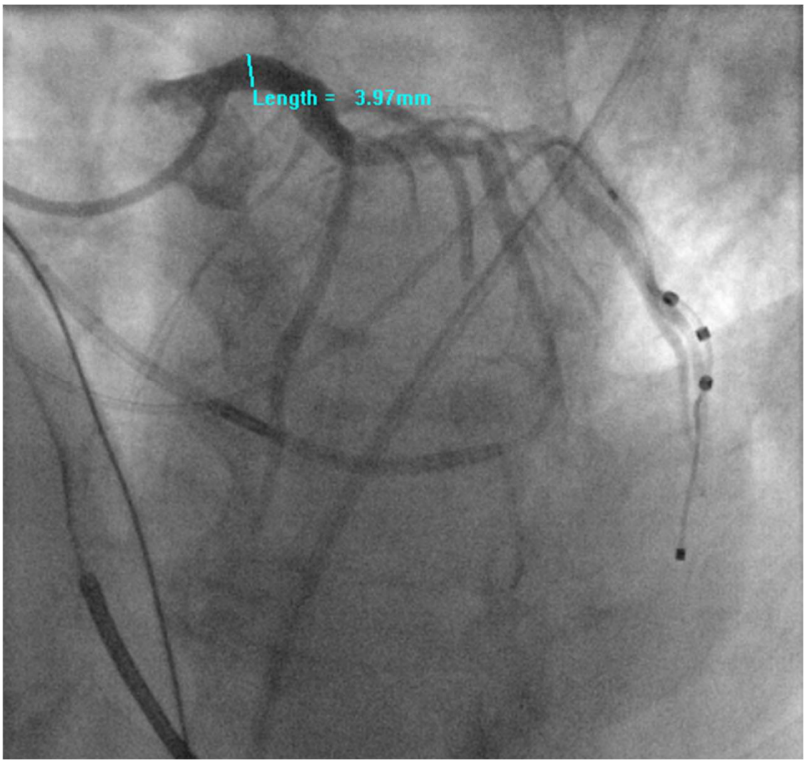

Figure 2.13*: Coronary Angiography with measurement of the left main stem coronary artery diameter (LAO cranial view).*

Oxygen content of blood was calculated as

1.36 x Haemoglobin x (Oxygen Saturation / 100) + 0.0031 x Partial pressure of oxygen

Where Haemoglobin is in grams per decilitre, oxygen saturation in percentage and pressure of oxygen in mmHg (kPa multiplied by a conversion factor of 7.5).

2.5 Methods used in Animal Experiments

2.5.1 Animal Handling

All animal experiments were performed in accordance with relevant legislation with personal, project and institutional licences granted under the UK Animals (Scientific Procedures) Act 1986, licence number 30/3322. At the end of the MRI/MRS experiment, the rats were terminally anaesthetised with 5% isoflurane in oxygen. Upon confirmation of deep anaesthesia (loss of the corneal reflex), euthanasia was performed by rapid excision of the heart.

2.5.2 Acipimox

A dose of 50 mg/kg body weight of acipimox was chosen based on work by other groups[307] and we performed pilot experiments on two animals to show this had peak effect in suppressing fatty acid levels over 1 to 2 hours post injection (see figure 2.14), hence we chose 1 hour as the timepoint for measurements.

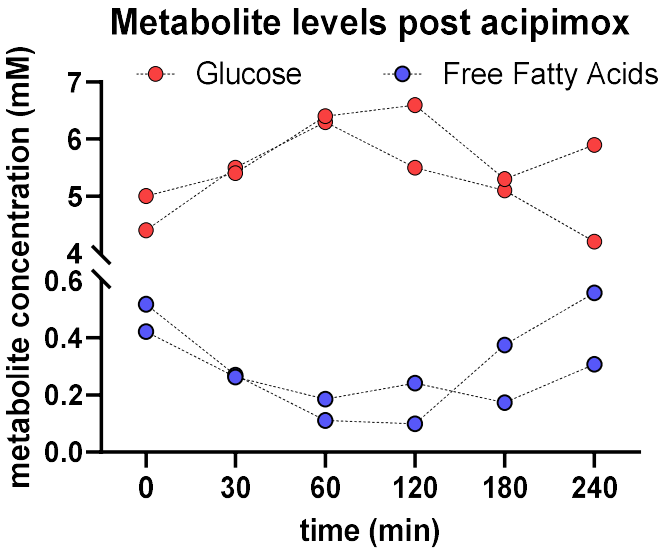

Figure 2.14*: Pilot data demonstrating levels of glucose and free fatty acids over two hours following an intraperitoneal injection of 50mg/kg acipimox into a healthy Wistar rat.*

2.5.3 MRI/MRS

Live animals were loaded into a horizontal bore 7T spectrometer (VARIAN) in a custom-made cradle. ECG monitoring was undertaken throughout. A CINE-FLASH sequence was used to assess cardiac function and volumes using a dual tuned $^{1}H/^{13}C$-volume coil and a four-channel ^{1}H-receive surface coil (Rapid Biomedical; FOV 51.2 x 51.2 mm^2, 1.6 mm axial slices, 128x128x8 matrix size, flip angle 15°, 4 averages). Hyperpolarized [1-^{13}C]pyruvate MRS was used to assess cardiac pyruvate dehydrogenase (PDH) flux, as described previously[308]. 1 ml of 80 mM hyperpolarized [1-^{13}C]pyruvate was injected into a tail vein over 10 s through a pre-implanted cannula.



***Figure 2.15**: Oxford Instruments Alpha system used to generate hyperpolarised [1-^{13}C]pyruvate*

A slice-selective MR spectrum (10 mm slab) was acquired from the cardiac region (60 acquisitions, 1 second TR, 15° Gaussian excitation pulse, 14 kHz bandwidth) using a two-element ^{13}C surface receive array coil (Rapid Biomedical) and volume ^{13}C excitation. Multi-

coil data were either reconstructed via the whitened singular value decomposition method[309], or were elementwise manually phased to the pyruvate peak and added in phase. The first 30 seconds of spectra following the first appearance of the pyruvate peak were summed and quantified using AMARES/jMRUI as previously described[270].

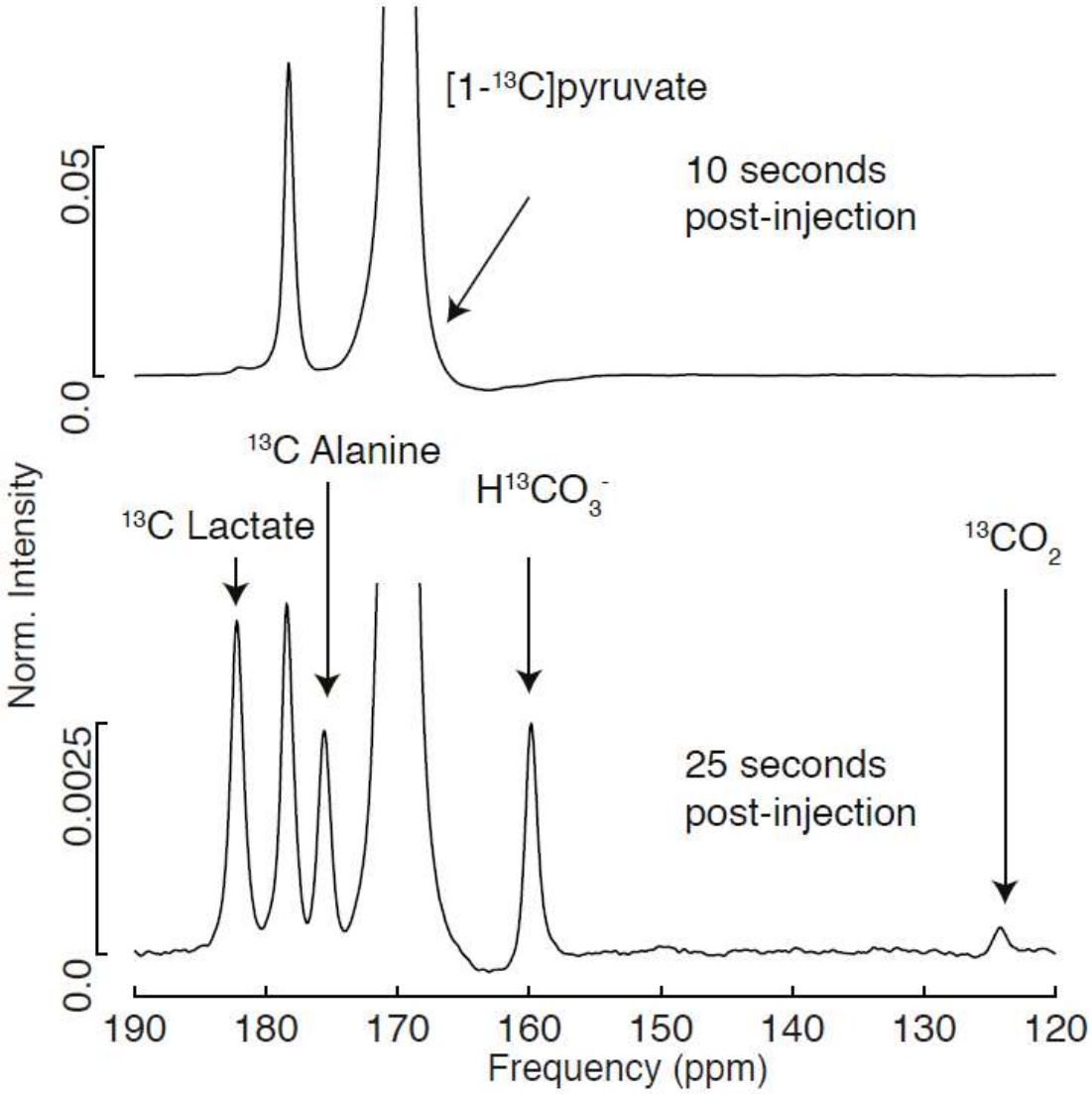

***Figure 2.16**: Labelled ^{13}C spectrum, courtesy of Dr Jack Miller*

Langendorff perfused hearts were lowered in a 20 mm ø borosilicate glass NMR tube into a vertical bore 12T MRI system (Magnex 500 MHz magnet / Varian DDR2 console) at constant hydrostatic pressure. Perfused hearts were placed in a temperature-controlled dual-tuned $^{31}P/^{1}H$ volume coil at 500 MHz, and localiser (FLASH gradient echo) images obtained to confirm that the entire heart was positioned within the sensitive region of the volume coil. Shimming was then performed manually on the whole sample with a third-order shimset, prior to the acquisition of fully-relaxed pulse/acquire ^{31}P FID spectroscopy (10 s TR, 10 kHz bandwidth, 50 μs hard pulse, 90° flip angle, 32 averages, total scan time 5 minutes). Data was quantified via a custom reimplementation of the AMARES algorithm (based on the OXSA toolkit) in MATLAB with prior knowledge explicitly taking into account the known spectral locations and J-coupling of ^{31}P metabolites.

2.5.4 Langendorff Perfusion

Rats were terminally anaesthetised with an intraperitoneal injection of sodium pentobarbital (700 μL) and hearts rapidly excised, weighed and arrested in ice-cold Krebs-Henseleit buffer (118 mM NaCl, 4.7 mM KCl, 1.2 mM $MgSO_4 \cdot 7H_2O$, 1.75 mM $CaCl_2 \cdot 2H_2O$, 0.5 mM Na_2EDTA, 11 mM glucose, 25 mM $NaHCO_3$, 1.2 mM KH_2PO_4) at 37 °C, oxygenated with 95% O_2, 5% CO_2. For each heart, the aorta was then dissected free and the heart rapidly cannulated via the aorta prior to the start of recirculating Langendorff-mode perfusion at constant pressure (100 mmHg). A clingfilm balloon filled with phenyl-phosphoric acid (PPA) acting as a concentration standard at 100 mM was inserted into the right ventricle, connected to a pressure transducer (ADInstruments) and data recording system (LabChart 8), and inflated with PPA to achieve an end-diastolic pressure of between

3-5 mmHg. As well as homeothermic perfusion with water-jacketed perfusion lines, the temperature of the heart was maintained with a Bruker BVT3000 variable temperature hot air system controlled via a Raspberry Pi Model 3. *In vitro* experiments with MR-compatible platinum Pt100 temperature probes revealed that homeostatic control was obtained to ±0.1°.

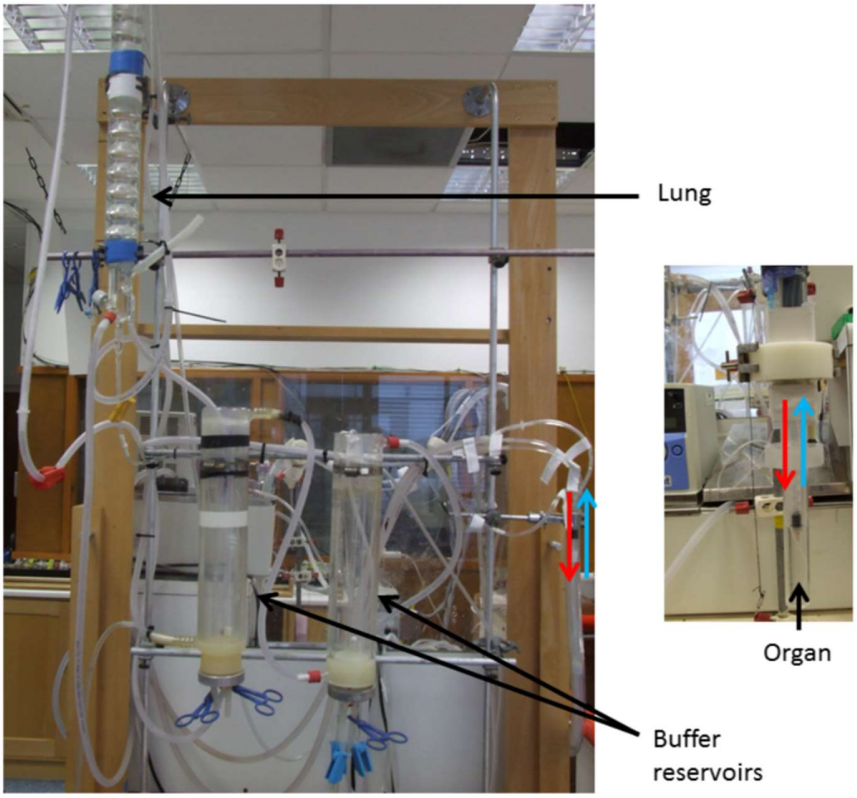

***Figure 2.17**: Langendorff perfusion apparatus*

2.6 Statistical Techniques

Statistical analysis is performed in SPSS statistics 25 (IBM, USA) with figures produced in Graphpad Prism (Graphpad holdings, USA).

Normality testing was performed with Kolmogorov-Smirnov tests. If data were distributed normally, then paired Student's t-tests used for paired datasets or ANOVA where there were more than two datasets (with post-hoc Bonferroni testing between datasets). If the data failed normality testing, Wilcoxon tests were used for paired data or Kruskal-Wallis tests for more than two datasets.

2.7 Ethics Overview

All research was in accordance with the Declaration of Helsinki. Specific authorisations are outlined below.

2.7.1 Human Research: Nicotinic Acid

The study was approved by the National Research Ethics Service (LREC no. 06/Q1607/38).

2.7.2 Human Studies: Substrate Selection

The study was approved by the National Research Ethics Service (REC reference 18/SC/0170).

2.7.3 Human Studies: Vasodilator

The study was approved by the University of Oxford Medical Sciences Interdivisional Research Ethics Committee (reference R64397/RE001).

2.8 Anthropometric and biochemical measurements

Heights and weights were measured using a digital station (Seca, UK) and were used to calculate Body Mass Index (BMI). Blood pressure was recorded as an average of 3 supine measures taken over 10 minutes (DINAMAP-1846-SX, Critikon Corp).

2.9 Blood Samples

Serum and plasma samples were centrifuged for 10 minutes at 11 g and 6°C. The supernatant was pipetted into individual sample vials and stored at -80°C in departmental freezers prior to transport to laboratories in Oxford University Hospitals NHS Foundation Trust for further analysis.

3 Chapter 3: The Effects of Nicotinic Acid on Cardiac Metabolism and Function

3.1 Introduction

3.1.1 Myocardial Metabolism

As discussed in 1.4.1, in the normal adult heart under resting conditions, most (60-90%) of myocardial ATP is generated by mitochondrial β-oxidation of free fatty acids, with a smaller (10-40%) contribution from glucose oxidation[85]. The heart alters substrate use depending on prevailing metabolic conditions, increasing fatty acid and ketone availability when fasting or increased glucose availability when feeding with no change in cardiac function in the healthy heart[62]. However, there is putative benefit from promoting one substrate over another in the energy-starved failing heart, as fatty acid oxidation provides less energy per unit oxygen consumed[310] and glucose oxidation produces a more negative energy of synthesis of ATP[96].

The Randle cycle[12], covered in greater detail in 1.4.1.4 page 19, is a process whereby glucose and fatty acid metabolism cross-regulate each other. Fatty acid metabolism inhibits glycolysis and glucose oxidation (citrate accumulation resulting in inhibition of Pyruvate dehydrogenase, Phosphofructokinase-1 and GLUT-4) and glucose oxidation inhibits fatty acid metabolism (via upregulation of acetyl CoA carboxylase and accumulated Acetyl CoA being converted to Malonyl CoA leading to inhibition of CPT-1)[82]. This helps auto-regulate substrate preference depending on available metabolites but it has been suggested that using drugs which inhibit beta-oxidation of free fatty acids may promote glucose oxidation and provide benefit for the failing heart.

3.1.2 Nicotinic Acid

Nicotinic acid (also known as niacin) is a well-known lipid lowering drug, having been used in clinical practice for over 50 years[311]. It decreases lipolysis by inhibiting hormone-sensitive triglyceride lipase[312] and reduces circulating lipids[313]. Nicotinic acid binds to a G-protein linked receptor on adipocytes known variously as 'protein upregulated in macrophages by interferon-γ', HM74 or GPR109a in humans and in mice as PUMA-G[314]. Binding to this receptor results in adenylate cyclase inhibition, reducing levels of cAMP and inhibiting PKA activity, which reduces the activity of triglyceride lipase[314].

Drugs which inhibit fatty acid metabolism such as nicotinic acid have been suggested as therapies for heart failure as a reduction in fatty acid availability will result in decreased myocardial fatty acid oxidation, promoting glycolysis and glucose oxidation via the Randle cycle. However, heart failure trials to date have not shown any benefit, with no improvement in ventricular function over 28 days[315] and mechanistic studies have shown short term reductions in systolic function[316-318]. The mismatch between the suggested benefits of nicotinic acid receptor agonists and their adverse effects on the myocardium is paradoxical. Nonetheless, acipimox is used in FDG-PET to stimulate myocardial glucose uptake, increasing glucose uptake to a similar extent as a euglycaemic insulin clamp[319, 320].

3.1.3 Intralipid

Intralipid is a lipid emulsion consisting primarily of polyunsaturated long-chain fatty acids: linoleic acid (C18), oleic acid (C18), palmitic acid (C16) and α-linolenic acid (C18). It is

discussed in greater detail in ***Error! Reference source not found.*** page ***Error! Bookmark not defined.***. Briefly, it is predominantly used to provide intravenous nutrition for people unable to take an oral diet, however it also has useful properties as an antidote for toxicity of local anaesthetics and other lipid-soluble drugs[251]. However, there are some cardiac effects including ischaemia-reperfusion protection[264] and positive inotropy[257].

3.1.4 Rationale

In these experiments, we set out to determine in what way nicotinic acid receptor agonists affected myocardial substrate metabolism and contractility. We hypothesized that, in the acute setting, inhibition of lipolysis via nicotinic acid receptor agonism would promote myocardial glucose oxidation. This would increase myocardial pyruvate dehydrogenase flux: we therefore set out to investigate this with hyperpolarized Carbon-13 (^{13}C) MRS in rodents. We hypothesized greater glucose oxidation over lipid oxidation, given a greater amount of ATP produced relative to oxygen consumption, would increase ATP production which would be buffered by an increase in myocardial phosphocreatine concentration. We therefore set out to investigate this in healthy human volunteers with Phosphorus-31 (^{31}P) MRS, giving an assay of the phosphocreatine / ATP (PCr/ATP) ratio. In both groups, we used magnetic resonance imaging to measure cardiac contractility.

In the human group, an infusion of Intralipid was used as a control to demonstrate the effect of increasing circulating free fatty acids on Phosphocreatine/ATP ratio and contractility. We hypothesized the heart would continue to use free fatty acids and there would be minimal change in PCr/ATP or contractility.

3.2 Methods

The experiments carried out are summarised in figure 3.1.

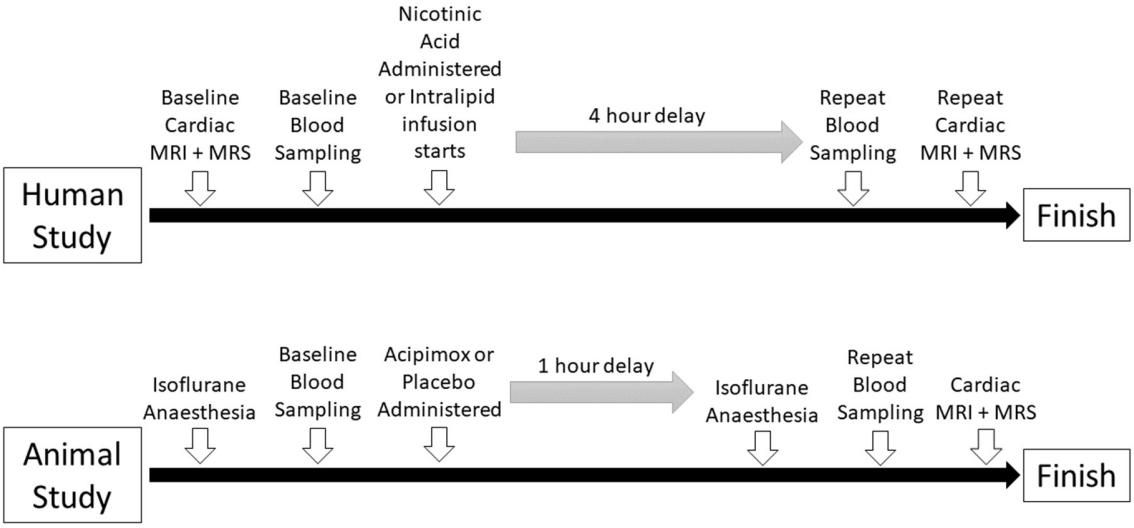

***Figure 3.1**: Overview of study methods.*

3.2.1 Human Experiment

Healthy human volunteers underwent MRI, MRS and blood sampling at baseline, 1 hour post a lipid modulation intervention and 4 hours post the intervention.

3.2.1.1 Recruitment

The study was approved by the National Research Ethics Service (LREC no. 06/Q1607/38) and conformed to the principles outlined in the Declaration of Helskini. All adult participants in this study were recruited on a voluntary basis by poster advertisement from the Oxfordshire area. The poster wording was explicit that normal "healthy" volunteers were needed, with no history of hypertension, diabetes or hypercholesterolaemia,

and no existing heart condition. Potential participants were screened briefly on the telephone and then fully assessed in the Department of Cardiovascular Medicine for exclusion criteria. Written informed consent was obtained from all participants, who were studied after an overnight fast. Participants were excluded if they were taking cardiovascular medication, had a current or past smoking habit, were diabetic (fasting serum glucose >7.0 mM), hyperlipidaemic (cholesterol >6.5 mM), hypertensive (>140/90 mmHg), or had an abnormal electrocardiograph. Participants with a history or clinical evidence of heart failure, obstructive sleep apnoea, valvular or congenital heart disease or contraindication to MR scanning were also excluded.

3.2.1.2 Anthropometric and biochemical measurements

Heights and weights were measured using a digital station (Seca, UK) and were used to calculate BMI. Blood pressure was recorded as an average of 3 supine measures taken over 10 minutes (DINAMAP-1846-SX, Critikon Corp). Venous blood was drawn during the experiments and sent for biochemical analysis of β-hydroxybutyrate, insulin, glucose and non-esterified free fatty acids (FFA, ABX Pentra System).

3.2.1.3 Fatty Acid Manipulation

To elevate free fatty acids, 20% Intralipid™ (Fresenius Kabi, UK) was infused intravenously at 60 ml/h with unfractionated heparin, as described in 2.1.1 page 58. Reduction of circulating free fatty acids (FFAs) was accomplished with a single 400 mg dose of nicotinic acid (Niaspan®, Abbot, UK).

3.2.1.4 Left Ventricular Imaging

All cardiac magnetic resonance (CMR) scans for the assessment of the left ventricle were performed on a 1.5 Tesla MR system (Siemens, Germany). Images for ventricular volumes and diastolic function were acquired using a steady state free precession (SSFP) sequence with an echo time (TE) of 1.5 ms, a repetition time (TR) of 3.0 ms, in plane resolution 1.5 x 1.5 mm^2, temporal resolution 47.84 ms, flip angle 60°, as previously described[321]. All imaging was performed supine, retrospectively cardiac gated and acquired during end-expiratory breath-hold. All analysis was performed using cmr42© (Circle Cardiovascular Imaging Inc, Calgary, Canada) as described in 2.3.1 page 61.

3.2.1.5 ^{31}Phosphorus Magnetic Resonance Spectroscopy

This is described in further detail in 2.3.2 page 62. All ^{31}P-MRS was performed at 3T (Siemens Tim Trio MR system, Erlangen, Germany) and spectra were acquired in fasted participants. Subjects lay prone with the left ventricle centred over a modified dual-tuned heart/liver ^{31}P/^{1}H surface transmit/surface receive loop/butterfly coil and a 3D-CSI technique performed. Analysis was performed as described in 2.3.2.1 page 64.

3.2.2 Animal Experiment

All animal experiments were performed in accordance with relevant legislation with personal, project and institutional licences granted under the UK Animals (Scientific

Procedures) Act 1986. Age and weight-matched male Wistar rats in four separate cohorts of eight animals each were used.

3.2.2.1 Metabolic interventions

Acipimox was used to lower circulating free fatty acids, as described in 2.1.3.1 page 59. The first cohort (Unfed Acipimox) were fasted overnight and received an intraperitoneal injection of 2 μl/g body weight of a solution containing 25 mg acipimox (Sigma Aldrich, Dorset, UK) in 1 ml sterile saline. The second cohort (Unfed Saline) were fasted overnight and received an intraperitoneal injection of 2 μl/g body weight sterile saline. The cohorts were mixed with a third investigator allocating the solutions for injection in a random fashion, so the investigators handling the animals were blinded to which received saline and which acipimox. A third cohort (Fed Acipimox) was allowed to feed ad libitum on normal rodent chow (60% carbohydrate) and injected with 2 μl/g body weight of the acipimox solution (50 mg/kg) and a fourth cohort (Fed) were allowed to feed on chow ad libitum and did not receive an injection.

Venous blood samples were taken immediately prior to IP injection from the saphenous vein using Li-heparin-coated collection tubes and then repeated one hour after the injection. Glucose was analysed with a point-of-care device (AccuCheck), FFAs with a spectrophotometric assay (Randox, Crumlin, UK) and insulin with an ELISA kit (Mercodia, Uppsala, Sweden).

3.2.2.2 MRI/MRS

One-hour post injection, rats were anaesthetised with 2% isoflurane and loaded into a horizontal bore 7T spectrometer for MRI and ^{13}C MRS as described in 2.5.3 page 82. 1 ml

of 80 mM hyperpolarized [1-^{13}C]pyruvate was injected into a tail vein over 10 s through a pre-implanted cannula for ^{13}C MRS.

3.2.2.3 Euthanasia

At the end of the MRI/MRS experiment, the rats were terminally anaesthetised with 5% isoflurane in oxygen. Upon confirmation of deep anaesthesia (loss of the corneal reflex), euthanasia was performed by rapid excision of the heart.

3.2.2.4 Langendorff Perfusion Experiment

Six rat hearts were retrograde-perfused in the Langendorff mode as described in 2.5.4 page 84. After perfusion, the heart was subsequently allowed to equilibrate for approximately a 10 minute period. In three of the hearts, acipimox was added to the perfusate to achieve a concentration of 0.78 mg/ml (equivalent to the estimated serum concentrations in experimental animals). 31P MRS was performed and rate pressure product recorded after the 10 minute equilibration period and after 30 minutes' perfusion.

3.3 Results

3.3.1 Baseline Characteristics of Human Study Participants

9 participants were recruited. 2 participated in the Intralipid arm of the study alone, 2 participated in the nicotinic acid arm alone and 5 participated in both arms. Baseline characteristics are shown in table 3.1

***Table 3.1**: Baseline characteristics of 9 participants (mean ± standard deviation)*

Characteristic	*Mean*
Age (y)	24 ± 3
Height (m)	1.71 ± 0.1
Body Mass Index (kg/m^2)	24.1 ± 2.0
Weight (kg)	71 ± 11
Systolic Blood Pressure (mmHg)	119 ± 10
Diastolic Blood Pressure (mmHg)	74 ± 8
Pulse Pressure (mmHg)	45 ± 9
Fasting Glucose (mmol/l)	4.5 ± 0.9
Fasting Cholesterol (mmol/l)	4.3 ± 0.7

3.3.2 Effects of Fatty Acid Elevation with Intralipid in Human Subjects

Intralipid resulted in elevated free fatty acids with reduced glucose, suggesting cardiac supply of fatty acids was elevated during the infusion. Contractility increased, while PCr/ATP ratio remained unchanged.

3.3.2.1 Circulating Substrates

Effects of fatty acid elevation are shown in Table 3.2 and Figure 3.2. As expected, 4 hours of Intralipid™/heparin infusion acutely elevated circulating FFAs (from 0.25 ± 0.14 mmol/L to 1.5 ± 0.61 mmol/l, $p < 0.0001$). Associated with this, during the infusion, circulating glucose levels fell (4.46 ± 0.62 mmol/l to 3.76 mmol/l, $p = 0.03$), insulin levels rose (0.2 ± 0.04 to 0.5 ± 0.22 mU/L, $p = 0.03$) and β-hydroxybutyrate levels increased, although not significantly (0.25 ± 0.13 mmol/l to 0.41 ± 0.21 mmol/l, $p = 0.09$).

3.3.2.2 Haemodynamics

FFA elevation was associated with a small, but statistically significant, increase in systolic blood pressure (mean 5 mmHg increase, p=0.042), but no change in diastolic blood pressure nor heart rate.

3.3.2.3 Cardiac Energetics and Function

Acute elevation of FFAs was associated with increased left ventricular ejection fraction (absolute increase +5.0%, LVEF baseline 62.9 ± 6.2% to 67.9 ± 6.4%, p<0.001). Peak circumferential systolic strain decreased and systolic radial strain increased during FFA elevation. The increased LVEF during FFA elevation was not associated with a change in myocardial PCr/ATP (baseline 2.16 ± 0.33 vs 4 h Intralipid™ Infusion, 2.09 ±0.35, p = 0.686).

***Table 3.2**: Changes in circulating metabolites, haemodynamics, myocardial energetics and ventricular systolic function with Intralipid infusion.*

	Baseline	***4-hour***	***P-value***
Circulating Metabolites			
Fatty Acids (mmol/l)	0.25 ± 0.14	1.5 ± 0.61	<0.001
d-β-hydroxybutyrate (mmol/l)	0.25 ± 0.13	0.41 ± 0.21	0.09
Glucose (mmol/l)	4.46 ± 0.62	3.76 ± 0.59	0.03
Insulin (mU/l)	0.2 ± 0.04	0.5 ± 0.22	0.03
Haemodynamics			
Systolic Blood Pressure (mmHg)	110 ± 8	115 ± 8	0.04
Diastolic Blood Pressure (mmHg)	65 ± 7	62 ± 5	0.24
Heart Rate (beats per minute)	55 ± 10	57 ± 10	0.77
Myocardial Energetics			
Myocardial PCr/ATP	2.16 ± 0.33	2.09 ±0.35	0.69
LV Systolic Function			
LVEF (%)	62.9 ± 6.2	67.9 ± 6.4	<0.001
Circumferential Strain (%)	-19.0 ± 2.5	-20.1 ± 2.4	0.03
Radial Strain (%)	36.1 ± 7.5	38.6 ± 7.2	0.04

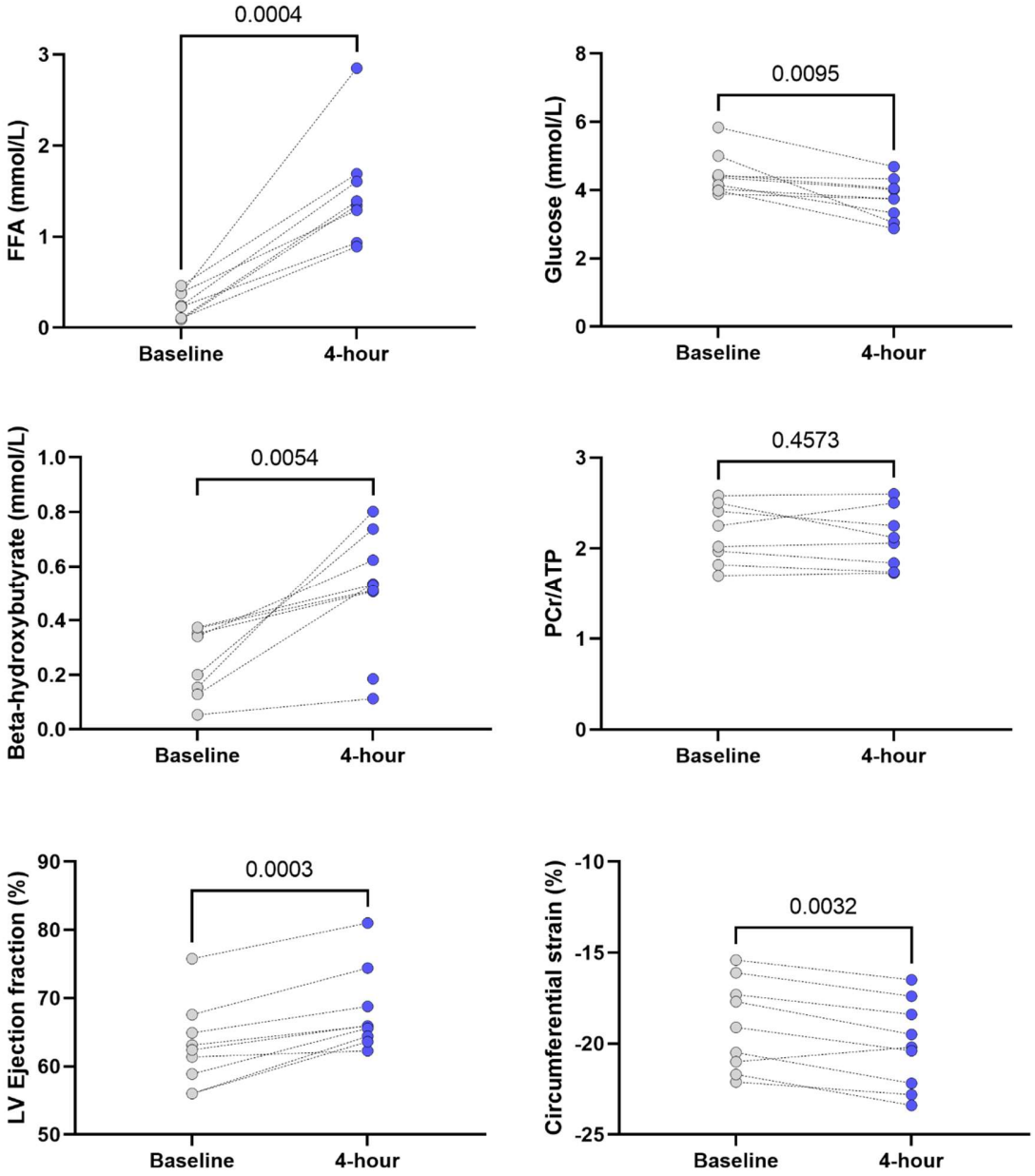

Figure 3.2*: Summary graphs of free fatty acids (FFA), glucose, beta-hydroxybutyrate, PCr/ATP ratio, left ventricular (LV) ejection fraction and circumferential strain before and during Intralipid infusion. P-values are shown by paired t-tests.*

3.3.3 Effects of Fatty Acid lowering with Nicotinic acid in Human Subjects

3.3.3.1 Circulating Substrates

See Table 3.3 and Figure 3.3. Four hours after nicotinic acid ingestion, circulating levels of FFAs fell (from baseline 0.19 ± 0.07 mmol/L to 0.03 ± 0.04mmol/L, $p < 0.001$). Circulating glucose levels, insulin and β-hydroxybutyrate levels were not statistically different (all $p > 0.05$).

3.3.3.2 Haemodynamics

There were no significant changes in systolic blood pressure, diastolic blood pressure or heart rate, although there was a (non-significant) trend towards a reduction in systolic blood pressure.

3.3.3.3 Cardiac Energetics and Function

Nicotinic acid caused a significant decrease in systolic function (absolute reduction 3.4%, LVEF baseline 64 ± 8% to 60 ± 7%, $p=0.027$). In line with this, peak circumferential systolic strain increased ($p = 0.005$), although radial strain did not significantly change. This was associated with a fall in myocardial PCr/ATP (baseline 2.16 ± 0.4 to 1.78 ± 0.14, $p < 0.05$).

***Table 3.3**: Changes in circulating metabolites, haemodynamics, myocardial energetics and ventricular systolic function following nicotinic acid.*

	Baseline	***4-hour***	***P-value***
Circulating Metabolites			
Fatty Acids (mmol/l)	0.19 ± 0.07	0.03 ± 0.04	0.009
d-β-hydroxybutyrate (mmol/l)	0.39 ± 0.07	0.29 ± 0.03	0.46
Glucose (mmol/l)	3.56 ± 0.91	3.44 ± 0.73	0.43
Insulin (mU/l)	0.21 ± 0.02	0.17 ± 0.05	0.15
Haemodynamics			
Systolic Blood Pressure (mmHg)	115 ± 12	108 ± 10	0.08
Diastolic Blood Pressure (mmHg)	62 ± 8	64 ± 5	0.65
Heart Rate (beats per minute)	59 ± 9	57 ± 8	0.77
Myocardial Energetics			
Myocardial PCr/ATP	2.16 ± 0.40	1.78 ± 0.14	0.04
LV Systolic Function			
LVEF (%)	63.5 ± 7.5	60.1 ± 7.1	0.03
Circumferential Strain (%)	-20.3 ± 4.1	-18.2 ± 4.0	0.005
Radial Strain (%)	40.3 ± 16.1	35.9 ± 15.0	0.24

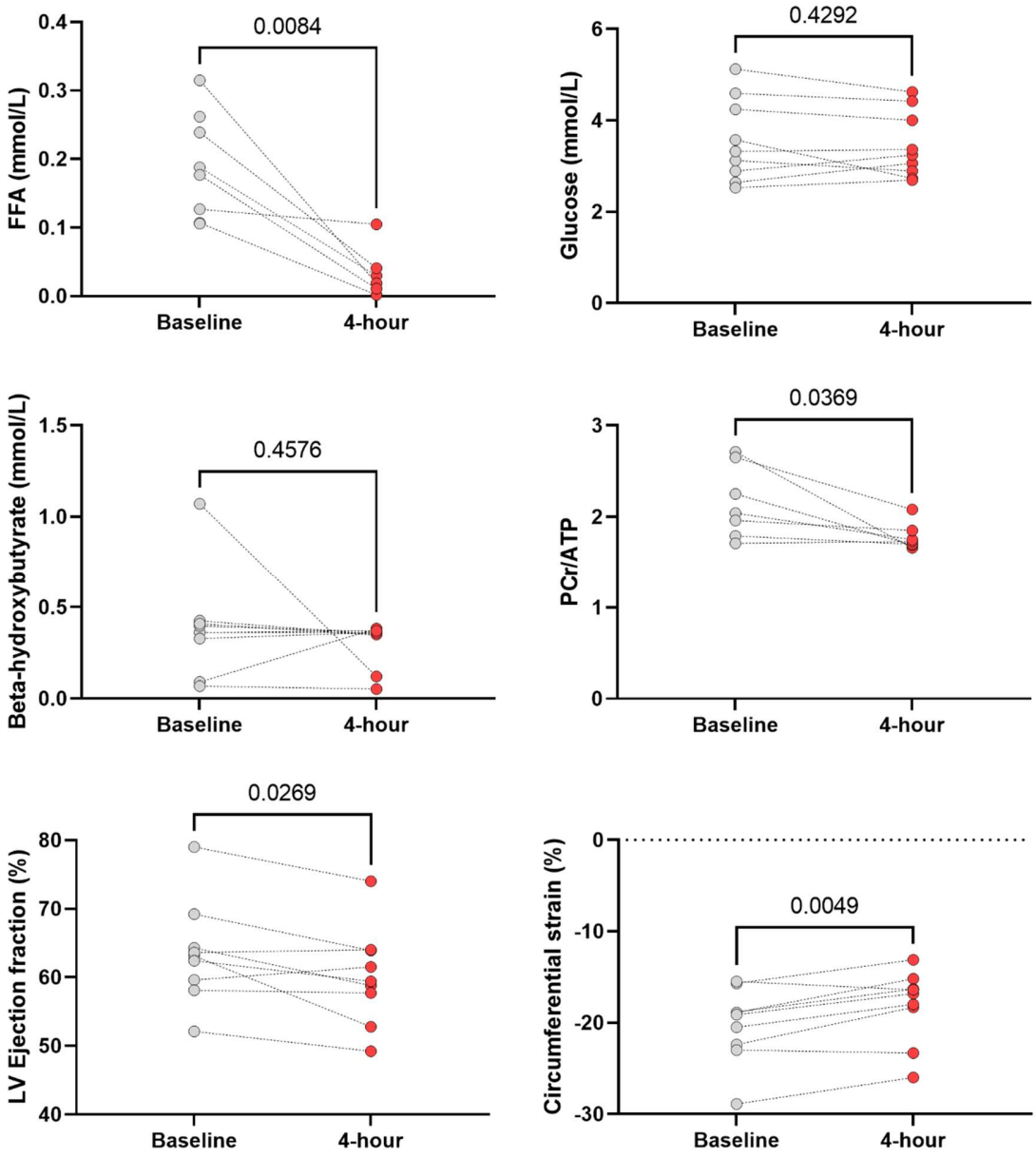

Figure 3.3: *Summary graphs of free fatty acids (FFA), glucose, beta-hydroxybutyrate, PCr/ATP ratio, left ventricular (LV) ejection fraction and circumferential strain before and following nicotinic acid administration. P-values are shown by paired t-tests.*

3.3.4 Pooled Data and Correlations in Human Subjects

Levels of β-hydroxybutyrate positively correlated with levels of free fatty acids ($R^2 = 0.21$, $p = 0.01$) and weakly negatively correlated with levels of glucose ($R^2 = 0.089$, $p = 0.03$), figure 3.4. Levels of free fatty acids positively correlated with ejection fraction ($R^2 = 0.204$, $p = 0.009$) and weakly negatively with global circumferential strain ($R^2 = 0.12$, $p = 0.048$), figure 3.4.

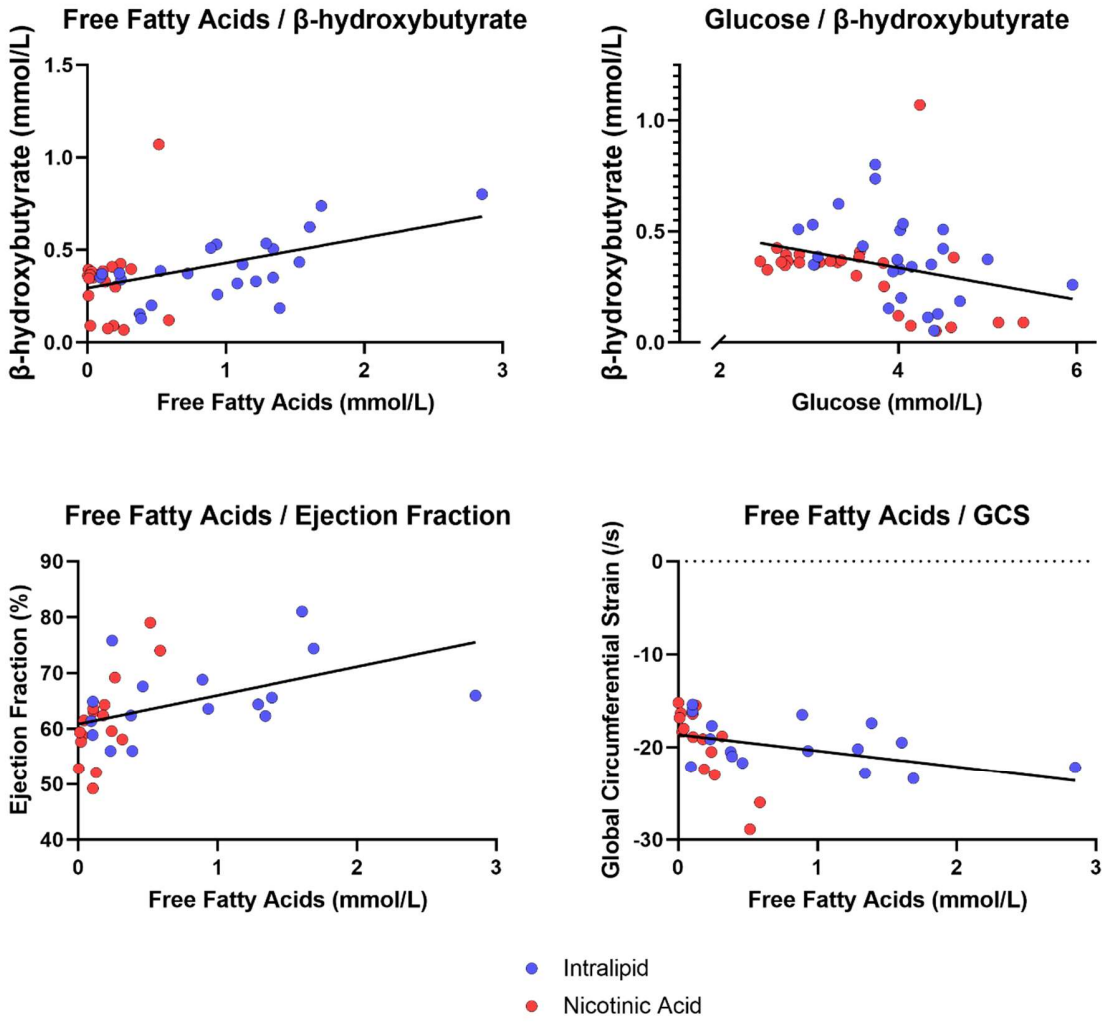

Figure 3.4: *Correlations of β-hydroxybutyrate with free fatty acids and glucose (upper panels) and correlations of free fatty acids with measures of contractility (lower panels) in data pooled from both arms of the study.*

Looking at the two arms of the experiment individually, strong correlations between metabolites and contractility were found in the nicotinic acid group (figure 3.5). Free fatty acids positively correlated with ejection fraction ($R^2 = 0.56$, $p = 0.001$), global radial strain ($R^2 = 0.57$, $p = 0.001$) and global circumferential strain ($R2 = 0.76$, $p < 0.001$). In this group, glucose concentrations also correlated with contractility: ejection fraction ($R^2 = 0.376$, $p = 0.007$), global radial strain ($R^2 = 0.3$, $p = 0.018$), global circumferential strain ($R^2 = 0.389$, $p = 0.006$).

In the Intralipid arm of the experiment, there was no association between free fatty acids and contractility, although glucose showed a negative correlation with ejection fraction ($R^2 = 0.29$, $p = 0.021$). Free fatty acids did however positively correlate with serum β-hydroxybutyrate ($R^2 = 0.46$, $p < 0.001$), while glucose showed a negative correlation with β-hydroxybutyrate ($R^2 = 0.17$, $p = 0.037$). These correlations are shown in figure 3.6.

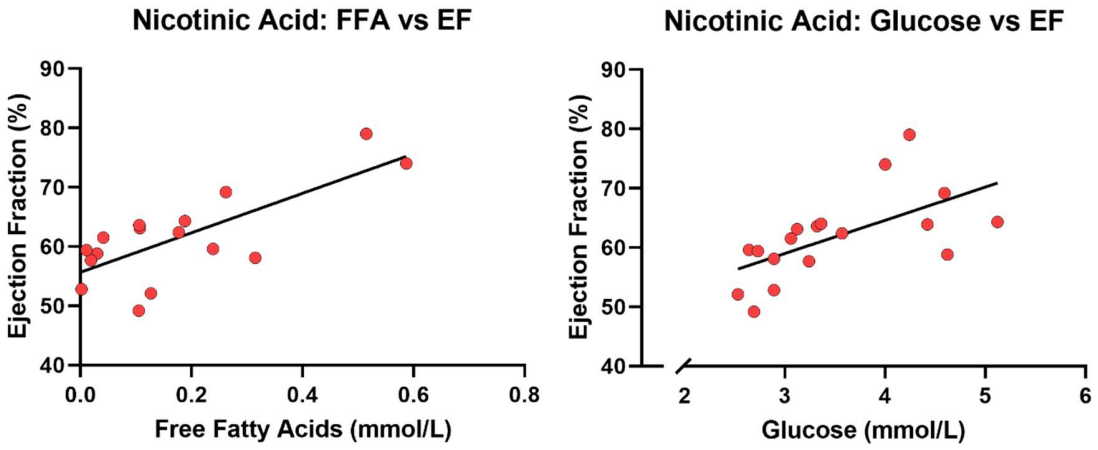

Figure 3.5: *Significant correlations in the nicotinic acid arm of the experiment.*

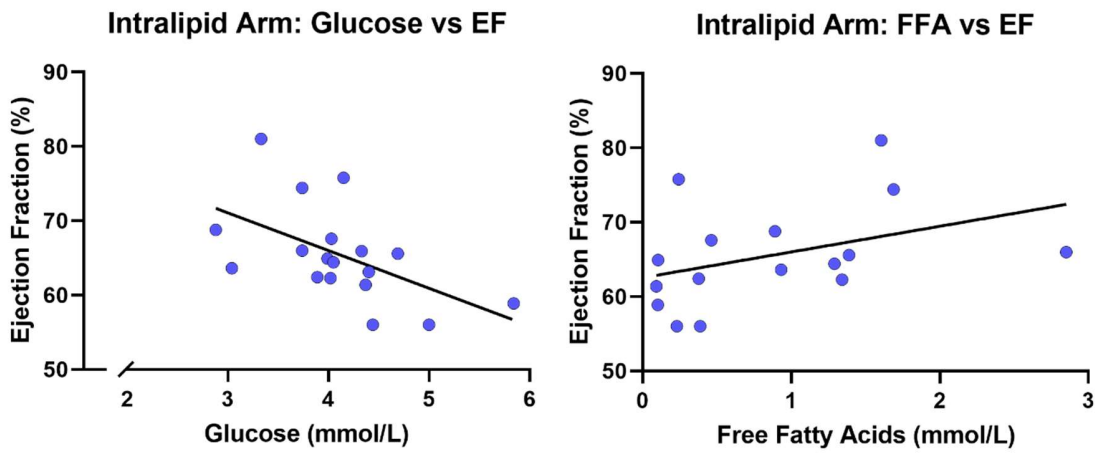

Figure 3.6: *Significant correlations in the Intralipid arm of the experiment.*

The change in free fatty acids positively correlated with change in β-hydroxybutyrate (R^2 = 0.375, p = 0.009), ejection fraction (R^2 = 0.438, p = 0.004) and negatively with change in global circumferential strain (R^2 = 0.552, p = 0.001), figure 3.7. No correlations were seen in individual group data for changes in values.

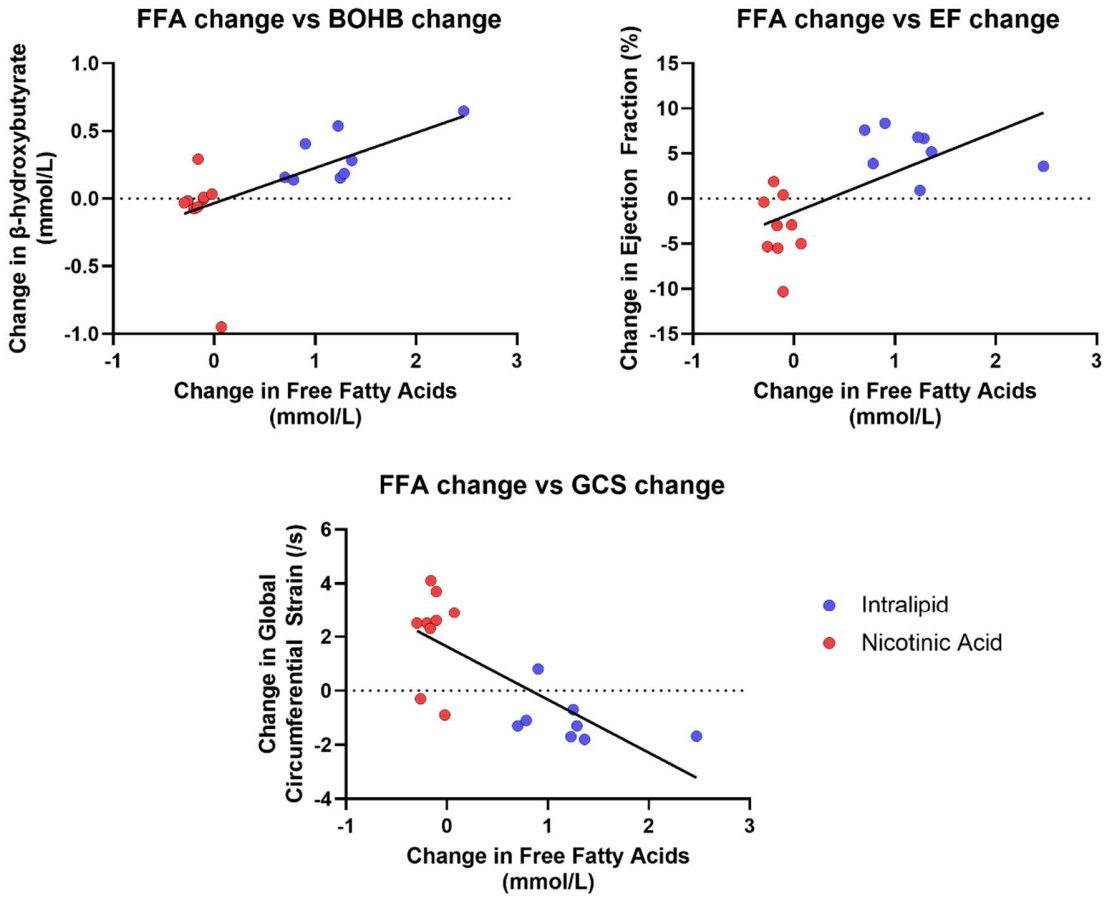

Figure 3.7 *Changes in serum free fatty acids correlated with changes in β-hydroxybutyrate (BOHB), ejection fraction (EF) and global circumferential strain (GCS).*

3.3.5 Whole Animal Experiment

3.3.5.1 Baseline Weights

There were small but statistically significant weight differences between fasted and fed groups ($p < 0.0001$, Table 4), which is likely due to the overnight fast.

Table 3.4: *Baseline weights of rats in the animal experiment by group*

Group	*Weight (g)*
Unfed + Acipimox	263 ± 12
Unfed + Saline	261 ± 9
Fed + Acipimox	290 ± 14
Fed	287 ± 12

3.3.5.2 Circulating Metabolites

See table 3.5 and figure 3.8. Acipimox caused a fall in FFAs and triacylglycerol (TAG) in the fasted animals, but no change in the fed animals, nor was there a change in the animals given saline. As expected, fasted animals given acipimox had significantly lower FFA ($p < 0.001$) than those given saline.

Beta-hydroxybutyrate was seen to rise only in the fasted animals injected with saline (from 0.65 ± 0.18 mmol/L to 1.17 ± 0.45 mmol/L, $p = 0.019$), while there was no significant change in fasted animals injected with acipimox. In the fed animals, levels were low throughout.

Blood glucose was higher in fed than fasted animals and there was a statistically significant increase in blood glucose in the fasted animals injected with acipimox (from 5. 4 ± 0.8 mmol/L to 6.4 ± 1.1 mmol/L, $p = 0.018$), which was not seen in the saline injected

animals, nor the fed animals injected with acipimox. Insulin levels were generally below the lower limit of assay detection in fasted animals. In fed animals, acipimox caused circulating insulin to fall ($p = 0.005$), and the fed animals given acipimox had significantly lower insulin than those not injected (0.55 ± 0.22 nU/L vs 1.18 ± 0.43 nU/L, $p = 0.002$). FFAs inversely correlated with glucose ($R^2 = 0.28$, $p = 0.003$) and positively correlated with beta-hydroxy-butyrate ($R^2 = 0.59$, $p < 0.001$).

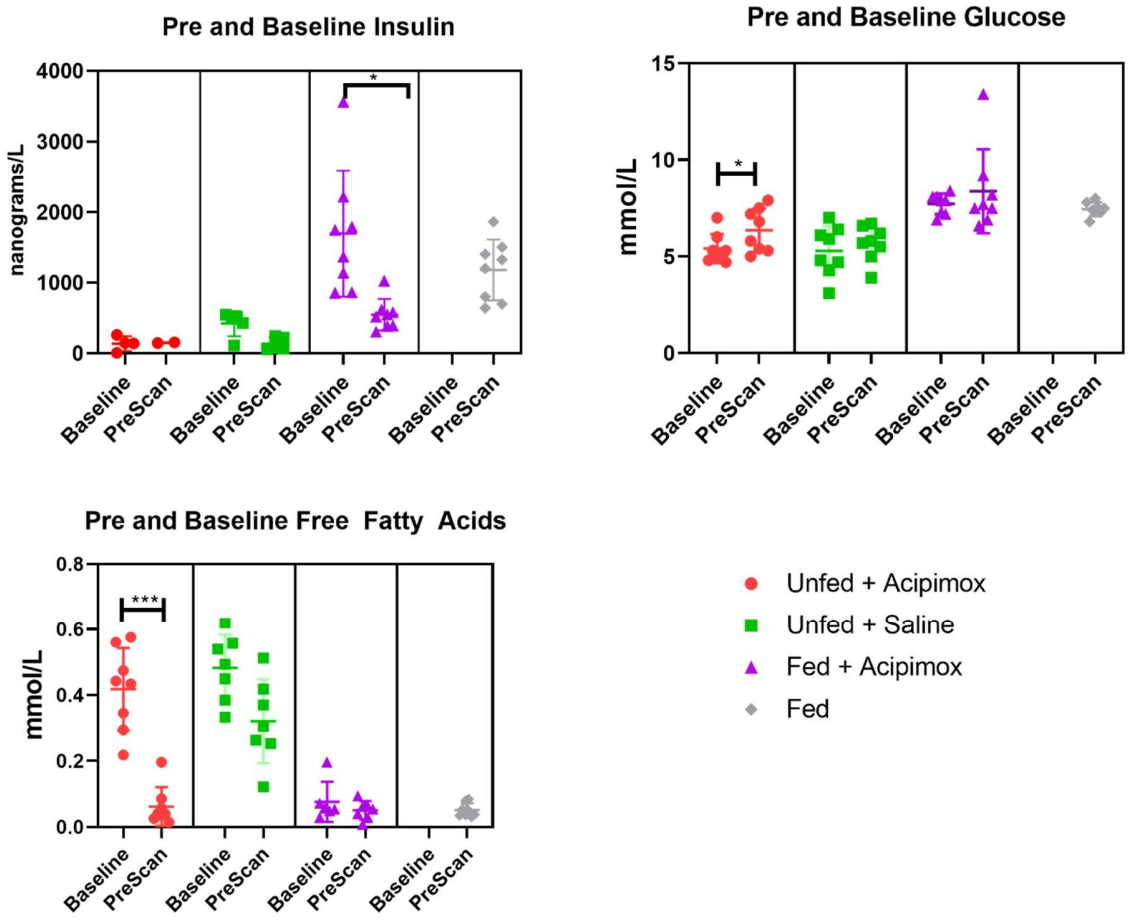

***Figure 3.8**: Circulating Metabolites in the animal experiment.*
** $p < 0.05$, ** $p < 0.01$, *** $p < 0.001$, **** $p < 0.0001$*

***Table 3.5**: Animal Circulating Metabolites. BLD = below limit of detection. P<0.05 highlighted*

		Unfed + Acipimox	***Unfed + Saline***	***Fed + Acipimox***	***Fed***
Glucose (mmol/L)	Baseline	5.4 ± 0.8	5.3 ± 1.3	7.7 ± 0.5	
	Pre-scan	6.4 ± 1.1	5.7 ± 0.9	8.4 ± 2.1	7.5 ± .4
	p-value (change)	***0.018***	0.379	0.434	
Free Fatty Acids (mmol/L)	Baseline	0.42 ± 0.13	0.48 ± 0.1	0.07 ± 0.06	
	Pre-scan	0.06 ± 0.06	0.32 ± 0.12	0.06 ± 0.02	0.05 ± 0.02
	p-value (change)	***< 0.001***	0.51	0.07	
Beta-hydroxy-butyrate (mmol/L)	Baseline	0.46 ± 0.19	0.65 ± 0.18	0.05 ± 0.05	
	Pre-scan	0.38 ± 0.31	1.17 ± 0.45	0.04 ± 0.03	0.03 ± 0.01
	p-value (change)	0.871	***0.019***	0.313	
Tri-acyl Glycerol (mmol/L)	Baseline	0.61 ± 0.41	0.67 ± 0.56	0.65 ± 0.88	
	Pre-scan	0.39 ± 0.35	0.83 ± 0.45	0.38 ± 0.47	0.83 ± 0.55
	p-value (change)	***0.002***	0.19	0.15	
Lactate (mmol/L)	Baseline	1.13 ± 0.16	0.85 ± 0.41	0.87 ± 0.98	
	Pre-scan	1.21 ± 0.35	1.02 ± 0.31	0.55 ± 0.6	1.32 ± 0.75
	p-value (change)	0.602	0.348	0.069	
Insulin (nU/L)	Baseline	BLD	BLD	1695 ± 891	
	Pre-scan	BLD	BLD	550 ± 222	1181 ± 432
	p-value (change)			***0.005***	

3.3.5.3 Contractility

In both fasted and fed animals, those given acipimox had lower cardiac contractility (table 3.6, figure 3.9). In a similar pattern to that seen in humans, fasted animals had lower LVEF (absolute reduction 8%, saline 68 ± 4% vs. acipimox 60 ± 3% p = 0.03) and also lower cardiac output indexed to body mass (368 ± 35 x 10^{-3} ml/min/g vs. 426 ± 53 x 10^{-3} ml/min/g, p = 0.02). In fed animals, the ejection fractions were not significantly changed by acipimox, however there was a difference in cardiac output indexed to body mass (395 ± 50 x 10^{-3} ml/min/g vs 471 ± 45 x 10^{-3} ml/min/g, p = 0.014). There were no significant differences between the two groups which had not received acipimox.

Table 3.6: *Animal Left Ventricular Contractility Data*

	Unfed + Acipimox	***Unfed + Saline***	***Fed + Acipimox***	***Fed***	***p-value (ANOVA)***
LVEF (%)	60 ± 3.1 ¥†‡	67.8 ± 3.6 ¥	67.5 ± 8.9 †	70.4 ± 3.5 ‡	***0.004***
Cardiac Output (ml/min)	97.2 ± 12.3 ⋆	111 ± 15.8 †	115 ± 18.4	135 ± 13 ⋆†	***< 0.001***
Cardiac Output index (ml/min.g x10^{3})	368 ± 35 ⋆	426 ± 53	395 ± 50 †	471 ± 45 †⋆	***0.001***

For post-hoc analyses (multiple comparisons with Tukey's test):
⋆ shows pairs of data significantly different at p < 0.001
‡ shows pairs of data significantly different at p < 0.01
† or ¥ shows pairs of data significantly different at p < 0.05

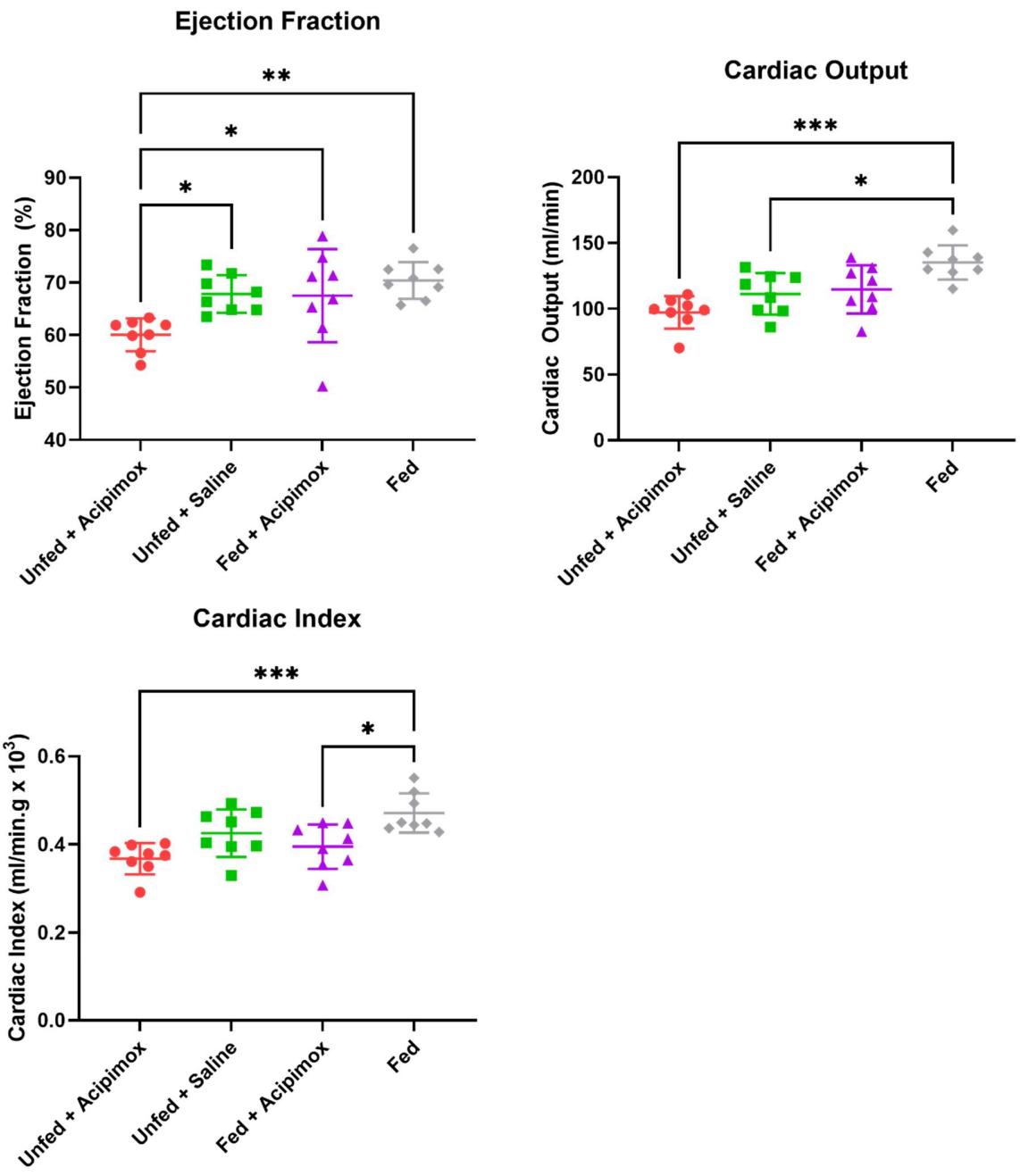

Figure 3.9: *Measures of contractility in animal data. Cardiac Index is cardiac output indexed to body mass in grams. * $p < 0.05$, ** $p < 0.01$, *** $p < 0.001$, **** $p < 0.0001$*

3.3.5.4 Hyperpolarized [1-^{13}C]pyruvate MRS

Values for the hyperpolarized data are summarised in table 3.7 and figure 3.10 and are given as summed spectra acquired every second over 30 seconds from the first appearance of the pyruvate peak, indexed to pyruvate peak height over the same time. Values are expressed as a ratio of signal intensity.

***Table 3.7**: Hyperpolarized [1-^{13}C]pyruvate MRS by metabolite and study arm of animal.*

	Unfed + Acipimox	***Unfed + Saline***	***Fed + Acipimox***	***Fed***	***p-value (ANOVA)***
Bicarbonate x 10^{-4}	486 ± 139 ‡†	182 ± 114 ‡⋆$	512 ± 130 ⋆#	726 ± 201 †$#	***<0.0001***
Lactate x 10^{-4}	993 ± 425 ‡	1220 ± 243 #	1620 ± 508	1970 ± 613 ‡#	***0.0013***
Alanine x 10^{-4}	145 ± 149	185 ± 159	176 ± 123	250 ± 97	0.473

Values are expressed as peak amplitude as a proportion of pyruvate peak amplitude in arbitrary units.
For post-hoc analyses (multiple comparisons with Tukey's test):
$ shows pairs of data significantly different at $p < 0.0001$
⋆ shows pairs of data significantly different at $p < 0.001$
‡ shows pairs of data significantly different at $p < 0.01$
 # or † shows pairs of data significantly different at $p < 0.05$

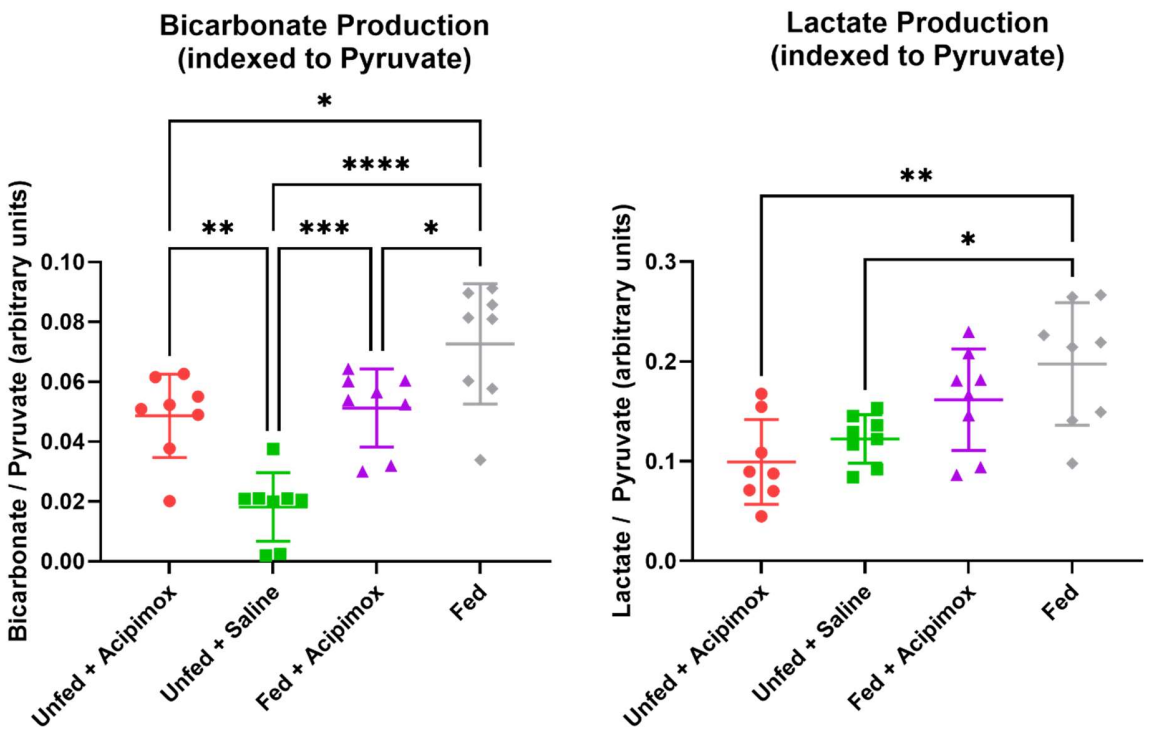

Figure 3.10: *Hyperpolarized [1-^{13}C]pyruvate MRS. * $p < 0.05$, ** $p < 0.01$, *** $p < 0.001$, **** $p < 0.0001$*

Fasted animals injected with acipimox had higher PDH flux (bicarbonate production) than those given the saline control ($p = 0.0019$). However, whilst elevated, bicarbonate production after Acipimox was 66% of that observed in fed animals ($p = 0.02$). PDH flux in fed rats given acipimox was also lower than that observed in fed animals ($p = 0.04$). Whilst Lactate Dehydrogenase (LDH) flux was higher in fed than fasted animals (0.18 ± 0.06 vs 0.11 ± 0.04, $p < 0.001$), acipimox administration did not alter lactate metabolism. There were no significant changes in alanine production.

3.3.5.5 Correlations in Animal Data

Across all groups, free fatty acids inversely correlated with bicarbonate production ($R^2 = 0.41$, $p < 0.001$), suggesting increasing reliance on glucose metabolism as fat availability declined. In the fasted animals, bicarbonate production was negatively correlated with cardiac index ($R^2 = 0.53$, $p = 0.001$), but there was no such correlation in fed animals. In the unfed animals, blood glucose correlated with bicarbonate production ($R^2 = 0.32$, $p = 0.021$) but there was no correlation in the fed group.

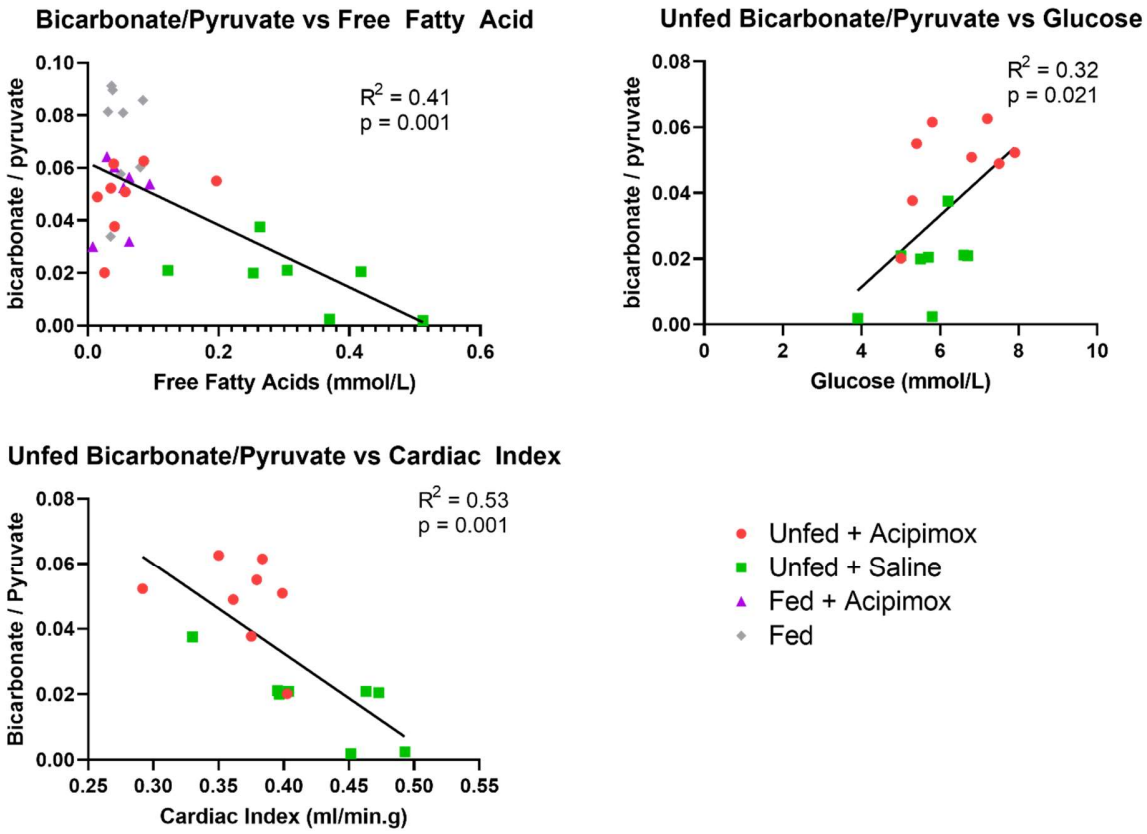

***Figure 3.11**, correlations between Hyperpolarized [1-^{13}C]pyruvate MRS, free fatty acids, glucose and cardiac index.*

In summary, in the fasted animals, acipimox increased bicarbonate production (indicating an increase in PDH flux), although not to the levels seen in animals allowed to feed *ad libitum*. In the fed animal, it had the opposite effect, reducing PDH flux. As there was no alteration in lactate production to indicate increased glycolysis, this would suggest a submaximal rise in glucose uptake and metabolism in the fasted rat and a fall in glucose uptake and metabolism in the fed rat.

3.3.6 Perfusion Experiment

See figure 3.12. For the most part, small declines were seen in both RPP and PCr/ATP over time, as would be expected for an *ex vivo* heart. However, no statistically significant changes between the acipimox and control groups were observed in any of the parameters measured.

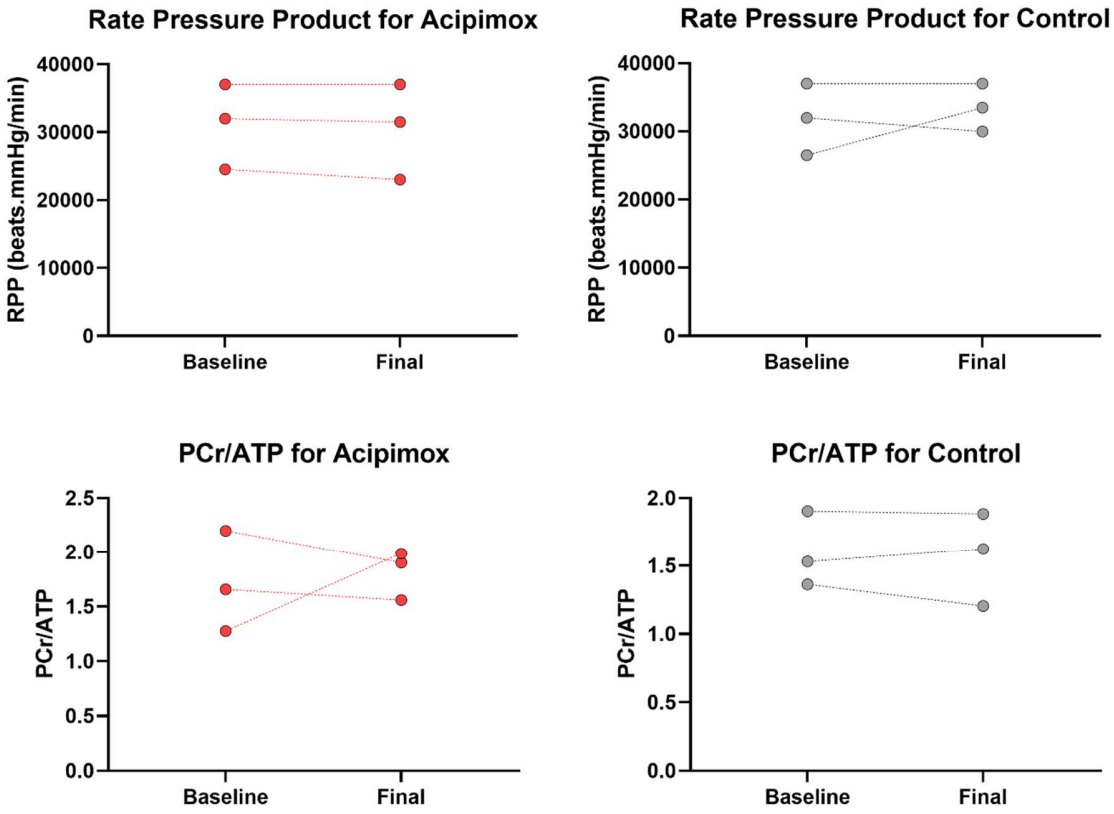

***Figure 3.12**: Rate Pressure Product and PCr/ATP ratio in the Langendorff perfused hearts given acipimox or controls perfused with Krebs buffer only.*

3.4 Discussion

Here we show that following nicotinic acid receptor agonist administration in the fasted state, there is a depression of contractile function in the human heart and a decrease in the human cardiac PCr/ATP ratio. In rats, the reduction in LV function was linked to a reduction in fatty acid availability and/or myocardial glucose oxidation.

3.4.1 Effects of Intralipid on the Fasted Human Heart

Elevation of free fatty acids with Intralipid correlated with an increased contractility demonstrated by increased left ventricular ejection fraction and reduced global circumferential strain. Intralipid has previously been shown to exert an inotropic effect[257]. Sympathetic nervous system activation[258] and increased intracellular calcium release[259] via GPR40[260] have been implicated as causative factors, although a beneficial metabolic effect from increased fat metabolism has been proposed, but never proven[263].

Although neither fatty acid uptake nor utilisation is recorded in this study, it is known that myocardial extraction and metabolism of fat from the bloodstream increases in correlation with arterial free fatty acid concentrations[59] and therefore reasonable to assume increased myocardial fatty acid uptake and utilisation occurred during this experiment, as serum free fatty acid levels were elevated. Likewise, plasma β-hydroxybutyrate was elevated: this, too is taken up and metabolised in proportion to its plasma concentrations[322], however when it is metabolised this inhibits fatty acid oxidation[322, 323]. Serum glucose falls and insulin rises as free fatty acids rise, in line with previous studies in this area[324]. Free fatty acids act to promote gluconeogenesis, act as a potent insulin secretagogue and yet impair insulin-mediated glucose transport in peripheral

tissues[325], so the previous studies on the net effects on myocardial glucose metabolism are conflicting.

There is not sufficient data in this study to show the individual changes in substrate metabolism of fatty acids, ketone and glucose owing to their cross-regulation. Increased free fatty acid metabolism results in build-up of mitochondrial citrate, inhibiting phosphofructokinase and slowing glycolytic flux, known as the glucose-fatty acid cycle or Randle cycle[12] so it is tempting to assume that fatty acid metabolism will predominate during Intralipid infusion, but the individual effects of elevated β-hydroxybutyrate and insulin cannot be discounted. PCr/ATP ratio did not significantly change during the experiment, suggesting that mitochondrial oxidative phosphorylation and ATP production was matched to ATP usage in the heart, irrespective of the prevailing source of metabolic substrate, as PCr/ATP is known to fall in situations where demand exceeds supply[326].

The correlations with free fatty acids and all measures of contractility suggests there is an effect from increasing plasma free fatty acids on contractility, although it is unclear from these data alone whether this is due to alterations in metabolism, a form of inotropic stimulation, or a combination of the two. This does raise the question of whether this inotropic effect could be seen in the failing heart, and this is the focus of later chapters in this thesis.

3.4.2 Effects of Nicotinic Acid on the Fasted Human Heart

Nicotinic acid caused a fall in circulating free fatty acids, as expected. β-hydroxybutyrate and glucose levels were not significantly different from baseline, while there was a trend to a fall in insulin. A decline in contractility occurred across all measures of systolic function (ejection

fraction and strain) and, associated with this, an 18% reduction of PCr/ATP. The PCr/ATP fall implies an impairment of oxidative phosphorylation, however a reduction in free fatty acid availability should simply result in increased glucose uptake and oxidation via the Randle cycle. Indeed, in PET studies on fasted volunteers, myocardial glucose uptake with nicotinic acid administration increases to a level comparable to insulin-glucose clamp[327], and it has previously been suggested that the increase in glucose metabolism would be sufficient to offset a loss of FFA availability[328]. PET can only show myocardial glucose uptake, and not metabolism. It is possible that glycolysis occurred but this was uncoupled from oxidative metabolism and glucose was diverted towards lactate and alanine production. As hyperpolarized [1-^{13}C]pyruvate MRS is able to answer these questions this study was back translated into animals.

3.4.3 Animal Hyperpolarized [1-^{13}C]Pyruvate Magnetic Resonance Spectroscopy

3.4.3.1 Hyperpolarized [1-^{13}C]Pyruvate Magnetic Resonance Spectroscopy in Healthy Fed Rats

These animals show are large bicarbonate/pyruvate ratio consistent with high pyruvate dehydrogenase flux. This would be consistent with high levels of serum glucose and high levels of insulin driving glucose uptake and that this uptake and oxidation are coupled. This would be expected given the carbohydrate rich nature of the chow (by weight 50% carbohydrate, 3% fat). In addition, low levels of circulating FFA (as shown in Table 3.5) would also result in a low level of myocardial fatty acid uptake and metabolism and hence minimal inhibition of pyruvate dehydrogenase, maximizing glucose oxidation through PDH. The elevated LDH (and

numerically ALAT) flux also suggest that increased glucose entry and glycolytic flux was occurring upstream of PDH.

3.4.3.2 Hyperpolarized [1-^{13}C]Pyruvate Magnetic Resonance Spectroscopy in Healthy Fasted Rats given Saline Placebo

In these animals, the bicarbonate/pyruvate ratio was low, demonstrating low pyruvate dehydrogenase flux. This would also be expected given that serum glucose and insulin were low (Table 3.5) and FFA levels high. As such FFA uptake and metabolism will dominate in the fasted state, causing inhibition of pyruvate dehydrogenase. In addition to pyruvate dehydrogenase inhibition, glucose supply would also not be elevated, and the lower LDH flux versus fed animals would also suggest that glycolytic flux was lower upstream of PDH.

3.4.3.3 Hyperpolarized [1-^{13}C]Pyruvate Magnetic Resonance Spectroscopy in Healthy Fasted Rats given the Nicotinic Acid Receptor Agonist Acipimox

These animals exhibited higher pyruvate dehydrogenase flux than fasted animals given the saline placebo, but lower than that seen in the fed rats. Here, as FFA levels were suppressed to levels comparable to the fed state (Table 3.5), it would be expected that FFA mediated inhibition of pyruvate dehydrogenase via the Randle cycle would be minimised, and pyruvate dehydrogenase flux elevated. However, we propose that although there was a small rise in serum glucose, as insulin levels remained low, glucose entry to the glycolytic pathway would not be increased to a level expected following CHO feeding, and that glucose entry into glycolysis upstream of PDH

may account for the difference and reduced pyruvate dehydrogenase flux compared to fed rats. This would be supported by the lowest LDH and ALAT flux being seen in these animals.

3.4.3.4 Hyperpolarized [1-^{13}C]Pyruvate Magnetic Resonance Spectroscopy in Healthy Fed Rats given the Nicotinic Acid Receptor Agonist Acipimox

Compared to the fed animals not given acipimox, the pyruvate dehydrogenase flux in fed animals given acipimox was lower and not significantly different from fasted animals given acipimox. As free fatty acid levels were low, Randle cycle mediated inhibition of glycolysis and glucose oxidation should be minimal in this group, one would expect similar PDH flux. However, while serum glucose was comparable to that seen in the fed animals not given acipimox, insulin levels were lower. We therefore hypothesise that the lower pyruvate dehydrogenase flux in this group was caused by a lower glucose supply to glycolysis, mediated by reduced insulin mediated GLUT4 uptake, which would have a direct effect to limit myocardial glucose uptake. While we only observed a non-significant trend towards a fall in insulin levels in human participants given nicotinic acid, this has been observed in other studies[316, 317]. The other possibility here would be a direct inhibition of PDH via acipimox, however diversion of pyruvate into other pathways (alanine and lactate) would be expected in this case, yet it is not seen here. In addition, there was no effect on function or energetics in isolated perfused hearts when given acipimox, makes a direct effect unlikely.

3.4.4 Cardiac Contractility in Healthy Rats

As in the humans, acipimox treatment depressed ejection fraction in the fasted rats. In line with this, in the fed rats, a significant lower cardiac output indexed to body weight was observed after acipimox injection. Interestingly, there was a negative correlation between cardiac index and pyruvate dehydrogenase flux in all of the fasted animals, possibly an indirect effect, as the animals with the greatest fall in FFA had the largest rise in pyruvate dehydrogenase flux.

3.4.5 31P Magnetic Resonance Spectroscopy and Contractility in Langendorff perfused hearts given nicotinic acid receptor agonists

There were no significant changes in contractility or PCr/ATP seen in isolated hearts exposed to acipimox compared to control hearts. This would suggest that the mechanisms of metabolic and contractile changes are not a result of direct effects of nicotinic acid receptor agonists on the heart.

3.4.6 Possible Mechanisms of Nicotinic Acid induced Ventricular Impairment

3.4.6.1 Glucose Stimulated Insulin Secretion

Nicotinic acid, and its acipimox derivative, act on the GPR109a receptor in adipose tissue to inhibit lipolysis[314]. GPR109a is also expressed in pancreatic beta cells: here, its activation reduced glucose stimulated insulin secretion via PPAR-γ and cAMP[329, 330], with the fall in insulin in turn reducing cellular glucose uptake and therefore metabolism in insulin sensitive tissues. This gives

rise to the clinical observation that nicotinic acid agonism impairs glucose tolerance and elevates serum glucose levels[331]. In this experiment, we see a fall in insulin despite glucose levels being unchanged, consistent with this.

Insulin activates myocardial GLUT-4 transporters[332], increases activity of enzymes involved in glycolysis such as phosphofructokinase[62] and pyruvate dehydrogenase itself, via pyruvate dehydrogenase kinase[333], hence myocardial substrate metabolism is shifted towards glucose by insulin.

3.4.6.2 Nicotinic Acid effects on Myocardial Metabolism and Contractility in the Fed State

In these animals, the impairment of glucose stimulated insulin secretion is seen to reduce circulating insulin in spite of a similar glucose level. This explains the reduced PDH flux in these animals. As free fatty acids are low in the fed state and remain low following the administration of the nicotinic acid receptor agonist, the myocardium is deprived of both fat and glucose, which can explain the reduction in contractility measured by indexed cardiac output.

3.4.6.3 Nicotinic Acid effects on Myocardial Metabolism and Contractility in the Fasted State

Despite the rise seen in glucose in the animals given nicotinic acid receptor agonists, insulin remains low, consistent with glucose stimulated insulin secretion inhibition. Levels of free fatty acids fall (consistent with inhibition of lipolysis in adipose tissue) and it would follow that myocardial fatty acid metabolism is reduced.

Hence, there are two competing effects on myocardial glucose oxidation. A reduction in fatty acid metabolism will act to promote glucose metabolism via the Randle cycle. However, low levels of circulating insulin will inhibit glucose metabolism. We therefore find PDH flux in fasted animals given acipimox to be higher than the fasted animals given saline (who have high levels of free fatty acids and low insulin), but not as high as animals allowed to feed (who have low levels of free fatty acids and high insulin). Hence, the myocardium remains starved of energetic substrate following the administration of a nicotinic acid receptor agonist in the fasted state: acetyl-CoA entry into the TCA cycle would be reduced from both glucose and fatty acid routes, effectively starving the heart of substrate to produce ATP.

This tallies with the reduction in contractility (ejection fraction) seen in both human and animal experiments: without adequate metabolic substrate to provide ATP for contraction, contractility is impaired. It also fits with the reduction in PCr/ATP seen in the human data: as ATP supply and demand become uncoupled, phosphocreatine concentration falls as a new equilibrium is established.

3.5 Conclusions

We have shown here that healthy heart function can be altered by limiting its supply of metabolic substrates, confirming the importance of myocardial substrate metabolism to function. In particular, we have shown that by reducing circulating fatty acids and inhibiting glucose-stimulated insulin secretion, nicotinic acid agonists starve the heart of substrate. While there was an increase in glucose metabolism in the fasted state, it appears to be insufficient to make up for the loss of fat and hence cardiac function was compromised as a result. In the fed state, glucose metabolism falls.

These observations shed light on why nicotinic acid agonists, such as acipimox, have failed to bring about benefits for heart failure. The use of nicotinic acid agonists in PET protocols to stimulate glucose uptake may give rise to falsely low readings of left ventricular function and skew its use as a research tool, although the metabolic impairment of dysfunctional myocardium may further increase sensitivity for detecting ischaemia.

4 Chapter 4: The Effects of Substrate Manipulation at Rest in Normal Hearts and in Heart Failure

4.1 Introduction

While the healthy heart at rest predominantly uses fatty acids to produce ATP (oxidative metabolism consisting of 60-90% fatty acids and 10-40% glucose), fatty acid oxidation is reduced in heart failure[334] while glucose oxidation is decreased, but as fatty acid oxidation is reduced relatively more, a relative 'substrate switch' towards glucose metabolism is seen [151]. The failing heart is also said to be inflexible, unable to switch from one fuel substrate to another as conditions dictate[85]. This is reviewed in further detail in section 1.4 page 13.

Increasing glucose oxidation has been pursued as a therapy for heart failure over the last 20 or more years. A biochemical advantage has been suggested, as the yield of ATP for oxygen consumption (P:O ratio) is greater for glucose than for fats and it produces a higher energy of synthesis for ATP production, yielding a greater Gibbs free energy[96]. Fatty acid metabolism, on the other hand, has received relatively little attention. In non-ischaemic cardiomyopathies, where oxygen supply is theoretically not limiting (at least not to the same degree as ischaemia/infarction driven heart failure), the oxygen sparing effect of enhanced glucose metabolism may not be beneficial, and indeed may reduce the overall ATP production.

To this point, studies have focussed on maximising glucose metabolism by inhibiting fatty acid transport or metabolism. Dichloroacetate increases PDH flux, and has been shown to improve cardiac function in the pressure overloaded and post-ischaemic rat heart[199, 200], and in small-scale human studies, has shown modest benefit in coronary artery disease[202], but in HFrEF

both improvement[27] and no change have been observed [203]. PDH activity can also be increased by inhibition of fatty acid oxidation, and trimetazidine[208], ranolazine[209], perhexiline[210] and etoxomir[211] have been shown in small studies to produce modest improvements in LV function[212] and myocardial energetics[213] in chronic ischaemic HFrEF. However, results have been largely disappointing, and these drugs have not gained traction in the treatment of HFrEF. This may be due the fact that the lower yield of ATP from glucose oxidation, when combined with the reduced uptake from insulin resistance in HFrEF [171, 335], the increase in ATP production via increased glucose oxidation is unlikely to fully compensate for the loss of fatty acid oxidation.

This current approach, to increase glucose oxidation due to its inherently lower P:O ratio, relies on two fundamental premises. Firstly, that the human failing heart is inflexible to substrate, and secondly that it has a fixed and reduced oxygen supply. Should the human failing heart be shown to be neither inflexible nor oxygen limited, this current therapeutic approach would be brought into question.

In order to investigate this, patients living with severe non-ischaemic HFrEF underwent either insulin-glucose infusion to increase glucose metabolism or Intralipid infusion to increase fatty acid metabolism with the order randomised. We then used non-invasive cardiovascular magnetic resonance to assess of cardiac function and cardiac energetics using ^{31}phosphorus magnetic resonance spectroscopy. To investigate the effects of the infusions on cardiac substrate use, $MV0_2$ and stroke work we further assessed this invasively with arterio-venous sampling and pressure volume loops.

4.2 Methods

The work in this chapter was approved by the National Research Ethics Service (REC reference 18/SC/0170) and conformed to the principles outlined in the Declaration of Helsinki.

We recruited 10 healthy volunteers and 20 participants with heart failure to undergo cardiac MRI and MRS during interventions to manipulate cardiac metabolic substrate in order to measure contractility, PCr/ATP ratio and creatine kinase flux. 5 of those who had participated in the heart failure MRI protocol and 4 separate volunteers underwent a research protocol during cardiac resynchronisation pacemaker implant involving paired coronary arteriovenous blood sampling, pressure-volume loop measurement and coronary artery flow measurements.

4.2.1 Recruitment

All healthy participants in this study were recruited on a voluntary basis by poster advertisement from the Oxfordshire area. The poster wording was explicit that normal "healthy" volunteers were needed. Participants with heart failure were recruited from heart failure clinics, cardiac MRI lists and from other studies where the participants had consented to future contact.

Potential participants were screened briefly on the telephone and then fully assessed in the Department of Cardiovascular Medicine for exclusion criteria. Written informed consent was obtained from all participants, who were studied after an overnight fast.

4.2.2 Inclusion and Exclusion Criteria

4.2.2.1 Inclusion Criteria

General Inclusion Criteria

- Participant is willing and able to give informed consent for participation in the study.
- Male or Female, aged at least 18 years old.

Additional inclusion criteria for Heart Failure Participants

- Heart failure as diagnosed by symptoms and signs of heart failure accompanied by echo or MRI derived measures of LV ejection fraction (as per European Society of Cardiology 2016 guidelines)

Additional inclusion criteria for heart failure participants undergoing CRT implantation

- CRT clinically indicated as per ESC guidelines
- Scheduled for CRT implantation as part of routine clinical care

Additional inclusion criteria for participants with pre-existing CRT pacemakers

- MRI conditional CRT device, under follow-up at Oxford University Hospitals NHS Foundation Trust.

4.2.2.2 Exclusion Criteria

General Exclusion Criteria

- Participant is unwilling or unable to give informed consent
- Any impediment to communication which, in the opinion of the investigator, might prevent the investigator communicating effectively with the patient during the study which could cause a safety or reliability concern.
- Any other condition which, in the opinion of the investigator, might affect the safety of the participant or reduce the reliability of the study results
- Involvement in any other research project where the procedures would affect the outcomes of this study.
- History of diabetes mellitus or taking diabetic medication
- Egg, or soya allergy (used in the manufacture of Intralipid)
- Disturbances of the normal fat metabolism (e.g. pathological hyperlipemia, lipoid nephrosis, acute pancreatitis)
- Severe liver damage, TB, pulmonary disease, anaemia, blood coagulation disorders, or recent fracture of pelvis or long bones.

Additional Exclusion Criteria for Participants Undergoing MRI Studies (except post-CRT implantation scans)

- Metal clips or metallic foreign body
- Prior injury to the eye involving fragments of metal
- Prior shrapnel injuries
- Any other metallic or electronic implants affected by the magnetic field

- History of severe claustrophobia
- Implanted pacemaker prior to commencement of trial
- History of chronic kidneys disease
- Female participant who is pregnant, lactating or planning pregnancy during the course of the study

Additional Exclusion Criteria for Healthy Controls

- A history of valvular heart disease
- LVEF under 57% (the defined lower bound of the normal CMR range[336])
- Coronary artery disease (known coronary artery disease greater than 25% stenosis)
- Known peptic ulcer disease (a contra-indication to nicotinic acid)
- Use of statins or fibrates (drugs which alter lipid handling)

Additional Exclusion Criteria for Participants with Heart Failure undergoing CRT

- Patient with known iodine contrast hypersensitivity
- Patient with uncontrolled atrial fibrillation or a baseline heart rate judged by the investigators to preclude the ability to pace at a heart rate simulating resting conditions.

Additional Exclusion Criteria for Participants with Heart Failure undergoing MRI (except post CRT implantation scans)

- Ischaemia as primary cause of heart failure (based on cardiac magnetic resonance diagnosis or the presence of obstructive coronary artery disease and echocardiographic regional wall motion abnormalities in the context of heart failure)

4.2.3 Substrate Manipulation

4.2.3.1 Fatty Acid Elevation

To elevate free fatty acids, 20% Intralipid™ (Fresenius Kabi, UK) was infused intravenously at 60 ml/h, as described in section 2.1.1, page 58. In those not taking anticoagulant medications, unfractionated heparin (Monoparin, CP Pharmaceuticals, UK) is concomitantly infused at 0.4 U/kg/min.

4.2.3.2 Fatty Acid Suppression

Reduction of circulating free fatty acids was accomplished with a single 250 mg dose of the nicotinic acid receptor agonist acipimox (Olbetam®, Pfizer, UK). 0.9% saline was infused at a rate of 60ml/H to provide an equivalent fluid load to other interventions.

4.2.3.3 Glucose Elevation

A euglycaemic hyperinsulinaemic clamp was used, as described in 2.1.2 page 58. Insulin (Actrapid™, Novo, Denmark) was infused at 0.8 mUnits/kg/min with an infusion of 20% Glucose titrated to maintain blood glucose measurements at around the baseline for participants.

Samples of venous blood were taken from a venous cannula up to every 5 minutes and tested with a point-of-care device (Freestyle Optimum Neo, Abbot, UK).

4.2.4 CMR study and protocol

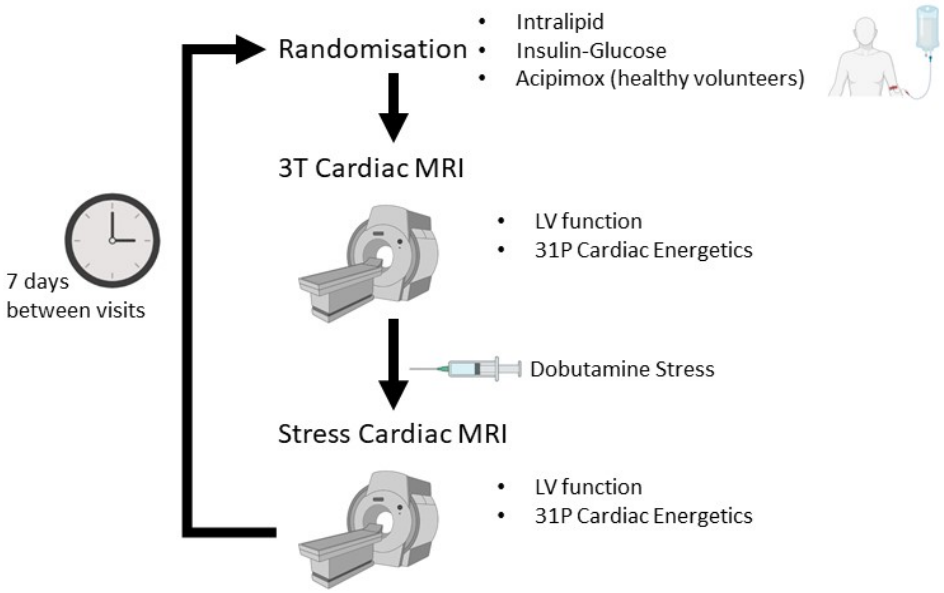

***Figure 4.1**: Summary diagram of CMR study*

The study is summarised in figure 4.1 Healthy volunteers attended for three visits, receiving one of acipimox, Intralipid or insulin-glucose infusions on each visit, the order determined via randomisation through a tool available on www.randomizer.org. Participants with heart failure attended for two visits and only receive Intralipid or insulin-glucose, again the order determined at random. There was an interval of at least 7 days between visits. Each visit would took place either in the morning following an overnight fast or in the afternoon following an early breakfast and fasting thereafter (minimum 9 hours).

4.2.4.1 Baseline Measurements

Baseline anthropometric measurements were collected at the first visit (height, weight, baseline blood pressure, hip-to-waist ratio) and a 12-lead ECG. In the case of the participants with heart failure, baseline cardiac volumes and phosphorus spectroscopy was carried out prior to metabolic interventions.

4.2.4.2 Substrate Manipulation

The euglycaemic clamp, Intralipid/heparin infusion or administration of acipimox occurred 1 hour prior to the start of the CMR protocol.

4.2.4.3 CMR protocol

More technical information on each segment of the protocol was described in 2.3 page 61. All scans were performed on a Siemens 3T Tim Trio system (Erlangen, Germany). The protocol ran in the following order:

4.2.4.3.1 31-Phosphorus 3D Chemical Shift Imaging

Subjects lay prone with their left ventricle positioned above the centre of a modified Heart-Liver ^{31}P coil at magnet iso-centre. Proton localisers and free induction decay inversion recovery curves were acquired. A 3D acquisition-weighted chemical shift imaging (CSI) was used: acquisition matrix size 16 x 16 x 8, FOV 240 x 240 x 200 mm, 10 averages at the centre of k-space, 1690 total acquisitions, voxel size 5.6ml, centred on a basal septal voxel with saturation bands over

chest wall and liver. The basal septal voxel was analysed with an in-house Matlab package (Matlab compiler runtime version 8.3, Mathworks, USA) and PCr/ATP ratio calculated using the average of the three ATP peaks.

4.2.4.3.2 Cardiac Volumes and Function

Using a 24 channel spine matrix and 6 channel body matrix steady state free precession cardiac volumes were acquired with long axis (HLA and VLA) and short axis (a short axis stack) during end-expiration breath hold. Manual contouring of the images at end-systole and end-diastole was performed using cvi42 version 5.10.1 (Circle Cardiovascular Imaging Inc, Calgary, Alberta, Canada).

4.2.4.3.3 Assessment of Creatine Kinase pseudo first order rate constant with Triple Repetition Saturation Transfer (TRIST)

The subject was positioned supine with a 10cm ^{31}P surface coil over their heart at magnet isocentre. Proton localisers were used to confirm position and a 1D-CSI sequence run prior to the main TRiST acquisition in order to scout the centre frequency and offsets for saturation pulses. The four Trist sequences (15s TR, 1.5s TR with γATP saturation, 9.5s TR with γATP saturation and 15s TR with control saturation, as outlined in chapter 2, section 2.3.3.

4.2.4.4 Blood Sampling

Baseline blood samples were taken one hour after substrate manipulation commenced. Venous blood was drawn during the experiments and sent for biochemical analysis of β-hydroxybutyrate, insulin, glucose and free fatty acids.

4.2.5 Invasive Study

The invasive sampling protocol is as set out in 2.4 page 75 and summarised in figure 4.2.

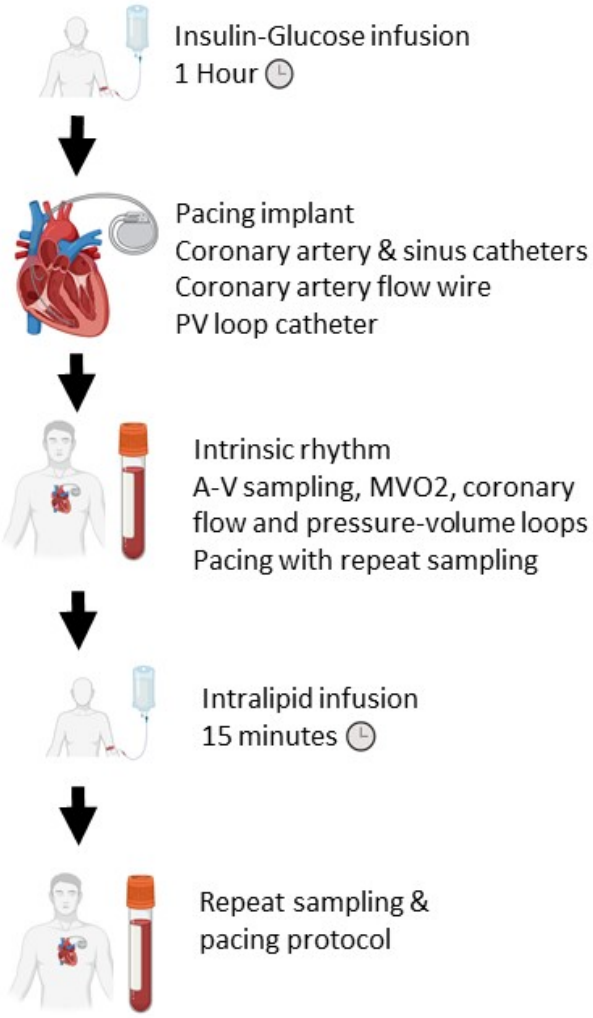

***Figure 4.2**: Invasive study summary diagram*

Participants were fasted overnight prior to the study. An hour prior to the pacemaker implant starting, a euglycaemic hyperinsulinaemic clamp was started (as per the description in 2.1.2 page 58). Once the pacemaker implant was complete, the coronary sinus and coronary artery

catheters, flow wire and impedance catheter were positioned. Sampling was undertaken in intrinsic rhythm and with rapid atrial (stress) pacing (see chapter 5 page 192). Pressure and volume measurements were also conducted during biventricular pacing as a comparator.

The euglycaemic clamp was then discontinued, a 60ml/H Intralipid infusion started and following 15 minutes, the pacing and sampling protocol was repeated.

4.3 Results

4.3.1 Healthy Volunteers

4.3.1.1 Baseline demographics

Demographic data is displayed in table 4.1. 10 volunteers were recruited, 3 of whom were male.

***Table 4.1**: Baseline Characteristics of the healthy volunteers*

	Mean	***Range***
Age	41	24-79
Height (m)	1.69	1.57-1.92
Weight (kg)	67	53-85
BMI (kg/m^2)	23.4	20.6-27.1
Hip:Waist Ratio	1.26	1.13-1.54

The volumes infused were not significantly different between groups (acipimox 214 ± 18 ml, insulin-glucose 234 ± 81 ml, Intralipid 259 ± 21 ml, $p = 0.14$).

4.3.1.2 Circulating Metabolites

Circulating metabolites prior to scanning are displayed in table 4.2 and figure 4.3. Free fatty acids were significantly elevated in the Intralipid group and low in the Acipimox and Insulin/Glucose groups, although not significantly different between the latter two groups. Glucose was lowest in the insulin/glucose group (relating to the pre-specified blood glucose level at which the euglycaemic clamp was set) and the acipimox group showed marginally higher levels than the Intralipid group. Insulin was highest in the insulin/glucose group and not significantly different

between the other two groups. Lactate was not significantly different between groups. Beta-hydroxybutyrate was elevated in the Intralipid group only.

Table 4.2: *Circulating venous metabolites 1hr after Acipimox, Insulin+Glucose infusion or Intralipid infusion.*

	Acipimox	***Insulin+Glucose***	***Intralipid***	***p-value*** (ANOVA)
NEFA (mmol/L)	0.09 ± 0.08	0.13 ± 0.10	3.06 ± 0.65	<0.0001
Glucose (mmol/L)	4.62 ± 0.4	3.29 ± 0.39	4.2 ± 0.34	<0.0001
Insulin (pmol/L)	36.3 ± 17.4	166 ± 67.0	39.0 ± 11.1	<0.0001
Lactate (mmol/L)	1.00 ± 0.29	1.03 ± 0.23	0.92 ± 0.18	0.48
BOHB (mmol/L)	0.01 ± 0.04	0.00 ± 0.00	0.50 ± 0.24	<0.0001

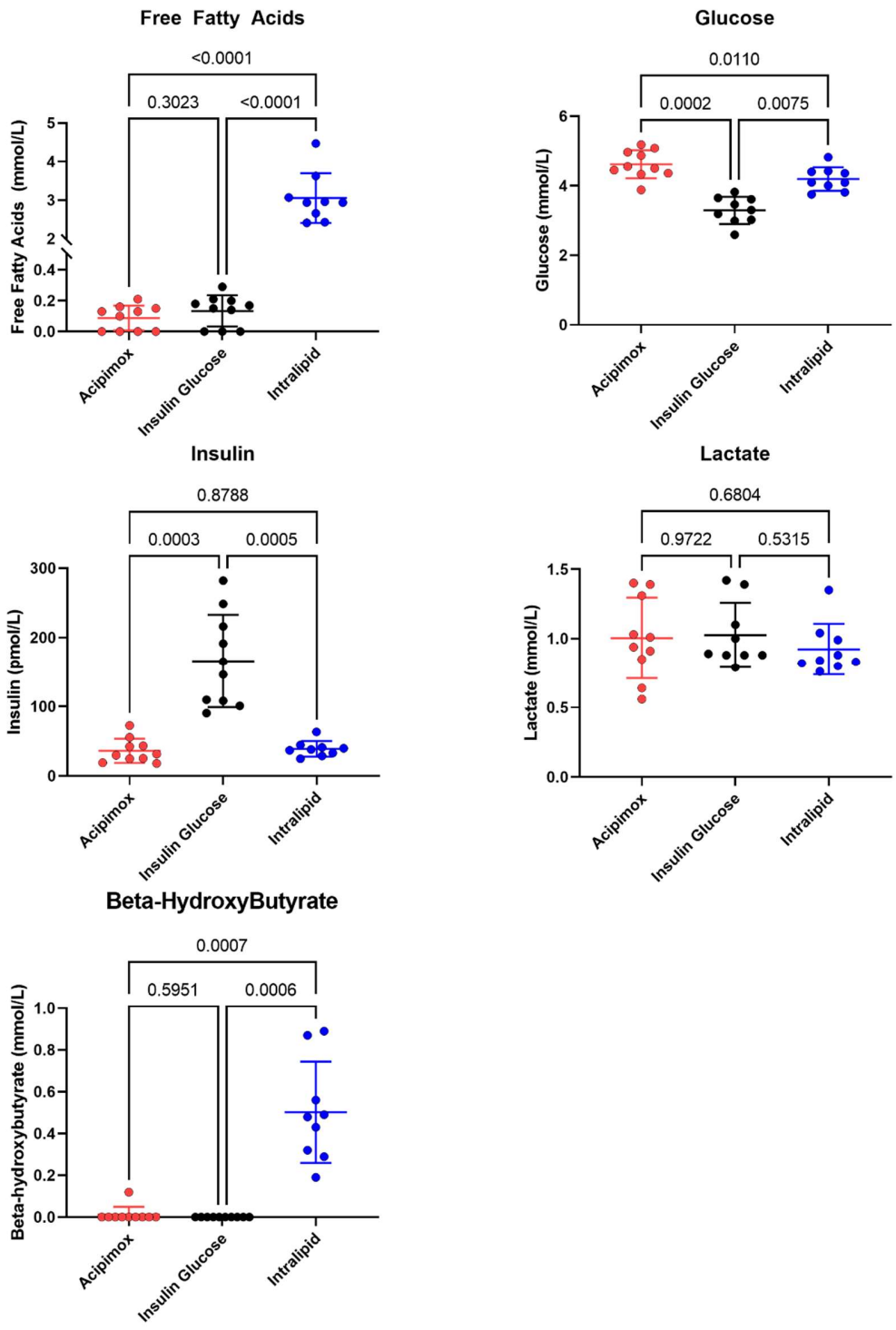

***Figure 4.3**: Circulating venous metabolites 1hr after Acipimox, Insulin+Glucose infusion or Intralipid infusion.*

4.3.1.3 Left Ventricular Volumes and Function

See table 4.3 and figure 4.4. In general, contractility was greater with Intralipid, seen with higher LV ejection fraction and LV stroke volume, lower LV end systolic volume and a trend towards higher cardiac output and cardiac index, but no significant differences between acipimox and insulin-glucose groups. In terms of strain measurements, only global radial strain showed a significant difference between arms (which mirrored the ejection fraction). Importantly, there were no significant differences in LV end diastolic volume.

***Table 4.3**: Left ventricular volumes and function in healthy volunteers*

	Acipimox	***Insulin+ Glucose***	***Intralipid***	***p-value (ANOVA)***
LVEF (%)	57.3 ± 3.1	58.1 ± 3.8	63 ± 3.4	***0.001***
LV-End Diastolic Volume (ml)	161 ± 25	153 ± 26	159 ± 31	0.10
LV-End Systolic Volume (ml)	69 ± 13	64 ± 12	59 ± 14	***<0.001***
LV-Stroke Volume (ml)	92 ± 14	89 ± 16	100 ± 19	***0.02***
Cardiac Output (L/min)	5.01 ± 0.84	4.94 ± 0.65	5.98 ± 1.18	***0.01***
Cardiac Index ($L/min/m^2$)	2.85 ± 0.46	2.8 ± 0.33	3.4 ± 0.64	***0.02***
3D Global Circumferential Strain (%)	-19.6 ± 4.0	-19.4 ± 1.7	-20.8 ± 2.6	0.55
3D Global Radial Strain (%)	35.2 ± 9.5	40.8 ± 7.2	45.1 ± 12.4	***0.01***
3D Global Longitudinal Strain (%)	-17.1 ± 2.4	-15.8 ± 2.6	-17.7 ± 2.4	0.28

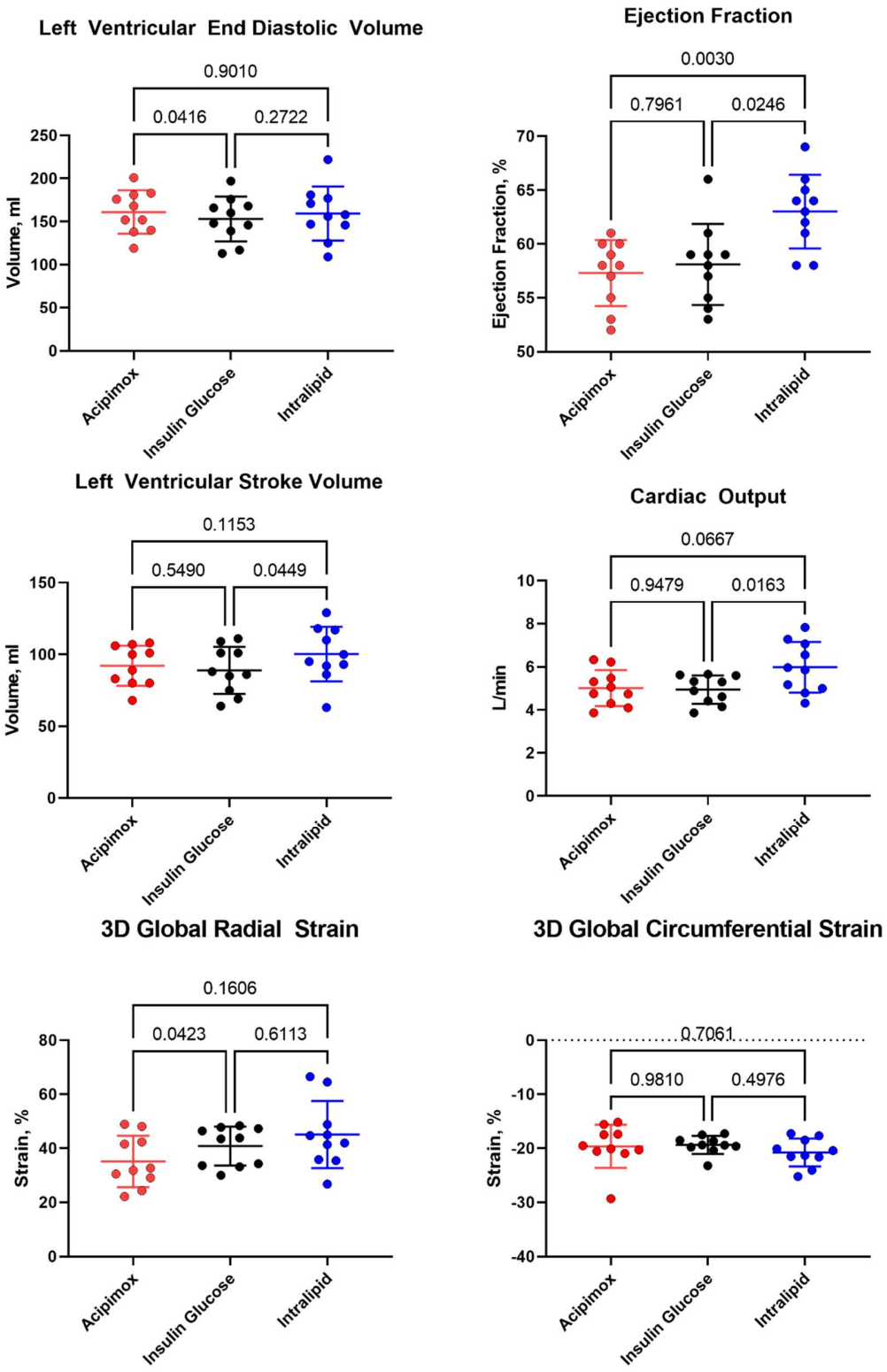

***Figure 4.4**: Left ventricular volumes and function in healthy volunteers*

4.3.1.4 Right Ventricular Volumes and Function

Here, the trends were the same as those seen in the LV with EF and SV being higher during Intralipid. However, statistically there were no significant differences seen in right ventricular function or volume between infusions. This may well be due to the larger variance in RV contouring measures (seen globally, e.g. in Hudsmith et al[337]) which would require a greater sample size to delineate differences than LV analysis.

Table 4.4: *Healthy Volunteer Right Ventricular Contractility and Volumes during substrate manipulation. RV, right ventricle; EF, ejection fraction; EDV, end diastolic volume; ESV, end systolic volume; SV, stroke volume*

	Acipimox	***Insulin + Glucose***	***Intralipid***	***p-value (ANOVA)***
RVEF (%)	62.7 ± 4.6	61.8 ± 6.3	64.4 ± 6.5	0.24
RV-EDV (ml)	147 ± 29	147 ± 34	151 ± 37	0.75
RV-ESV (ml)	56 ± 16	57 ± 21	55 ± 21	0.75
RV-SV (ml)	91 ± 14	90 ± 16	95 ± 18	0.77

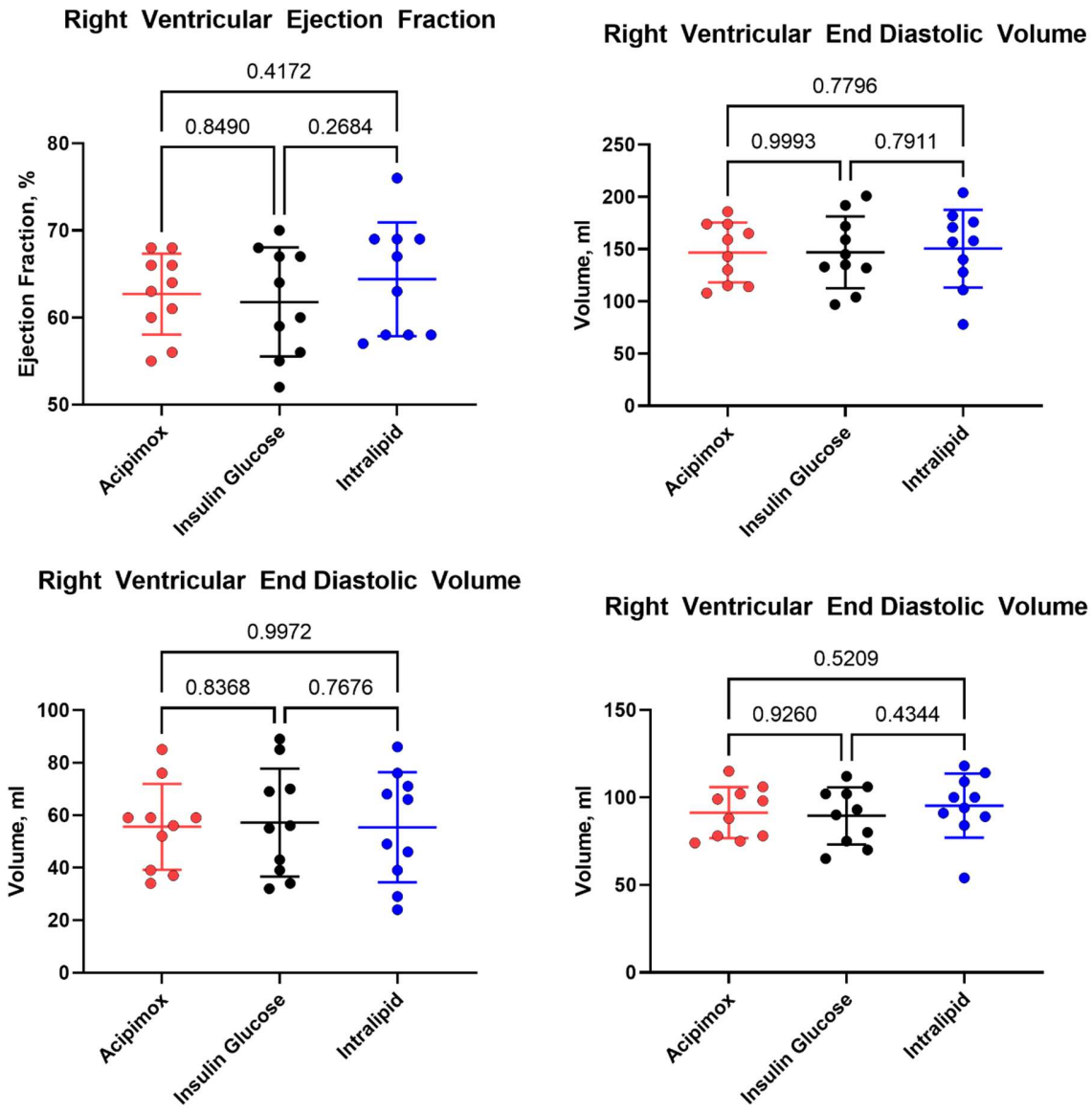

Figure 4.5: *Healthy Volunteer Right Ventricular Volumes and Function during substrate manipulation*

4.3.1.5 Haemodynamics and Calculated Cardiac Work

Haemodynamics and calculated cardiac work are displayed in table 4.5 and figure 4.6. There was a trend towards a higher systolic blood pressure with Intralipid. Stroke work (calculated as the product of systolic blood pressure and stroke volume) showed a trend towards being lowest in the Intralipid group and highest with acipimox, however this trend was reversed in cardiac work (calculated as the product of systolic blood pressure, stroke volume and heart rate), with Intralipid cardiac work being significantly higher than that of the insulin-glucose group, although the acipimox and insulin-glucose infusions produced similar cardiac work. There were no significant trends, however, with rate pressure product.

Table 4.5: *Healthy Volunteer Haemodynamics and calculated cardiac work during substrate manipulation*

	Acipimox	***Insulin + Glucose***	***Intralipid***	***p-value (ANOVA)***
Systolic Blood Pressure (mmHg)	115 ± 15	115 ± 13	127 ± 25	0.37
Heart Rate (bpm)	59 ± 9	58 ± 10	62 ± 12	0.31
Stroke work (mmHg.ml)	5678 ± 1148	5348 ± 1024	5007 ± 1132	***0.03***
Cardiac work (mmHg.ml/min x 10^3)	419 ± 121	419 ± 97	508 ± 106	***0.02***
Rate Pressure Product (mmHg.bpm)	6806 ± 1276	6659 ± 1882	7961 ± 1380	0.16

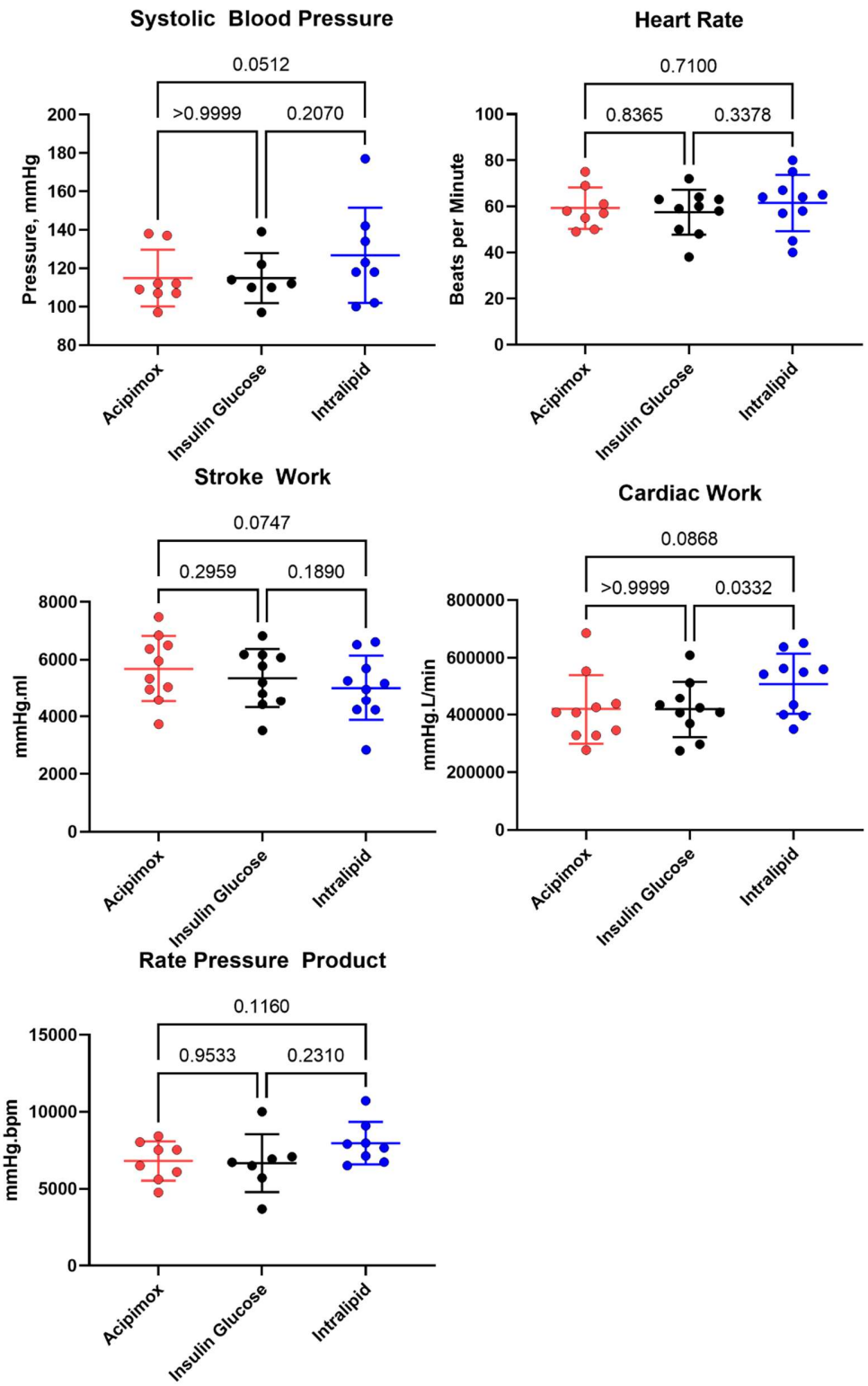

Figure 4.6: *Healthy Volunteer Haemodynamics and calculated cardiac work during substrate manipulation*

4.3.1.6 31-Phosphorous Magnetic Resonance Spectroscopy

Results for ^{31}P MRS are shown in table 4.6 and figure 4.7. PCr/ATP values were higher in the insulin-glucose group and lower in the acipimox group, with the Intralipid group sitting in between but not significantly different from the other two groups. The pseudo first-order creatine kinase forward rate constant was significantly higher in the Intralipid group, with the acipimox values sitting in between but not significantly different from the other two groups. Creatine kinase flux (calculated as the product of PCR x CK_{kf}, with PCr calculated as PCr/ATP x 5.7, a literature reference value for [ATP] in the healthy heart [135]) was significantly higher in the Intralipid group than the insulin glucose group, with acipimox again sitting between but not significantly different from the other two groups. The ratio of cardiac work to CK flux was not significantly different during the different interventions within the healthy heart group (acipimox 2.08 ± 1.82, Insulin-glucose 2.1 ± 1.23, Intralipid 1.9 ± 1.28, ANOVA p-value 0.69, p-values between groups all >0.9).

There were no significant correlations between PCr/ATP and resting cardiac work (rate pressure product R^2 0.06, p 0.24; cardiac index R^2 0.004, p 0.57; ejection fraction R^2 0.03, p 0.38) across all three infusions.

***Table 4.6**: Normal Heart ^{31}P MRS data for PCr/ATP, CK k_f and CK Flux during the different substrate altering interventions*

	Acipimox	***Insulin-Glucose***	***Intralipid***	***p-value***
PCr/ATP ratio	1.82 ± 0.29	2.05 ± 0.3	1.98 ± 0.34	0.138
CK Rate Constant (/s)	0.29 ± 0.11	0.21 ± 0.09	0.34 ± 0.13	***0.024***
CK Flux (μmol/g/s)	2.77 ± 1.06	2.37 ± 0.93	3.45 ± 1.48	0.051

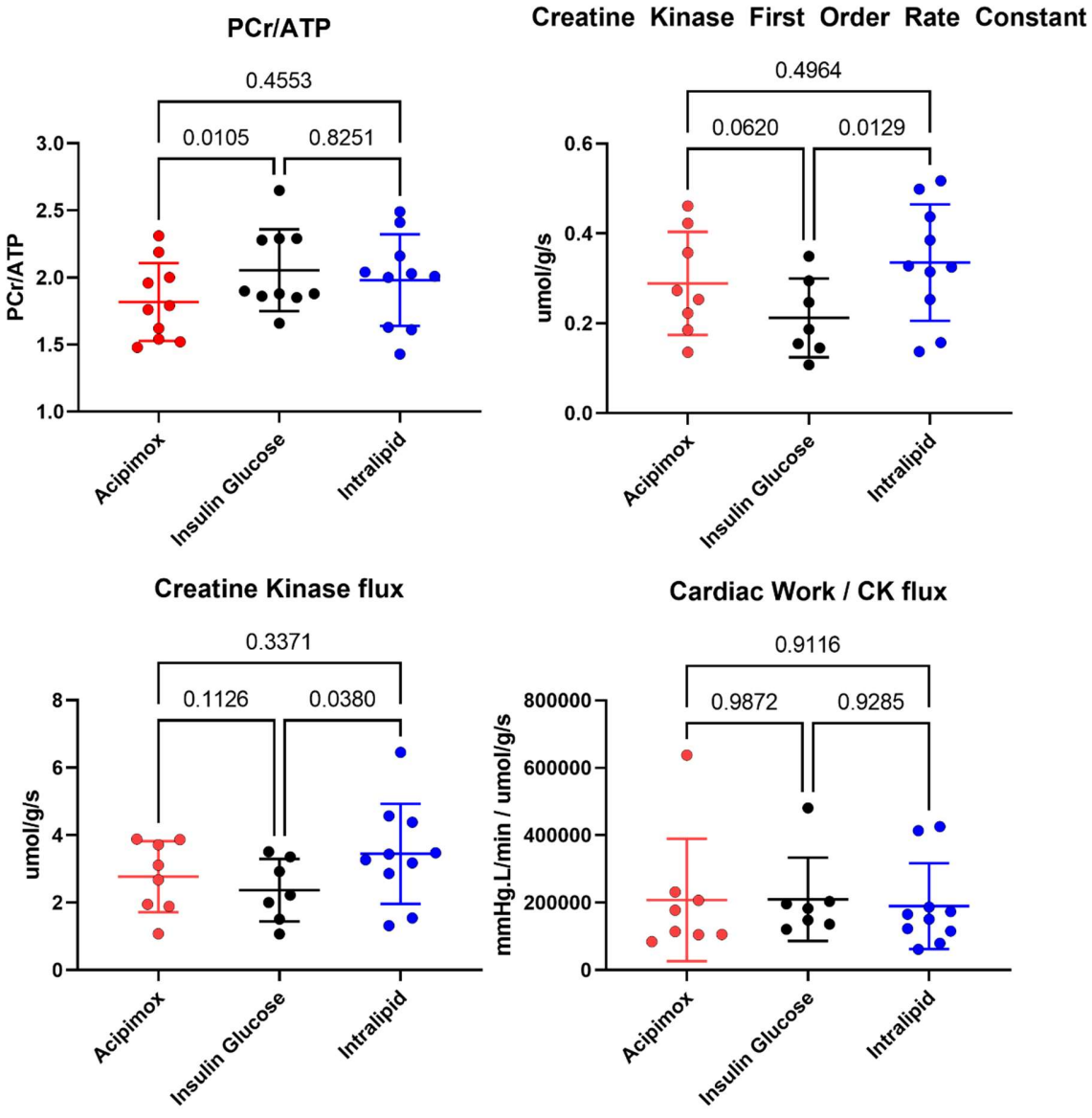

***Figure 4.7**: Normal Heart ^{31}P MRS data for PCr/ATP, CK k_f and CK Flux during the different substrate altering interventions*

4.3.2 Heart Failure

4.3.2.1 Baseline Demographics

Demographic data for the group is presented in table 4.7. 20 volunteers were recruited, 7 of whom were female. Compared to the healthy volunteers, those recruited with heart failure were older (vs 41.3 ± 19.7 years old, p = 0.001), had a trend towards higher BMI (vs 23.4 ± 2.6, p =0.06) and were more likely to be male.

Table 4.7. *Baseline data for the Heart Failure cohort*

	Mean	***Range***
Age	63	38-79
Height (m)	1.72	1.57-1.9
Weight (kg)	78.4	51.8-95
BMI (kg/m^2)	26.7	18.6-37.6
Hip:Waist Ratio	1.11	0.98-1.34
Baseline LV ejection fraction (%)	34.9	18-48
NYHA class	II	II-III
Baseline systolic BP (mmHg)	127	100-156
Baseline diastolic BP (mmHg)	68	55-98

The cohort were on maximum tolerated doses of goal directed medical therapy for heart failure, as shown below in table 4.8.

Table 4.8: *Drug therapy in heart failure cohort*

Drug Class	***Number (Proportion) of Participants***
Diuretic	9 (45%)
ACE inhibitor / ARB	10 (50%)
Beta-blocker	17 (85%)
ARNI	10 (50%)
Aldosterone Antagonist	16 (80%)

4.3.2.2 Circulating Metabolites

Metabolites were measured once a baseline state was established, i.e. an hour into the infusion. As expected, the Intralipid infusion elevated circulating free fatty acids. Insulin was higher with insulin-glucose infusion. Again, β-hydroxybutyrate was higher with an Intralipid infusion.

***Table 4.9**: Venous Circulating Metabolites one hour into infusion in the heart failure group*

	Insulin + Glucose	***Intralipid***	***p-value***
Free Fatty Acids (mmol/L)	0.23 ± 0.2	2.96 ± 1.77	***<0.001***
Glucose (mmol/L)	4.97 ± 0.86	5.5 ± 0.69	0.06
Insulin (pmol/L)	357 ± 214	91 ± 65	***<0.001***
Lactate (mmol/L)	1.16 ± 0.21	1.17 ± 0.34	0.75
Beta-hydroxybutyrate (mmol/L)	0.01 ± 0.04	0.41 ± 0.42	***0.01***

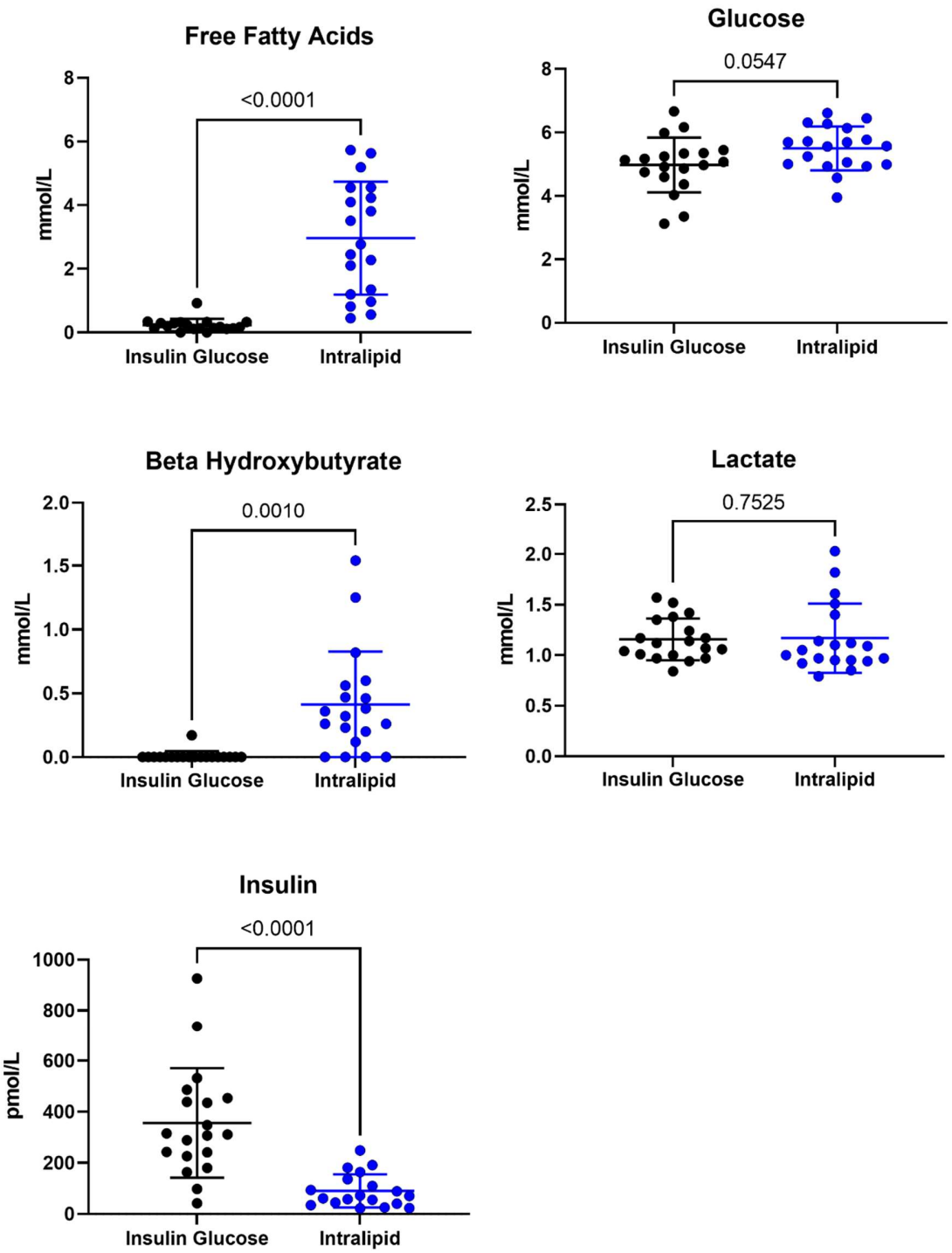

Figure 4.8: *Venous metabolites and Insulin 1 hour after substrate altering intervention in the heart failure group*

4.3.2.3 Left Ventricular Volumes and Function

See table 4.10 and figure 4.9. Contractility, if assessed by LV ejection fraction, was highest in the Intralipid group, representing an average increase of 5% over the pre-intervention values in absolute terms, with insulin-glucose not significantly differing from basal conditions. This was driven by a difference in end systolic volume, with end diastolic volume not significantly differing between the interventions, suggesting contractility differences was the main determinant of LVEF change. There was a trend towards greater radial and circumferential strain values in the Intralipid arm, with it being significantly different to insulin-glucose but not when compared to the baseline.

Table 4.10: *The effect of substrate manipulation on left ventricular volumes and function in the heart failure cohort*

	Baseline	***Insulin + Glucose***	***Intralipid***	***p-value (ANOVA)***
LVEF (%)	34.9 ± 9.1	33.7 ± 8.2	39.9 ± 9.3	***<0.001***
LV-EDV (ml)	254 ± 81	258 ± 83	250 ± 83	0.37
LV-ESV (ml)	166 ± 73	176 ± 74	156 ± 75	***<0.001***
LV-SV (ml)	80 ± 25	83 ± 23	93 ± 22	***<0.001***
Cardiac Output (L/min)	5.54 ± 1.6	5.43 ± 1.37	6.48 ± 1.36	***<0.001***
Cardiac Index (L/min/m^2)	2.92 ± 0.79	2.83 ± 0.63	3.39 ± 0.7	***<0.001***
3D Global Circumferential Strain (%)	-10.8 ± 3.1	-10 ± 2.5	-11.2 ± 3.3	0.138
3D Global Radial Strain (%)	15.5 ± 5.9	15.6 ± 7	17.4 ± 6.8	0.272
3D Global Longitudinal Strain (%)	-6.6 ± 2.8	-7 ± 3.4	-6.7 ± 4.5	0.79

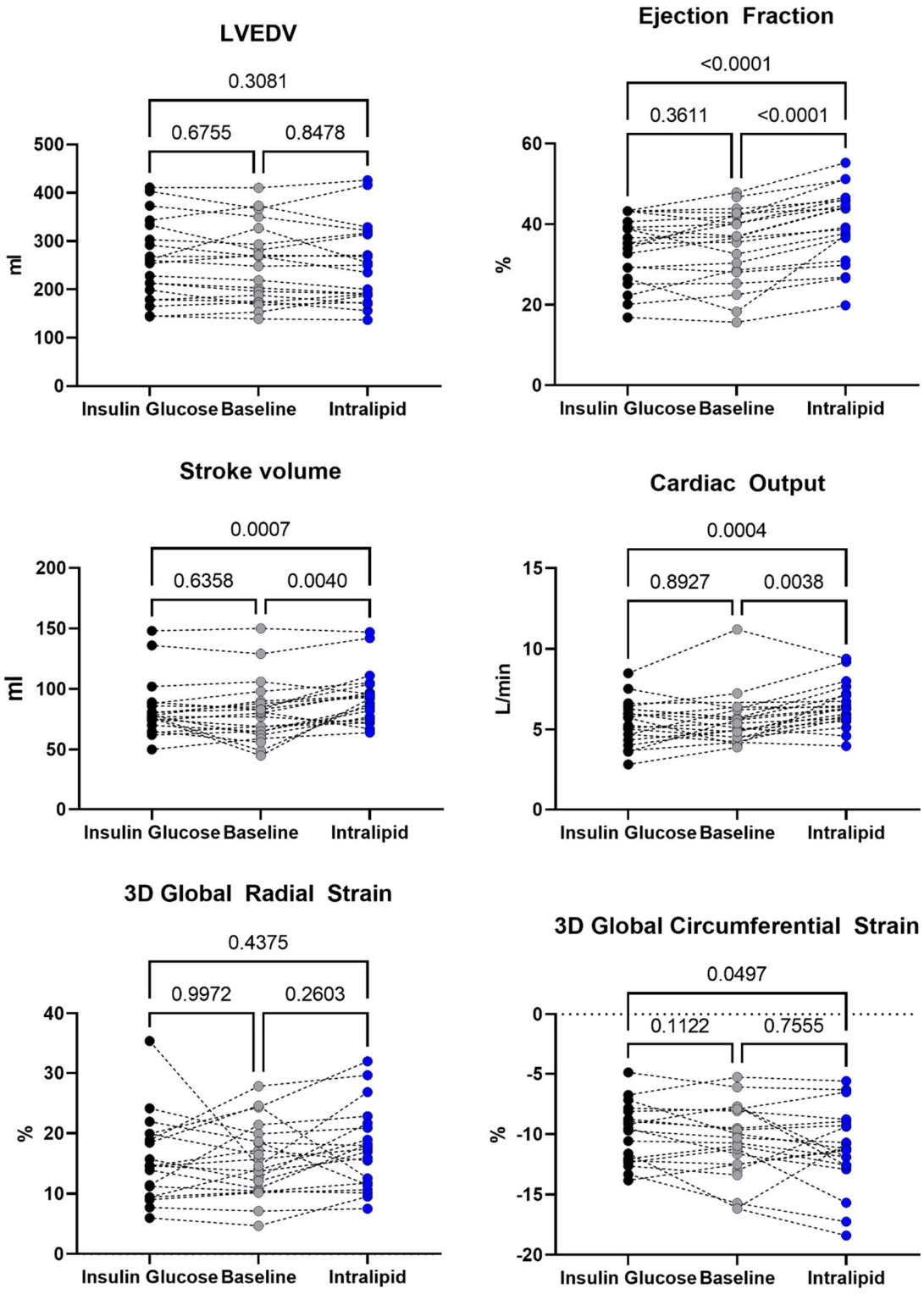

Figure 4.9: *The effect of substrate manipulation on left ventricular volumes and function in the heart failure cohort*

4.3.2.4 Right Ventricular Contractility and Volumes

See table 4.11 and figure 4.10. Like in the left ventricle, ejection fraction was highest with Intralipid and not significantly different from baseline with insulin-glucose. RV end diastolic volume did not significantly differ across the interventions and the increased ejection fraction was driven by a reduced end systolic volume. The matched increase in stroke volume across the ventricles would suggest the LV changes are not driven by increases in e.g. valvular regurgitation.

Table 4.11: *The effect of substrate manipulation on right ventricular volumes and function in the heart failure cohort.*

	Baseline	***Insulin + Glucose***	***Intralipid***	***p-value (ANOVA)***
RVEF (%)	50.3 ± 11.6	51.5 ± 10.2	56.8 ± 10.4	***0.02***
RV-EDV (ml)	158 ± 45	161 ± 48	161 ± 42	0.58
RV-ESV (ml)	82 ± 42	81 ± 40	73 ± 39	0.063
RV-SV (ml)	76 ± 18	80 ± 18	88 ± 15	***<0.01***

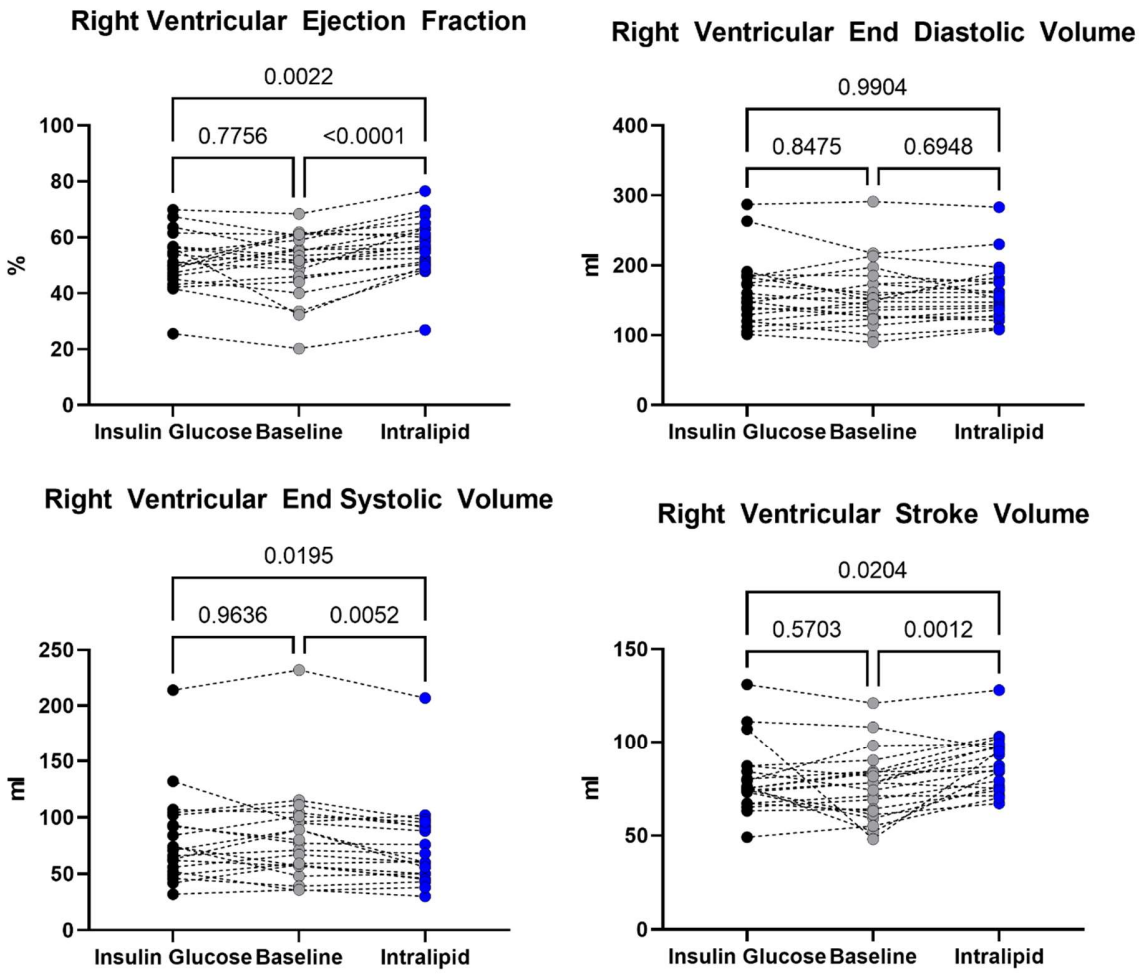

***Figure 4.10**: The effect of substrate manipulation on right ventricular volumes and function in the heart failure cohort*

4.3.2.5 Haemodynamics and Calculated Cardiac Work

See table 4.12 and figure 4.11. There was a trend towards a lower heart rate, cardiac work and rate pressure product in the insulin-glucose arm and higher in the Intralipid arm. Blood pressure was not significantly different.

Table 4.12: *Haemodynamics and calculated cardiac work during substrate manipulation in heart failure*

	Baseline	***Insulin + Glucose***	***Intralipid***	***p-value (ANOVA)***
Systolic Blood Pressure (mmHg)	125 ± 17	119 ± 20	122 ± 20	0.27
Heart Rate (bpm)	69 ± 12	65 ± 12	69 ± 13	***0.03***
Stroke work (mmHg.ml)	5877 ± 2297	5590 ± 1692	6151 ± 1737	0.08
Cardiac work (mmHg.ml/min x 10^3)	495 ± 169	466 ± 148	549 ± 163	***0.02***
Rate Pressure Product (mmHg.bpm)	8432 ± 1646	7736 ± 2014	8419 ± 2378	0.10

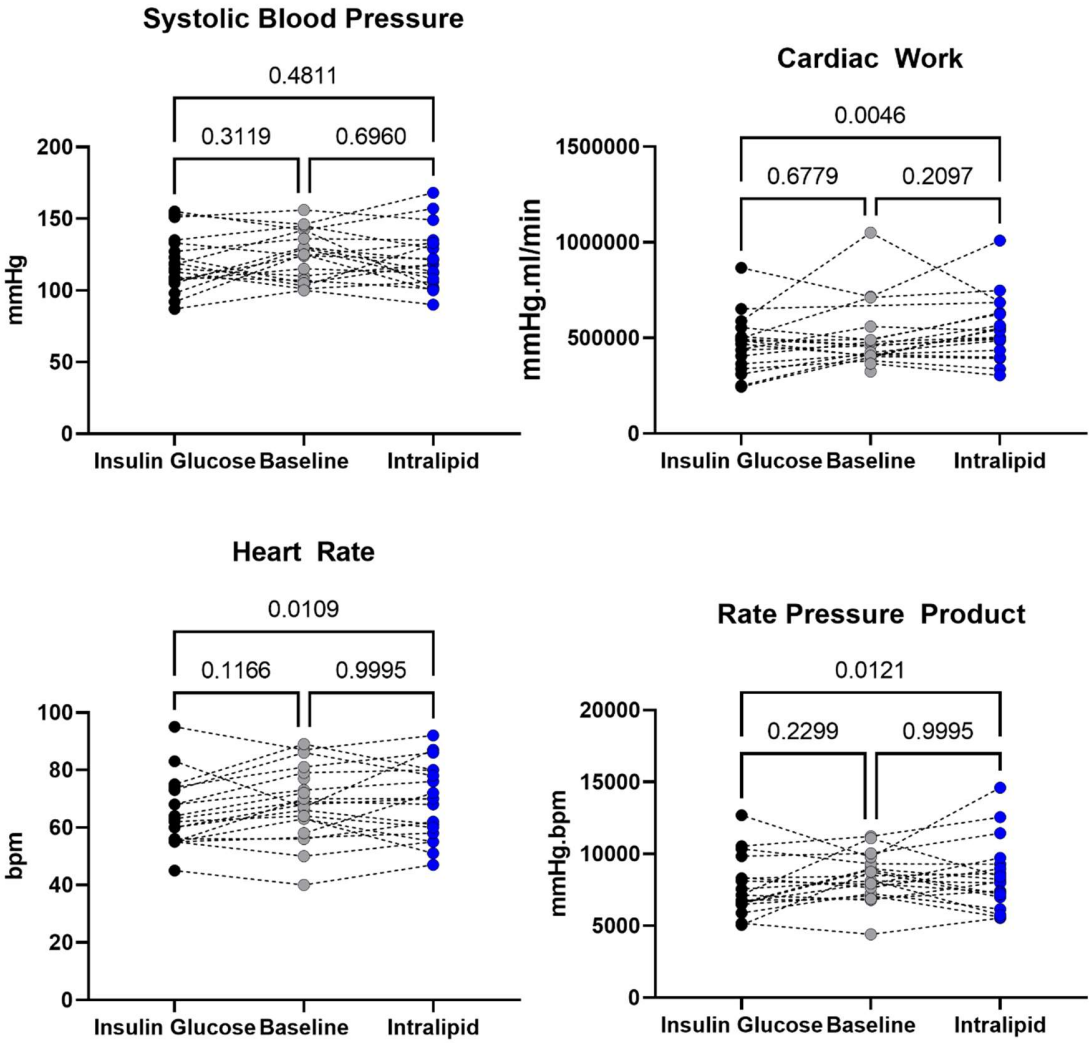

Figure 4.11: *Haemodynamics and calculated cardiac work during substrate manipulation in heart failure*

4.3.2.6 31-Phosphorus Magnetic Resonance Spectroscopy

PCr/ATP was higher in the Intralipid arm than in the Insulin-glucose arm. For 9 participants, baseline (pre infusion) PCr/ATP data was available, however there were no significant differences when compared with the two invasive arms. Creatine kinase pseudo first order rate constant and creatine kinase flux were not significantly different between the two arms.

Table 4.13: *Heart failure cohort ^{31}P MRS data for PCr/ATP, CK k_f and CK Flux during the different substrate altering interventions*

	Insulin-Glucose	***Intralipid***	***p-value***
PCr/ATP ratio	1.86 ± 0.25	2.01 ± 0.33	***0.02***
CK Rate Constant (/s)	0.201 ± 0.132	0.229 ± 0.19	0.53
CK Flux (μmol/g/s)	1.87 ± 1.16	2.36 ± 2.32	0.33

Table 4.14: *Heart failure cohort ^{31}P MRS data for PCr/ATP for subjects where matched baseline data was available.*

	Baseline	***Insulin-Glucose***	***Intralipid***	***p-value***
PCr/ATP ratio	2.04 ± 0.48	1.88 ± 0.25	2.03 ± 0.39	0.39

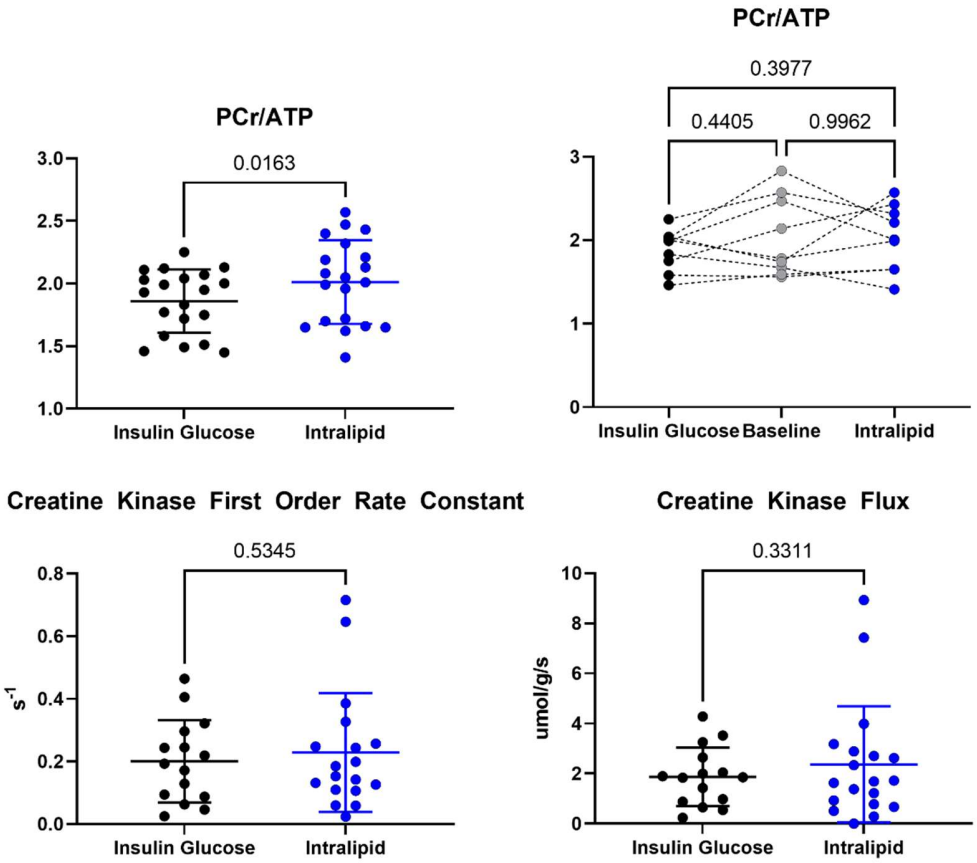

Figure 4.12: *Heart failure cohort ^{31}P MRS data for PCr/ATP, CK k_f and CK Flux during the different substrate altering interventions*

There were significant positive correlations between PCr/ATP at rest and several resting values of cardiac contractility: cardiac output (R^2 0.12, p = 0.018), cardiac index (R^2 0.19, p 0.007) or rate pressure product (R^2 0.17, p = 0.005), however not with ejection fraction (R^2 0.03, p = 0.19), see figure 4.12.

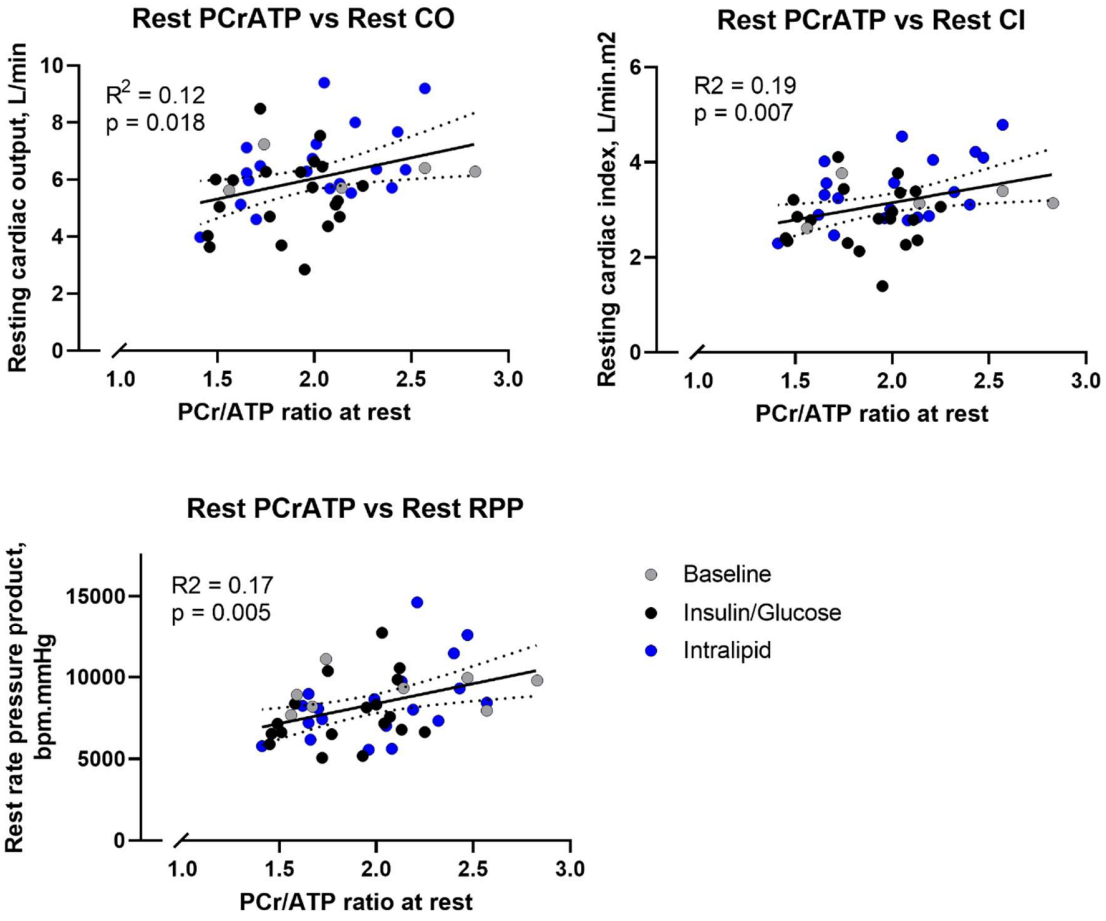

Figure 4.13: *Correlations between PCr/ATP and resting measures of left ventricular contractility in the heart failure cohort during substrate manipulation.*

4.3.3 Comparisons between Healthy Volunteers and Heart Failure Patients and Pooled Data

4.3.3.1 PCr/ATP

See figure 4.14. PCr/ATP ratio was not significantly different between the healthy and heart failure groups receiving Intralipid, however in the heart failure group it was trended towards being lower during insulin-glucose infusion.

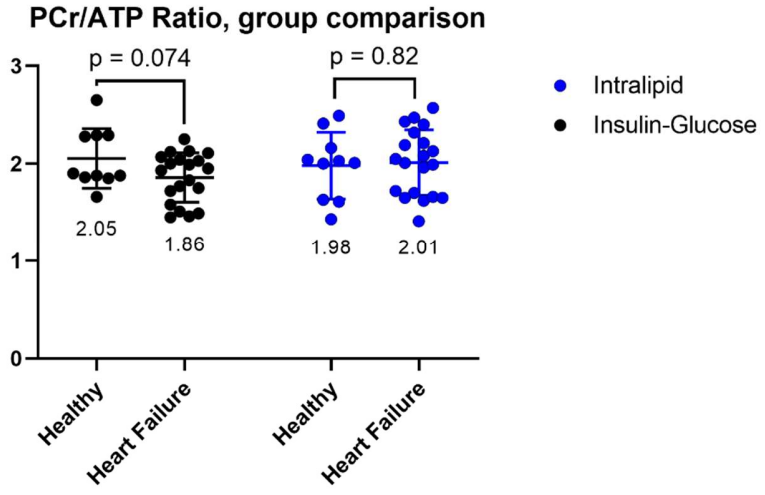

***Figure 4.14**: PCr/ATP comparison between healthy and heart failure groups receiving insulin-glucose and Intralipid infusions. Mean for each group is displayed.*

4.3.3.2 Creatine Kinase First Order Forward Rate Constant and Creatine Kinase Flux

See figure 4.15. Flux and rate constant were not significantly different between healthy and heart failure groups given insulin-glucose infusions, but in the healthy volunteers, they were both significantly higher than the healthy group given the Intralipid infusion.

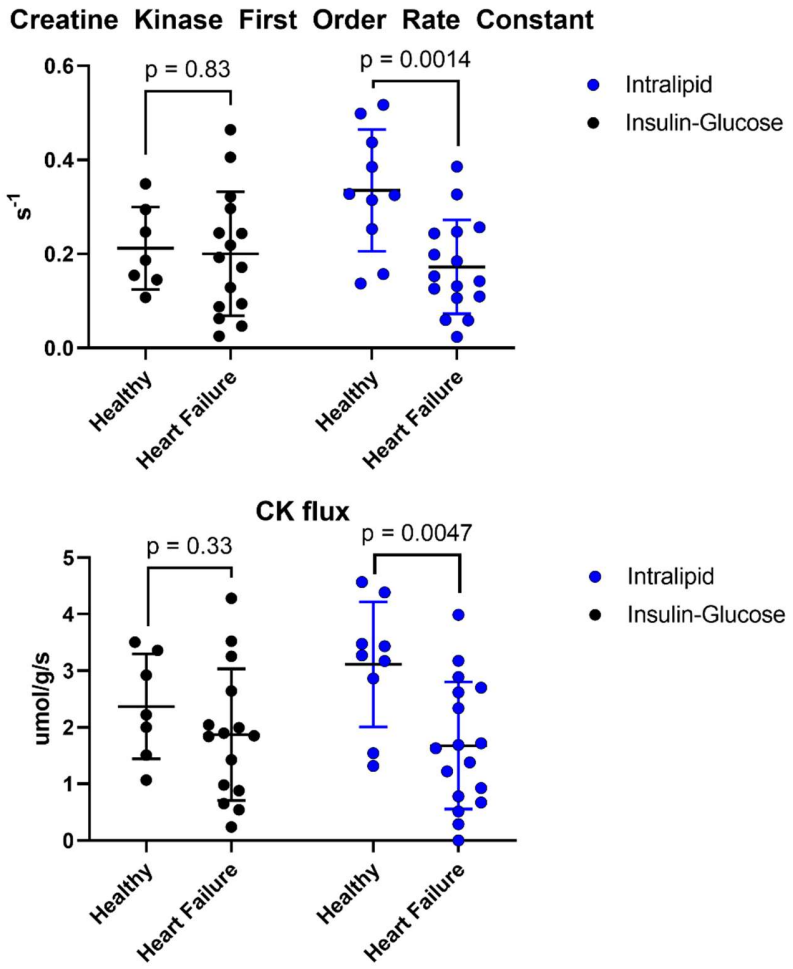

Figure 4.15*: Creatine kinase measurement comparison between healthy and heart failure groups receiving Intralipid and insulin-glucose infusions.*

4.3.3.3 Cardiac Work and Rate Pressure Product

There were no significant differences between groups by infusion arm in measures of contractility.

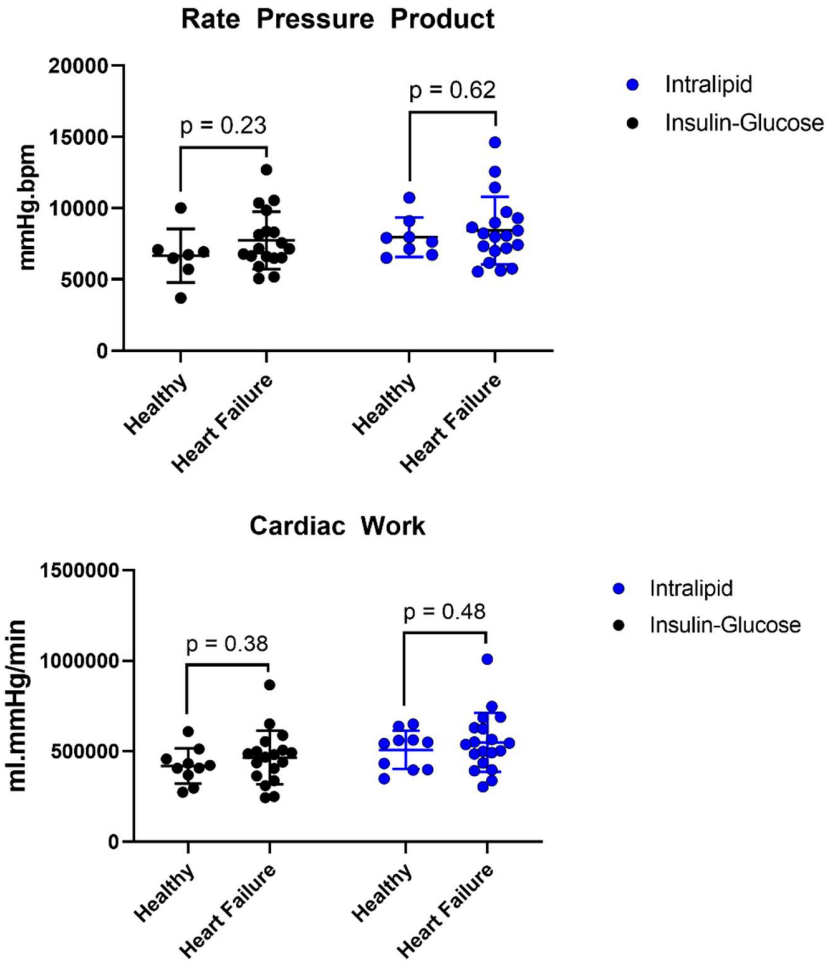

***Figure 4.16**: differences in rate pressure product and cardiac work by arms of the experiment.*

4.3.4 Invasive Data

4.3.4.1 Demographics

Baseline demographic data is displayed in table 4.15. 9 volunteers participated in this arm of the study, five of whom had participated in the CMR study. 5 were male and 4 female. There were no significant demographic differences from the invasive cohort in either demographics or medications.

Table 4.15: *Baseline Data for the Invasive subgroup*

	Mean	***Median***	***Range***
Weight (kg)	84.5	87.6	73-102
Height (m)	1.76	1.78	1.62-1.9
BMI (kg/m^2)	28.2	28.6	21.4-34.5
Hip: Waist Ratio	1.08	1.09	0.94-1.24
6 minute walk distance (m)	410	404	207-581
Baseline LVEF (%)	31	35	20-37
NYHA class	-	II	II-III

Table 4.16*: Medical therapy in the invasive group*

Drug	***Number (Proportion) of Participants***
Diuretic	7 (70%)
ACE inhibitor / ARB	3 (30%)
Beta-blocker	9 (90%)
ARNI	7 (70%)
Aldosterone Antagonist	6 (60%)

4.3.4.2 Metabolites

Data is shown in figure 4.17 and table 4.17. As expected, Intralipid significantly elevated serum free fatty acids and the insulin-glucose infusion significantly elevated serum insulin. As in the cardiac MR study, ketone bodies were produced during Intralipid infusion but were below the limit of assay detection during insulin-glucose. Lactate and glucose were not significantly different.

Table 4.17: *Left mainstem arterial metabolite concentrations in HFrEF during substrate manipulation in the invasive study*

	Insulin Glucose	***Intralipid***	***p-value***
Intrinsic rhythm			
Glucose (mmol/L)	5.34 ± 0.67	5.54 ± 0.79	0.49
Free Fatty Acids (mmol/L)	0.98 ± 0.57	3.29 ± 1.56	***0.001***
Insulin (pmol/L)	201 ± 85	52 ± 16.7	***<0.01***
Β-*Hydroxybutyrate* (mmol/L)	0	0.1 ± 0.15	0.08
Lactate (mmol/L)	0.75 ± 0.08	0.77 ± 0.19	0.69

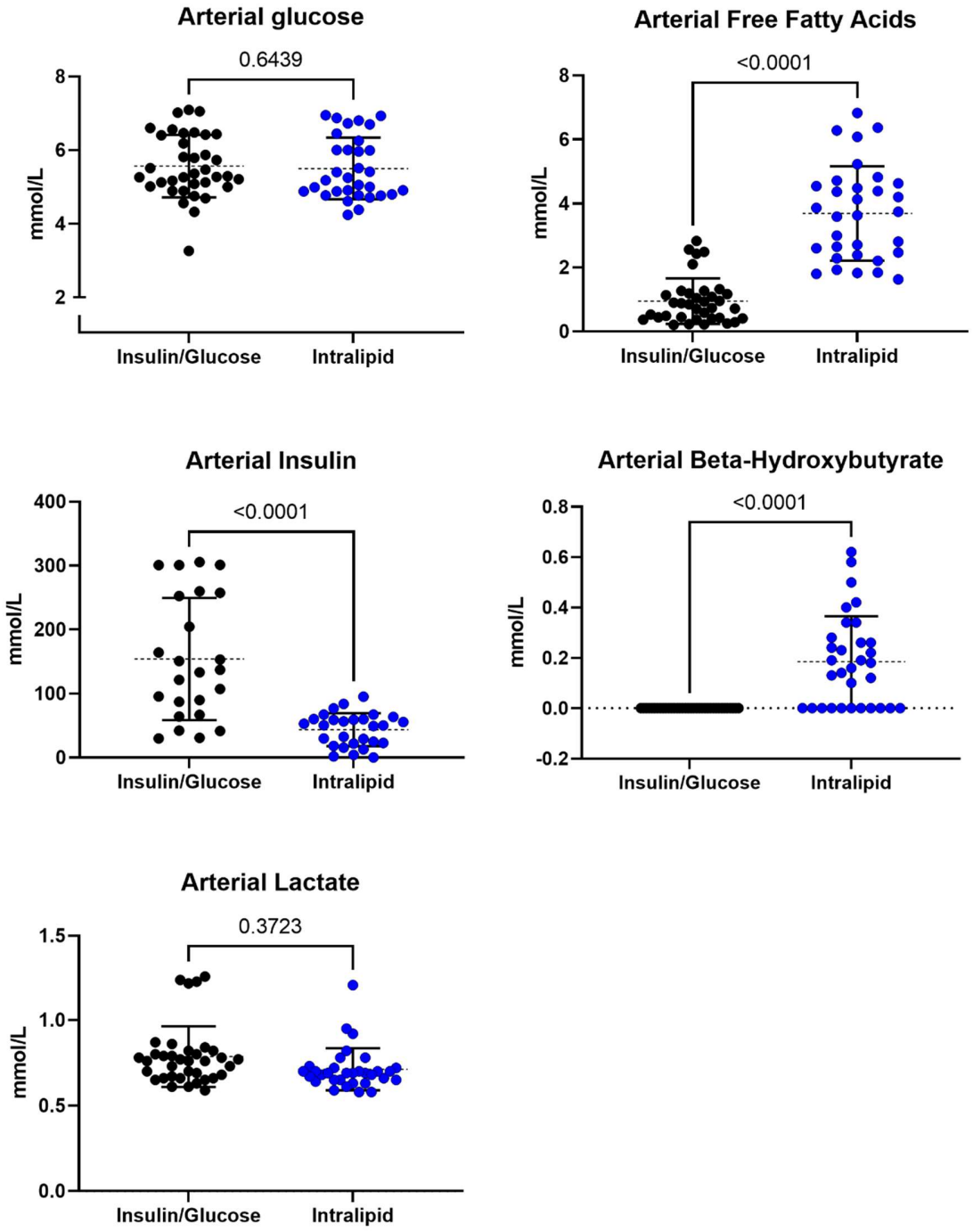

Figure 4.17: *Left mainstem arterial metabolite concentrations during substrate manipulation in the invasive study*

There was a positive correlation between coronary arterial free fatty acids in the invasive study and those in the same patients during the CMR study ($R^2 = 0.8$, $p = 0.003$), however no significant correlation was seen with glucose ($R^2 = 0.09$, $p = 0.48$), figure 4.18.

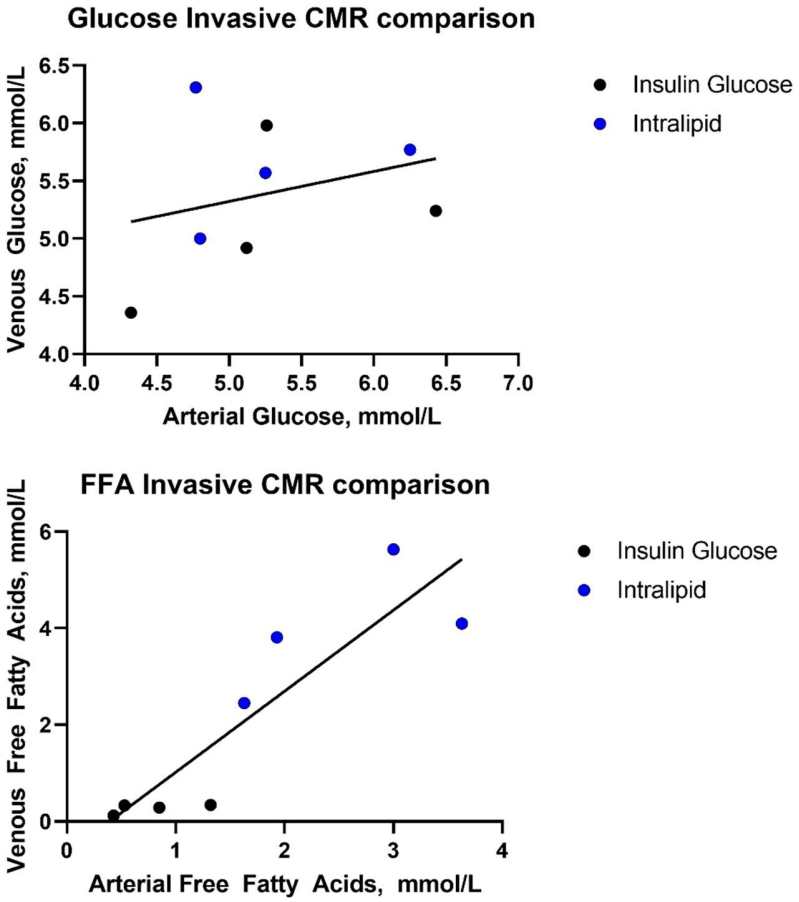

***Figure 4.18**: Correlations between resting arterial coronary sinus bloods in invasive studies and venous bloods at baseline in CMR studies on participants in both parts of the study.*

4.3.4.3 Arteriovenous Oxygen Extraction

See table 4.18 and figure 4.19. Oxygen content is calculated as (Haemoglobin x 1.36) x (Oxygen Saturation / 100) + (Partial Pressure of oxygen x 0.0031). Oxygen extraction is calculated as left main flow x Oxygen content.

In general, oxygen usage is greater in the Intralipid arm. Extraction per unit of blood (oxygen content difference) is greater and the MVO2 is greater still, whether in intrinsic rhythm or during slow BiV pacing (with a trend towards higher extraction during BiV pacing).

Table 4.18: *Arteriovenous differences in oxygen content and extraction during substrate manipulation*

	Insulin + Glucose	***Intralipid***	***p-value***
Left Main coronary artery flow (ml/s)	2.8 ± 1.15	3.12 ± 0.82	0.46
Oxygen content difference (ml/dl)	7.53 ± 3.76	9.92 ± 4.09	***<0.01***
Oxygen extraction (MVO2) (ml/min)	14 ± 9.29	18.5 ± 8.4	***0.02***

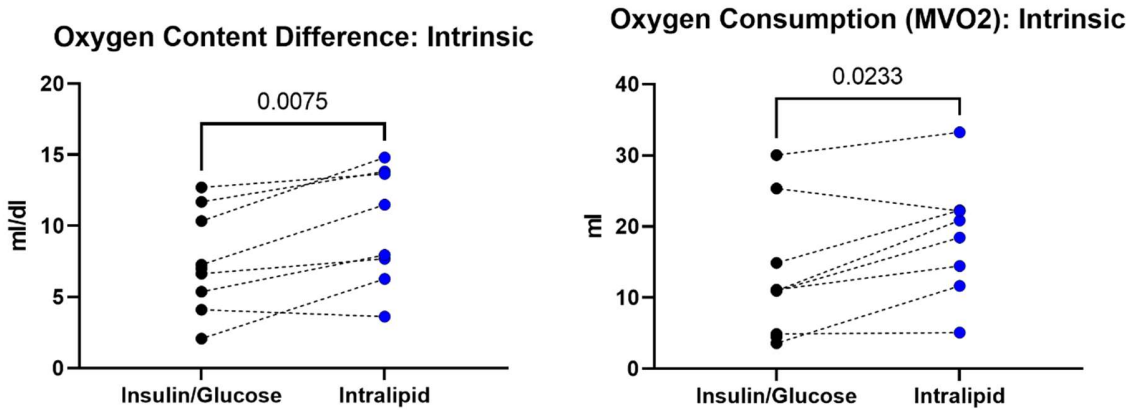

Figure 4.19: *Arteriovenous differences in oxygen content and extraction during substrate manipulation*

4.3.4.4 Arteriovenous Metabolite Extraction

See table 4.19 and figure 4.20. In intrinsic rhythm, glucose extraction was higher during the insulin-glucose infusion and free fatty acid extraction and beta-hydroxybutyrate extraction higher during Intralipid infusion. There was a similar trend seen in biventricular pacing, although it did not reach significance.

Table 4.19: *Arteriovenous metabolite uptake in HFrEF during substrate manipulation in the invasive study*

	Insulin + Glucose	***Intralipid***	***p-value***
Glucose (μmol/min)	96 ± 53	45 ± 36	***0.02***
Free Fatty Acids (μmol/min)	10 ± 11	72 ± 43	0.06
B -*hydroxybutyrate* (μmol/min)	0	8.9 ± 18	0.22
Lactate (μmol/min)	34 ± 35	35 ± 32	0.53

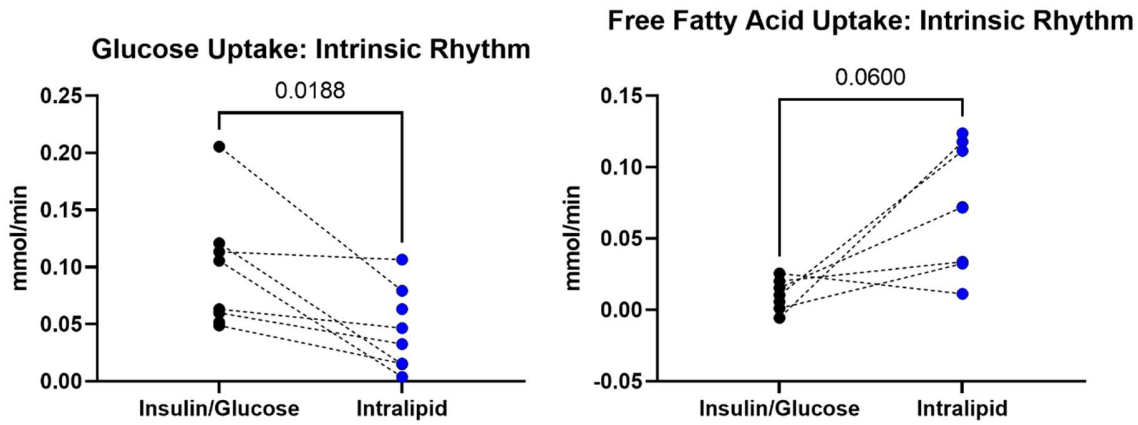

Figure 4.20*: Arteriovenous metabolites in heart failure during substrate manipulation in the invasive study*

ATP generation was calculated assuming total oxidation of each substrate taken up (31mmol of ATP per mmol Glucose, 105mmol of ATP per mmol of free fatty acid, 12.5mmol of ATP per mmol of lactate, 20mmol of ATP per mmol of beta-hydroxybutyrate[338]), see table 4.20.

There was a strong trend towards a higher total ATP in the Intralipid infusion arm, with it being almost 2 fold higher (p=0.08). The same trends as in total uptake were seen: increased glucose during insulin-glucose and increased fatty acids during Intralipid, see figure 4.21.

Table 4.20: *ATP produced per metabolite as a percentage of total ATP production in HFrEF during substrate manipulation in the invasive study*

	Insulin + Glucose	***Intralipid***	***p-value***
Intrinsic rhythm			
Total ATP (mmol/min)	4.6 ± 2.27	8.78 ± 5.14	0.08
Glucose (%)	70 ± 14	17 ± 16	***0.002***
Free Fatty Acids (%)	19 ± 26	73 ± 17	***0.009***
Β*-hydroxybutyrate* (%)	0	1.9 ± 3.4	0.2
Lactate (%)	11 ± 13	7.5 ± 5.4	0.5

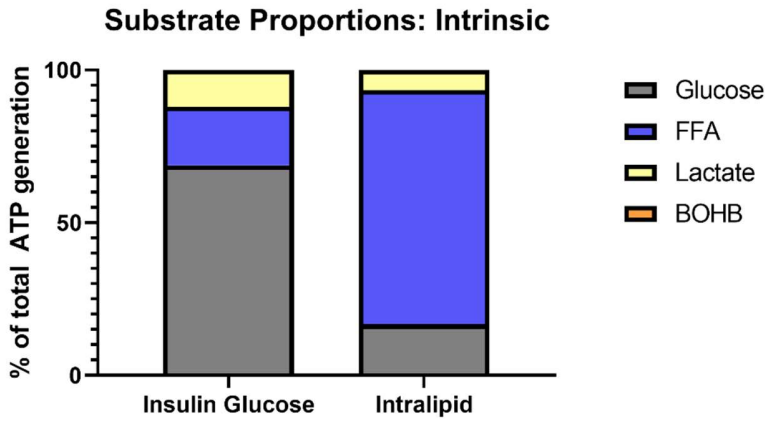

Figure 4.21: *Proportion of ATP production by substrate, during resting intrinsic rhythm*

There was a strong positive correlation seen between circulating levels of free fatty acids and their uptake (R^2 = 0.648, p = 0.0003, figure 4.22), however there was no correlation between insulin and glucose uptake(R^2 = 0.09, p = 0.34, figure 4.22). This is likely due to the fact that the different participants would have different sensitivities to insulin.

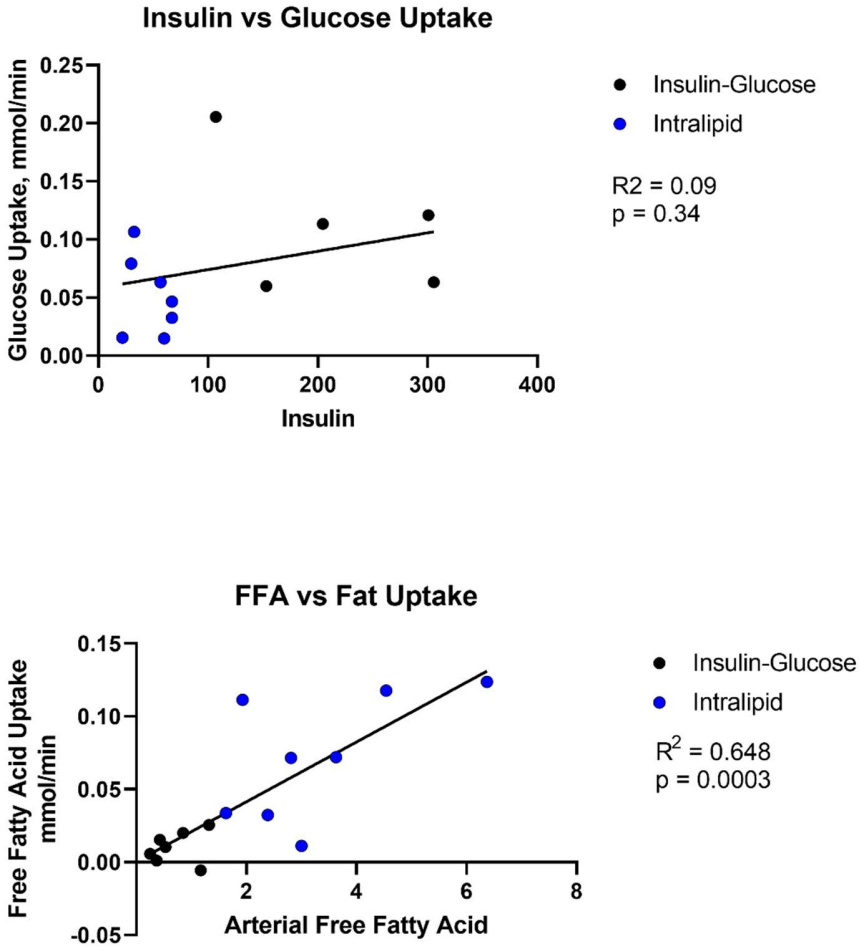

Figure 4.22: *Correlations between arterial metabolites and substrate uptake.*

When total oxygen consumption is calculated based on uptake of each substrate (assuming complete oxidation with glucose requiring 135ml/mmol, lactate 56ml/mmol, β-hydroxybutyrate 101ml/mmol and free fatty acid requiring 515ml/mmol[338]), the correlation in the insulin-glucose arm approaches significance (line slope 0.27, $R^2 = 0.525$, $p = 0.065$, figure 4.23) while there is no correlation in the Intralipid arm (line slope 0.14, $R^2 = 0.0096$, $p=0.82$). As noted elsewhere, the

concentration of free fatty acids circulating in the Intralipid arm is supra-physiological, so whether this correlation would hold during physiological range infusions is unclear.

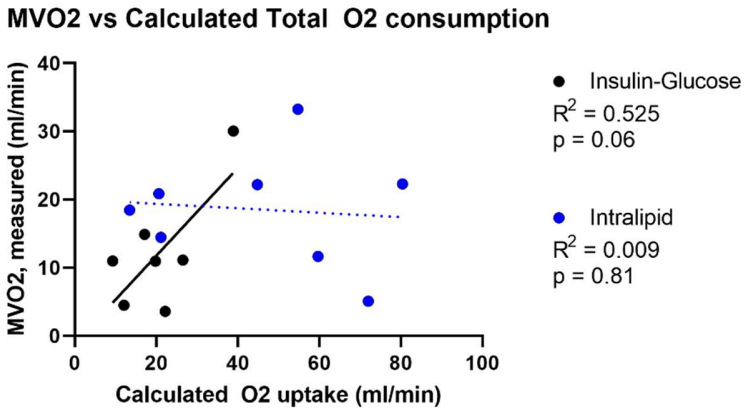

Figure 4.23: *MVO2 compared to total oxygen required to fully oxidise all metabolites*

4.3.4.5 Invasive Measures of Contractility

Comparing infusions in intrinsic rhythm and during biventricular pacing, there were no significant differences in LV ejection fraction or other volume-dependent measures of contractility (stroke work, calculated as pressure-volume loop area, or cardiac work, calculated as stroke work multiplied by heart rate, table 4.21, figure 4.24).

However, there were differences in pressure dependent measures of work: a trend towards being higher in the Intralipid arm. Comparing Insulin-glucose infusion to Intralipid during biventricular pacing, this trend was reproduced (table 4.22, figure 4.25).

***Table 4.21**: Invasive measures of contractility in intrinsic rhythm*

	Insulin/Glucose	***Intralipid***	***p-value***
LV Ejection Fraction (%)	36.4 ± 9.2	35.7 ± 15.5	0.85
LV Stroke Work (mmHg.ml)	9771 ± 3544	9272 ± 4805	0.68
Cardiac Work (L.mmHg/min)	720 ± 367	705 ± 476	0.88
LV dP/dT (mmHg/s)	663 ± 112	688 ± 92	0.12
LV ESP (mmHg)	97.6 ± 17.3	102 ± 16.4	0.23
LV ESP-EDP (LVDP, mmHg)	84 ± 15.1	89.8 ± 16.4	0.1

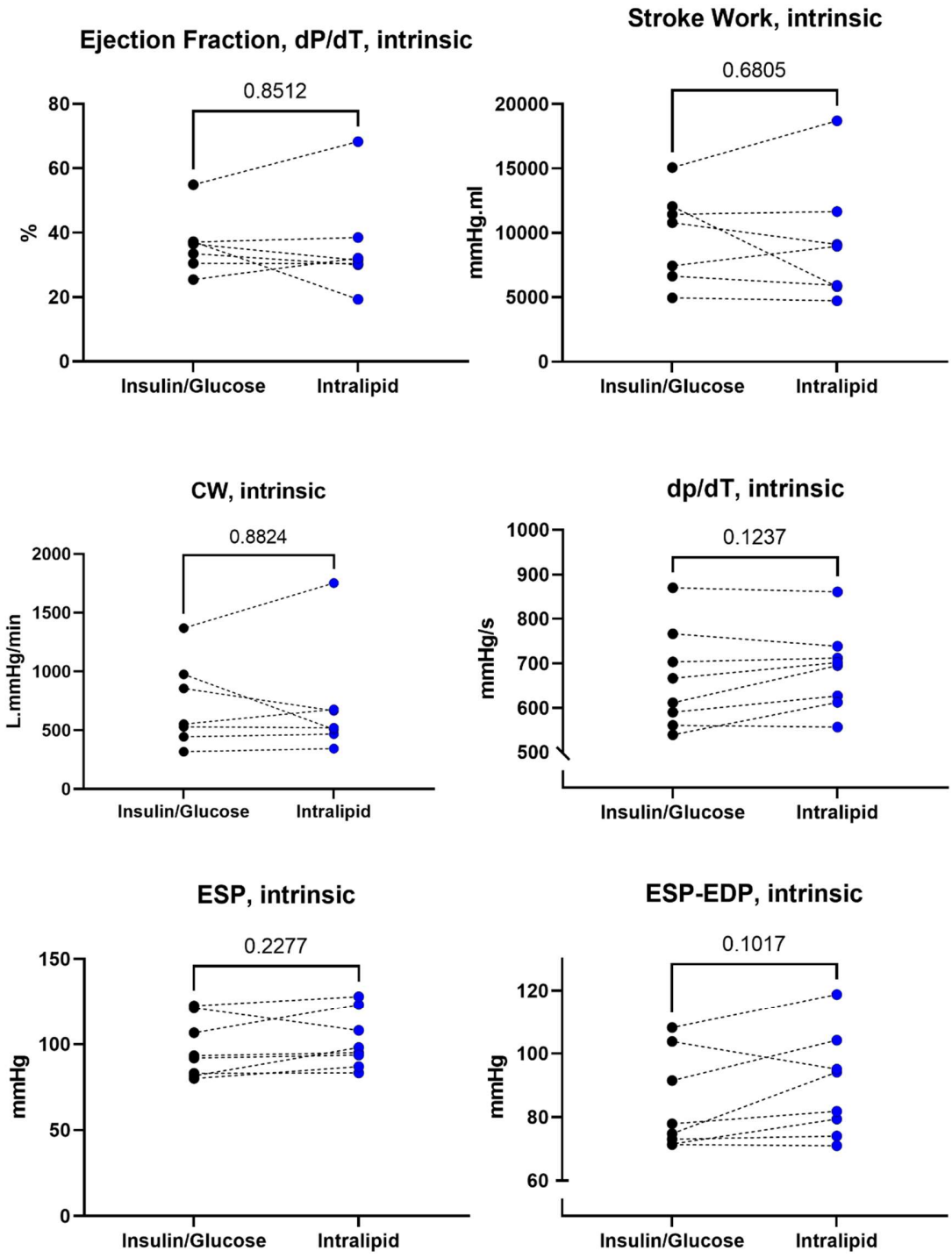

Figure 4.24*: The effect of Substrate modulation on Invasive measures of resting contractility in intrinsic rhythm in patients with heart failure with reduced ejection fraction. Intrinsic, intrinsic rhythm. Ejection fraction calculated using highest and lowest dP/dt measurements (ejection fraction, dP/dt). CW, cardiac work; ESP end systolic pressure; ESP-EDP, end systolic – end diastolic pressure.*

***Table 4.22**: Invasive measures of contractility during biventricular paced rhythm. Ejection fraction calculated using highest and lowest dP/dt measurements (ejection fraction, dP/dt). ESP end systolic pressure; ESP-EDP, end systolic – end diastolic pressure.*

	Insulin/Glucose	***Intralipid***	***p-value***
Ejection Fraction (%)	37.9 ± 10.9	38.6 ± 10.2	0.75
Stroke Work (mmHg.ml)	14392 ± 9061	16676 ± 15073	0.45
Cardiac Work (L.mmHg/min)	1102 ± 862	1372 ± 1519	0.37
dP/dt (mmHg/s)	741 ± 112	808 ± 113	0.08
ESP (mmHg)	97 ± 14.2	105 ± 14	0.11
ESP-EDP (mmHg)	84.9 ± 13.4	91.6 ± 12.2	0.12

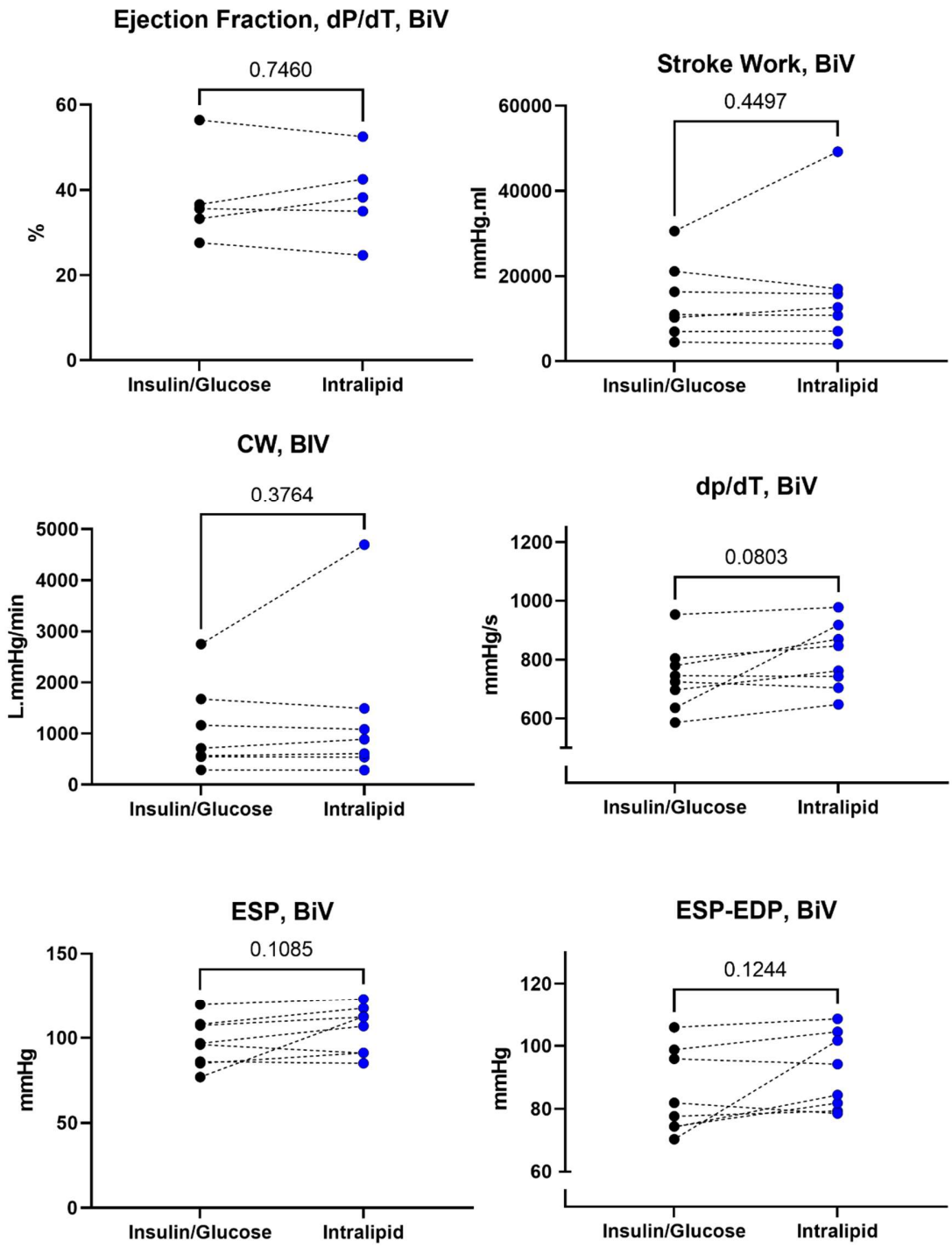

Figure 4.25*: Invasive measures of contractility during biventricular paced rhythm (BiV). Ejection fraction calculated using highest and lowest dP/dt measurements (ejection fraction, dP/dt). CW, cardiac work; ESP end systolic pressure; ESP-EDP, end systolic – end diastolic pressure.*

Cardiac work positively correlated with myocardial oxygen consumption (R^2 = 0.32, p = 0.04, figure 4.26), as has been demonstrated previously.

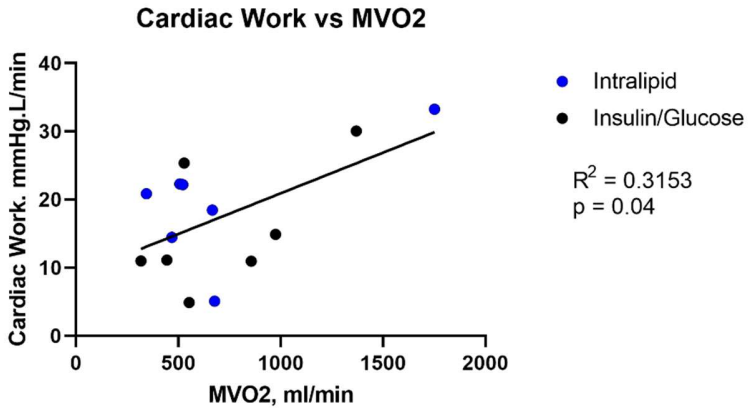

Figure 4.26: *Correlation between oxygen consumption (MVO2) and cardiac work during substrate manipulation in HFrEF in intrinsic rhythm*

4.4 Discussion

4.4.1 The Failing Heart Demonstrates Substrate Flexibility

The healthy heart showed no energetic differences (no significant PCr/ATP change) with euglycaemic clamp or Intralipid infusion, suggesting it is able to balance energy demand for workload with uptake of substrate, irrespective of the prevailing metabolic conditions.

Contrary to the view commonly taken in the literature[85], where the failing heart is regarded as being metabolically inflexible, we have shown here that substrate uptake can change depending on the prevailing circulating metabolites, with fatty acid uptake in particular being proportion to circulating free fatty acids, as has been shown elsewhere. Glucose uptake was increased by euglycaemic clamp while fatty acid uptake was proportional to arterial concentration.

Many studies show fatty acid uptake and oxidation are reduced[147, 150, 339] in heart failure, however we have here shown that simply providing more substrate, more is taken up. We cannot comment on the extent and destinations of metabolism, although the relative increase in MVO2 would suggest a greater degree of free fatty acid oxidation. There was greater glucose uptake in the euglycaemic clamp arm, although the correlation between insulin and glucose uptake was poor, presumably due to varying insulin sensitivity between participants.

It has previously been shown in heart failure that there is a 'substrate switch'[151] to glucose forming the predominant substrate, with fatty acid metabolism downregulated. These data would suggest that, where additional free fatty acids are taken up, ATP production may be increased; and that PCr/ATP ratios in the heart failure and healthy groups receiving Intralipid are not significantly different suggests a greater supply of free fatty acids rebalances the relationship between substrate uptake and oxidation with energy demand. This would be consistent with ideas that

glucotoxicity and lipotoxicity can be damaging to the myocardium[340] and that achieving a balance of substrates is of benefit.

4.4.2 Intralipid Increases Contractility in both Healthy and Failing Hearts

In both the healthy and failing hearts there was an increase in left ventricular ejection fraction and cardiac output during Intralipid infusion and a trend towards an increase in developed pressures measured invasively. Given that contractility and preload are inherently linked, it was important that this was observed without a difference in either LV end diastolic volume or volume infused, making it unlikely that differences in preload were responsible for the observed differences in contractility.

It is unclear if the mechanisms are the same in either arm, however. The healthy hearts saw an increase in creatine kinase rate constant (CK k_f) and creatine kinase flux but no alteration in PCr/ATP during Intralipid, while the failing hearts showed an increase in PCr/ATP but no k_f change during Intralipid. In the normal hearts, the increase in CK flux was driven by a change in CKk_f and that ATP produced was able to match the increase in demand as phosphocreatine (represented by PCr/ATP ratio) did not fall. In heart failure, CKk_f did not increase in spite of the higher workload, suggesting that the creatine kinase enzyme was not able to further increase its activity. The rise in PCr/ATP suggests ATP production was higher, hence the only way to increase ATP delivery is via increasing the (previously reduced) phosphocreatine concentration. Whether CKk_f can increase further is tested in chapter 5.

We have confirmed in the invasive study that there was increased free fatty acid uptake and total substrate uptake, which (if fully oxidised) should provide a greater amount of ATP than the substrate uptake measured during the euglycaemic clamp.

Intralipid is known to exert an inotropic effect[257] via sympathetic nervous system activation[258] and increased intracellular calcium release[259] via GPR40 activation[260], hence it would be expected that there would be increased contractility in both healthy and failing hearts, although most heart failure participants were taking beta blockers. This increased demand for ATP may be stimulating the increase in CKk_f seen in the healthy hearts. However, this would not account for the increased PCr/ATP ratio seen in the failing heart, hence increased substrate oxidation may be occurring compared to the euglycaemic clamp or baseline conditions.

4.4.3 Myocardial Oxygen Delivery Does Not Limit Substrate Oxidation at Rest

We find increased oxygen uptake during Intralipid infusion. This is in keeping with data showing fatty acids such as palmitate have a higher P:O ratio (i.e. more oxygen is required per amount of ATP produced) than glucose. As MVO_2 increases while PCr/ATP does not fall during Intralipid infusion in either healthy or heart failure groups (indeed, rising in the heart failure group), this implies mitochondrial oxidative metabolism and ATP production is sufficient to keep up with demand of ATP. When put together with lactate being consumed rather than produced, this strongly implies oxygen supply was not limiting in these cases of non-ischaemic cardiomyopathy.

This is highly relevant, for two reasons. Inotropes such as dobutamine are associated with elevated mortality[42, 341], where impaired sarcoplasmic reticulum calcium release results in inefficient coupling between contraction and mitochondrial ATP production, hence a progressive

energy deficit[42] and oxygen efficiency is decreased[342]. It is important that this increased ATP demand is met by increased oxidative metabolism to allow function to be sustained.

Secondly, the argument for targeting glucose oxidation as a therapeutic strategy in heart failure is based on the more favourable P:O ratio[328], hence if oxygen delivery is not limiting in heart failure then this argument is void. Arguments advancing the idea of increasing myocardial glucose metabolism as a treatment for heart failure have expanded from hypotheses and research on ischaemia[209] and carried over this assumption. Here, we show this to likely not be the case, in line with other noninvasive studies where no deprivation of oxygen was found in heart failure[343].

4.4.4 There is no energetic benefit from euglycaemic clamp over Intralipid infusion in heart failure

PCr/ATP has shown to be predictive of mortality in heart failure[141] and has a close link to performance under stress[344] and diastolic function[345], therefore any treatment changing this variable may be worthy of future investigation as a therapeutic for heart failure.

It may be that, in the healthy heart, the couplings between oxidation to produce ATP, ATP transfer and ATP utilisation are the closest (hence there is no significant difference in PCr/ATP), while in failing hearts ATP production, transfer and use are less well coupled, leading to rises in PCr/ATP as substrate oxidation increases out of proportion to what can be transported by the creatine kinase system (and other shuttles). Healthy hearts may be able to uncouple any of the steps of fat uptake, oxidation and ATP production, maintaining a constant PCr/ATP ratio and either diverting excess fats which enter the myocyte into anaplerotic pathways or uncoupling oxidative phosphorylation to produce heat.

One of the reasons suggested for increased glucose oxidation being beneficial in heart failure is the greater Gibbs free energy of synthesis of ATP thus produced[96]. Changing the rate of substrate supply will not change the Gibbs free energy of synthesis but changing the types of substrate oxidised will. That increased availability of lipid brought about a rise in PCr/ATP would suggest that in the failing heart it is not free energy of synthesis that dictates the PCr/ATP ratio but rather the rate of energetic substrate supply which is limiting, as long as there is flexibility to metabolise different substrates and oxygen supply is not limiting. Where this rate of substrate supply is increased via fats which can more easily enter the cell, mitochondrial ATP production may increase and the concentration of available phosphocreatine is restored to near normal levels.

In animal models of pressure overload induced failure, TCA intermediates were significantly depleted in spite of increased glycolysis as they were diverted into de novo amino acid synthesis, however this phenotype could be prevented with a high fat diet[167]. It may be that provision of excess fats in this experiment similarly provides alternative substrate when glucose is diverted elsewhere.

4.4.5 Energetics Limit Contractility in the Failing Heart, but not the Healthy Heart

Correlations between resting cardiac output, cardiac index and rate pressure product and PCr/ATP ratio are seen in heart failure, however these correlations do not exist in the healthy population. It seems likely that energetics are a limiting factor for contractility in heart failure but in the healthy heart, it is not the case. This may suggest both a better match between energy

demand and substrate uptake and also a 'buffer' or 'reserve' of energy in the healthy heart that must be depleted before the available concentration of phosphocreatine becomes limiting.

4.4.6 There is a greater degree of uncoupling of substrate uptake from oxidative metabolism with Intralipid than with glucose

Maximal possible ATP production calculated from substrate uptake nearly doubled with the Intralipid infusion, however cardiac work increased by just under 20%. This would imply that some of these substrates are not contributing to ATP production or that the ATP produced is not coupled to contraction. Fatty acids are known to activate uncoupling proteins[224] and it may be that these substrates are oxidised but the energy is wasted by proton leak across the inner mitochondrial membrane.

The line slope of the MVO2 compared to the total calculated requirement for oxygen consumption would imply that not all substrate taken up is fully oxidised and we can infer from the change in slope and loss of correlation that uncoupling of uptake and oxidation is more variable but generally greater during Intralipid infusion. This would fit with the higher calculated ATP production from substrate uptake during Intralipid infusion, again disproportionate to the small increase in cardiac work and further suggesting that there is more substrate being taken up but not used to produce ATP during Intralipid infusion. Note that a direct comparison between the two arms of the study may be misleading as Intralipid infusion elevates levels of free fatty acids in the bloodstream to supraphysiological levels, while a mid-range physiological euglycaemic clamp was used. Therefore, uptake of fat may be expected to be proportionately greater than that

of glucose; whether this provides a long term physiological benefit or if any gains are outweighed by lipid accumulation within the myocytes is worth questioning and would require further study.

Even with euglycaemic clamp, the slope of the line of measured MVO_2 vs calculated oxygen consumption is less than 1, so this would imply some of these substrates are being taken up and not oxidised. This is a known issue in heart failure with glycolysis not being coupled to glucose oxidation[169] and lipid accumulation taking place within myocytes, being diverted into toxic metabolites associated with mitochondrial dysfunction[228].

It was previously thought uncoupling was deleterious, energy wasting process with detrimental effects in heart failure[328]. However, evidence of positive effects is emerging[346]. Uncoupling proteins have protective roles against ischaemia-reperfusion injury, with UCP3 being vital for protection[227], with the mechanism believed to be a reduction in generation of ROS[347]. Increased expression of UCP2 inhibits oxidative stress induced myocyte death[348] and UCPs have been implicated in ischaemic preconditioning[349].

Could uncoupling proteins have protective roles in heart failure outside ischaemia? Reactive oxygen species play a significant role in the development and progression of heart failure[350], hence the protective roles against ROS may by relevant, running contrary to older ideas that fatty acid metabolism could induce ROS formation and hence promote heart failure[328]. Data is limited, although there are effects of increased UCP2 expression on mitochondrial calcium uptake and excitation-contraction coupling[351]. Given the relatively higher PCr/ATP ratio seen in Intralipid treatment, it would seem less likely that any energy wasting occurred in this heart failure cohort and it may be that uncoupling has a beneficial effect in contractility and metabolism.

It is unknown if increased diversion of substrate into anaplerosis can have beneficial effects in heart failure or not[89]. Many of the factors controlling the pool of TCA cycle intermediates are

dysregulated in heart failure, hence there may be an imbalance between anaplerosis and TCA cycle flux. In pressure overload hypertrophy, there is increased anaplerotic flux into the TCA cycle[153], a consistent finding in remodelling in cardiac hypertrophy to facilitate growth. There may be a role for increased diversion of substrate into anaplerosis, indirectly bringing about beneficial effects via replacement of TCA intermediates to allow myocyte growth and allow an overloaded heart to accommodate increased volume. Therefore, an increased supply of substrate in heart failure may bring about wider benefits than energy production alone via providing intermediates for anaplerosis and the discrepancy seen here between total ATP calculated from substrate uptake and mechanical energy required for cardiac work may be beneficial.

4.5 Limitations

4.5.1 Different methods between invasive and noninvasive arms

Only 5 of those in the CMR arm participated in the invasive study, with additional volunteers who had not undergone CMR. Therefore we are forced to assume all invasive studies are representative of the larger group of CMR studies and vice versa. The patients were carefully selected as nonischaemic cardiomyopathies without diabetes and it is reasonable to assume the mechanisms are similar, although worth noting that the precise genetic mechanism is frequently unknown in each case.

Only 15 minutes elapsed between the insulin-glucose infusion finishing, the Intralipid infusion starting and sampling commencing. This differs from the 7-day wash out period between studies in the CMR experiment and the 1-hour period to reach steady state in the CMR experiment.

Nonetheless, we were able to confirm increased uptake of fat following starting the Intralipid infusion, so a substrate switch presumably occurred.

Of the patients in the invasive arm, all received some form of sedation. 7 of the 9 had conscious sedation with opiate and barbiturate while 2 had general anaesthetic: the 2 with general anaesthetic had total intravenous anaesthesia (TIVA) with propofol used in small quantities as an induction agent and an opiate and barbiturate used for maintenance. A literature search did not find any effects of opiates or barbiturates on cardiac substrate metabolism. The same was true for propofol, however it is dissolved in Intralipid; although typically no more than 5ml of 2% propofol was used, this did not seem to significantly alter the effect of the euglycaemic clamp compared to the other participants.

4.5.2 Supraphysiological levels of circulating free fatty acids

While we have managed to bring about a substrate switch experimentally, it is important to bear in mind that these represent supra-physiological levels of arterial insulin and arterial free fatty acids, hence we cannot refute the assertion that the failing heart is metabolically inflexible under physiological changes in substrate supply. However, we have shown increased fat uptake (driven by higher circulating free fatty acid levels) correlates with increased contractility and a higher PCr/ATP ratio in heart failure, therefore treatments targeting increased fatty acid uptake and oxidation remain very worthy of future research.

4.5.3 Metabolic Fates and Other Metabolites

A key limitation is that we can only demonstrate substrate uptake by the myocardium and cannot comment on oxidation rates or diversion into other pathways. The discrepancies between calculated oxygen consumption and measured oxygen consumption with Intralipid and insulin-glucose imply this is occurring but to what extent is unclear. It may be that the euglycaemic clamp, rather than promoting glucose oxidation, rather promotes glyconeogenesis. Likewise, the free fatty acids in Intralipid may be drawn into TAG stores within the myocyte and thereafter into other fates such as ceramide. Interestingly, other studies have shown no features of lipotoxicity in the hearts of diabetics with heart failure exposed to Intralipid infusions for 8 hours[352]. Our assumption is that the improved PCr/ATP ratio seen during Intralipid infusion is a product of increased beta-oxidation of fat: rather it may be a result of downstream signalling triggered by increased cellular fat uptake. Other techniques such as ^{1}H spectroscopy or dynamic nuclear polarisation studies would be necessary to probe these pathways and longer term studies would be required to ascertain whether the elevated PCr/ATP ratio persists and if it translates into longer term improvements in outcome.

Free fatty acids, beta-hydroxybutyrate, lactate and glucose, while representing a large part of myocardial substrate, do not represent the entirety. Amino acids, TCA cycle intermediates and a full breakdown of different length fats would also be desirable, and shed further light on metabolic fates of substrate.

Likewise, we did not directly measure oxygen availability or its metabolic fate following uptake into the cell, only inferring this from changes in oxygen uptake and a lack of lactate production. This could better be measured with labelled oxygen studies, e.g. kinetics of ^{15}O labelled oxygen.

4.5.4 Discordant Invasive and Noninvasive Measures

Inconsistent with the MRI data, ejection fraction and other data using volumes were not significantly different between arms of the study. However, there was a difference with ventricular pressure measurements (dP/dt, developed pressure and end-systolic pressure). We hypothesized that, within a dyssynchronous ventricle, there was torqueing and twisting of the conductance catheter which may have increased with greater inotropy.

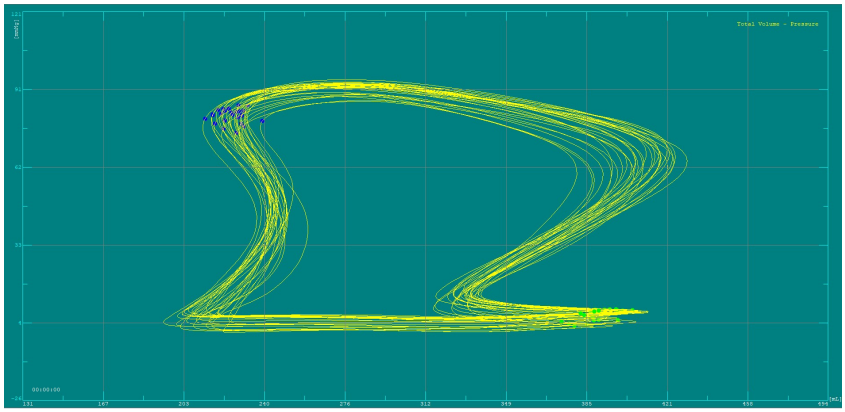

Figure 4.27*: Unusually shaped pressure-volume loop recorded in intrinsic rhythm.*

4.6 Summary

To sum up, we are able to refute many of the assertions upon which the putative benefit of increasing glucose oxidation are based: at rest, the heart is not inflexible, oxygen appears to be not limiting and myocardial energetics are not improved by glucose oxidation.

However, to be a truly effective treatment for heart failure, increasing free fatty acid metabolism also has to be effective at higher heart rates and conditions of stress. This is addressed in chapter 5.

5 Chapter 5: The Effects of Substrate Manipulation at Stress in Normal Hearts and in Heart Failure

5.1 Introduction

Many heart failure patients are symptomatic only during exertion (NYHA class II-III symptoms, 65% of the UK heart failure population[36]), hence the ideal treatment for heart failure would be one that not only improves cardiac function at rest but also increases the ability to do work at higher loads. Cardiac work requires ATP, hence given the link between manipulating substrate supply to the myocardium and ATP production, it is an attractive option to increase the ATP needed for contraction during exercise.

There is relatively little known about cardiac metabolism under stress, especially in the failing heart (as detailed in 1.5.4 page 38). Neglia in 2007 found, in dilated cardiomyopathy, glucose uptake did not change significantly between resting and rapid pacing compared to healthy volunteers where there was a doubling of glucose uptake; while fatty acid uptake and oxidation increased under stress in the heart failure group[147]. If the failing heart is oxygen starved, then increased glucose oxidation under stress should be advantageous, given the favourable P:O ratio. However, fat yields a greater amount of ATP per mole of substrate and may be advantageous as a more easily accessible source of energy.

In a continuation of the experiment in chapter 4, we looked at energy and substrate metabolism in healthy and failing hearts during either dobutamine or rapid pacing stress. We aimed to find how increased energy demand under stress affected ATP flux and substrate profile and whether substrate manipulation could alter the heart's maximal ability to do work.

5.2 Methods

The data presented here mark a continuation of the study presented in chapter 4, using the same participants. Inclusion and exclusion criteria remain the same.

5.2.1 CMR

The CMR protocol was extended with the STReST acquisition described in 2.3.3, page 66, with additional cine imaging in horizontal and vertical long axis orientations for biplane left ventricular function.

Stress was provided with dobutamine, targeted to 65% of the participant's maximal heart rate for age. Heart rate and blood pressure were monitored throughout and dobutamine was titrated in 2 minute intervals. At the end of the protocol, prior to heart rate returning to normal, blood samples were taken for glucose, insulin, lactate, β-hydroxybutyrate and free fatty acids.

5.2.2 Invasive Protocol

During the invasive arm of the study, data was acquired during rapid atrial pacing (or rapid right ventricular pacing if the subject was in atrial fibrillation) and rapid biventricular pacing. Again, heart rate was targeted to 65% of maximal heart rate for age.

5.3 Results

5.3.1 Healthy Volunteers

5.3.1.1 Venous Metabolites in Healthy Volunteers

See figure 5.1 and table 5.1. As expected, free fatty acids were high with Intralipid and were low with acipimox, while insulin was highest in the insulin/glucose arm and was lowest with acipimox. Again, beta-hydroxybutyrate was highest with the Intralipid infusion.

***Table 5.1**: Circulating metabolites at stress in healthy volunteers (venous blood taken immediately following dobutamine infusion)*

	Acipimox	***Insulin/Glucose***	***Intralipid***	***p-value*** (ANOVA)
Free Fatty Acids (mmol/L)	0.826 ± 0.623	1.5 ± 0.746	3.03 ± 0.803	***0.0045***
Glucose (mmol/L)	4.34 ± 0.31	4.45 ± 0.56	5.19 ± 1.2	0.14
Insulin (pmol/L)	42.7 ± 22.6	242 ± 159	102 ± 80.1	***0.04***
Lactate (mmol/L)	1.22 ± 0.38	1.42 ± 0.48	1.14 ± 0.4	0.4
Beta-hydroxybutyrate (mmol/L)	0.15 ± 0.15	0.3 ± 0.15	1.37 ± 0.65	***0.0011***

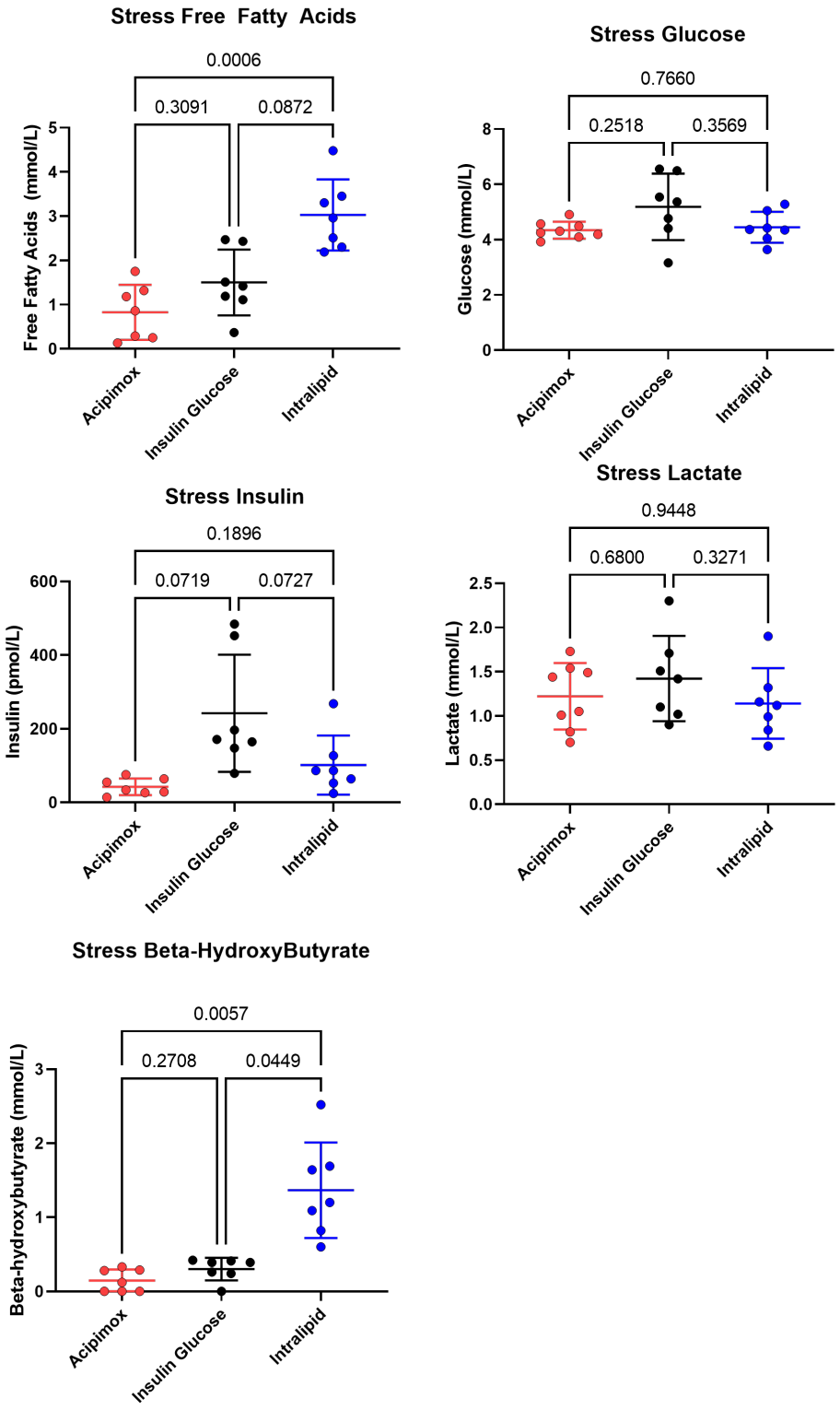

***Figure 5.1**: Circulating metabolites at stress in healthy volunteers (venous blood taken immediately following dobutamine infusion)*

Free fatty acids rose in the acipimox and insulin-glucose arms, although did not significantly change in the Intralipid infusion (although they were already high). Glucose rose in the insulin-glucose arm and did not significantly change in the other two infusion arms. Insulin rose in the Intralipid arm but did not significantly change with the other infusions. Lactate did not change significantly on stress with any infusion. Beta-hydroxybutyrate rose during insulin-glucose and Intralipid infusions but not with acipimox.

***Table 5.2**: Change from baseline to stress in venous blood in healthy volunteers*

	Acipimox	***Insulin/Glucose***	***Intralipid***	***p-value*** (ANOVA)
Free Fatty Acids (mmol/L)	0.74 ± 0.6	1.38 ± 0.79	0.1 ± 0.77	***0.014***
Glucose (mmol/L)	-0.24 ± 0.35	2.33 ± 2.16	0.24 ± 0.5	***0.016***
Insulin (pmol/L)	5.7 ± 16.6	91.8 ± 144	65.4 ± 77.4	0.15
Lactate (mmol/L)	0.21 ± 0.41	0.55 ± 0.59	0.15 ± 0.49	0.16
Beta-hydroxybutyrate (mmol/L)	0.13 ± 0.18	0.3 ± 0.15	0.41 ± 0.15	***0.007***

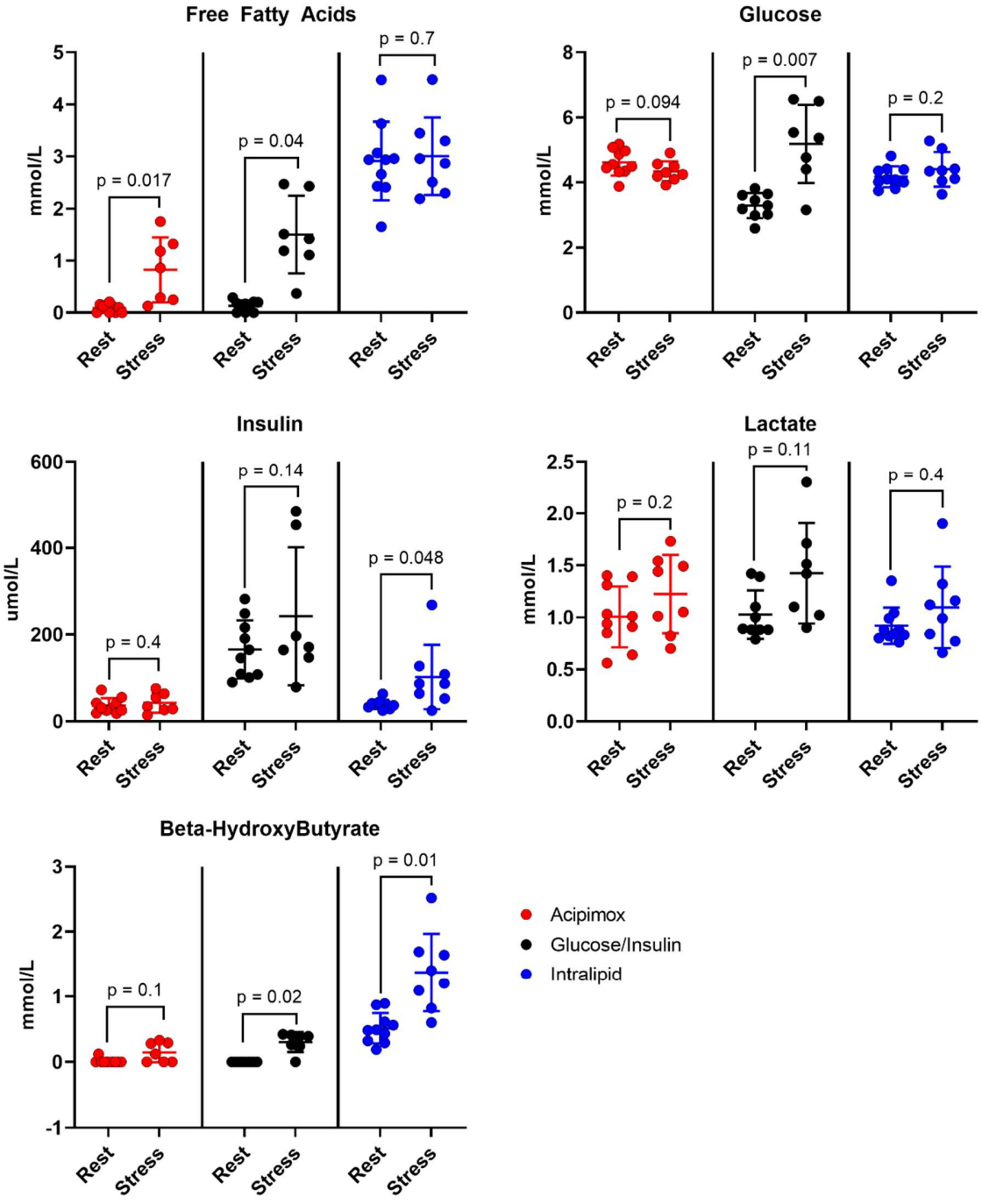

***Figure 5.2**: Changes in venous metabolites in healthy volunteers between rest and stress. Paired t-tests are shown.*

5.3.1.2 Haemodynamics and Cardiac Work under Stress in Healthy Volunteers

There was a trend towards a higher rate pressure product and cardiac work in the Intralipid arm, although there were no significant differences between the groups in terms of the rate pressure product change between rest and stress. Blood pressure measurements are non-invasive. The target heart rate of 65% maximal predicted heart rate for age was achieved in 9/10 volunteers.

***Table 5.3**: Haemodynamics and Cardiac Work in healthy volunteers during dobutamine stress*

	Acipimox	***Insulin/Glucose***	***Intralipid***	***p-value*** (ANOVA)
Rest				
Systolic Blood Pressure (mmHg)	115 ± 15	115 ± 13	127 ± 25	0.37
Heart Rate (bpm)	59 ± 9	58 ± 10	62 ± 12	0.31
Rate Pressure Product (mmHg.bpm x 10^3)	5.68 ± 1148	5.35 ± 1024	5.01 ± 1132	***0.03***
Stroke Work (ml.mmHg x 10^3)	419 ± 121	419 ± 97	508 ± 106	***0.02***
Cardiac Work (ml.mmHg/min x 10^3)	6806 ± 1276	6659 ± 1882	7961 ± 1380	0.16
Stress				
Systolic Blood Pressure (mmHg)	144 ± 17	142 ± 9.6	152 ± 13	0.21
Heart Rate (bpm)	108 ± 13	113 ± 12	110 ± 12	0.44
Rate Pressure Product (mmHg.bpm x 10^3)	15.1 ± 3	15.4 ± 2	17.1 ± 2	0.16
Stroke Work (ml.mmHg x 10^3)	9.57 ± 3.98	9.09 ± 1.73	9.34 ± 2.26	0.23
Cardiac Work (ml.mmHg/min x 10^3)	854 ± 276	736 ± 217	999 ± 197	0.09
Stress – Rest Difference				
Systolic Blood Pressure (mmHg)	29 ± 28	43 ± 50	25 ± 17	0.47
Heart Rate (bpm)	49 ± 15	53 ± 7.5	49 ± 10	0.68
Rate Pressure Product (mmHg.bpm x 10^3)	8.27 ± 3.21	8.74 ± 2.34	9.17 ± 1.45	0.82
Stroke Work (ml.mmHg x 10^3)	3.95 ± 3.75	3.21 ± 1.36	4.15 ± 1.37	0.39
Cardiac Work (ml.mmHg/min x 10^3)	449 ± 248	319 ± 214	472 ± 189	0.08

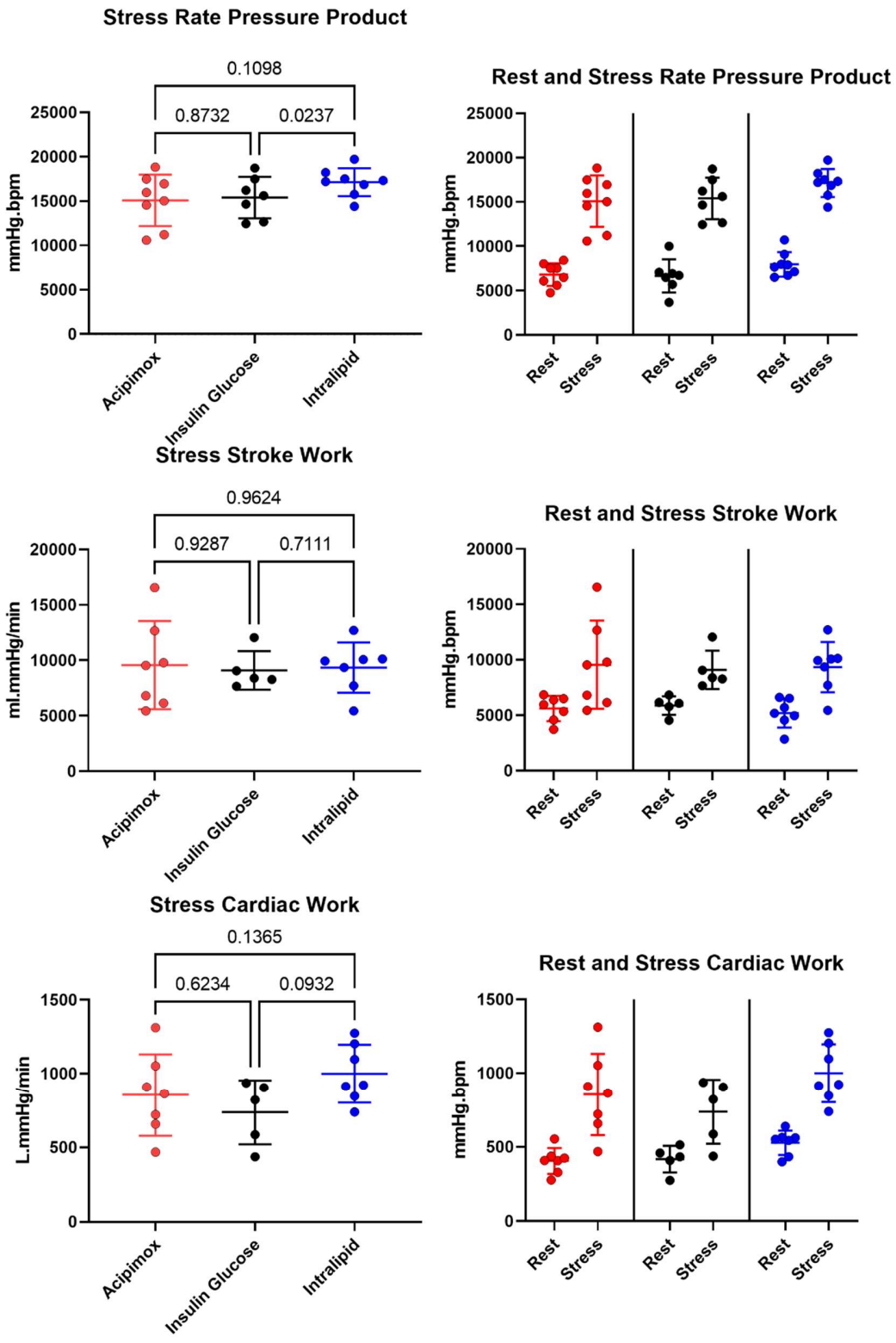

***Figure 5.3**: Haemodynamics and Cardiac Work in Healthy Volunteers*

5.3.1.3 Contractility and Volume changes under stress in healthy volunteers

The contractility differences between the arms in healthy volunteers under stress was minimal, although there was a trend to higher cardiac output and cardiac index in the Intralipid group and lower in the insulin-glucose group.

***Table 5.4**: Left Ventricular Volumes and Contractility At Rest and During Stress*

	Acipimox	***Insulin/Glucose***	***Intralipid***	***p-value*** (ANOVA)
Stress Volumes				
Left Ventricular End Diastolic Volume (ml)	129 ± 39	136 ± 23	125 ± 28	0.31
Left Ventricular End Systolic Volume (ml)	25 ± 6	32 ± 16	23 ± 10	0.38
Left Ventricular Stroke Volume (ml)	104 ± 33	104 ± 20	101 ± 21	0.22
Left Ventricular Ejection Fraction (%)	80 ± 3	82 ± 4	82 ± 5	0.57
Cardiac Output (L/min)	11.2 ± 3.2	11.0 ± 1.4	11.1 ± 1.9	0.15
Cardiac Index ($L/min/m^2$)	6.30 ± 1.75	6.14 ± 0.82	6.08 ± 1.02	0.1
Change Rest to Stress				
Left Ventricular End Diastolic Volume (ml)	-7 ± 20	-8 ± 17	-9 ± 13	0.96
Left Ventricular End Systolic Volume (ml)	-30 ± 11	-20 ± 32	-22 ± 10	0.47
Left Ventricular Stroke Volume (ml)	+23 ± 23	+13 ± 21	+13 ± 7	0.27
Left Ventricular Ejection Fraction (%)	+21 ± 4	+18 ± 8	+16 ± 5	0.24
Cardiac Output (L/min)	+6.19 ± 2.85	+4.99 ± 2.74	+5.33 ± 1.38	0.27
Cardiac Index ($L/min/m^2$)	+3.45 ± 1.52	+2.84 ± 1.52	+2.93 ± 0.78	0.23

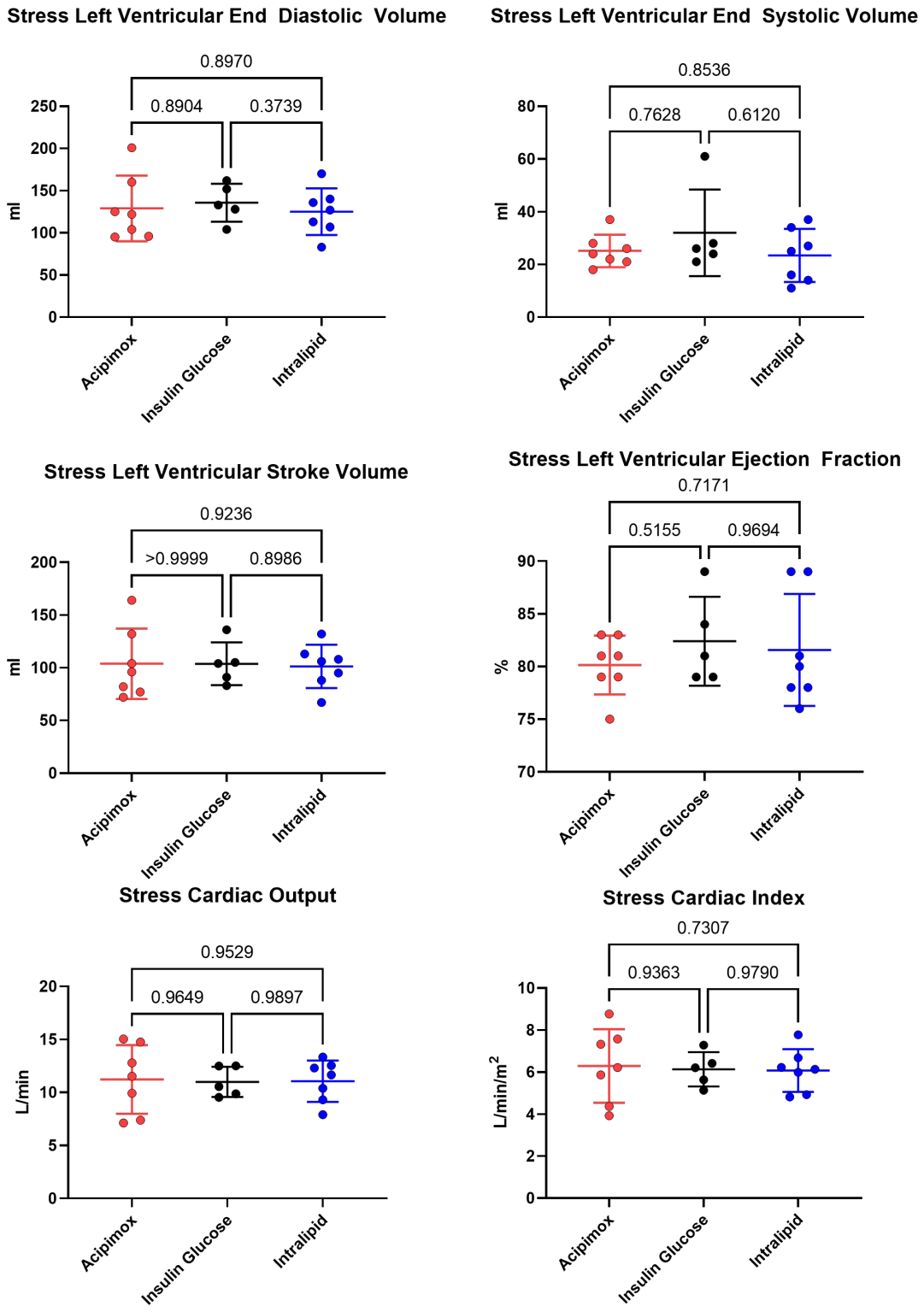

***Figure 5.4**: CMR volumes during dobutamine stress in healthy volunteers*

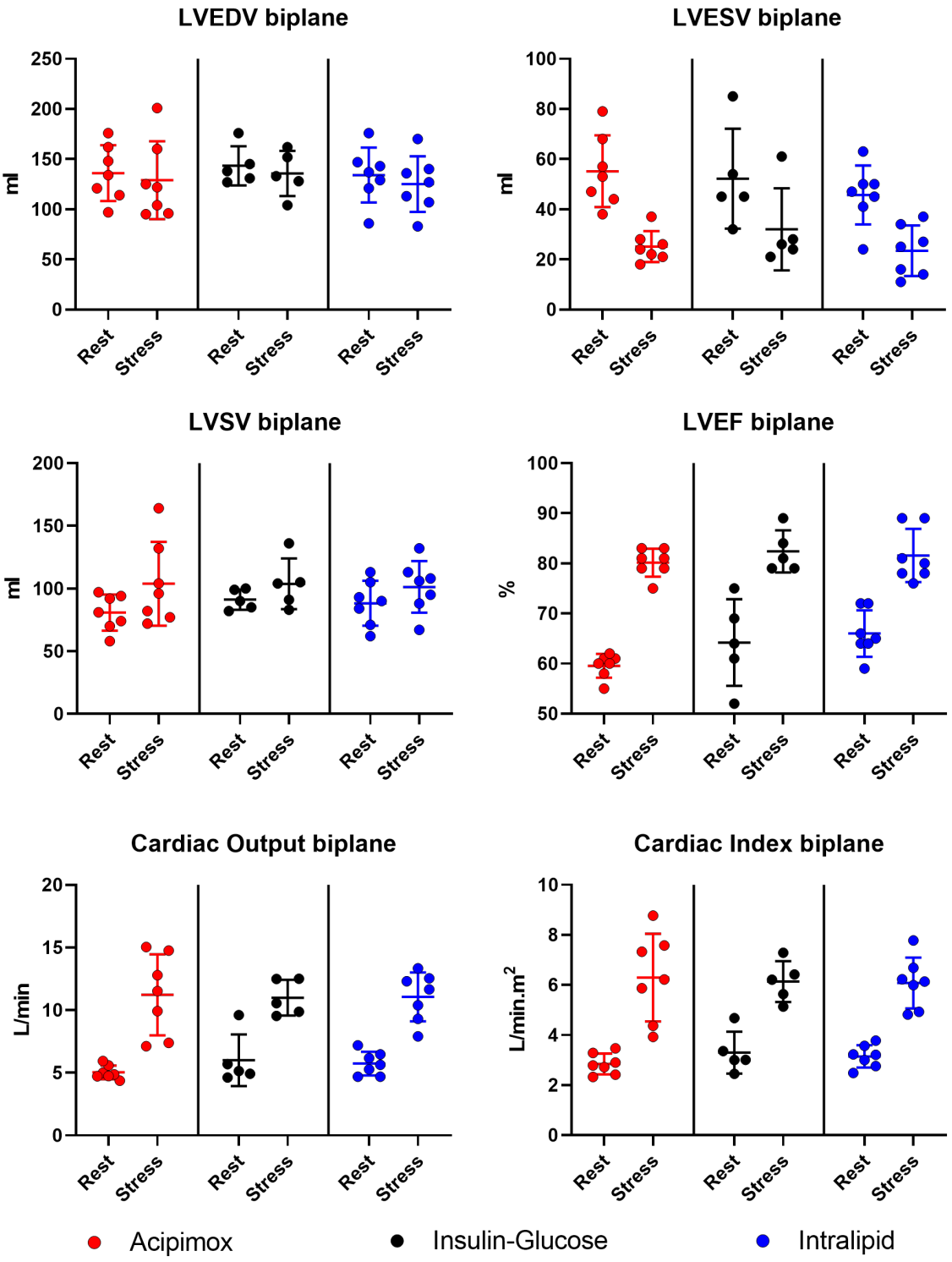

***Figure 5.5**: Changes in CMR volumes between rest and stress in healthy volunteers*

5.3.1.4 Correlations at Stress in Healthy Volunteers

There were significant positive correlations seen between the resting PCr/ATP and the stress stroke volume ($R^2 = 0.35$, $p = 0.007$) and the stress cardiac work ($R^2 = 0.27$, $p = 0.022$), however these correlations were not significant at rest (resting stroke volume $R^2 = 0.18$, $p = 0.07$; resting cardiac work $R^2 = 0.005$, $p = 0.77$).

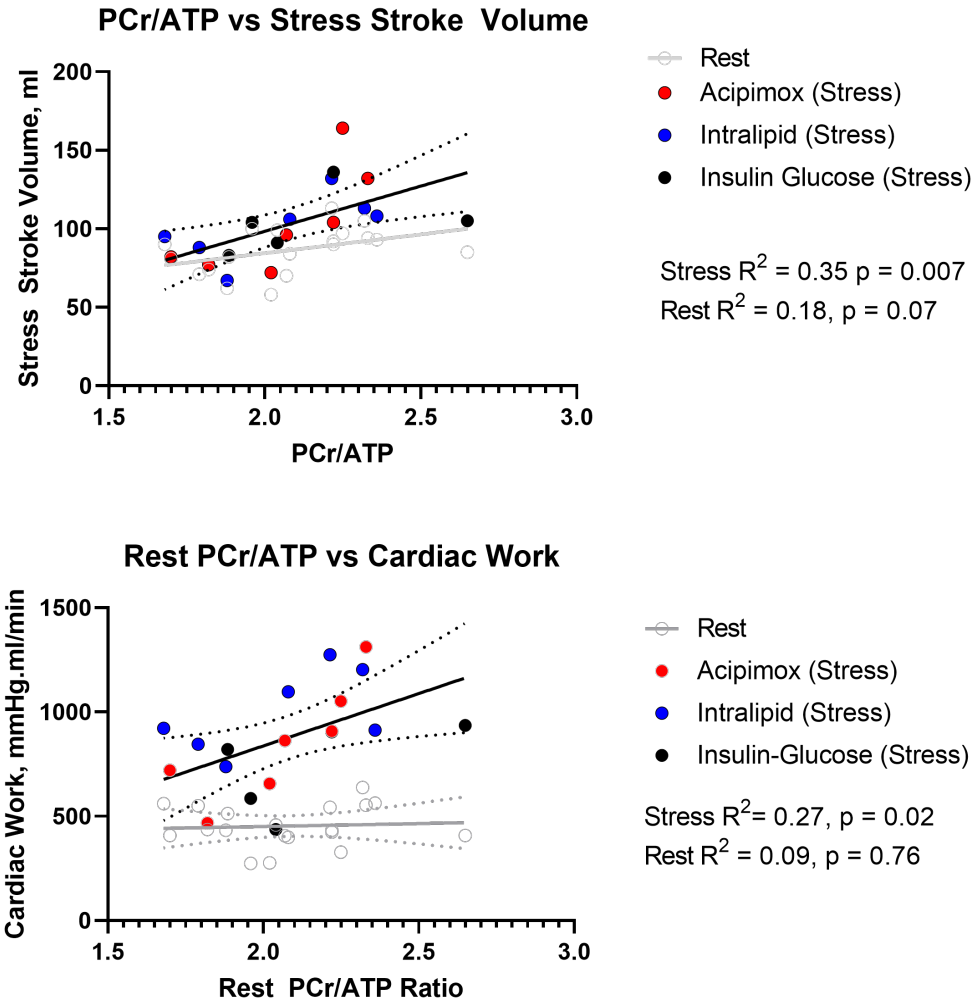

***Figure 5.6**: Correlations between PCr/ATP at rest and measures of contractility and haemodynamics. SV = Stroke Volume*

5.3.1.5 ^{31}P MRS Under Stress in Healthy Volunteers

There were no significant differences in stress creatine kinase first order rate constant between groups, nor was there a significant change from rest to stress seen. Across all measurements, creatine kinase first order rate constant was 0.21 s^{-1} at rest and 0.24 s^{-1} at stress, p = 0.47.

***Table 5.5**: Stress Creatine Kinase First Order Rate Constant (Ck_{kf})*

	Acipimox	***Insulin/Glucose***	***Intralipid***	***p-value*** (ANOVA)
CK Rate Constant (s^{-1})	0.28 ± 0.1	0.19 ± 0.14	0.26 ± 0.17	0.41
PCr/ATP	2.59 ± 0.81	2.17 ± 0.52	2.11 ± 0.68	0.1
CK flux (umol/g/s)	4.72 ± 1.75	2.79 ± 1.8	3.26 ± 2.83	0.36

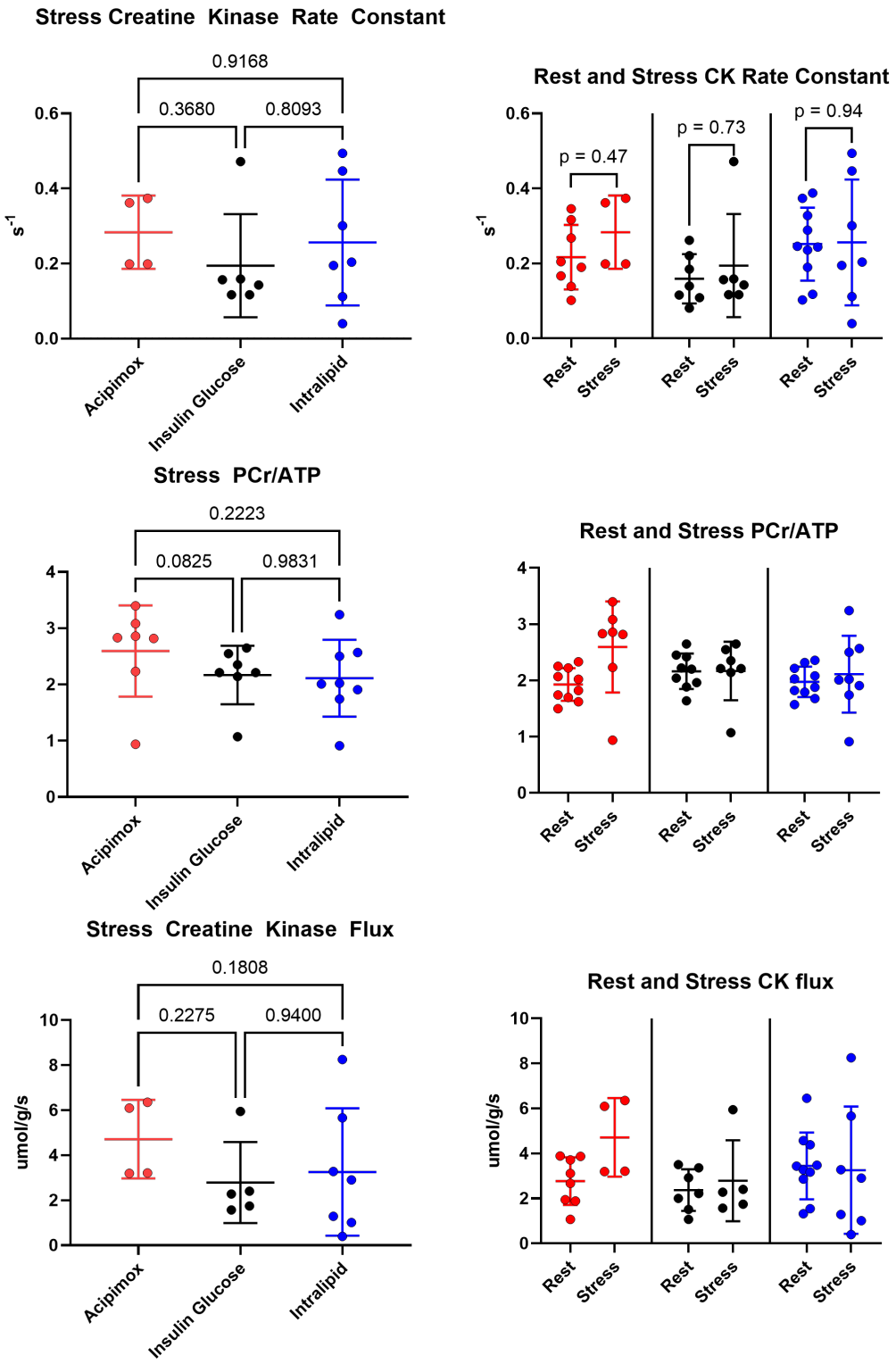

***Figure 5.7**: Rest and stress Creatine Kinase First Order Rate Constant (Ck $_{kf}$), PCr/ATP ratio and CK flux.*

5.3.2 Heart Failure Volunteers

5.3.2.1 Venous Metabolites in Healthy Volunteers during Stress CMR scanning

As expected, free fatty acids during stress were significantly higher in the Intralipid infusion group compared to insulin-glucose. Surprisingly, insulin was not significantly higher in the insulin-glucose infusion group compared to Intralipid.

Free fatty acids rose under stress in the insulin glucose group although the rise did not reach significance in the insulin-glucose group (although the levels were already high here). Insulin rose significantly under stress in the Intralipid group, although there was no significant change in the insulin-glucose infusion group. Ketone levels rose under stress in both groups, although the rise was greater in the insulin-glucose group.

Compared to healthy volunteers, β-hydroxybutyrate was higher at stress during Intralipid infusion in healthy volunteers than those with heart failure (healthy 1.37 ± 0.65 mmol/L vs heart failure 0.64 ± 0.35 mmol/L, $p = 0.002$), with a trend in the same direction during insulin-glucose infusion (healthy 0.26 ± 0.18 mmol/L vs heart failure 0.11 ± 0.21 mmol/L, $p = 0.09$). Comparing levels of free fatty acids, these were higher at stress in healthy volunteers on the insulin-glucose infusion (healthy 1.5 ± 0.75 mmol/L vs heart failure 0.8 ± 0.51 mmol/L, $p = 0.01$), while in those on the Intralipid infusion, they remained at supra-physiological levels and not significantly different (healthy 3.03 ± 0.8 mmol/L vs heart failure 3.47 ± 1.86 mmol/L, $p = 0.55$). No significant differences were seen elsewhere.

***Table 5.6**: Venous metabolites at stress in heart failure volunteers*

	Insulin/Glucose	***Intralipid***	***p-value*** (t-test)
Rest			
Free Fatty Acids (mmol/L)	0.23 ± 0.2	2.96 ± 1.77	***<0.001***
Glucose (mmol/L)	4.97 ± 0.86	5.5 ± 0.69	0.06
Insulin (pmol/L)	357 ± 214	91 ± 65	***<0.001***
Lactate (mmol/L)	1.16 ± 0.21	1.17 ± 0.34	0.75
Beta-hydroxybutyrate (mmol/L)	0.01 ± 0.04	0.41 ± 0.42	***0.01***
Stress			
Free Fatty Acids (mmol/L)	0.8 ± 0.51	3.47 ± 1.86	***<0.0001***
Glucose (mmol/L)	4.96 ± 0.83	5.08 ± 0.52	0.9
Insulin (pmol/L)	350 ± 645	193 ± 160	0.24
Lactate (mmol/L)	1.23 ± 0.23	1.18 ± 0.24	0.27
Beta-hydroxybutyrate (mmol/L)	0.11 ± 0.21	0.64 ± 0.35	***<0.0001***
Change from Rest to Stress			
Free Fatty Acids (mmol/L)	0.58 ± 0.58	0.38 ± 0.89	0.51
Glucose (mmol/L)	0.08 ± 1.04	- 0.49 ±0.29	0.13
Insulin (pmol/L)	-1 ± 616	103 ± 125	0.58
Lactate (mmol/L)	-0.02 ± 0.36	0.09 ± 0.26	0.24
Beta-hydroxybutyrate (mmol/L)	0.27 ± 0.18	0.11 ± 0.21	***0.02***

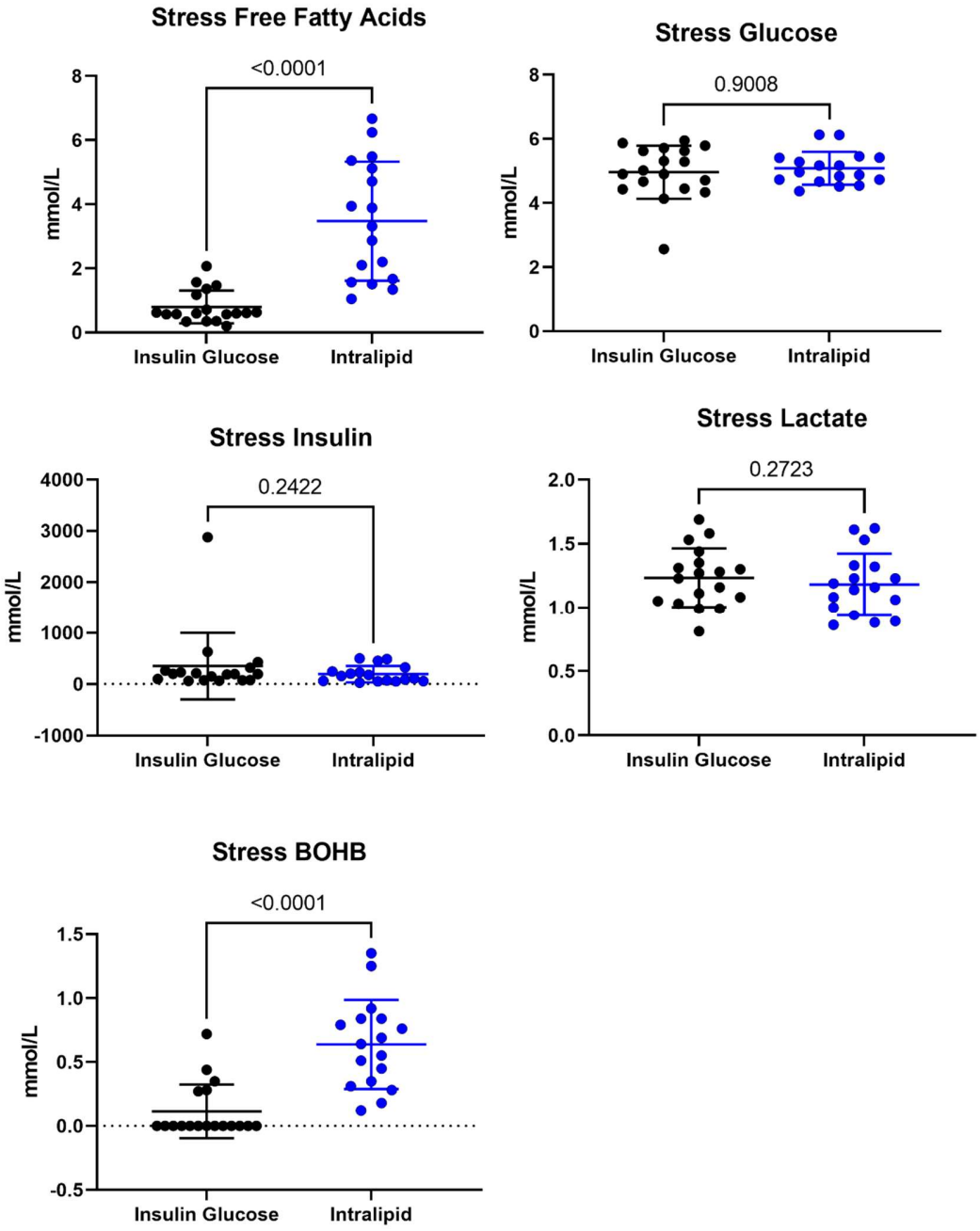

***Figure 5.8**: Venous metabolites at stress in heart failure volunteers*

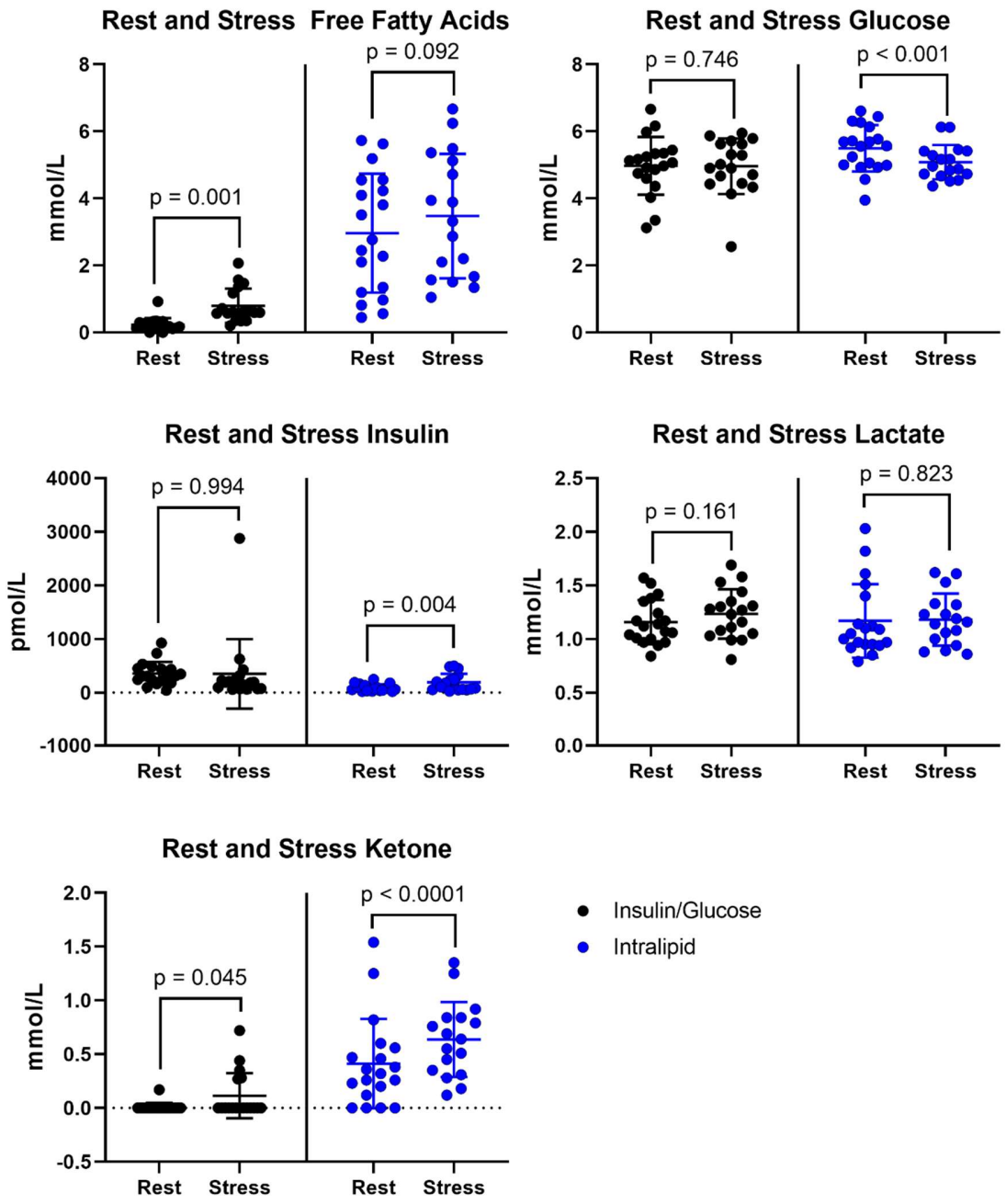

***Figure 5.9**: Venous metabolites at rest and stress in heart failure volunteers*

5.3.2.2 Contractility and Volume changes in heart failure volunteers during stress CMR scanning

See figures 5.10 and 5.11 and table 5.7. Stress volumes and contractility were not significantly different between the arms of the study. There was a trend towards a lower increase in the Intralipid arm, which may relate to higher resting contractility.

***Table 5.7**: Volumes During Stress in Heart Failure Volunteers*

	Insulin/Glucose	***Intralipid***	***p-value*** (t-test)
Stress			
Left Ventricular End Diastolic Volume (ml)	197 ± 86	185 ± 86	0.79
Left Ventricular End Systolic Volume (ml)	107 ± 70	104 ± 79	0.85
Left Ventricular Stroke Volume (ml)	91 ± 26	88 ± 30	0.76
Left Ventricular Ejection Fraction (%)	49 ± 12	51 ± 16	0.48
Cardiac Output (L/min)	9.02 ± 2.9	8.83 ± 3.21	0.5
Cardiac Index (L/min/m^2)	4.61 ± 1.64	4.65 ± 1.32	0.55
Change from Rest to Stress			
Left Ventricular End Diastolic Volume (ml)	-42 ± 34	-50 ± 75	0.64
Left Ventricular End Systolic Volume (ml)	-51 ± 35	-40 ± 55	0.29
Left Ventricular Stroke Volume (ml)	+10 ± 17	-3 ± 31	0.2
Left Ventricular Ejection Fraction (%)	+13 ± 10	+8 ± 15	0.16
Cardiac Output (L/min)	+3.55 ± 2.49	+2.34 ± 3.25	0.12
Cardiac Index (L/min/m^2)	+1.8 ± 1.2	+1 ± 1.64	0.07

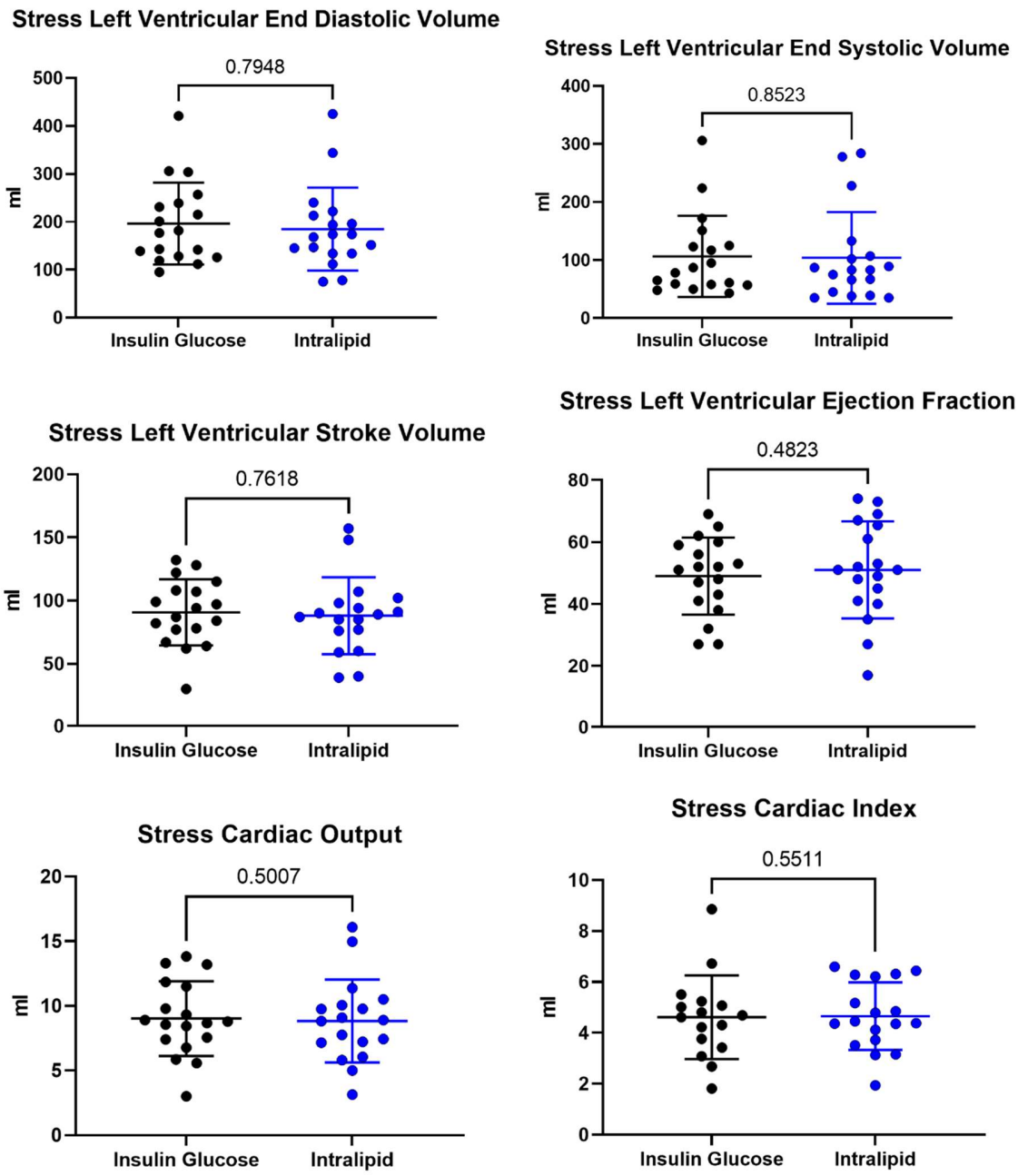

***Figure 5.10**: Stress Contractility in Heart Failure Volunteers*

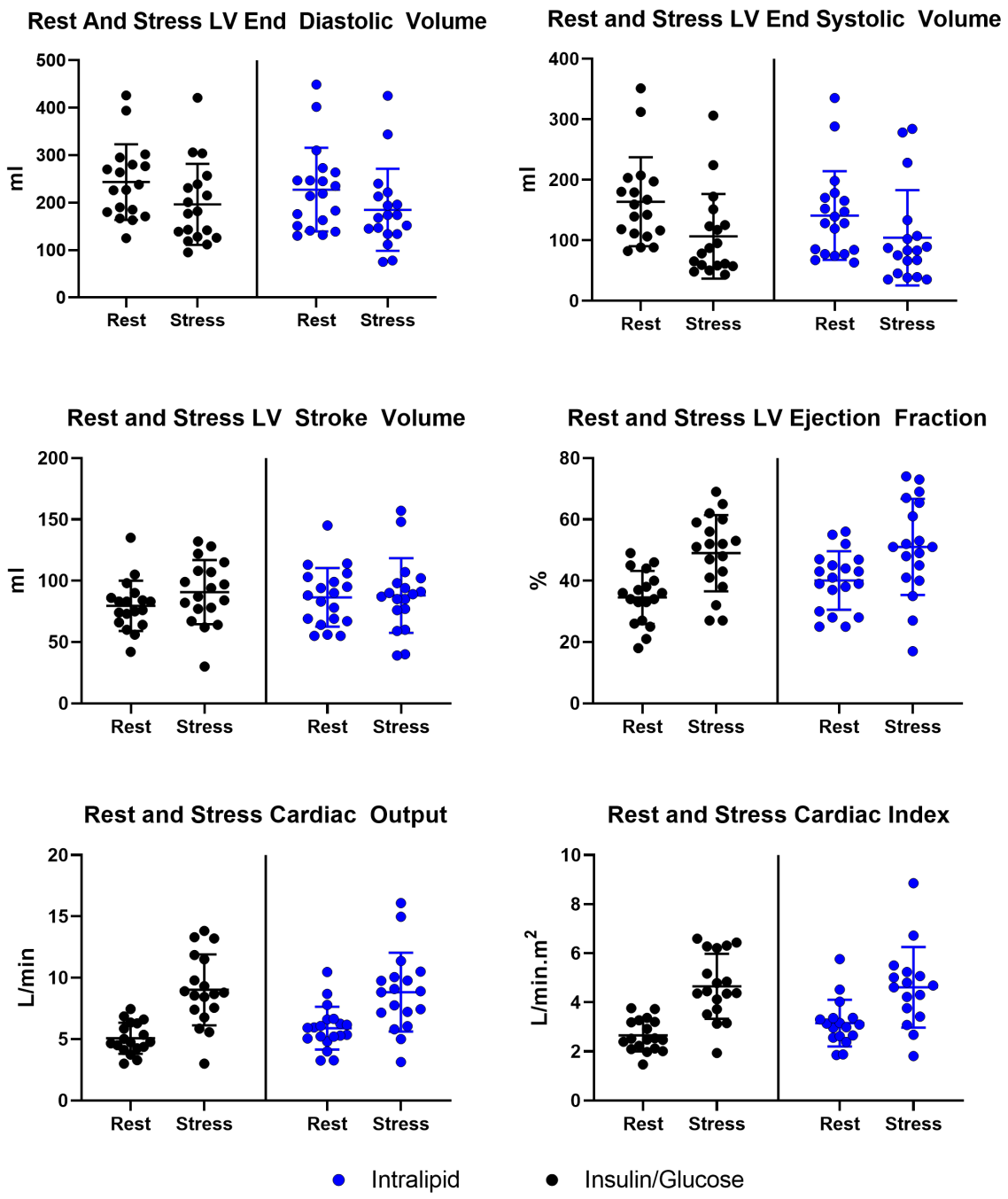

***Figure 5.11**: Rest and Stress Contractility in Heart Failure Volunteers*

5.3.2.3 Haemodynamics and Cardiac Work under Stress in Heart Failure Volunteers

See figure 5.12 and 5.13 and table 5.8. Stress stroke work and cardiac work were higher in the Intralipid arm compared to insulin-glucose.

Unlike the healthy volunteers, cardiac work did not change significantly between rest and stress. Stroke work fell slightly in the insulin-glucose arm. What changes that did take place were not significantly different between the arms of the study.

***Table 5.8**: Rest and Stress Haemodynamics and Cardiac Work in Volunteers with Heart Failure*

	Insulin/Glucose	***Intralipid***	***p-value*** (t-test)
Rest			
Heart Rate (bpm)	65 ± 12	69 ± 13	***0.001***
Mean Arterial Pressure (mmHg)	84 ± 12	85 ± 15	0.47
Rate Pressure Product (mmHg.bpm x 10^3)	7736 ± 2014	8419 ± 2378	***0.001***
Stroke Work (ml.mmHg x 10^3)	5.59 ± 1692	6.15 ± 1737	***0.004***
Cardiac Work (ml.mmHg/min x 10^3)	466 ± 148	549 ± 163	***0.0005***
Stress			
Heart Rate (bpm)	103 ± 8	103 ± 9	0.18
Mean Arterial Pressure (mmHg)	85 ± 17	83 ± 12	0.59
Rate Pressure Product (mmHg.bpm x 10^3)	13 ± 2.3	13.2 ± 2.8	0.4
Stroke Work (ml.mmHg x 10^3)	4.49 ± 1.54	5.15 ± 1.67	***0.02***
Cardiac Work (ml.mmHg/min x 10^3)	463 ± 168	525 ± 166	***0.009***
Stress - Rest			
Heart Rate (bpm)	39 ± 12	35 ± 13	***0.006***
Mean Arterial Pressure (mmHg)	0.7 ± 13.6	-5.9 ± 29.8	0.38
Rate Pressure Product (mmHg.bpm x 10^3)	4.93 ± 3.1	3.66 ± 5.07	0.28
Stroke Work (ml.mmHg x 10^3)	-0.99 ± 1.85	- 1.2 ± 2.99	0.64
Cardiac Work (ml.mmHg/min x 10^3)	-2.41 ± 181	-49.4 ± 301	0.34

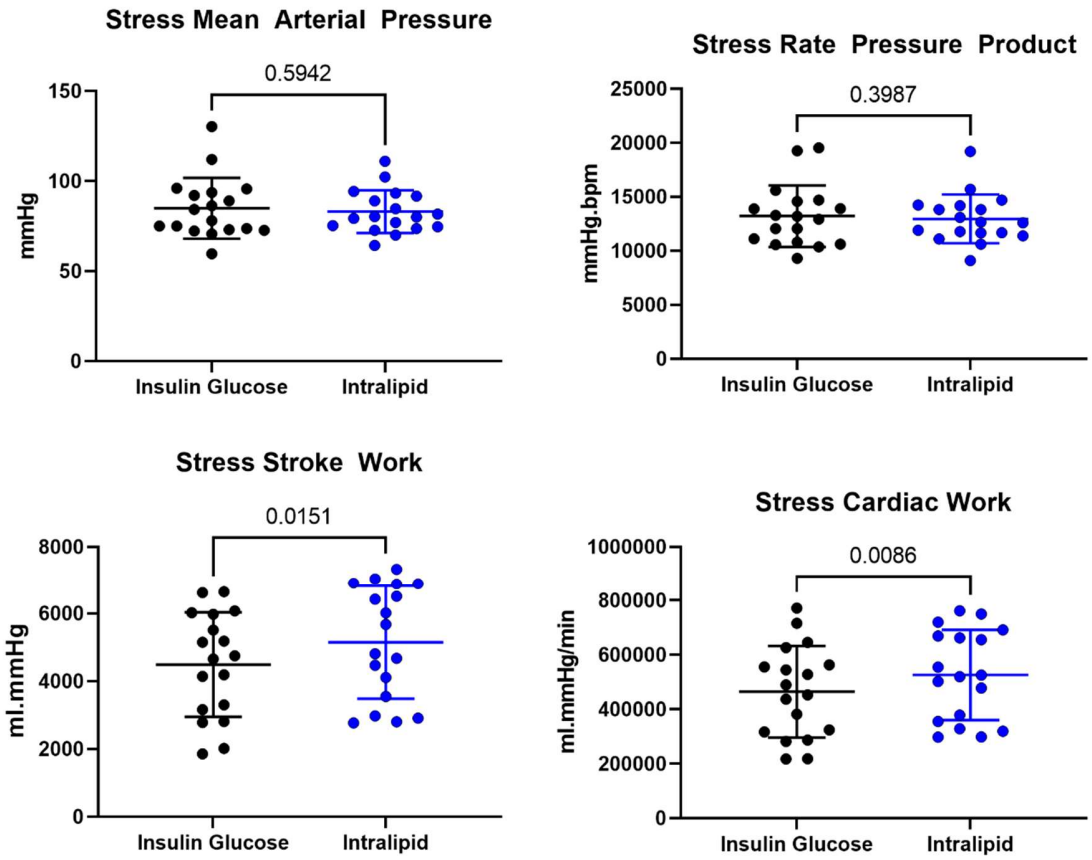

***Figure 5.12**: Haemodynamics in heart failure volunteers during CMR stress*

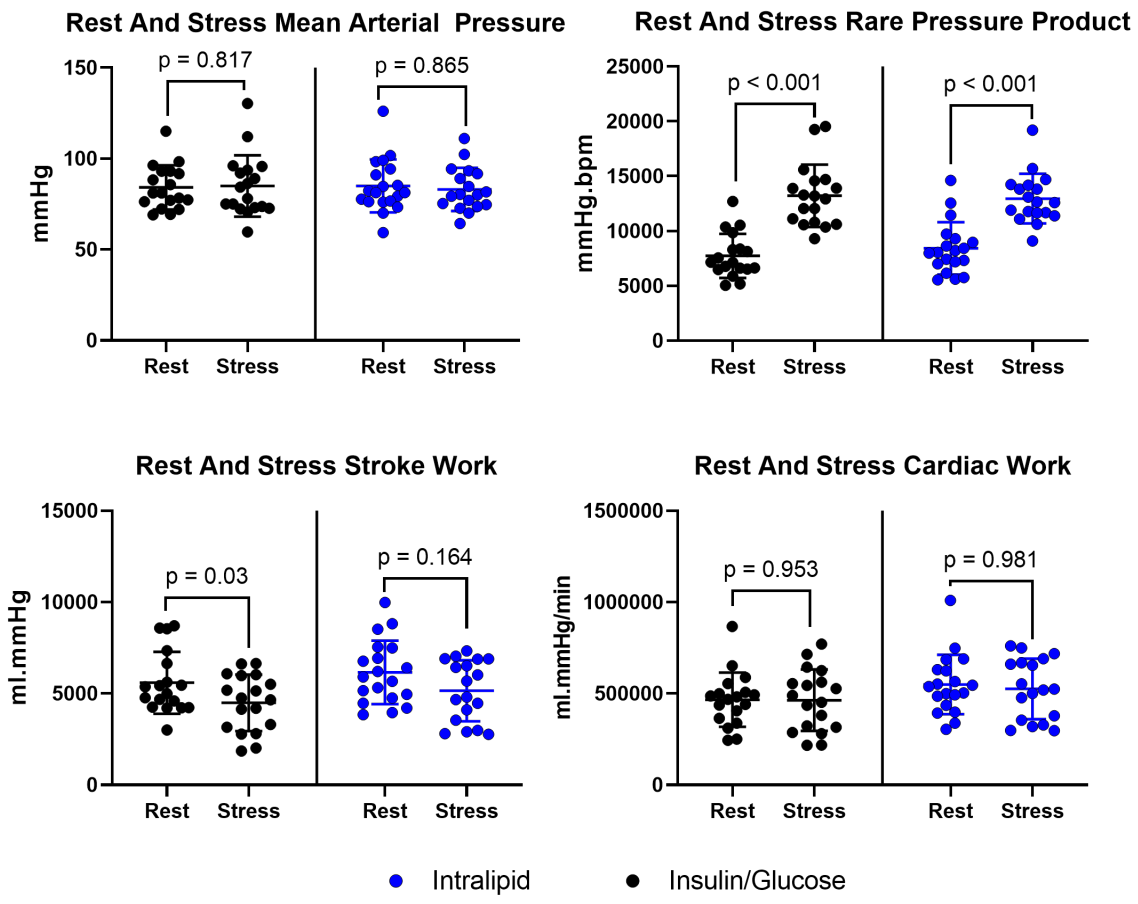

***Figure 5.13**: Rest and Stress Haemodynamics in heart failure volunteers*

5.3.2.4 ^{31}P MRS under stress in Heart Failure

Stress creatine kinase first order rate constant was not significantly different between arms of the study, nor was there a significant difference between rest and stress measures.

***Table 5.9**: Stress Creatine Kinase First Order Rate Constant in Heart Failure at stress*

	Insulin/Glucose	***Intralipid***	***p-value*** (t-test)
CK First Order Rate Constant (s^{-1})	0.37 ± 0.35	0.29 ± 0.21	0.36
PCr/ATP	1.88 ± 0.49	1.87 ± 0.65	0.63
CK flux (umol/g/s)	3.61 ± 3.12	2.85 ± 2.09	0.35

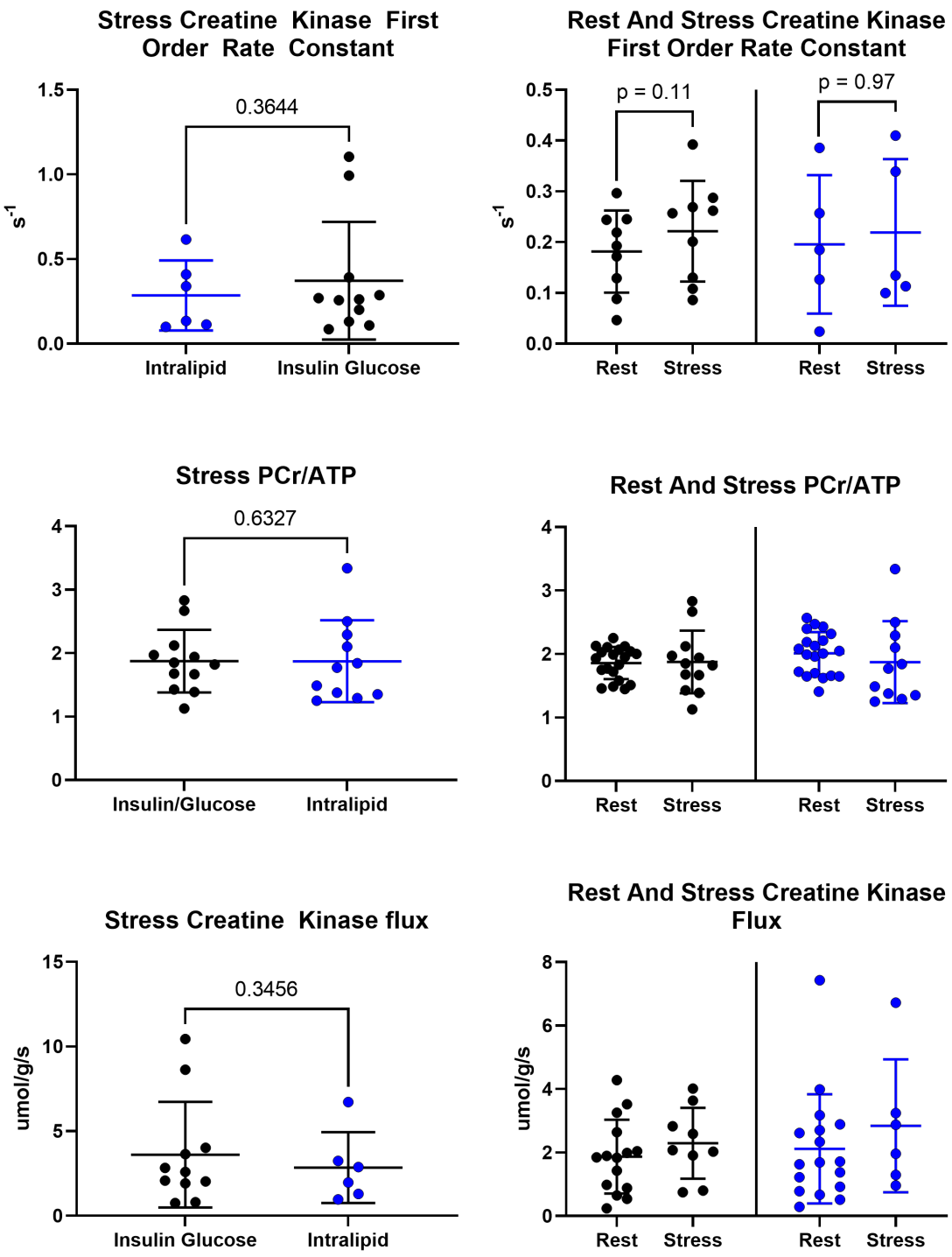

***Figure 5.14**: Stress ^{31}P Creatine Kinase First Order Rate Constant, PCr/ATP ratio and flux, with comparison to rest values in Heart Failure*

Resting PCr/ATP positively correlated with the cardiac index under stress (R^2 = 0.25, p = 0.003) and the rate pressure product at stress (R^2 = 0.2, p = 0.006) but not the stress cardiac work (R^2 = 0.08, p = 0.08).

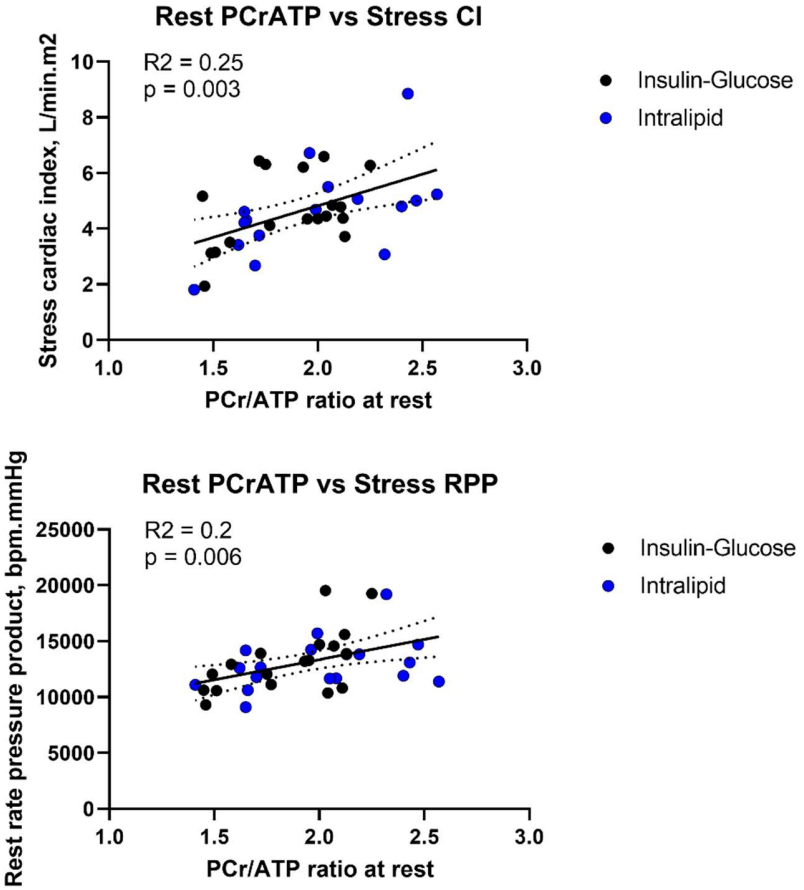

***Figure 5.15**: Correlations between resting PCr/ATP and stress haemodynamics in heart failure*

5.3.3 Invasive Data

5.3.3.1 Arterial Metabolites in Heart Failure Volunteers

Data is shown in table 5.10. Free fatty acid levels were significantly higher, as was beta-hydroxybutyrate. Insulin was numerically higher, although this also did not reach significance.

***Table 5.10**: Left mainstem arterial metabolite concentrations during rapid atrial pacing and substrate manipulation, during the invasive study, in the HFrEF group.*

	Insulin Glucose	***Intralipid***	***p-value (t-test)***
Glucose (mmol/L)	5.4 ± 1.22	5.47 ± 0.87	0.85
Free Fatty Acids (mmol/L)	0.96 ± 0.66	3.78 ± 1.47	***0.0001***
Insulin (pmol/L)	138 ± 102	40.7 ± 27.7	0.082
Β*-Hydroxybutyrate* (mmol/L)	0	0.2 ± 0.2	***0.028***
Lactate (mmol/L)	0.76 ± 0.19	0.71 ± 0.09	0.95

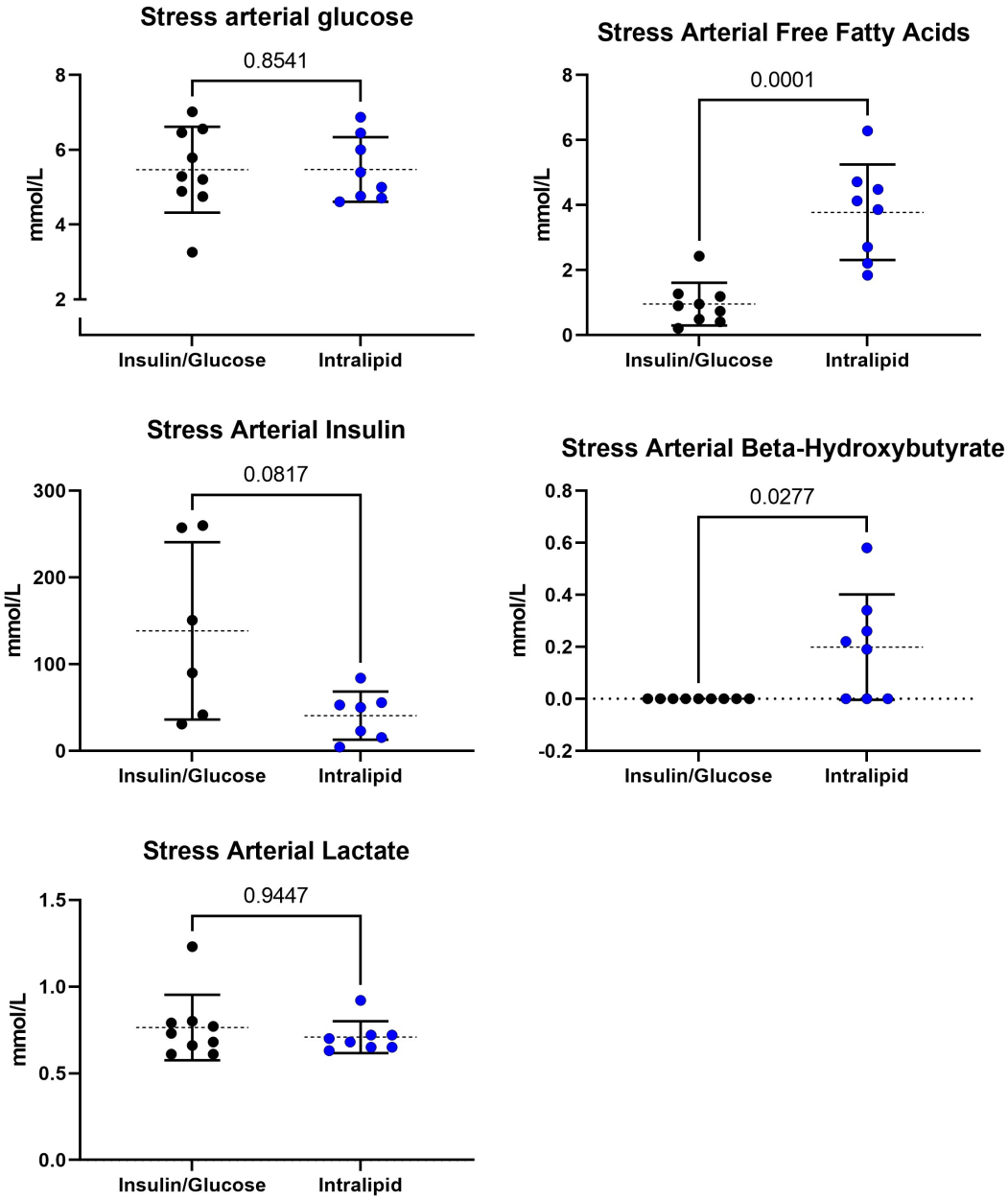

***Figure 5.16**: Left mainstem arterial metabolite concentrations during rapid atrial pacing and substrate manipulation, during the invasive study, in the HFrEF group.*

5.3.3.2 Arteriovenous Metabolite Extraction

See tables 5.11 and figure 5.17. As in the resting data, glucose extraction is higher with the insulin-glucose infusion while fatty acid extraction is higher with the Intralipid infusion, although the trend is less strong.

***Table 5.11**: Arteriovenous metabolite uptake during rapid atrial pacing and substrate manipulation, during the invasive study, in the HFrEF group.*

	Insulin/Glucose	***Intralipid***	***p-value***
Glucose (μmol/min)	63 ± 57	32 ± 28	0.09
Free Fatty Acids (μmol/min)	28 ± 32	68 ± 51	0.15
Β*-hydroxybutyrate* (μmol/min)	0	14 ± 26	0.18
Lactate (μmol/min)	25 ± 34	19 ± 63	0.28

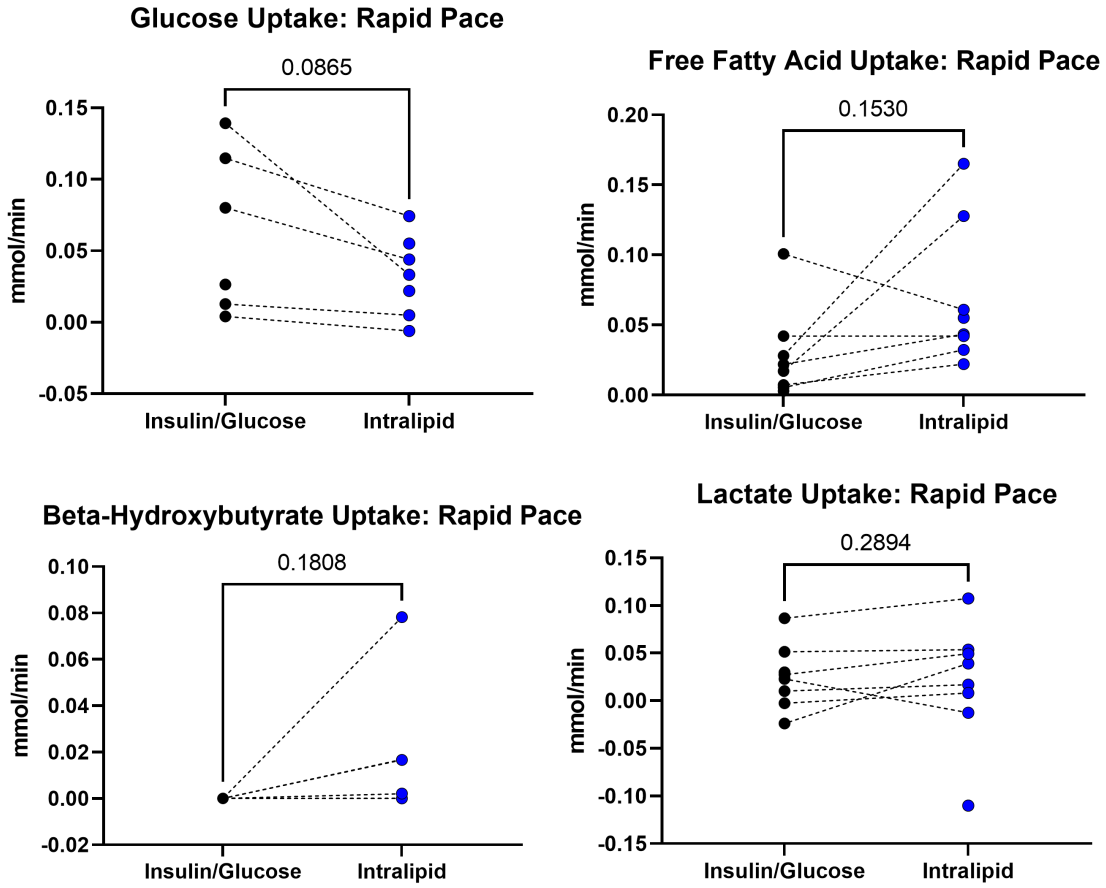

***Figure 5.17**: Arteriovenous metabolite uptake during rapid atrial pacing and substrate manipulation, during the invasive study, in the HFrEF group*

Glucose extraction generally fell under stress and fat extraction increased on the insulin-glucose infusion (although these changes were not statistically significant), while there was relatively minimal change on the Intralipid infusion.

***Table 5.12**: Rest and Stress comparison of cardiac arteriovenous metabolite uptake in patients with HFrEF*

	Intrinsic Rhythm	***Rapid Atrial Pacing***	***p-value***
Glucose-Insulin			
Glucose (μmol/min)	96 ± 53	63 ± 57	0.95
Free Fatty Acids (μmol/min)	10 ± 11	28 ± 32	0.32
β -hydroxybutyrate (μmol/min)	0	0	-
Lactate (μmol/min)	34 ± 35	25 ± 34	0.58
Intralipid			
Glucose (μmol/min)	45 ± 36	32 ± 28	0.16
Free Fatty Acids (μmol/min)	72 ± 43	68 ± 51	0.9
β -hydroxybutyrate (μmol/min)	8.9 ± 18	14 ± 26	0.19
Lactate (μmol/min)	35 ± 32	19 ± 63	0.35

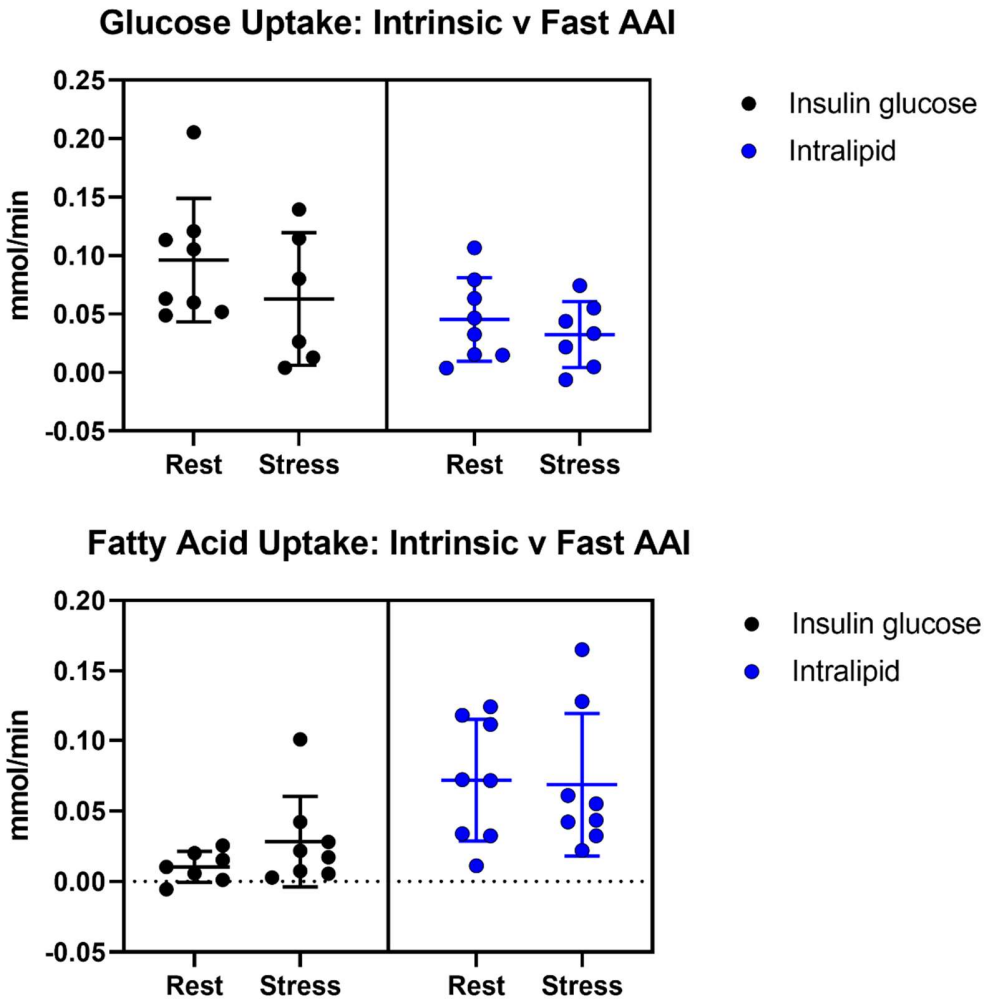

***Figure 5.18**: Rest and Stress comparison of cardiac arteriovenous metabolite uptake in patients with HFrEF. Intrinsic, intrinsic rhythm; Fast AAI, rapid atrial pacing.*

ATP generation was calculated assuming total oxidation of each substrate taken up (31mmol of ATP per mmol Glucose, 105mmol of ATP per mmol of free fatty acid, 12.5mmol of ATP per mmol of lactate, 20mmol of ATP per mmol of beta-hydroxybutyrate[338]), see table 5.13.

The trends seen above are reproduced, with fatty acid uptake becoming predominant in the insulin-glucose arm on rapid pacing, although not changing significantly in the fatty acid arm.

***Table 5.13**: ATP produced per metabolite as a percentage of total ATP production during stress*

	Insulin/Glucose	***Intralipid***	***p-value***
Total ATP (mmol/min)	5.81 ± 5.05	9.5 ± 6.25	0.19
Glucose (%)	44 ± 16	15 ± 10	***0.013***
Free Fatty Acids (%)	65 ± 27	75 ± 13	0.4
B ***-hydroxybutyrate*** (%)	0	4.2 ± 6.7	0.15
Lactate (%)	1 ± 16	6.1 ± 5.6	0.39

***Table 5.14**: Comparison between rest and stress of proportional ATP production by substrate*

	Intrinsic Rhythm	***Rapid Atrial Pacing***	***p-value***
Insulin-Glucose			
Glucose (%)	70 ± 14	44 ± 16	***0.04***
Free Fatty Acids (%)	19 ± 26	65 ± 27	0.06
B ***-hydroxybutyrate*** (%)	0	0	-
Lactate (%)	11 ± 13	1 ± 16	0.21
Intralipid			
Glucose (%)	17 ± 16	15 ± 10	0.56
Free Fatty Acids (%)	73 ± 17	75 ± 13	0.74
B ***-hydroxybutyrate*** (%)	1.9 ± 3.4	4.2 ± 6.7	***0.001***
Lactate (%)	7.5 ± 5.4	6.1 ± 5.6	0.1

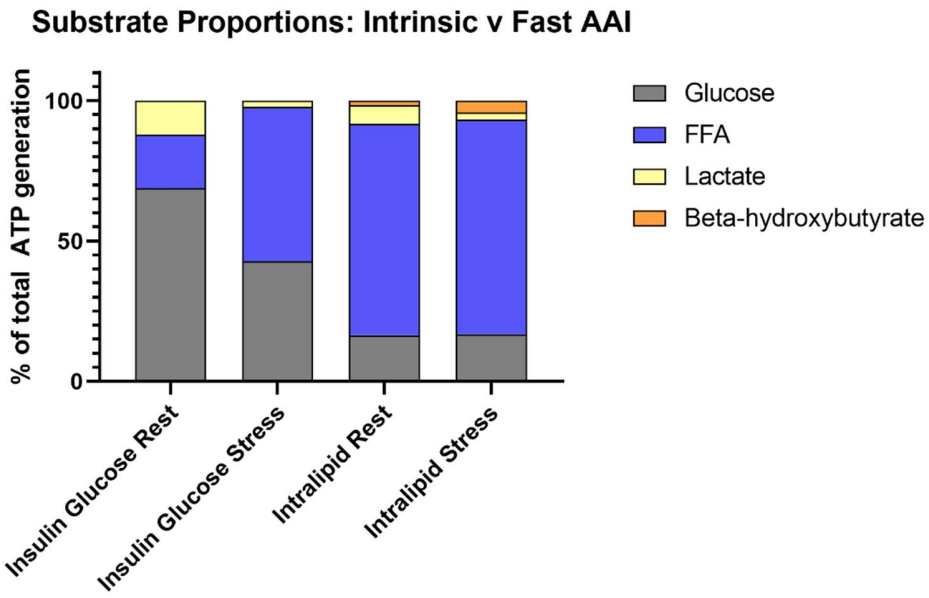

Figure 5.19*: ATP generation per substrate as proportion of the total. Fast AAI, rapid atrial pacing.*

There was no significant change in total calculated ATP production between rest and stress in glucose (intrinsic rhythm 4.6 ± 2.27 mmol/min vs rapid pace 5.81 ± 5.05 mmol/min, p = 0.48) or Intralipid (intrinsic rhythm 8.78 ± 5.14 mmol/min vs rapid pace 9.5 ± 6.25 mmol/min, p = 0.86).

5.3.3.3 Arteriovenous Oxygen Extraction

When the data is analysed together, oxygen extraction during rapid pacing was higher than that during intrinsic rhythm or slow biventricular pacing.

***Table 5.15**: Cardiac arteriovenous oxygen difference and extraction in HFrEF, during rapid atrial pacing, and substrate manipulation*

	Insulin/Glucose	***Intralipid***	***p-value***
Oxygen content difference (ml/dl)	8.61 ± 4.14	8.84 ± 4.48	0.72
Oxygen extraction (MVO2) (ml/min)	17.3 ± 9.67	21.3 ± 4.5	0.14

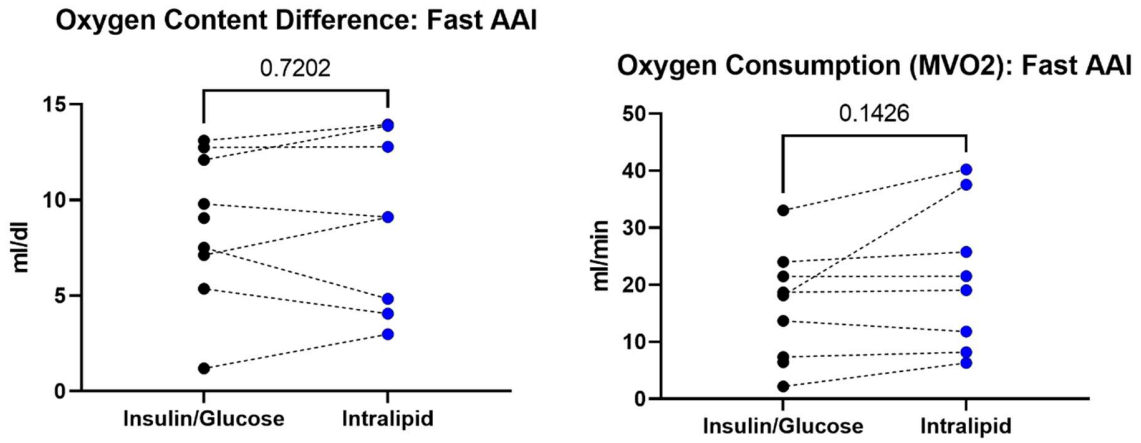

***Figure 5.20**: Arteriovenous oxygen extraction at stress in patients with HFrEF. Fast AAI, rapid atrial pacing.*

There was a numerical increase in MVO_2 from intrinsic rhythm to fast pacing, however this only trended towards significance (p = 0.08) in the insulin-glucose arm and was not significant in the Intralipid arm (p = 0.26). The increase in MVO_2 from rest to stress was not significantly different between the insulin-glucose and Intralipid arms of the study (insulin-glucose +3.2 ± 4.89 ml/min vs Intralipid +2.47 ± 6.01 ml/min, p = 0.74).

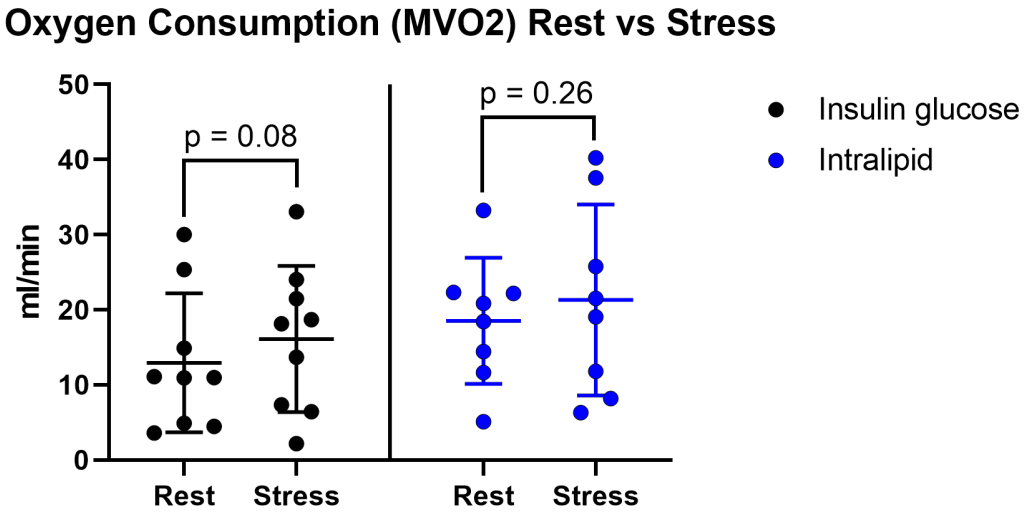

Figure 5.21*: Oxygen consumption at stress compared to that at rest (intrinsic rhythm compared to rapid atrial pacing).*

Similar positive correlations were seen between the MVO2 and the calculated total oxygen consumption in each arm (Insulin-Glucose slope 0.12, $R^2 = 0.405$, p = 0.09; Intralipid slope 0.13, $R^2 = 0.424$, p = 0.08, Figure 5.20).

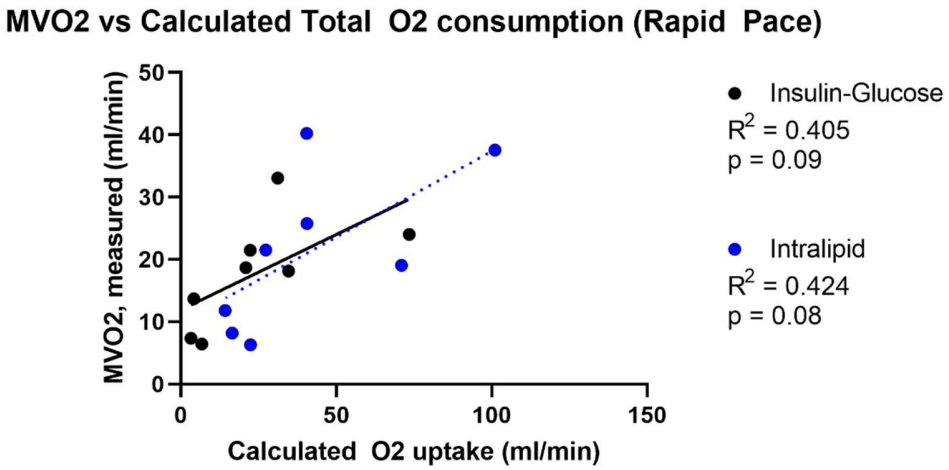

***Figure 5.22**: Calculated oxygen uptake (based on the complete oxidation of each substrate taken up) compared to measured oxygen uptake (MVO2).*

5.3.3.4 Invasive Measures of Contractility during Rapid pacing

As in the rest data, there were no significant differences in volumetric measures of cardiac contractility, however on pressure based measures of contractility, the Intralipid group trended towards producing higher values. Comparing rest to stress values, with Intralipid there was a smaller fall in stroke work and a trend towards a greater rise in dP/dt.

***Table 5.16**: Invasive measures of contractility during rapid atrial pacing in HFrEF, and the change from intrinsic rhythm (rest) to rapid pacing (stress)*

	Insulin/Glucose	***Intralipid***	***p-value***
Rapid Atrial Pacing Stress			
LV Ejection Fraction (%)	22 ± 10.1	21.8 ± 12.8	0.96
Stroke Work (mmHg.ml)	5461 ± 1887	5151 ± 1300	0.74
Cardiac Work (L.mmHg/min)	552 ± 174	705 ± 476	0.48
dP/dT (mmHg/s)	752 ± 111	807 ± 119	0.06
ESP (mmHg)	92.8 ± 8.5	100.3 ± 10.7	0.08
LVDP (mmHg)	82.3 ± 10.1	89.5 ± 11.9	0.08
Stress – Rest			
LV Ejection Fraction (%)	- 7.0 ± 5.1	- 4.1 ± 4.6	0.15
Stroke Work (mmHg.ml)	-3428 ± 2402	- 2549 ± 1900	***0.05***
Cardiac Work (L.mmHg/min)	-52 ± 245	-5 ± 205	0.34
dP/dT (mmHg/s)	106 ± 68	143 ± 117	0.19
ESP (mmHg)	4.8 ± 9.5	1.7 ± 10.4	0.39
LVDP (mmHg)	1.7 ± 5.7	0.3 ± 8.8	0.64

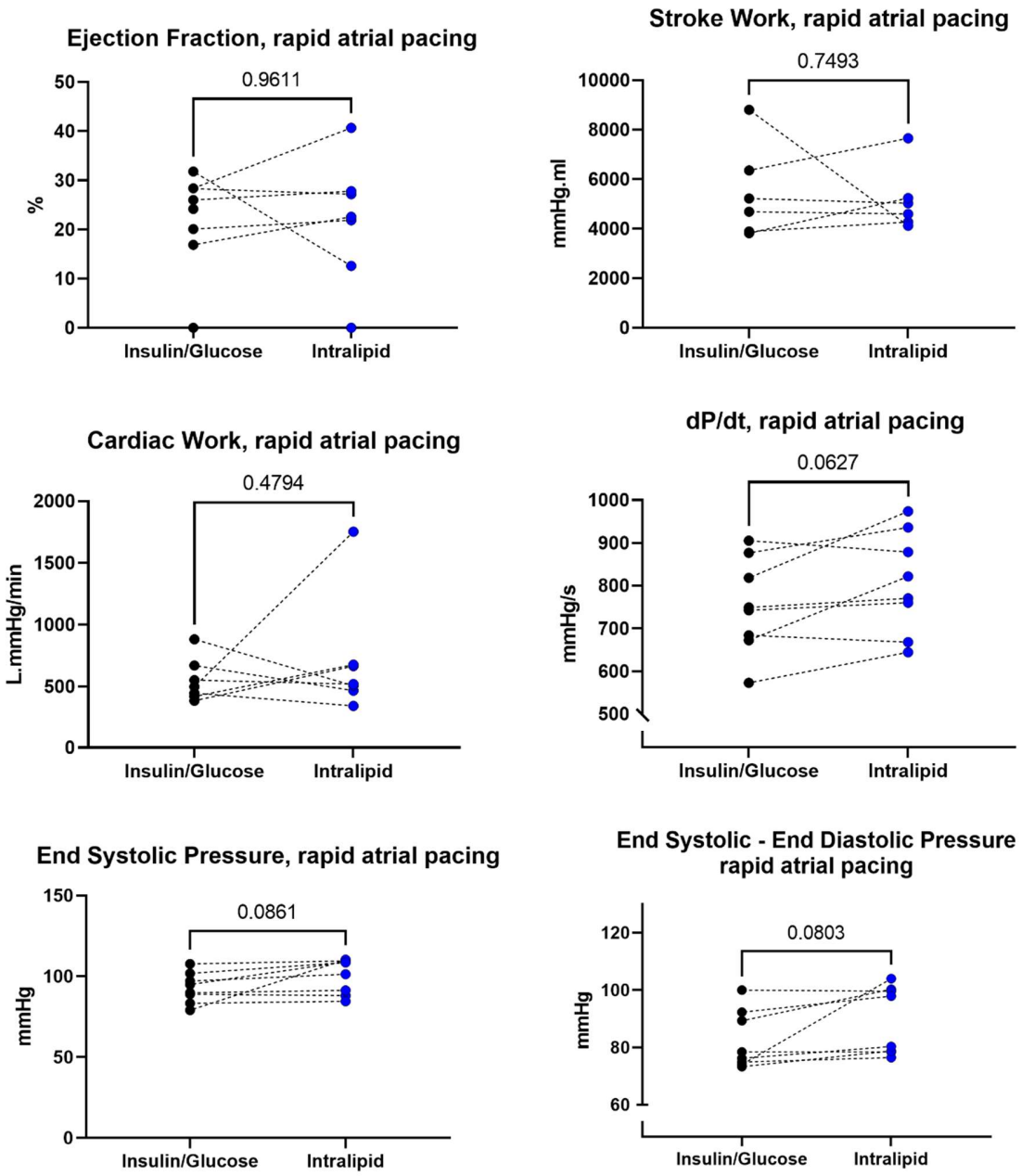

***Figure 5.23**: Invasive Measures of Contractility during rapid pacing in HFrEF. CW, cardiac work.*

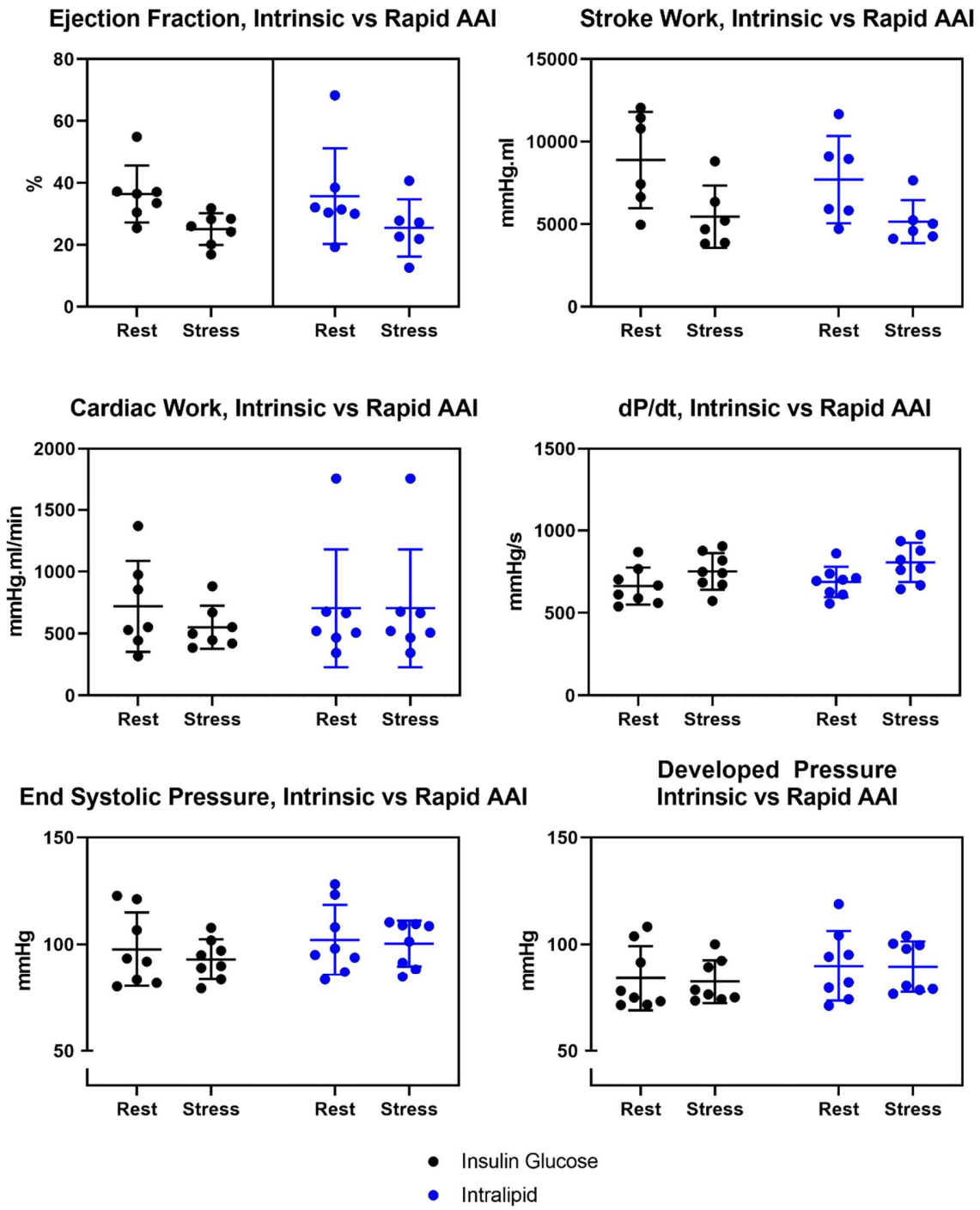

***Figure 5.24**: Rest (intrinsic rhythm) and Stress (Rapid AAI, rapid atrial pacing) invasive measures of contractility in HFrEF*

5.3.3.5 Invasive Measures of Contractility during Rapid Biventricular Pacing

As in the rapid atrial pacing, measures of pressure (dP/dt and left ventricular developed pressure) were higher during biventricular pacing with Intralipid. However, there were no differences between insulin-glucose infusion and Intralipid in terms of the change from slow biventricular pacing to rapid biventricular pacing.

***Table 5.17**: Cardiac contractility during rapid biventricular pacing and compared between slow and rapid biventricular pacing in patients with HFrEF*

	Insulin/Glucose	***Intralipid***	***p-value***
Rapid Biventricular Pacing Stress			
LV Ejection Fraction (%)	39.2 ± 16.7	36.9 ± 12	0.62
Stroke Work (mmHg.ml)	10555 ± 6446	10094 ± 5841	0.55
Cardiac Work (L.mmHg/min)	1003 ± 585	817 ± 432	0.06
dP/dt (mmHg/s)	849 ± 121	941 ± 163	***0.04***
ESP (mmHg)	96.8 ± 13.3	103 ± 12.7	0.09
LVDP (mmHg)	85 ± 13.1	92.7 ± 11.9	***0.03***
Stress – Rest			
LV Ejection Fraction (%)	- 3.2 ± 4.4	-1.8 ± 4.2	0.57
Stroke Work (mmHg.ml)	-1140 ± 1550	-1150 ± 1850	0.98
Cardiac Work (L.mmHg/min)	176 ± 155	229 ± 171	0.32
dP/dT (mmHg/s)	123 ± 104	165 ± 120	0.33
ESP (mmHg)	0.2 ± 4.4	1.7 ± 4.0	0.44
LVDP (mmHg)	-0.1 ± 5.7	-1.0 ± 4.0	0.77

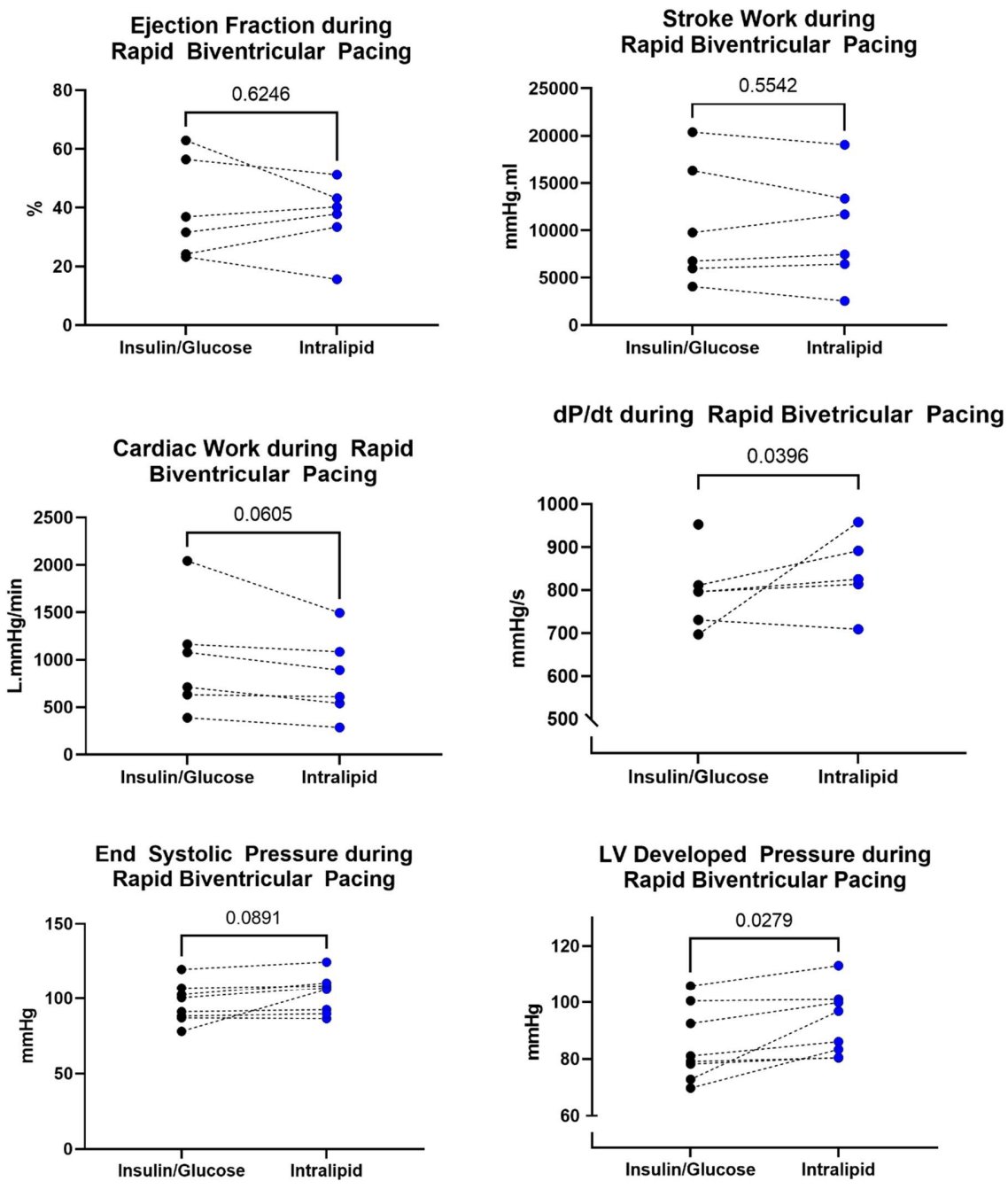

***Figure 5.25**: Measures of Contractility during Rapid Biventricular Pacing in HFrEF patients*

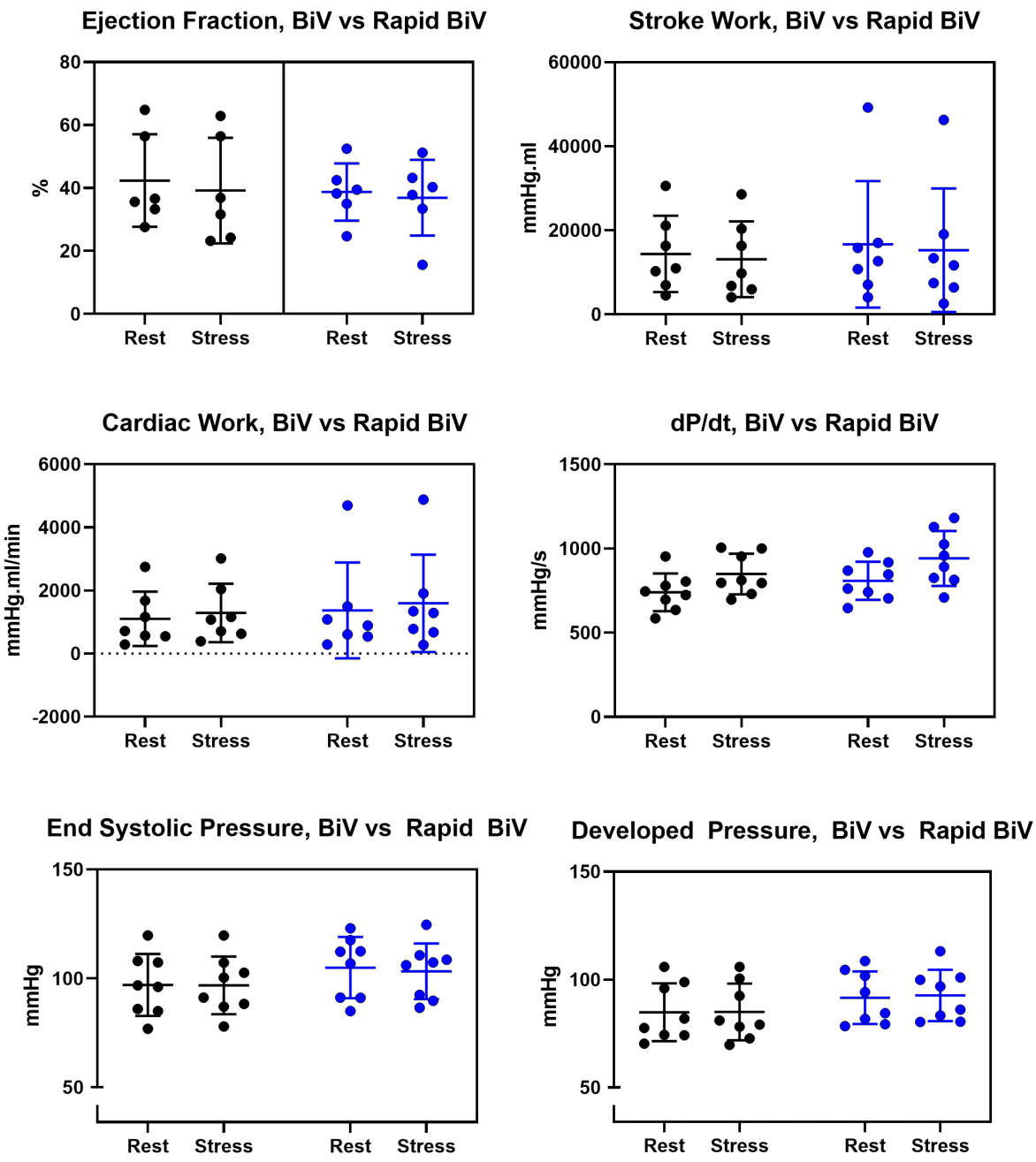

***Figure 5.26**: Comparison of slow biventricular pacing (rest) and rapid biventricular pacing (stress) in cardiac contractility. Black circles (left) represent insulin-glucose infusion while blue circles (right) represent Intralipid infusion. BiV, biventricular pacing.*

5.4 Discussion

5.4.1 The failing heart retains flexibility to take up different substrates under stress

In chapter 4, I demonstrated flexible substrate uptake depending upon the prevailing concentrations of circulating free fatty acids or insulin. In the data presented in this chapter, we have shown changes of uptake on stress in spite of the infusions ongoing at the time, with a general move towards an increased reliance on free fatty acids and decreased reliance upon glucose, even during the euglycaemic clamp. This runs contrary to both ideas around the inflexibility of the failing heart[85] although is in line with previous studies with rapid pacing and arteriovenous sampling[147] where fatty acid uptake and oxidation rose during rapid pacing in patients with dilated cardiomyopathy.

We have shown that substrate selection may not simply be a passive change in uptake that reflects changes in arterial supply. Whilst AAI pacing has previously been shown to increase fatty acid uptake in the fasted state in HFrEF[147] and dobutamine stress increases fatty acid uptake in animal models of pacing induced heart failure[353], we have shown that even during a glucose-insulin infusion, rapid atrial pacing increases cardiac extraction of fatty acids despite no change in arterial fatty acid supply, and that Glucose uptake was numerically (but not significantly) reduced. As this increased uptake of fatty acids occurred without a change in arterial supply it implies that the heart in HFrEF has active substrate selection and preference to fatty acids during rapid contraction.

5.4.1.1 Glucose Uptake Fell During Stress

On all infusions and modalities, glucose uptake fell during stress. Glucose would appear a more logical substrate for stress metabolism were the heart to be oxygen-limited, however this appears not to be the case for the hearts studied here as MVO_2 rose from rest to stress and there was no significant lactate efflux suggestive of anaerobic metabolism. The higher ATP yield per molecule of substrate may influence the shift from glucose to fat with capacity to take up substrate being the limiting factor rather than oxygen consumption.

As discussed in chapter 1 section 1.4.1.2.1 and section 1.4.1.3.1, there are many interacting signals which determine substrate preference under stress[57], however the extent to which these function in heart failure is unknown. In healthy subjects and animal models, glucose uptake and oxidation has been shown to increase in response to stress[354], however, the response of the failing heart to stress remains under-investigated. Exercise or ischaemic stress cause translocation of GLUT-4 transporters for increased glucose uptake in response to HIF-1α and AMPK[355] activation, although the exact mechanisms leading to GLUT-4 activation are not well understood[356]. In skeletal muscle, calcium stimulates glucose uptake[357], although this pathway is yet to be looked at closely in the cardiac myocyte. Indeed, in animal hearts, AMPK activation at low levels was shown to increase glycogenolysis rather than cause glucose uptake[358]: given that these patients had been established on a euglycaemic clamp for an hour or more prior to the sampling, it may be that they had laid down glycogen stores which would be used during the short runs of rapid pacing. A future direction may be to monitor glucose uptake serially during more prolonged rapid pacing.

In animal models of prolonged rapid pacing induced heart failure, glucose oxidation has been shown to fall[138]. The need to maintain a sufficient $NADH/NAD^+$ ratio for aerobic glycolysis is

limiting at medium to high workload, as these agents cannot be shuttled between mitochondria and cytosol with sufficient speed[128], which may limit glucose uptake.

Some of the processes which would normally increase glucose metabolism may be deficient in the failing heart. Calcium increases inotropy and chronotropy, with mitochondrial calcium increasing in the healthy heart in response, acting on PDH to increase carbohydrate oxidation[359], however calcium handling is remodelled in heart failure, with a smaller calcium transient amplitude in contraction[360]. HIF-1 increases glycolysis while inhibiting PDH[73], however HIF-1 protein levels are chronically increased in heart failure[361]. Finally, increased Pi and activation of AMPK would be expected to activate glucose uptake, glycolysis and fatty acid oxidation[362, 363], however phosphotransfer is dysfunctional in heart failure and these signals may not be fed back from sites of ATP use to the mitochondria[100]. Taken together, this may explain the relative preference for fatty acids, as many of the signals required to increase glucose uptake are dysfunctional.

5.4.1.2 Fatty Acid was taken up preferentially in Heart Failure

Fatty acid uptake rose during stress in heart failure with the insulin-glucose infusion but did not significantly change from being the predominant energetic substrate between rest and stress on the Intralipid infusion. This challenges the concepts in the literature where glucose was thought to be the preferential substrate at stress, so is also worthy of further discussion.

AMPK has been shown to activate myocardial fat oxidation via inhibition of acetyl CoA carboxylase and a reduction in cytosolic malonyl CoA[364, 365] in responses to changes in the AMP/ATP or Cr/PCr ratios, which may be relevant in rapid pacing stress as ATP demand increases. Exercise induces PGC-1 activation in skeletal muscle[366] (although response to increased

ATP demand has not been tested in cardiac muscle), while MAP kinase activates PPARα[367]. While these processes are not fully elucidated in health or heart failure, it is known that rapid pacing reduces cytosolic malonyl-CoA, increasing β-oxidation[55]. Further work is required to tie these biochemical pathways together and fully explain the observations here but it may be, as with glucose, the response to exercise is different in the failing heart as the normal signalling pathways do not function as they should.

As in the resting phase, calculated ATP production was almost 2 times higher during the Intralipid infusion than the euglycaemic clamp during stress, suggesting that not all the substrate taken up contributed to energy production. Nontheless, some indices (a lower fall in ejection fraction and a greater increase in dP/dt would suggest a benefit from increased fat supply and a benefit from favouring this fuel under stress.

5.4.2 In the Healthy Heart, Substrate Metabolised does not impact Stress Cardiac Work

While trends were seen in the healthy group, there were no significant differences in cardiac performance under dobutamine stress comparing Intralipid, insulin-glucose or acipimox. It is of interest that the reduction in contractility with a nicotinic acid receptor agonist which was observed in chapter 3 can be overcome with dobutamine in the healthy heart: in fact there was a rise in free fatty acids from baseline, suggesting the lipolytic effect of catecholamines[60, 119] partially overcomes the inhibition from nicotinic receptor agonists.

5.4.3 In The Failing Heart, there is no Change in Cardiac Work during Dobutamine Stress but Cardiac Work remains higher with Intralipid Infusion

In the CMR experiment, rest and stress cardiac work are remarkably similar. Even though heart rate rose, changes in stroke volume and blood pressure counter this to leave stroke work lower and hence cardiac work unchanged; while there was a significant reduction in LV stroke work with insulin-glucose, this was not present with Intralipid. This may demonstrate a heart functioning at the upper limit of its ability to do work in the rested state, unable to further increment this output in the stress state, whereas in the healthy heart, cardiac work could increase significantly. It cannot be a surprise that the calculated amounts of ATP produced from all substrates are not significantly different in the invasive study at rest compared to at stress. It is known that beta adrenoreceptors are downregulated in the failing heart[368, 369] and the response to inotropes is desensitised[370], however the similarity between cardiac work is striking.

This is consistent with the PCr/ATP ratio at rest being predictive of both resting and stress contractility in the heart failure group but only stress measures in the resting heart. This may suggest that, in healthy volunteers, resting PCr/ATP can determine peak cardiac performance, while other factors are more important at rest, while in heart failure, the heart is continuously at peak performance, determined by the PCr/ATP ratio. This is consistent with work elsewhere demonstrating PCr/ATP determines performance under stress[345]. It neatly follows that Intralipid, which was shown in chapter 4 to elevate resting PCr/ATP ratio, increased maximal cardiac work and in invasive studies showed greater increases in developed pressure from rest to stress. This may relate to the higher ATP yield from free fatty acid compared to glucose[155, 156] or the

metabolic limitations of maintaining a high rate of glucose oxidation, such as maintaining a low $NADH/NAD^+$ ratio for glycolysis[128].

5.4.4 There is no Significant Change in Oxygen Consumption in the Failing Heart during Rapid Pacing

The minimal increase in oxygen uptake under stress parallels the lack of significant change in cardiac work seen in the invasive and CMR sides of the study, although the stressors are different. Oxygen consumption did not seem to be limiting in either CMR or invasive arms of the study, with PCr/ATP ratios maintained and no significant lactate efflux.

The difference between MVO_2 with insulin-glucose compared to with Intralipid was less marked (although still higher) on stress than in the rest measurements, presumably a result of the shift towards increased fatty acid uptake seen with rapid pacing. In animal models of heart failure (e.g. rapid pacing in dogs), oxygen consumption per beat decreased during catecholamine stress[370], while human studies using PET during dobutamine in volunteers with dilated cardiomyopathy, myocardial efficiency (the ratio of noninvasively determined stroke work to oxygen consumption) actually improved[342]. This may be due to changes in ATP utilisation or reductions in uncoupling at stress. Further work is needed to understand the molecular mechanisms underlying these alterations in the healthy and the failing heart.

5.5 Limitations

5.5.1 Metabolic Fates

In addition to the limitations expressed in chapter 4 over monitoring of metabolic fates, it is worth noting in particular that we only measured glucose uptake from the myocyte and did not measure glycogenolysis, which has been shown to provide glucose for oxidation under stress[358].

5.5.2 Rapid pacing and dobutamine may not be equivalent

Catecholamines are known to stimulate lipolysis and mobilisation of lipid from adipocytes[60, 119]. Therefore, a rise in circulating lipids during stress is to be expected during dobutamine infusion. Also, reduced sensitivity to insulin has been previously observed during longer term Intralipid infusion in healthy volunteers[371]. In this case, this may be causing a feedback mechanism to increase insulin secretion during the time of the infusion. Likewise, the rise in glucose seen in the euglycaemic clamp under stress can be accounted for by the effects of Catecholamines on glucose metabolism. β_2 adrenoreceptor stimulation elevates blood glucose via inhibition of insulin secretion, activation of gluconeogenesis and glycogenolysis and secretion of glucagon and cortisol[372].

Dobutamine also has positive inotropic effects on the heart and vasodilator effects on the peripheral vasculature, which are not present with rapid pacing which only has a chronotropic effect. Therefore, the energy requirements may not be equivalent, even though heart rate was matched. This may also explain the fall in ejection fraction during rapid atrial pacing contrasting

with the unchanged values in rapid biventricular pacing and the rise seen during dobutamine stress CMR.

5.5.3 Venous Sampling in the CMR Experiment

It cannot be assumed that changes seen represent metabolic alterations during stress alone as approximately 90 minutes elapse between the baseline measure and the start of stress, so this may represent further metabolic changes taking place during the infusion.

6 Chapter 6: The Effect of Vasodilator Stress on Cardiac Function and Energetics

6.1 Introduction and Rationale

6.1.1 Myocardial Energy Use

Mechanical work done by the heart is proportional to heart rate, stroke volume and end systolic pressure (the latter two generating ventricular wall tension). Myocardial oxygen consumption (and therefore ATP production) is again proportional to this, although the slope of the curve is modified by the effects of catecholamines or myocardial substrate[17].

In this chapter, we quantify the ATP flux through creatine kinase instead of oxygen uptake. Creatine kinase transfer carries roughly 80% of ATP, with the remainder being split between adenylate kinase (~15%) and glycolysis (~5%). Therefore, by comparing changes in the same human subject, we can draw conclusions about the efficiency of the heart in using ATP for mechanical work as preload and afterload changes.

^{31}P Cardiac MRS will allow us to study the turnover of ATP within the myocardium. We can therefore use it to directly test energy demand and ascertain how it varies with contractile state.

6.1.2 Vasodilators and Venodilators

A vasodilator will cause preferential dilation of the arteriolar beds, reducing systemic vascular resistance and therefore mean arterial pressure. The initial effect will be a loss of afterload on the ventricle and a change in the shape of the pressure-volume loop based on the end systolic

pressure-volume relationship (ESPVR) with an increase in the stroke volume based on this relationship.

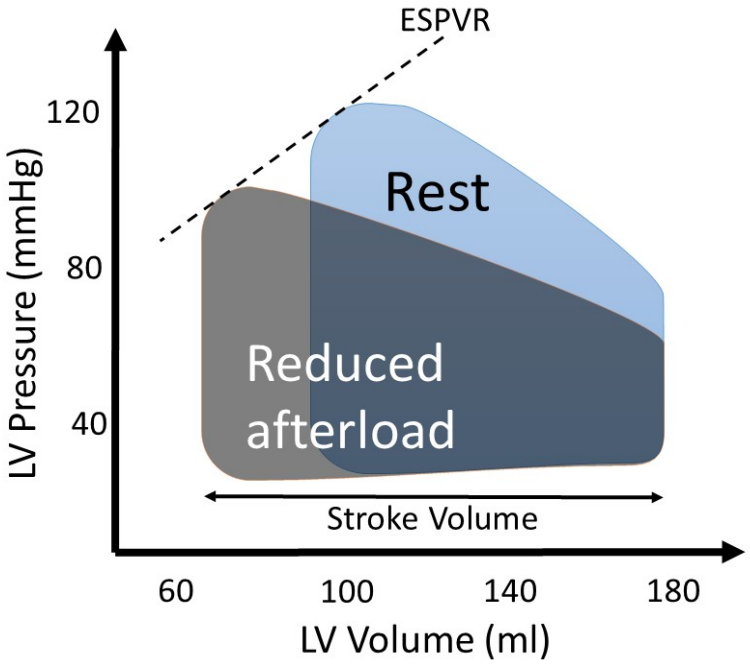

Figure 6.1*: Changes in pressure-volume loops with afterload change*

A venodilator will preferentially act upon the large central capacitance veins (e.g. the splanchnic circulation), reducing the filling of the heart. This will cause a fall in the left ventricular end diastolic volume (LVEDV) and left ventricular end diastolic pressure (LVEDP) – i.e. a fall in preload – and hence a reduction in myofibrillar stretch and a decline in stroke volume by Frank-Starling mechanisms.

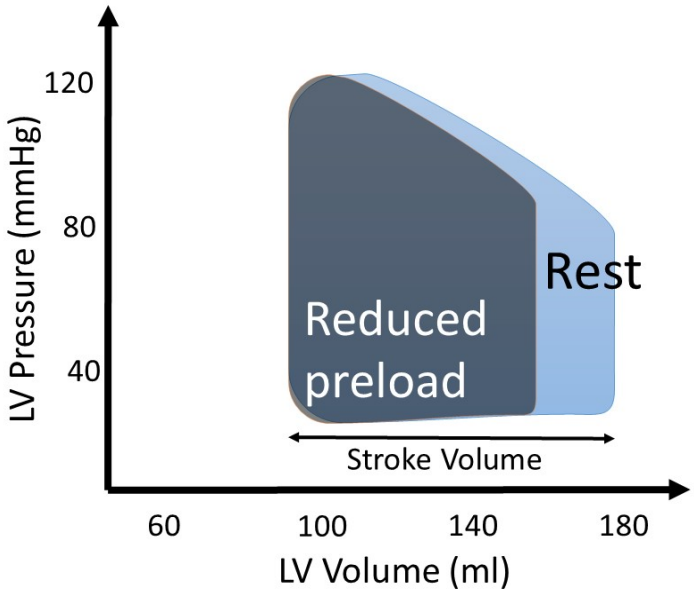

***Figure 6.2**: Changes in pressure-volume loops with preload change*

If a drug such as glyceryl trinitrate (GTN) is applied in sufficient doses, it has combined vasodilator and venodilator effects. The net effects are a fall in both afterload and preload, although the individual effects on a circulation will depend upon the state of the heart and the circulation.

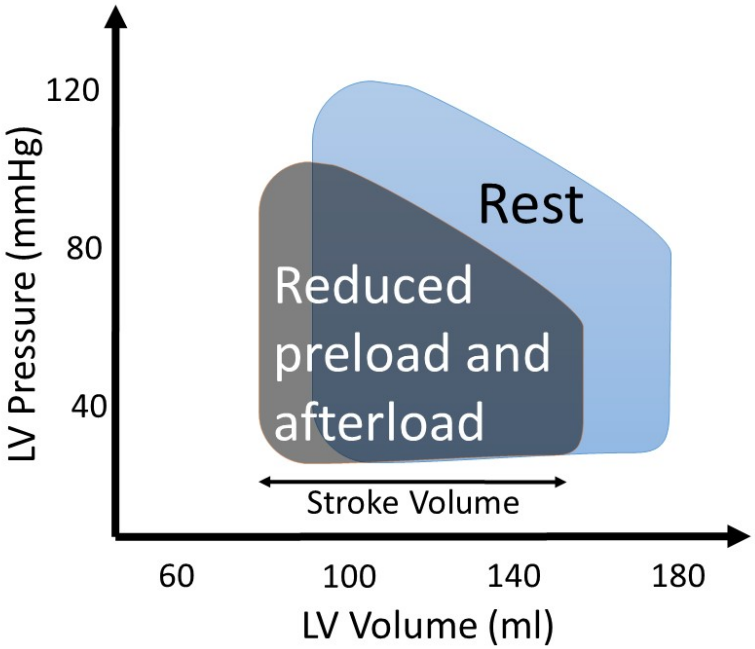

***Figure 6.3**: Changes in pressure-volume loops with preload and afterload changes*

In decompensated cardiac failure, the heart is stretched by preload beyond the point where Frank-Starling laws will increase stroke volume while high afterload increases the energy required for each contraction. In these circumstances, reducing preload and afterload will increase stroke volume without compromising blood pressure and hence GTN can be a useful treatment for these patients. Long term administration of vasodilator therapy has been shown to improve mortality in heart failure[373].

In the healthy circulation, the response is different. The drop in preload causes a fall in stroke volume and when combined with a fall in systemic vascular resistance, this causes a drop in mean arterial pressure[374]. This causes a rapid arterial baroreflex sympathetic response to increase the inotropy and chronotropy of the heart in an attempt to offset these changes (altering the ESPVR line's slope). Reductions in preload and afterload with increased inotropic stimulation would be

expected to cause myocardial oxygen efficiency to fall and ATP requirement per unit work done to increase.[17, 52, 53]

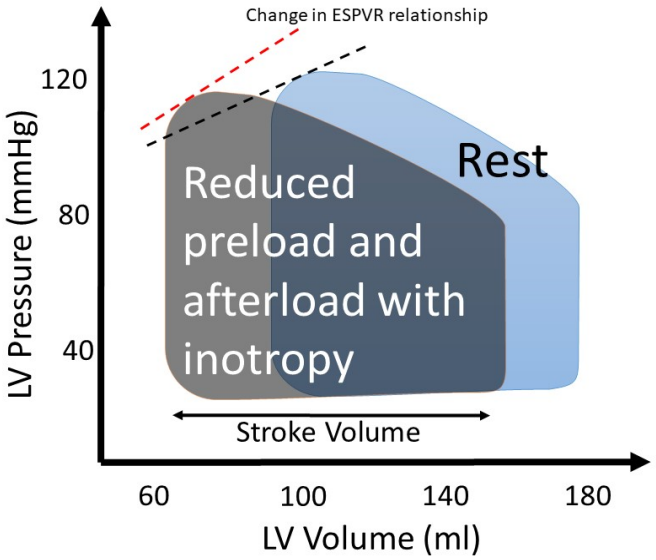

***Figure 6.4**: Changes in pressure-volume loops with preload and afterload changes and inotropy*

Therefore we would expect to find, when GTN is administered in sufficient quantities, a fall in preload leading to increased inotropy and chronotropy driven by reflex sympathetic action to maintain blood pressure. We would predict from the above that energetic demand would be higher, even though the cardiac output may be similar. Studies have shown increased MVO2 in the human heart following their administration[375]. We hypothesized this was due to a loss of mechanical efficiency[376] (i.e. the difference between ATP requirement and mechanical work done due to relative changes in unloaded or external cardiac work) in the heart following loss of preload.

6.1.3 Effects of GTN on Myocardial Oxygen Consumption and Oxidative Phosphorylation

Historical studies have shown increased myocardial oxygen demand in humans during administration of nitrate in spite of unchanged cardiac output[375], while in isolated hearts or preparations of myocytes, there was a reduction in oxygen uptake[377, 378]. On the organelle level, GTN inhibits oxidative phosphorylation in isolated mitochondria[379] via nitric oxide induced inhibition of complex IV of the respiratory chain[380], therefore mitochondrial oxygen uptake and ATP production declines.

6.1.4 Experimental Rationale

In totality, we would predict that the heart faces an increased energy demand from the loss of mechanical efficiency and a loss of energy supply from a loss of mitochondrial efficiency. This provides a model for the failing heart where there is both mitochondrial dysfunction and a mechanical inefficiency from a large, dilated ventricle. We would further hypothesize that sustained high energy demand provides a model for progression of heart failure and being able to mimic the changes in high energy phosphate metabolism may pave the way for metabolic interventions targeting the condition.

6.2 Methods

10 Healthy volunteers were recruited via word of mouth, emails to departmental mailing lists, social media postings and posters located in University Departments.

Exclusion criteria were as follows:

- Any history of cardiac disease (valvular heart disease, coronary artery disease or known impaired ejection fraction)
- Any metabolic disturbance (a history of diabetes or taking diabetic medication, hypothyroidism or anaemia)
- Any condition which would contraindicate nitrate based medications (glaucoma, hypotension or taking existing nitrate-based medications)
- Any contra-indication to cardiac MRI scanning (metallic clips/foreign bodies, injuries to the eye, shrapnel injuries, metallic or electronic implants including pacemakers, pregnancy)
- Involvement in any other research projects where the procedures may affect the outcomes of the trial

6.2.1 CMR Protocol

The aim was to collect cine imaging, PCr/ATP ratio and CK_{kf} data in baseline and veno and vasodilatory states. Briefly, the protocol was as follows:

1. Baseline ^{31}P 3D-CSI
2. Baseline cine imaging
3. ^{31}P TRIST sequence
4. GTN infusion started and 15-25 minutes allowed for rate to stabilise
5. STRESS extension of TRIST sequence
6. Repeat cine imaging
7. Repeat ^{31}P 3D-CSI

Further detail on 1, 2, 3 and 5 can be found in chapter 2, sections 2.3.1 and 2.3.2. The study is summarised in figure 6.5.

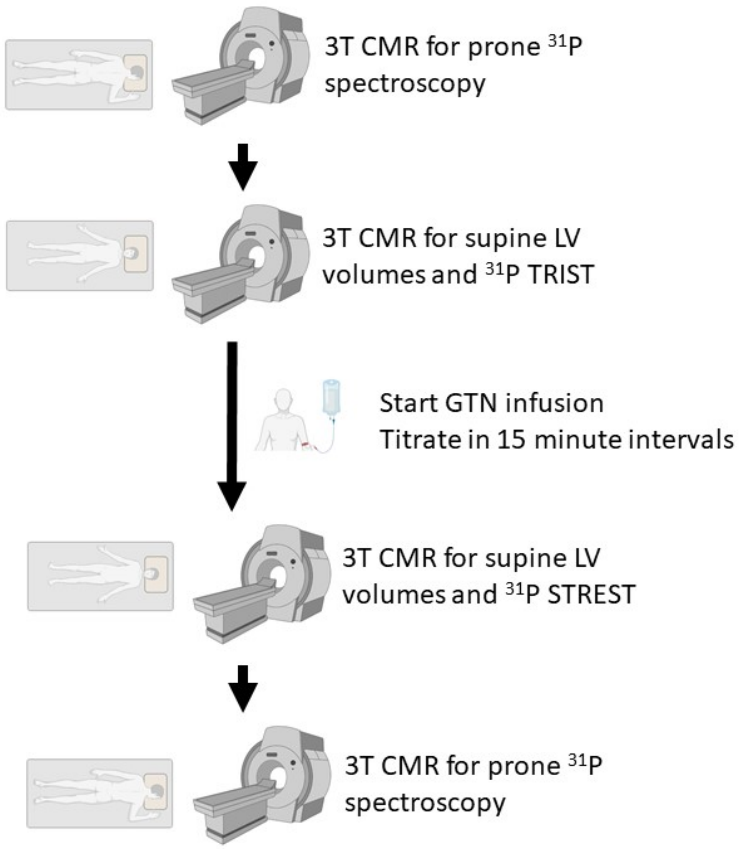

***Figure 6.5**: Study diagram*

For 4, a 1mg/ml GTN infusion was started at a rate of 3ml/h and titrated at 5 minute intervals with a target of a 15mmHg fall in mean arterial pressure (but not to lower MAP below 70mmHg). The infusion was maintained through 5, 6, and 7.

In order to protect the participant from sitting upright whilst hypotensive, an anterior element only (16 channel body matrix) was used for the cine imaging in 6, with the patient supine. The participant was then rolled into a prone position for 7.

6.3 Results

6.3.1 Participant Characteristics

Participant characteristics are in table 6.1. One participant was unusually tall (2.09m) and had previously rowed at a competitive level, another was a running enthusiast, however no participant undertook more than 8 hours a week of aerobic exercise at high intensity.

Table 6.1*: Participant characteristics for study volunteers for the vasodilator experiment.*

	Mean	Range
Age	38	26-63
Height (m)	1.76	1.64-2.09
Weight (kg)	71	59-107
BMI	22.6	18.5-27.8

6.3.2 Ventricular volumes and haemodynamics

***Table 6.2**: 5-minute averaged haemodynamic values collected during GTN infusion.*

	Baseline	***During GTN***	***p-value (t-test)***
Mean arterial pressure (mmHg)	78 ± 7	65 ± 6	***<0.0001***
Heart rate (bpm)	63 ± 7	72 ± 11	***<0.0001***
Rate pressure product (mmHg.bpm)	6929 ± 976	7214 ± 1051	0.06
Calculated stroke work (ml.mmHg)	7708 ± 2782	6071 ± 2660	***<0.0001***
Calculated cardiac work (L.mmHg.bpm)	491 ± 140	422 ± 114	***0.02***

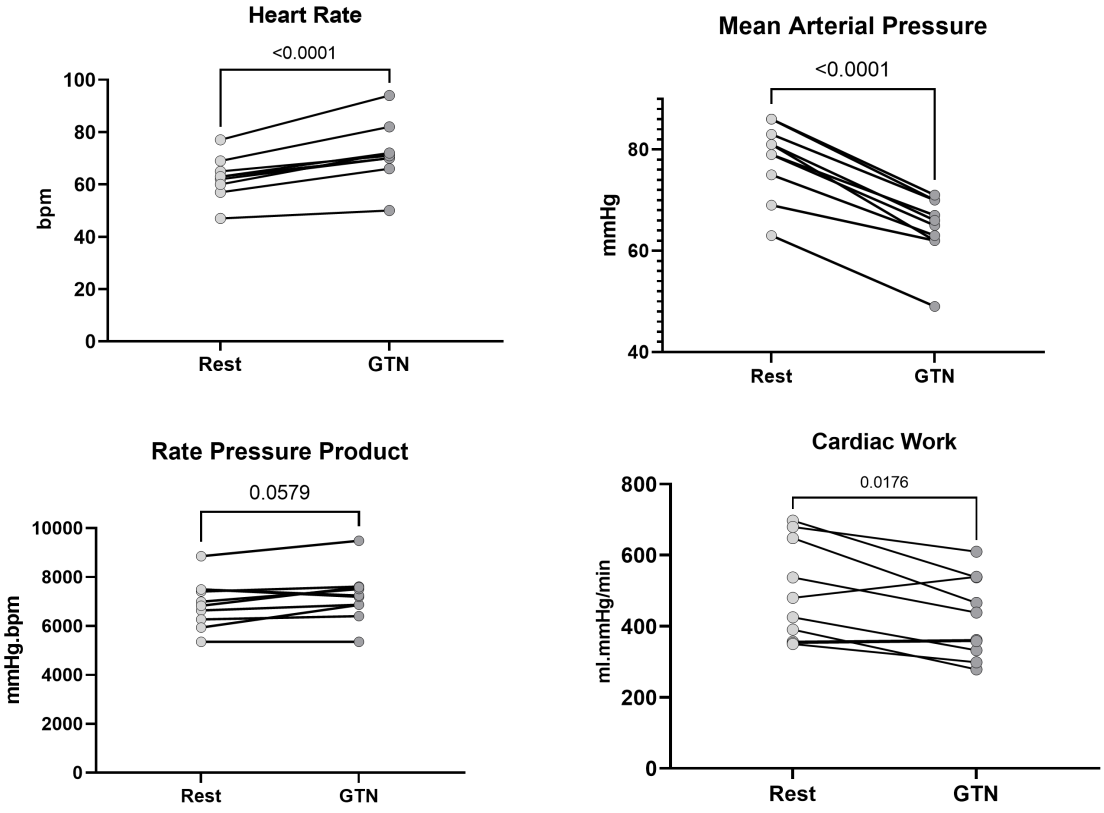

***Figure 6.6**: Haemodynamic changes before and during GTN infusion*

MAP fell by an average of 13mmHg (slightly short of the target overall). There was the predicted heart rate rise from baroreceptor reflex activation. The calculated stroke work and cardiac work both fell, driven by the lower mean arterial pressure.

Left and right ventricular volumes are shown in table 6.3 and figure 6.7. Both left and right ventricular end diastolic volume fell (by 20ml), as did right atrial area (by an average of $3cm^2$), in keeping with the reduction in preload. Left and right ventricular end systolic volume fell in order to maintain stroke volume, with left ventricular ejection fraction increasing. Combined with the increased heart rate, cardiac output did not significantly change.

Table 6.3*: Left and right ventricular volumes before and during GTN infusion.*

	Baseline	During GTN	p-value (t-test)
Left ventricular end diastolic volume (ml)	161 ± 51	141 ± 52	***<0.0001***
Left ventricular end systolic volume (ml)	64 ± 22	48 ± 18	***<0.0001***
Left ventricular stroke volume (ml)	97 ± 30	93 ± 35	0.24
Left ventricular ejection fraction (%)	61 ± 3	66 ± 4	***0.0002***
Cardiac output (L/min)	6.24 ± 1.46	6.49 ± 1.43	0.37
Cardiac index ($L/min.m^2$)	3.35 ± 0.5	3.47 ± 0.3	0.4
Right atrial area (cm^2)	23.3 ± 7.8	20.9 ± 6.7	***0.04***
Right ventricular end diastolic volume (ml)	161 ± 54	148 ± 64	***0.01***
Right ventricular end systolic volume (ml)	70 ± 26	61 ± 29	***0.03***
Right ventricular ejection fraction (ml)	59 ± 3	60 ± 3	0.46

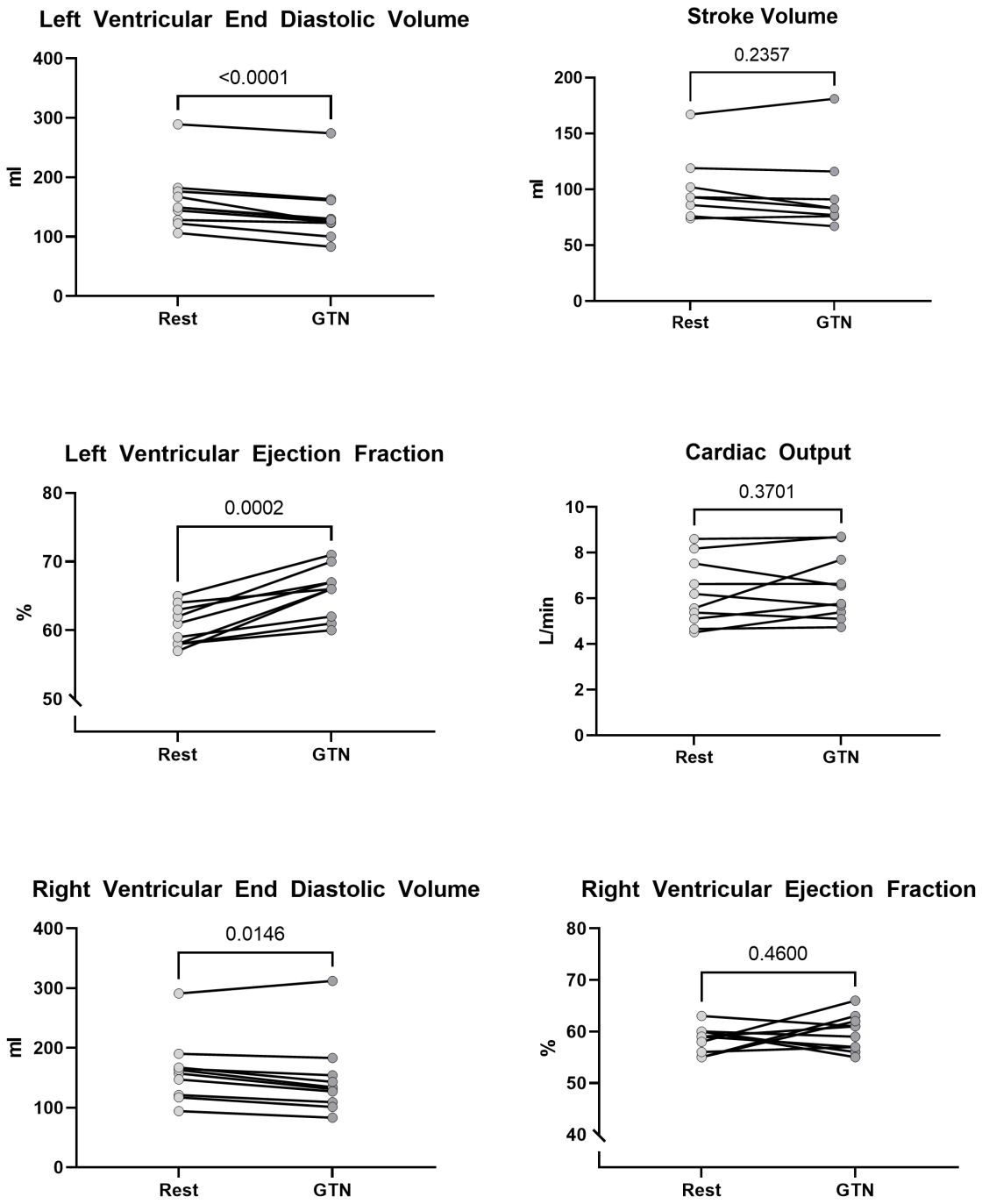

***Figure 6.7**: Volume changes before and during GTN infusion.*

6.3.3 ^{31}P Spectroscopy

***Table 6.4**: Spectroscopic values before and during GTN infusion.*

	Baseline	***During GTN***	***p-value (t-test)***
PCr/ATP ratio	2.17 ± 0.2	1.99 ± 0.22	0.054
CK forward pseudo first order rate constant (s^{-1})	0.158 ± 0.068	0.249 ± 0.091	***0.006***
Creatine kinase flux (umol/g/s)	1.79 ± 0.79	2.59 ± 1.07	***0.03***

There is a significant trend towards a decline in the PCr/ATP ratio from baseline to the GTN infusion, with only one participant showing a small rise. By a single-tailed paired t-test, the change is significant ($p = 0.0274$). This would suggest a mismatch between ATP supply from oxidative phosphorylation (reduced) or ATP demand (increased).

There is a large increase in both CK_{kf} (58%) and CK flux (45%), demonstrating increased ATP transfer and confirming the elevated ATP demand in the vaso- and venodilated state, in spite of the reduction in non-invasively estimated workload.

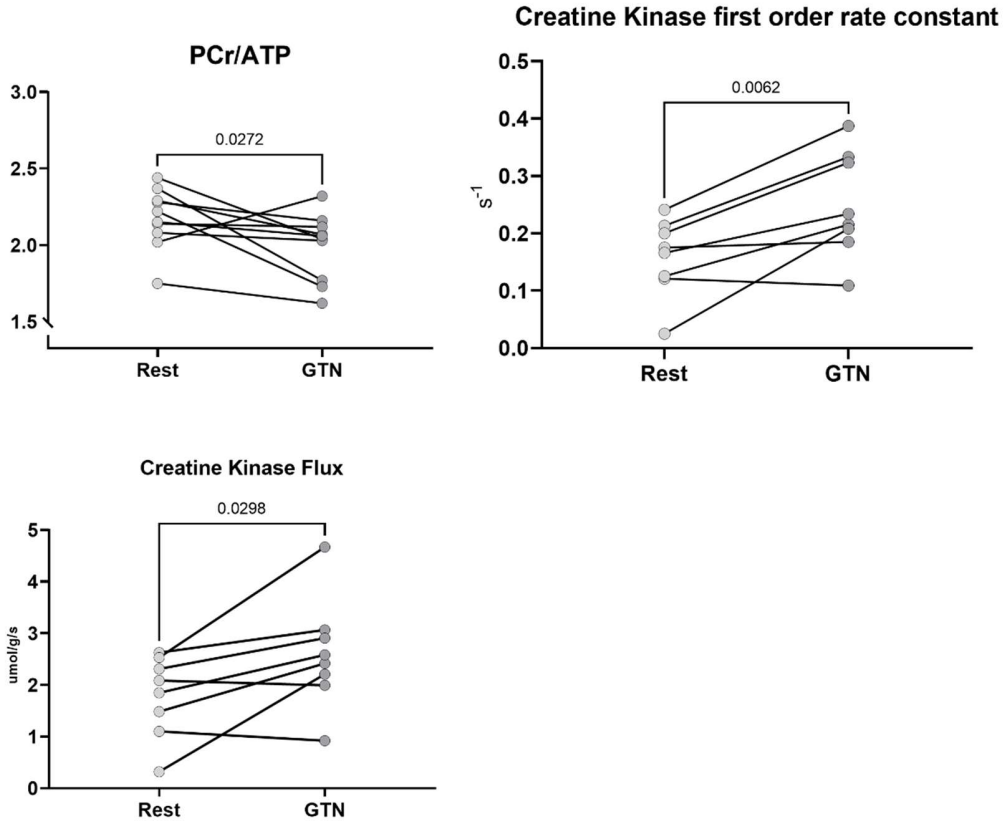

***Figure 6.8**: [31]P Spectroscopic Measurements before and during GTN infusion in the vasodilator experiment*

6.3.4 Correlations

There was a strong positive correlation between the baseline PCr/ATP value and the change in stroke volume (R^2 = 0.658, p = 0.004), where those with the lowest PCr/ATP levels had the largest falls in stroke volume while those with the highest were able to preserve or even increase their stroke volume.

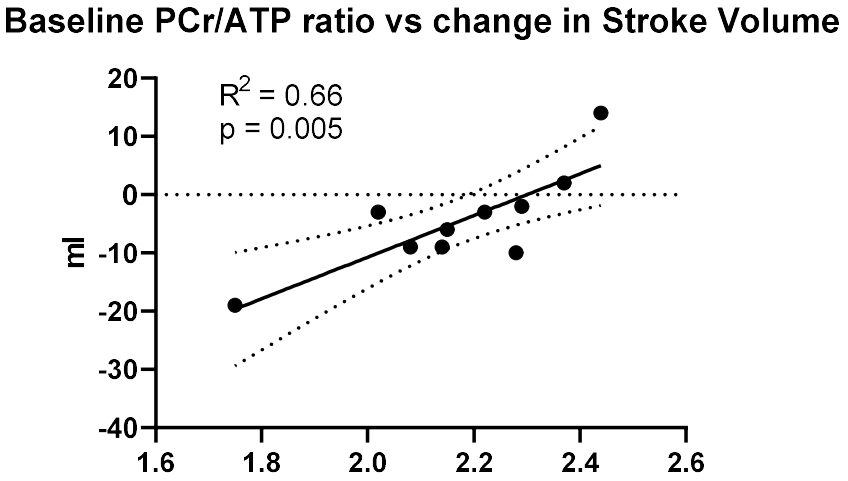

Figure 6.9*: Baseline PCr/ATP ratio compared to change in stroke volume before and during vasoplegic stress*

The change in CK_{kf} was positively correlated with the change in stroke volume (R^2 = 0.578, p = 0.028): those with the smallest rise in CK_{kf} showed the largest falls in stroke volume while those with the largest rises in CK_{kf} were able to preserve or even increase their stroke volume.

At rest, there was a close positive correlation between CK_{kf} and rate pressure product (R^2 = 0.563, p = 0.03), although the correlation with CK flux and RPP was less strong, (R^2 = 0.404, p = 0.09) but gained significance on the removal of an outlier (R^2 = 0.78, p = 0.008). During GTN administration, this correlation was lost.

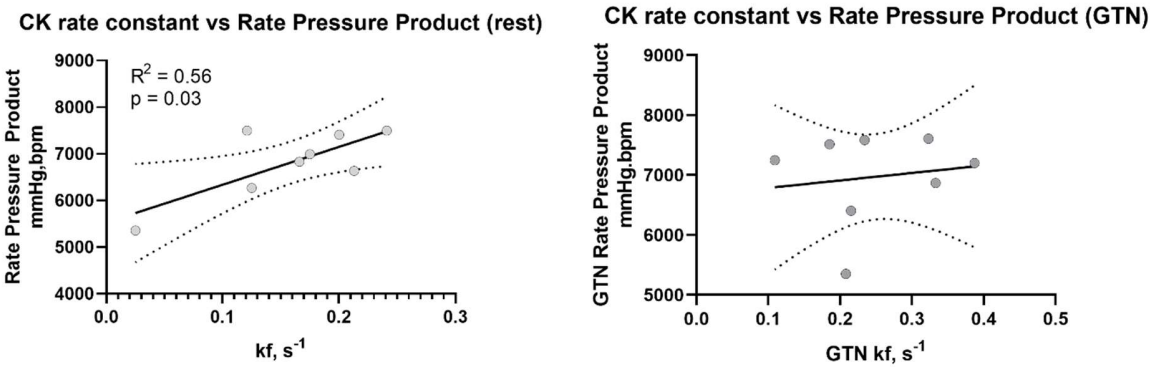

***Figure 6.10**: Creatine kinase first order rate constant correlated with rate pressure product at rest and during vasoplegic stress (GTN)*

6.4 Discussion

Combined venodilation and vasodilation cause a fall in afterload and preload with a reflex increase in contractility and heart rate to compensate for the fall in mean arterial pressure. Although the LVEDV fell by an average of 20mL, these reflex actions maintained or even increased cardiac output.

6.4.1 Effect of Nitrate on Energy Metabolism

Here we have reconciled previous data from historical studies demonstrating increased myocardial oxygen demand in humans given nitrate[375] but a decrease in demand in isolated hearts or myocardial tissue preparations[377]. The data presented here shows that there is a greatly increased ATP demand and delivery, demonstrated by the rise in CK flux, but suggests this exceeds mitochondrial oxidative phosphorylation supply, hence the fall in PCr/ATP as phosphocreatine is depleted. This would be in line with data showing GTN inhibiting oxidative phosphorylation in isolated mitochondria[379] via nitric oxide induced inhibition of complex IV of the respiratory chain[380].

While GTN relieves angina through its well-known vascular effects to reduce ischaemia, we have demonstrated profound effects on myocardial energy metabolism.

6.4.2 Calculated Cardiac Work and Energy Demand

Although the calculated indices of cardiac energy consumption (rate pressure product, stroke work and cardiac work) all fell, there were large increases in CK_{kf} and CK flux, indicating large

increases in demand for ATP consistent with our understanding of preload dominating energetic efficiency in the healthy heart. These increases were disproportionately larger (greater than those usually seen in dobutamine stress), which demonstrates the inadequacy of non-invasive calculations of myocardial energy output to fully demonstrate cardiac energy demand. The rise in CKk_f was slightly higher than that recorded with a Dobutamine infusion targeted to a 65% target heart rate[381].

Participants with the highest baseline PCr/ATP ratio or the largest increases in CKk_f were able to preserve their stroke volume. This suggests that both a large pool of energy reserve in the form of phosphocreatine and an ability to increase the turnover and delivery of ATP are key in meeting the physiological challenge of veno- and vasodilation.

Rate pressure product is known to be a good surrogate for myocardial oxygen consumption: we show here that it correlates well with the CK_{kf} and CK flux at rest, demonstrating a correlation with ATP usage. That this correlation is lost under vasodilator stress may demonstrate the differing response of hearts to adrenergic stimulation[53] or alternatively may indicate pathways other than creatine kinase (e.g. adenylate kinase or glycolysis) being used to channel ATP.

6.4.3 Flexibility in Myocardial Energy Delivery Protects Against Vasodilator Stress

These studies demonstrate the importance of a large reserve of phosphocreatine and the ability to increase creatine kinase activity to maintain cardiac performance under stress and suggests why in heart failure, where PCr/ATP ratio is typically low[382], the heart cannot readily increase cardiac output, resulting in shortness of breath on exertion. Athletes typically have similar resting CK

flux and CK_{kf} to normal individuals but while the flux and CK_{kf} increased under stress in these normal individuals, they did not alter significantly during Dobutamine stress in athletes[381]. In aortic stenosis, the PCr/ATP is lower than healthy hearts but CK_{kf} was preserved, with reduction in overall CK flux as the heart transitioned to failure[383].

Continuous pressure overload (in aortic constriction[384]) or rapid pacing[385] are techniques used to induce heart failure experimentally, however the mechanisms are still unclear. Clinically, there is a parallel with cardiomyopathy induced by incessant tachycardia[386], continuous right ventricular pacing[387] or cardiac dysfunction in sepsis (where there is vasoplegia, although other mechanisms may supervene)[388]. Generally, hearts working at high workload for prolonged periods of time will fail.

In rapid pacing induced heart failure, falls in myocardial ATP[389] and Na-K-ATPase activity[390] are observed and it has been previously speculated that it is an imbalance between energy supply and demand may contribute to the progression of heart failure. Indeed, targeting mitochondrial function has proven protective against canine pacing-induced heart failure[391] and provision of an increased fat supply proved protective in pressure overload induced failure[167]. The experimental model here recapitulates this imbalance over the short term and the energetic observations may be relevant to heart failure in general.

If PCr/ATP ratio is protective against negative ventricular performance changes during stress, given we have demonstrated the ability to manipulate PCr/ATP in heart failure in chapter 4 and demonstrate beneficial effects from fat metabolism during stress in chapter 5, we can hypothesize that metabolic manipulation may be protective against heart failure progression owing to prolonged stress. Further research in this field may be of use.

6.5 Limitations

6.5.1 Other Physiological Effects of Nitric Oxide

Nitric Oxide has multiple physiological effects, and it is difficult to fully account for all of their impacts within this study. For instance, Nitric Oxide is known to be involved in altering the response to the arterial baroreflex, inhibiting heart rate response[392], therefore the full haemodynamic effects of a change in preload and afterload may not be directly modelled. Another good example is Nitric Oxide's neuromodulatory properties in altering noradrenaline and adrenaline release from autonomic nerves[393].

6.5.2 Cohort Containing Mixed Athletic Ability / Body Morphology

This small cohort of 10 had a variety of participants, although one unusually tall participant (2.09m tall) skewed the results with a high ventricular size, perhaps increased by his prior history of competitive rowing.

7 Summary and Future Directions

Chapter 1 discussed myocardial energy in the round, from the uptake of substrates to produce ATP, the oxidative processes required to produce ATP from the substrates, the shuttling of ATP through phosphocreatine to its sites of use and the requirements for energy based on the mechanics of contraction. In the healthy human heart, fat and glucose are responsible for the majority of ATP production, approximately 60-90% coming from fat and 40-10% from glucose, although these ratios change depending upon the prevailing mix of metabolic substrates in the blood stream, in addition to changes in conditions of the heart such as stress or ischaemia. The mix of substrates metabolised is important as glucose carries a lower oxygen requirement per unit ATP produced and produces a higher Gibbs free energy of hydrolysis of ATP when oxidised, whereas free fatty acids have a higher yield of ATP per mole of substrate. In the failing heart, concentrations of ATP and phosphocreatine are reduced. Substrate metabolism is closely linked to this and fatty acid uptake and oxidation declines as heart failure progresses, while glucose uptake and glycolysis increase, although pyruvate oxidation decreases, leaving the heart an "engine out of fuel." Altering substrate metabolism has therefore become an attractive prospect as a treatment for heart failure and increasing glucose metabolism (either directly or indirectly via inhibiting fatty acid metabolism) has been trialled in heart failure, with mixed results. However, there are several evidence gaps in the literature. Firstly, little is known about metabolism during increased workloads in heart failure, even though the majority of patients with heart failure complain of mostly exertional symptoms. Secondly, most of the research into the effects of cardiac metabolic manipulation has focussed on glucose metabolism, while the effects of increased fat metabolism has been neglected. This thesis therefore aims to compare the relative benefits of

increased glucose and increased fat metabolism, at rest and at stress and tie together the links between metabolism and function.

In chapter 2, the combined methods for the thesis are summarised. Cardiac ^{31}Phosphorus magnetic resonance spectroscopy forms an important tool for the research and methods to determine myocardial phosphocreatine/ATP (PCr/ATP) ratio and the pseudo-first-order rate constant of creatine kinase (CK_{kf}) are described, along with cardiac magnetic resonance imaging techniques to non-invasively determine cardiac function. ^{13}Carbon cardiac magnetic resonance spectroscopy is described in an animal model using hyperpolarized [1-^{13}C]pyruvate as a tracer of glucose metabolism. Finally, an invasive protocol is described where paired arteriovenous sampling of coronary arterial and coronary venous blood is combined with coronary artery flow measurements by flow wire and left ventricular pressure volume loops recorded via impedance catheter. The blood samples are analysed for oxygen content in addition to free fatty acids, glucose, β-hydroxybutyrate and lactate. Common to these experiments, I describe interventions to elevate fat uptake and oxidation (Intralipid, a lipid emulsion), interventions to reduce uptake and oxidation of fat (nicotinic acid receptor agonists such as nicotinic acid and acipimox, which inhibit lipolysis and lower circulating free fatty acids) and the effects of a mid-physiological euglycaemic clamp to increase glucose uptake and metabolism.

In chapter 3, the effects of lipid emulsion infusion are compared to nicotinic acid receptor agonists, hypothesizing that inhibiting lipolysis will promote glucose metabolism and improve myocardial function. Instead, an increase in contractility is observed with the lipid emulsion and a reduction with the nicotinic acid, along with a fall in myocardial PCr/ATP. To explain these observations, a rodent model is dosed with a nicotinic acid receptor agonist and undergoes ^{13}Carbon cardiac magnetic resonance with hyperpolarized [1-^{13}C]pyruvate, demonstrating a

reduction in glucose uptake compared to placebo. This is explained by an inhibition of glucose stimulated insulin secretion by the nicotinic acid receptor agonist; when combined with the reduction in fat availability this starves the heart of metabolic substrate and induces metabolic and contractile impairment.

In chapter 4, the effects of substrate manipulation in healthy individuals and those with nonischaemic dilated cardiomyopathy are compared and contrasted. In healthy hearts, lipid emulsion, euglycaemic clamp and acipimox are compared, with the effect that the lipid emulsion increases contractility (an average 5% ejection fraction increase) and increases ATP flux through the creatine kinase ATP transfer system. In the failing hearts, lipid emulsion is compared to euglycaemic clamp. Again, an increase in contractility is seen, although this time the PCr/ATP ratio is found to be elevated during the Intralipid infusion and the creatine kinase first order rate constant is unchanged. When measured invasively, the failing heart was found to be more flexible than previously supposed, able to take up increased amounts of free fatty acids during the lipid infusion and glucose during the euglycaemic clamp. The lipid infusion increased myocardial oxygen uptake, although this did not impair function. We concluded from these data that the failing heart is able to display a greater deal of substrate flexibility than previously thought, that myocardial oxygen demand is not a limiting factor in the failing heart and that metabolism of fats confers contractile and energetic benefits in the failing heart.

In chapter 5, the effects on substrate manipulation during stress are considered, in a continuation of the experiments in chapter 4. The same individuals are subjected to stress with dobutamine targeted to 65% of maximal heart rate for age in the magnetic resonance experiment and a rapid pacing intervention in the interventional experiment. This time, there were no significant differences between the arms in the healthy volunteers but in participants with heart failure,

maximum achieved cardiac work was higher during Intralipid infusion than during the euglycaemic clamp. During rapid pacing, even when on a euglycaemic clamp, the heart exhibited a preference for increasing fatty acid uptake, again showing a greater degree of substrate flexibility, and was not limited by oxygen consumption.

In chapter 6, the effects of vasoplegic stress on the healthy heart were tested. Vasoplegia reduces afterload on the heart but also causes a drop in preload and thereby reduces cardiac output. Baroreceptor responses cause sympathetic nervous system activation to restore blood pressure and thereby increase inotropy and chronotropy of the heart. Glyceryl trinitrate was used for this purpose, which also has toxic effects on the electron transport chain and impairs mitochondrial ATP production. Thereby, the energetic demands of the heart are increased and its supply is reduced. We observed 50% increases in CKk_f with falls in PCr/ATP ratio in these healthy volunteers as energy supply did not keep pace with demand. Within this cohort, we observed that those with the highest starting PCr/ATP ratios and the greatest ability to increase CKk_f were the most protected against falls in cardiac function. This neatly models heart failure, where constant high energy demand causes ATP depletion and confirms the myocardial metabolism as a target for future interventions in heart failure.

Several future directions can be anticipated. The most important finding is an improvement in cardiac function and metabolism with increased free fatty acid supply to the myocardium, however this is a short term study using an infusion as an intervention and the data would have to be better understood and studied in the long term. Firstly, this study does not establish the fates of myocardial metabolites after entering the cell and the use of substrates for alternative fates such as anaplerosis should be better studied. Secondly, the longer term effects of increased fatty acid

metabolism may be studied, for instance by using fibrate type drugs which agonise PPARα or other novel approaches.

8 Reference

1. Meakins J. Modern Muscle Physiology and Circulatory Failure. Annals of Internal Medicine 1932;***6***(4):506-513.
2. Krebs HA, Johnson WA. Metabolism of ketonic acids in animal tissues. The Biochemical journal 1937;***31***(4):645-660.
3. Olson RE, Schwartz WB. Myocardial Metabolism in Congestive Heart Failure. Medicine 1951;***30***(1):21-42.
4. Goulston A. A Note on the Beneficial Effect of the Ingestion of Cane Sugar in Certain Forms of Heart Disease. British Medical Journal 1911;***1***(2620):615-615.
5. Sodi-Pallares D*, et al.* Effects of an intravenous infusion of a potassium-glucose-insulin solution on the electrocardiographic signs of myocardial infarction: A preliminary clinical report*. The American Journal of Cardiology 1962;***9***(2):166-181.
6. Opie LH. The glucose hypothesis: Relation to acute myocardial ischaemia. Journal of Molecular and Cellular Cardiology 1970;***1***(2):107-115.
7. MAROKO PR*, et al.* Effect of Glucose-Insulin-Potassium Infusion on Myocardial Infarction following Experimental Coronary Artery Occlusion. Circulation 1972;***45***(6):1160-1175.
8. Opie LH, Owen P. Effect of glucose-insulin-potassium infusions on arteriovenous differences of glucose and of free fatty acids and on tissue metabolic changes in dogs with developing myocardial infarction. The American Journal of Cardiology 1976;***38***(3):310-321.
9. Rogers WJ*, et al.* Reduction of hospital mortality rate of acute myocardial infarction with glucose-insulin-potassium infusion. American heart journal 1976;***92***(4):441-454.
10. Wargovich TJ*, et al.* Myocardial metabolic and hemodynamic effects of dichloroacetate in coronary artery disease. The American Journal of Cardiology 1988;***61***(1):65-70.
11. Stacpoole PW. The pharmacology of dichloroacetate. Metabolism 1989;***38***(11):1124-44.
12. Randle PJ*, et al.* The glucose fatty-acid cycle. Its role in insulin sensitivity and the metabolic disturbances of diabetes mellitus. Lancet 1963;***1***(7285):785-9.
13. Lopaschuk GDW, S. R.; Olley, P. M.; Davies, N. J. Etomoxir, a carnitine palmitoyltransferase I inhibitor, protects hearts from fatty acid-induced ischemic injury independent of changes in long chain acylcarnitine. Circulation Research 1988;***63***(6):1036-1043.
14. Clarke K*, et al.* Temporal relation between energy metabolism and myocardial function during ischemia and reperfusion. Am J Physiol 1987;***253***(2 Pt 2):H412-21.
15. Cocco G*, et al.* Effects of a new metabolic modulator, ranolazine, on exercise tolerance in angina pectoris patients treated with beta-blocker or diltiazem. J Cardiovasc Pharmacol 1992;***20***(1):131-8.
16. Sabbaha HN, Stanley WC. Partial fatty acid oxidation inhibitors: a potentially new class of drugs for heart failure. European Journal of Heart Failure 2002;***4***(1):3-6.
17. Suga H. Ventricular energetics. Physiological Reviews 1990;***70***(2):247-277.
18. Korvald C*, et al.* Myocardial substrate metabolism influences left ventricular energetics in vivo. Am J Physiol Heart Circ Physiol 2000;***278***(4):H1345-51.
19. Scholz TD*, et al.* Effect of substrate on mitochondrial NADH, cytosolic redox state, and phosphorylated compounds in isolated hearts. American Journal of Physiology-Heart and Circulatory Physiology 1995;***268***(1):H82-H91.

20. Laughlin MR, Heineman FW. The Relationship between Phosphorylation Potential and Redox State in the Isolated Working Rabbit Heart. Journal of Molecular and Cellular Cardiology 1994;***26***(12):1525-1536.
21. Mallet RT, Bünger R. Energetic modulation of cardiac inotropism and sarcoplasmic reticular Ca2+ uptake. Biochimica et biophysica acta 1994;***1224***(1):22-32.
22. Van Der Lee KA*, et al.* Effects of fatty acids on uncoupling protein-2 expression in the rat heart. Faseb j 2000;***14***(3):495-502.
23. Faadiel Essop M, Opie LH. Metabolic therapy for heart failure. European Heart Journal 2004;***25***(20):1765-1768.
24. Hermann HP*, et al.* Haemodynamic effects of intracoronary pyruvate in patients with congestive heart failure: an open study. Lancet 1999;***353***(9161):1321-3.
25. Hermann HP*, et al.* Improved systolic and diastolic myocardial function with intracoronary pyruvate in patients with congestive heart failure. Eur J Heart Fail 2004;***6***(2):213-8.
26. Kalay N*, et al.* Effects of intermittent and long-term glucose-insulin-potassium infusion in patients with systolic heart failure. Exp Clin Cardiol 2008;***13***(2):85-8.
27. Bersin RM*, et al.* Improved hemodynamic function and mechanical efficiency in congestive heart failure with sodium dichloroacetate. J Am Coll Cardiol 1994;***23***(7):1617-24.
28. Chandler MP*, et al.* Short-Term Treatment With Ranolazine Improves Mechanical Efficiency in Dogs With Chronic Heart Failure. Circulation Research 2002;***91***(4):278-280.
29. Vitale C*, et al.* Trimetazidine improves left ventricular function and quality of life in elderly patients with coronary artery disease. European Heart Journal 2004;***25***(20):1814-1821.
30. Ponikowski P*, et al.* 2016 ESC Guidelines for the diagnosis and treatment of acute and chronic heart failure. European Heart Journal 2016;***37***(27):2129-U130.
31. Mosterd A, Hoes AW. Clinical epidemiology of heart failure. Heart 2007;***93***(9):1137-1146.
32. Jones NR*, et al.* Prognosis following a diagnosis of heart failure and the role of primary care: a review of the literature. BJGP Open 2017;***1***(3):bjgpopen17X101013-bjgpopen17X101013.
33. Ng ACT, Bax JJ. Hyperdynamic left ventricular function and the prognostic implications for heart failure with preserved ejection fraction. Eur Heart J 2020;***41***(12):1258-1259.
34. Konstam MA. Seeking therapeutic precision in heart failure: is ejection fraction really the way? Deconstructing the CHARM of heart failure with mid-range ejection fraction. European Journal of Heart Failure 2018;***20***(8):1240-1242.
35. Shah SJ*, et al.* Phenomapping for novel classification of heart failure with preserved ejection fraction. Circulation 2015;***131***(3):269-79.
36. (NICOR) NIfHOaR. National Heart Failure Audit 2020 (2018/19 data). In: National Institute for Health Outcomes and Research (NICOR); 2020.
37. Vedin O*, et al.* Significance of Ischemic Heart Disease in Patients With Heart Failure and Preserved, Midrange, and Reduced Ejection Fraction: A Nationwide Cohort Study. Circ Heart Fail 2017;***10***(6).
38. Mann DL, Felker GM. Mechanisms and models in heart failure: a translational approach. Circulation research 2021;***128***(10):1435-1450.
39. McMurray JJV*, et al.* Angiotensin–Neprilysin Inhibition versus Enalapril in Heart Failure. New Engl J Med 2014;***371***(11):993-1004.
40. Group DI. The effect of digoxin on mortality and morbidity in patients with heart failure. New Engl J Med 1997;***336***(8):525-533.
41. Teerlink JR*, et al.* Cardiac myosin activation with omecamtiv mecarbil in systolic heart failure. New Engl J Med 2021;***384***(2):105-116.

42. Maack C, *et al.* Treatments targeting inotropy. Eur Heart J 2018.
43. Ahmad T, *et al.* Why has positive inotropy failed in chronic heart failure? Lessons from prior inotrope trials. European journal of heart failure 2019;***21***(9):1064-1078.
44. Packer M, *et al.* Hemodynamic and clinical limitations of long-term inotropic therapy with amrinone in patients with severe chronic heart failure. Circulation 1984;***70***(6):1038-1047.
45. Lim HS. Cardiac Power Output Revisited. Circ Heart Fail 2020;***13***(10):e007393.
46. Tan LB. Cardiac Pumping Capacity and Prognosis in Heart Failure. The Lancet 1986;***328***(8520):1360-1363.
47. NELSON RR, *et al.* Hemodynamic Predictors of Myocardial Oxygen Consumption During Static and Dynamic Exercise. Circulation 1974;***50***(6):1179-1189.
48. Khalafbeigui F, *et al.* Left ventricular systolic pressure-volume area correlates with oxygen consumption. Am J Physiol 1979;***237***(5):H566-9.
49. Suga H, *et al.* Ventricular systolic pressure-volume area as predictor of cardiac oxygen consumption. Am J Physiol 1981;***240***(1):H39-44.
50. Nozawa T, *et al.* Relation between oxygen consumption and pressure-volume area of in situ dog heart. American Journal of Physiology-Heart and Circulatory Physiology 1987;***253***(1):H31-H40.
51. Klocke FJ, *et al.* Mechanism of increase of myocardial oxygen uptake produced by catecholamines1. American Journal of Physiology-Legacy Content 1965;***209***(5):913-918.
52. Suga H, *et al.* Mechanical efficiency of the left ventricle as a function of preload, afterload, and contractility. Heart and Vessels 1985;***1***(1):3-8.
53. Ohgoshi Y, *et al.* Sensitivities of cardiac O2 consumption and contractility to catecholamines in dogs. American Journal of Physiology-Heart and Circulatory Physiology 1991;***261***(1):H196-H205.
54. Murashige D, *et al.* Comprehensive quantification of fuel use by the failing and nonfailing human heart. Science (New York, NY) 2020;***370***(6514):364-368.
55. Goodwin GW, Taegtmeyer H. Regulation of fatty acid oxidation of the heart by MCD and ACC during contractile stimulation. Am J Physiol 1999;***277***(4):E772-7.
56. Lopaschuk GD, *et al.* Myocardial Fatty Acid Metabolism in Health and Disease. Physiological Reviews 2010;***90***(1):207-258.
57. Saks V, *et al.* Molecular system bioenergetics: regulation of substrate supply in response to heart energy demands. J Physiol 2006;***577***(Pt 3):769-77.
58. Goldberg Ira J, *et al.* Lipid Metabolism and Toxicity in the Heart. Cell Metabolism 2012;***15***(6):805-812.
59. Wisneski JA, *et al.* Myocardial metabolism of free fatty acids. Studies with 14C-labeled substrates in humans. The Journal of clinical investigation 1987;***79***(2):359-366.
60. Lafontan M, Langin D. Lipolysis and lipid mobilization in human adipose tissue. Prog Lipid Res 2009;***48***(5):275-97.
61. Boden G, Shulman GI. Free fatty acids in obesity and type 2 diabetes: Defining their role in the development of insulin resistance and β-cell dysfunction. European Journal of Clinical Investigation 2002;***32***(SUPPL. 3):14-23.
62. Stanley WC, *et al.* Myocardial substrate metabolism in the normal and failing heart. Physiol Rev 2005;***85***(3):1093-129.
63. Nguyen TD, Schulze PC. Lipid in the midst of metabolic remodeling – Therapeutic implications for the failing heart. Advanced Drug Delivery Reviews 2020.
64. Chakravarthy MV, *et al.* Identification of a physiologically relevant endogenous ligand for PPARα in liver. Cell 2009;***138***(3):476-488.

65. Khan SA, *et al.* ATGL-catalyzed lipolysis regulates SIRT1 to control PGC-1 α /PPAR- α signaling. Diabetes 2015;***64***(2):418-426.
66. Karwi QG, *et al.* Allosteric, transcriptional and post-translational control of mitochondrial energy metabolism. Biochemical Journal 2019;***476***(12):1695-1712.
67. Muoio DM, *et al.* Peroxisome proliferator-activated receptor- α regulates fatty acid utilization in primary human skeletal muscle cells. Diabetes 2002;***51***(4):901-909.
68. Burkart EM, *et al.* Nuclear receptors PPAR β / δ and PPAR α direct distinct metabolic regulatory programs in the mouse heart. The Journal of clinical investigation 2007;***117***(12):3930-3939.
69. Aubert G, *et al.* Perturbations in the gene regulatory pathways controlling mitochondrial energy production in the failing heart. Biochimica Et Biophysica Acta (BBA)-Molecular Cell Research 2013;***1833***(4):840-847.
70. Huss JM, *et al.* Estrogen-Related Receptor α Directs Peroxisome Proliferator-Activated Receptor α Signaling in the Transcriptional Control of Energy Metabolism in Cardiac and Skeletal Muscle. Molecular and Cellular Biology 2004;***24***(20):9079-9091.
71. Sheeran FL, Pepe S. Mitochondrial Bioenergetics and Dysfunction in Failing Heart. Adv Exp Med Biol 2017;***982***:65-80.
72. Gélinas R, *et al.* AMPK activation counteracts cardiac hypertrophy by reducing O-GlcNAcylation. Nature communications 2018;***9***(1):1-17.
73. Papandreou I, *et al.* HIF-1 mediates adaptation to hypoxia by actively downregulating mitochondrial oxygen consumption. Cell Metabolism 2006;***3***(3):187-197.
74. Slot JW, *et al.* Translocation of the glucose transporter GLUT4 in cardiac myocytes of the rat. Proceedings of the National Academy of Sciences 1991;***88***(17):7815-7819.
75. Russell RR, *et al.* Compartmentation of hexokinase in rat heart. A critical factor for tracer kinetic analysis of myocardial glucose metabolism. The Journal of clinical investigation 1992;***90***(5):1972-1977.
76. Wisneski JA, *et al.* Metabolic fate of extracted glucose in normal human myocardium. J Clin Invest 1985;***76***(5):1819-27.
77. Chandramouli C, *et al.* Myocardial glycogen dynamics: new perspectives on disease mechanisms. Clinical and Experimental Pharmacology and Physiology 2015;***42***(4):415-425.
78. Stanley WC, *et al.* Regulation of myocardial carbohydrate metabolism under normal and ischaemic conditions: potential for pharmacological interventions. Cardiovascular research 1997;***33***(2):243-257.
79. Oldfield GS, *et al.* Effects of preoperative glucose-insulin-potassium on myocardial glycogen levels and on complications of mitral valve replacement. The Journal of thoracic and cardiovascular surgery 1986;***91***(6):874-878.
80. Goldfarb AH, *et al.* Intensity and duration effects of exercise on heart cAMP, phosphorylase, and glycogen. Journal of Applied Physiology 1986;***60***(4):1268-1273.
81. Liedtke AJ. Alterations of carbohydrate and lipid metabolism in the acutely ischemic heart. Progress in cardiovascular diseases 1981;***23***(5):321-336.
82. Hue L, Taegtmeyer H. The Randle cycle revisited: a new head for an old hat. American Journal of Physiology-Endocrinology and Metabolism 2009;***297***(3):E578-E591.
83. Cotter DG, *et al.* Ketone body metabolism and cardiovascular disease. Am J Physiol Heart Circ Physiol 2013;***304***(8):H1060-76.
84. Fukao T, *et al.* Pathways and control of ketone body metabolism: on the fringe of lipid biochemistry. Prostaglandins, leukotrienes and essential fatty acids 2004;***70***(3):243-251.

85. Karwi QG, *et al.* Loss of Metabolic Flexibility in the Failing Heart. Frontiers in cardiovascular medicine 2018;***5***:68.
86. Sweatt AJ, *et al.* Branched-chain amino acid catabolism: unique segregation of pathway enzymes in organ systems and peripheral nerves. American Journal of Physiology-Endocrinology and Metabolism 2004;***286***(1):E64-E76.
87. Bergman BC, *et al.* Myocardial glucose and lactate metabolism during rest and atrial pacing in humans. J Physiol 2009;***587***(Pt 9):2087-99.
88. Gibala MJ, *et al.* Anaplerosis of the citric acid cycle: role in energy metabolism of heart and skeletal muscle. Acta Physiologica Scandinavica 2000;***168***(4):657-665.
89. Des Rosiers C, *et al.* Cardiac anaplerosis in health and disease: food for thought. Cardiovascular Research 2011;***90***(2):210-219.
90. Vincent G, *et al.* Citrate release by perfused rat hearts: a window on mitochondrial cataplerosis. American Journal of Physiology-Endocrinology and Metabolism 2000;***278***(5):E846-E856.
91. Mitchell PD. *Chemiosmotic coupling and energy transduction*: Glynn Research; 1968.
92. Veech RL. The therapeutic implications of ketone bodies: the effects of ketone bodies in pathological conditions: ketosis, ketogenic diet, redox states, insulin resistance, and mitochondrial metabolism. Prostaglandins, Leukotrienes and Essential Fatty Acids 2004;***70***(3):309-319.
93. Veech RL. The determination of the redox states and phosphorylation potential in living tissues and their relationship to metabolic control of disease phenotypes. Biochem Mol Biol Educ 2006;***34***(3):168-79.
94. Veech RL, *et al.* Ketone bodies, potential therapeutic uses. IUBMB Life 2001;***51***(4):241-247.
95. Korvald C, *et al.* Myocardial substrate metabolism influences left ventricular energetics in vivo. Am J Physiol-Heart C 2000;***278***(4):H1345-H1351.
96. Sato K, *et al.* Insulin, ketone bodies, and mitochondrial energy transduction. FASEB J 1995;***9***(8):651-8.
97. Kim DK, *et al.* Effects of beta-hydroxybutyrate on oxidative metabolism and phosphorylation potential in canine heart in vivo. Am J Physiol 1991;***260***(6 Pt 2):H1767-73.
98. Veech RL. The determination of the redox states and phosphorylation potential in living tissues and their relationship to metabolic control of disease phenotypes. Biochem Mol Biol Edu 2006;***34***(3):168-179.
99. Ingwall JS. *ATP and the Heart*. Boston: Kluwer Academic Publishers; 2002.
100. Tian R, Ingwall JS. Energetic basis for reduced contractile reserve in isolated rat hearts. Am J Physiol 1996;***270***(4 Pt 2):H1207-16.
101. Chen W, *et al.* Regulation of the Ca2+ gradient across the sarcoplasmic reticulum in perfused rabbit heart. A 19F nuclear magnetic resonance study. Circ Res 1998;***83***(9):898-907.
102. Tian R, *et al.* Role of MgADP in the development of diastolic dysfunction in the intact beating rat heart. J Clin Invest 1997;***99***(4):745-51.
103. Dzeja PP, Terzic A. Phosphotransfer networks and cellular energetics. Journal of Experimental Biology 2003;***206***(12):2039-2047.
104. Cain DF, Davies RE. Breakdown of adenosine triphosphate during a single contraction of working muscle. Biochemical and Biophysical Research Communications 1962;***8***(5):361-366.
105. Honda H, *et al.* Cyclical changes in high-energy phosphates during the cardiac cycle by pacing-Gated 31P nuclear magnetic resonance. Circulation journal : official journal of the Japanese Circulation Society 2002;***66***(1):80-6.

106. Pucar D, *et al.* Cellular energetics in the preconditioned state: protective role for phosphotransfer reactions captured by 18O-assisted 31P NMR. J Biol Chem 2001;***276***(48):44812-9.
107. Guzun R, *et al.* Modular organization of cardiac energy metabolism: energy conversion, transfer and feedback regulation. Acta Physiologica 2015;***213***(1):84-106.
108. Balaban RS, *et al.* Relation between work and phosphate metabolite in the in vivo paced mammalian heart. Science (New York, NY) 1986;***232***(4754):1121-3.
109. Naumova AV, *et al.* Regulation of murine myocardial energy metabolism during adrenergic stress studied by in vivo 31P NMR spectroscopy. Am J Physiol Heart Circ Physiol 2003;***285***(5):H1976-9.
110. Schaefer S, *et al.* Metabolic response of the human heart to inotropic stimulation: in vivo phosphorus-31 studies of normal and cardiomyopathic myocardium. Magn Reson Med 1992;***25***(2):260-72.
111. Bittl JA, Ingwall JS. Reaction rates of creatine kinase and ATP synthesis in the isolated rat heart. A 31P NMR magnetization transfer study. J Biol Chem 1985;***260***(6):3512-7.
112. Balaban RS, *et al.* Role of calcium in metabolic signaling between cardiac sarcoplasmic reticulum and mitochondria in vitro. American Journal of Physiology-Cell Physiology 2003;***284***(2):C285-C293.
113. Bose S, *et al.* Metabolic network control of oxidative phosphorylation: multiple roles of inorganic phosphate. J Biol Chem 2003;***278***(40):39155-65.
114. Saks V, *et al.* Cardiac system bioenergetics: metabolic basis of the Frank-Starling law. The Journal of Physiology 2006;***571***(2):253-273.
115. Arad M, *et al.* AMP-Activated Protein Kinase in the Heart. Circulation Research 2007;***100***(4):474-488.
116. Hiraoka T, *et al.* Studies of the effects of beta-adrenergic agonists on the regulation of pyruvate dehydrogenase in the perfused rat heart. Journal of Biological Chemistry 1980;***255***(16):7604-7609.
117. Depre C, *et al.* Cyclic AMP suppresses the inhibition of glycolysis by alternative oxidizable substrates in the heart. J Clin Invest 1998;***101***(2):390-7.
118. Collins-Nakai RL, *et al.* Epinephrine increases ATP production in hearts by preferentially increasing glucose metabolism. Am J Physiol 1994;***267***(5 Pt 2):H1862-71.
119. Wahrenberg H, *et al.* Importance of beta-adrenoceptor function in fat cells for lipid mobilization. Eur J Clin Invest 1992;***22***(6):412-9.
120. Awan MM, Saggerson ED. Malonyl-CoA metabolism in cardiac myocytes and its relevance to the control of fatty acid oxidation. Biochemical Journal 1993;***295***(1):61-66.
121. Goodwin GW, *et al.* Energy provision from glycogen, glucose, and fatty acids on adrenergic stimulation of isolated working rat hearts. American Journal of Physiology - Heart and Circulatory Physiology 1998;***274***(4 43-4):H1239-H1247.
122. Goodwin GW, *et al.* Regulation of energy metabolism of the heart during acute increase in heart work. Journal of Biological Chemistry 1998;***273***(45):29530-29539.
123. Hall JL, *et al.* Increased cardiac fatty acid uptake with dobutamine infusion in swine is accompanied by a decrease in malonyl CoA levels. Cardiovascular Research 1996;***32***(5):879-885.
124. Carley AN, Lewandowski ED. Triacylglycerol turnover in the failing heart. Biochimica et Biophysica Acta (BBA)-Molecular and Cell Biology of Lipids 2016;***1861***(10):1492-1499.
125. Bergman BC, *et al.* Myocardial FFA metabolism during rest and atrial pacing in humans. Am J Physiol Endocrinol Metab 2009;***296***(2):E358-66.

126. Gertz EW, *et al.* Myocardial substrate utilization during exercise in humans. Dual carbon-labeled carbohydrate isotope experiments. J Clin Invest 1988;***82***(6):2017-25.
127. Randle PJ. Regulatory interactions between lipids and carbohydrates: the glucose fatty acid cycle after 35 years. Diabetes/metabolism reviews 1998;***14***(4):263-283.
128. Kobayashi K, Neely JR. Control of maximum rates of glycolysis in rat cardiac muscle. Circulation Research 1979;***44***(2):166-175.
129. Starling RC, *et al.* Human myocardial ATP content and in vivo contractile function. Mol Cell Biochem 1998;***180***(1-2):171-7.
130. Beer M, *et al.* Absolute concentrations of high-energy phosphate metabolites in normal, hypertrophied, and failing human myocardium measured noninvasively with (31)P-SLOOP magnetic resonance spectroscopy. J Am Coll Cardiol 2002;***40***(7):1267-74.
131. Hardy CJ, *et al.* Altered myocardial high-energy phosphate metabolites in patients with dilated cardiomyopathy. Am Heart J 1991;***122***(3 Pt 1):795-801.
132. Conway MA, *et al.* Detection of low phosphocreatine to ATP ratio in failing hypertrophied human myocardium by 31P magnetic resonance spectroscopy. Lancet 1991;***338***(8773):973-6.
133. Zervou S, *et al.* Augmentation of Creatine in the Heart. Mini reviews in medicinal chemistry 2016;***16***(1):19-28.
134. Shen W, *et al.* Progressive loss of creatine maintains a near normal DeltaG approximately (ATP) in transgenic mouse hearts with cardiomyopathy caused by overexpressing Gsalpha. J Mol Cell Cardiol 2010;***48***(4):591-9.
135. Weiss RG, *et al.* ATP flux through creatine kinase in the normal, stressed, and failing human heart. Proceedings of the National Academy of Sciences of the United States of America 2005;***102***(3):808-13.
136. Bottomley PA, Weiss RG. Noninvasive Localized MR Quantification of Creatine Kinase Metabolites in Normal and Infarcted Canine Myocardium. Radiology 2001;***219***(2):411-418.
137. Rider OJ, *et al.* Effects of catecholamine stress on diastolic function and myocardial energetics in obesity. Circulation 2012;***125***(12):1511-9.
138. Schroeder MA, *et al.* Hyperpolarized (13)C magnetic resonance reveals early- and late-onset changes to in vivo pyruvate metabolism in the failing heart. Eur J Heart Fail 2013;***15***(2):130-40.
139. Willis BC, *et al.* Impaired oxidative metabolism and calcium mishandling underlie cardiac dysfunction in a rat model of post-acute isoproterenol-induced cardiomyopathy. Am J Physiol Heart Circ Physiol 2015;***308***(5):H467-77.
140. Rayner JJ, *et al.* The relative contribution of metabolic and structural abnormalities to diastolic dysfunction in obesity. Int J Obes (Lond) 2017.
141. Neubauer S, *et al.* Myocardial Phosphocreatine-to-ATP Ratio Is a Predictor of Mortality in Patients With Dilated Cardiomyopathy. Circulation 1997;***96***(7):2190-2196.
142. Phan TT, *et al.* Heart failure with preserved ejection fraction is characterized by dynamic impairment of active relaxation and contraction of the left ventricle on exercise and associated with myocardial energy deficiency. J Am Coll Cardiol 2009;***54***(5):402-9.
143. Tian R, *et al.* Failure to maintain a low ADP concentration impairs diastolic function in hypertrophied rat hearts. Circulation 1997;***96***(4):1313-9.
144. Bottomley PA, *et al.* Metabolic rates of ATP transfer through creatine kinase (CK Flux) predict clinical heart failure events and death. Sci Transl Med 2013;***5***(215):215re3.
145. Lygate CA, *et al.* The creatine kinase energy transport system in the failing mouse heart. J Mol Cell Cardiol 2007;***42***(6):1129-36.

146. Lygate CA, Neubauer S. Metabolic flux as a predictor of heart failure prognosis. Circ Res 2014;***114***(8):1228-30.
147. Neglia D*, et al.* Impaired myocardial metabolic reserve and substrate selection flexibility during stress in patients with idiopathic dilated cardiomyopathy. Am J Physiol Heart Circ Physiol 2007;***293***(6):H3270-8.
148. Brown DA*, et al.* Expert consensus document: Mitochondrial function as a therapeutic target in heart failure. Nat Rev Cardiol 2017;***14***(4):238-250.
149. Zhang L*, et al.* Cardiac insulin-resistance and decreased mitochondrial energy production precede the development of systolic heart failure after pressure-overload hypertrophy. Circ Heart Fail 2013;***6***(5):1039-48.
150. Shibayama J*, et al.* Metabolic remodeling in moderate synchronous versus dyssynchronous pacing-induced heart failure: integrated metabolomics and proteomics study. PLoS One 2015;***10***(3):e0118974.
151. Peterzan MA*, et al.* Metabolic remodeling in hypertrophied and failing myocardium: a review. Am J Physiol Heart Circ Physiol 2017;***313***(3):H597-H616.
152. Yonekura Y*, et al.* Regional myocardial substrate uptake in hypertensive rats: a quantitative autoradiographic measurement. Science (New York, NY) 1985;***227***(4693):1494-1496.
153. Sorokina N*, et al.* Recruitment of compensatory pathways to sustain oxidative flux with reduced carnitine palmitoyltransferase I activity characterizes inefficiency in energy metabolism in hypertrophied hearts. Circulation 2007;***115***(15):2033-41.
154. Thomassen A*, et al.* Myocardial substrate utilization and amino acid metabolism in chronic coronary artery disease. Z Kardiol 1987;***76 Suppl 5***:19-25.
155. How O-J*, et al.* Influence of substrate supply on cardiac efficiency, as measured by pressure-volume analysis in ex vivo mouse hearts. American Journal of Physiology-Heart and Circulatory Physiology 2005;***288***(6):H2979-H2985.
156. Burkhoff D*, et al.* Influence of metabolic substrate on rat heart function and metabolism at different coronary flows. Am J Physiol 1991;***261***(3 Pt 2):H741-50.
157. Bloom MW*, et al.* Heart failure with reduced ejection fraction. Nature Reviews Disease Primers 2017;***3***(1):1-19.
158. Tuunanen H*, et al.* Decreased Myocardial Free Fatty Acid Uptake in Patients With Idiopathic Dilated Cardiomyopathy: Evidence of Relationship With Insulin Resistance and Left Ventricular Dysfunction. Journal of Cardiac Failure 2006;***12***(8):644-652.
159. Sack MN*, et al.* Fatty acid oxidation enzyme gene expression is downregulated in the failing heart. Circulation 1996;***94***(11):2837-42.
160. Heather LC*, et al.* Fatty acid transporter levels and palmitate oxidation rate correlate with ejection fraction in the infarcted rat heart. Cardiovascular Research 2006;***72***(3):430-437.
161. Noordali H*, et al.* Cardiac metabolism - A promising therapeutic target for heart failure. Pharmacol Ther 2017.
162. Karbowska J*, et al.* Peroxisome proliferator-activated receptor alpha is downregulated in the failing human heart. Cellular & molecular biology letters 2003;***8***(1):49-53.
163. Bugger H*, et al.* Proteomic remodelling of mitochondrial oxidative pathways in pressure overload-induced heart failure. Cardiovasc Res 2010;***85***(2):376-84.
164. Cheng L*, et al.* Cardiomyocyte-restricted peroxisome proliferator-activated receptor- δ deletion perturbs myocardial fatty acid oxidation and leads to cardiomyopathy. Nature medicine 2004;***10***(11):1245-1250.

165. Khan RS, *et al.* Rescue of heart lipoprotein lipase-knockout mice confirms a role for triglyceride in optimal heart metabolism and function. American Journal of Physiology-Endocrinology and Metabolism 2013;***305***(11):E1339-E1347.
166. Diakos NA, *et al.* Evidence of Glycolysis Up-Regulation and Pyruvate Mitochondrial Oxidation Mismatch During Mechanical Unloading of the Failing Human Heart: Implications for Cardiac Reloading and Conditioning. JACC Basic Transl Sci 2016;***1***(6):432-444.
167. Umbarawan Y, *et al.* Glucose is preferentially utilized for biomass synthesis in pressure-overloaded hearts: evidence from fatty acid-binding protein-4 and -5 knockout mice. Cardiovascular Research 2018;***114***(8):1132-1144.
168. Pound KM, *et al.* Substrate–Enzyme Competition Attenuates Upregulated Anaplerotic Flux Through Malic Enzyme in Hypertrophied Rat Heart and Restores Triacylglyceride Content. Circulation Research 2009;***104***(6):805-812.
169. Lei B, *et al.* Paradoxical downregulation of the glucose oxidation pathway despite enhanced flux in severe heart failure. J Mol Cell Cardiol 2004;***36***(4):567-76.
170. Hopkins TA, *et al.* Control of cardiac pyruvate dehydrogenase activity in peroxisome proliferator-activated receptor-alpha transgenic mice. Am J Physiol Heart Circ Physiol 2003;***285***(1):H270-6.
171. Swan JW, *et al.* Insulin resistance in chronic heart failure: relation to severity and etiology of heart failure. J Am Coll Cardiol 1997;***30***(2):527-32.
172. Horton JL, *et al.* Mitochondrial protein hyperacetylation in the failing heart. JCI Insight 2016;***1***(2).
173. Zhang X, *et al.* Abstract 18978: Lysine Acetylation of Pyruvate Dehydrogenase Reduces Enzymatic Activity and Contributes to Impaired Substrate Metabolism in the Failing Myocardium. Circulation 2014;***130***(suppl_2):A18978-A18978.
174. Mangmool S, *et al.* beta-Adrenergic Receptor and Insulin Resistance in the Heart. Biomol Ther (Seoul) 2017;***25***(1):44-56.
175. Lehmann LH, *et al.* A proteolytic fragment of histone deacetylase 4 protects the heart from failure by regulating the hexosamine biosynthetic pathway. Nature medicine 2018;***24***(1):62.
176. Erickson JR, *et al.* Diabetic hyperglycaemia activates CaMKII and arrhythmias by O-linked glycosylation. Nature 2013;***502***(7471):372-376.
177. Aubert G, *et al.* The Failing Heart Relies on Ketone Bodies as a Fuel. Circulation 2016;***133***(8):698-705.
178. Bedi KC, Jr., *et al.* Evidence for Intramyocardial Disruption of Lipid Metabolism and Increased Myocardial Ketone Utilization in Advanced Human Heart Failure. Circulation 2016;***133***(8):706-16.
179. Janardhan A, *et al.* Altered systemic ketone body metabolism in advanced heart failure. Texas Heart Institute journal 2011;***38***(5):533-8.
180. Hasselbaink DM, *et al.* Ketone bodies disturb fatty acid handling in isolated cardiomyocytes derived from control and diabetic rats. Biochemical Journal 2003;***371***(3):753-760.
181. Russell RR, 3rd, Taegtmeyer H. Changes in citric acid cycle flux and anaplerosis antedate the functional decline in isolated rat hearts utilizing acetoacetate. The Journal of Clinical Investigation 1991;***87***(2):384-390.
182. Schugar RC, *et al.* Cardiomyocyte-specific deficiency of ketone body metabolism promotes accelerated pathological remodeling. Molecular metabolism 2014;***3***(7):754-769.
183. Uchihashi M, *et al.* Cardiac-specific Bdh1 overexpression ameliorates oxidative stress and cardiac remodeling in pressure overload–induced heart failure. Circulation: Heart Failure 2017;***10***(12):e004417.

184. Lai L, *et al.* Energy Metabolic Reprogramming in the Hypertrophied and Early Stage Failing Heart. Circulation: Heart Failure 2014;**7**(6):1022-1031.
185. Li T, *et al.* Defective Branched-Chain Amino Acid Catabolism Disrupts Glucose Metabolism and Sensitizes the Heart to Ischemia-Reperfusion Injury. Cell Metabolism 2017;***25***(2):374-385.
186. Tian R, *et al.* Unlocking the secrets of mitochondria in the cardiovascular system: path to a cure in heart failure—a report from the 2018 National Heart, Lung, and Blood Institute Workshop. Circulation 2019;***140***(14):1205-1216.
187. Murphy MP. How mitochondria produce reactive oxygen species. Biochemical journal 2009;***417***(1):1-13.
188. Maack C, *et al.* Oxygen free radical release in human failing myocardium is associated with increased activity of rac1-GTPase and represents a target for statin treatment. Circulation 2003;***108***(13):1567-1574.
189. Huang Q, *et al.* Thioredoxin-2 inhibits mitochondrial reactive oxygen species generation and apoptosis stress kinase-1 activity to maintain cardiac function. Circulation 2015;***131***(12):1082-1097.
190. Luongo TS, *et al.* The mitochondrial Na+/Ca 2+ exchanger is essential for Ca 2+ homeostasis and viability. Nature 2017;***545***(7652):93-97.
191. Denton RM, McCormack JG. The calcium sensitive dehydrogenases of vertebrate mitochondria. Cell calcium 1986;**7**(5-6):377-386.
192. Aroor AR, *et al.* Insulin resistance and heart failure: molecular mechanisms. Heart Fail Clin 2012;***8***(4):609-617.
193. Bertero E, Maack C. Calcium Signaling and Reactive Oxygen Species in Mitochondria. Circ Res 2018;***122***(10):1460-1478.
194. Dzeja PP, *et al.* Reduced activity of enzymes coupling ATP-generating with ATP-consuming processes in the failing myocardium. Molecular and Cellular Biochemistry 1999;***201***(1):33-40.
195. Trico D, *et al.* Abnormal Glucose Tolerance Is Associated with a Reduced Myocardial Metabolic Flexibility in Patients with Dilated Cardiomyopathy. J Diabetes Res 2016;***2016***:3906425.
196. Morrow DA, Givertz MM. Modulation of myocardial energetics: emerging evidence for a therapeutic target in cardiovascular disease. In: Am Heart Assoc; 2005.
197. Lopaschuk GD, *et al.* Cardiac Energy Metabolism in Heart Failure. Circulation Research 2021;***128***(10):1487-1513.
198. Halbirk M, *et al.* Short-term changes in circulating insulin and free fatty acids affect Nt-pro-BNP levels in heart failure patients. International journal of cardiology 2010;***144***(1):140-142.
199. Liu B, *et al.* Cardiac efficiency is improved after ischemia by altering both the source and fate of protons. Circ Res 1996;***79***(5):940-8.
200. Lydell CP, *et al.* Pyruvate dehydrogenase and the regulation of glucose oxidation in hypertrophied rat hearts. Cardiovasc Res 2002;***53***(4):841-51.
201. Bøgh N, *et al.* Increasing carbohydrate oxidation improves contractile reserves and prevents hypertrophy in porcine right heart failure. Scientific reports 2020;***10***(1):1-9.
202. Wargovich TJ, *et al.* Myocardial metabolic and hemodynamic effects of dichloroacetate in coronary artery disease. Am J Cardiol 1988;***61***(1):65-70.
203. Lewis JF, *et al.* Effects of dichloroacetate in patients with congestive heart failure. Clin Cardiol 1998;***21***(12):888-92.

204. Pierce GN, Philipson K. Binding of glycolytic enzymes to cardiac sarcolemmal and sarcoplasmic reticular membranes. Journal of Biological Chemistry 1985;***260***(11):6862-6870.
205. Kusuoka H, Marban E. Mechanism of the diastolic dysfunction induced by glycolytic inhibition. Does adenosine triphosphate derived from glycolysis play a favored role in cellular Ca2+ homeostasis in ferret myocardium? The Journal of clinical investigation 1994;***93***(3):1216-1223.
206. Lewis AJ, *et al.* Hyperpolarized 13C and 31P magnetic resonance spectroscopy identify pyruvate dehydrogenase as a therapeutic target in obesity cardiomyopathy. Journal of Cardiovascular Magnetic Resonance 2015;***17***(Suppl 1):O16.
207. Lopaschuk GD, *et al.* Beneficial effects of trimetazidine in ex vivo working ischemic hearts are due to a stimulation of glucose oxidation secondary to inhibition of long-chain 3-ketoacyl coenzyme a thiolase. Circulation research 2003;***93***(3):e33-e37.
208. Kantor PF, *et al.* The antianginal drug trimetazidine shifts cardiac energy metabolism from fatty acid oxidation to glucose oxidation by inhibiting mitochondrial long-chain 3-ketoacyl coenzyme A thiolase. Circ Res 2000;***86***(5):580-8.
209. Sabbah HN, *et al.* Ranolazine, a partial fatty acid oxidation (pFOX) inhibitor, improves left ventricular function in dogs with chronic heart failure. J Card Fail 2002;***8***(6):416-22.
210. Lee L, *et al.* Metabolic modulation with perhexiline in chronic heart failure: a randomized, controlled trial of short-term use of a novel treatment. Circulation 2005;***112***(21):3280-8.
211. Schmidt-Schweda S, Holubarsch C. First clinical trial with etomoxir in patients with chronic congestive heart failure. Clin Sci (Lond) 2000;***99***(1):27-35.
212. Jatain S, *et al.* Metabolic manipulation in dilated cardiomyopathy: Assessing the role of trimetazidine. Indian Heart J 2016;***68***(6):803-808.
213. Fragasso G, *et al.* Effects of metabolic modulation by trimetazidine on left ventricular function and phosphocreatine/adenosine triphosphate ratio in patients with heart failure. Eur Heart J 2006;***27***(8):942-8.
214. Kolwicz SC, *et al.* Cardiac-Specific Deletion of Acetyl CoA Carboxylase 2 Prevents Metabolic Remodeling During Pressure-Overload Hypertrophy. Circulation Research 2012;***111***(6):728-738.
215. Choi YS, *et al.* Preservation of myocardial fatty acid oxidation prevents diastolic dysfunction in mice subjected to angiotensin II infusion. Journal of Molecular and Cellular Cardiology 2016;***100***:64-71.
216. Stanley WC, *et al.* Dietary Fat and Heart Failure: Moving From Lipotoxicity to Lipoprotection. Circulation Research 2012;***110***(5):764-776.
217. Steinbusch LKM, *et al.* Absence of fatty acid transporter CD36 protects against Western-type diet-related cardiac dysfunction following pressure overload in mice. American Journal of Physiology-Endocrinology and Metabolism 2011;***301***(4):E618-E627.
218. Lahey R, *et al.* Dietary fat supply to failing hearts determines dynamic lipid signaling for nuclear receptor activation and oxidation of stored triglyceride. Circulation 2014;***130***(20):1790-1799.
219. Wiggers H, *et al.* Influence of insulin and free fatty acids on contractile function in patients with chronically stunned and hibernating myocardium. American Journal of Physiology-Heart and Circulatory Physiology 2005;***289***(2):H938-H946.
220. Boehm EA, *et al.* Increased uncoupling proteins and decreased efficiency in palmitate-perfused hyperthyroid rat heart. American Journal of Physiology-Heart and Circulatory Physiology 2001;***280***(3):H977-H983.

221. Demine S, *et al.* Mitochondrial Uncoupling: A Key Controller of Biological Processes in Physiology and Diseases. Cells 2019;***8***(8).
222. Nedergaard J, Cannon B. The 'novel' 'uncoupling' proteins UCP2 and UCP3: what do they really do? Pros and cons for suggested functions. Exp Physiol 2003;***88***(1):65-84.
223. Vozza A, *et al.* UCP2 transports C4 metabolites out of mitochondria, regulating glucose and glutamine oxidation. Proceedings of the National Academy of Sciences 2014;***111***(3):960-965.
224. Jiménez-Jiménez J, *et al.* Fatty acid activation of the uncoupling proteins requires the presence of the central matrix loop from UCP1. Biochimica et Biophysica Acta (BBA) - Bioenergetics 2006;***1757***(9):1292-1296.
225. Ruiz-Ramírez A, *et al.* Cell Death and Heart Failure in Obesity: Role of Uncoupling Proteins. Oxidative Medicine and Cellular Longevity 2016;***2016***:9340654.
226. Krauss S, *et al.* The mitochondrial uncoupling-protein homologues. Nature Reviews Molecular Cell Biology 2005;***6***(3):248-261.
227. Ozcan C, *et al.* Role of uncoupling protein 3 in ischemia-reperfusion injury, arrhythmias, and preconditioning. American Journal of Physiology-Heart and Circulatory Physiology 2013;***304***(9):H1192-H1200.
228. Sharma S, *et al.* Intramyocardial lipid accumulation in the failing human heart resembles the lipotoxic rat heart. The FASEB Journal 2004;***18***(14):1692-1700.
229. Chokshi A, *et al.* Ventricular Assist Device Implantation Corrects Myocardial Lipotoxicity, Reverses Insulin Resistance, and Normalizes Cardiac Metabolism in Patients With Advanced Heart Failure. Circulation 2012;***125***(23):2844-2853.
230. Tsushima K, *et al.* Mitochondrial Reactive Oxygen Species in Lipotoxic Hearts Induce Post-Translational Modifications of AKAP121, DRP1, and OPA1 That Promote Mitochondrial Fission. Circulation Research 2018;***122***(1):58-73.
231. Haemmerle G, *et al.* Defective Lipolysis and Altered Energy Metabolism in Mice Lacking Adipose Triglyceride Lipase. Science (New York, NY) 2006;***312***(5774):734-737.
232. Koves TR, *et al.* Mitochondrial Overload and Incomplete Fatty Acid Oxidation Contribute to Skeletal Muscle Insulin Resistance. Cell Metabolism 2008;**7**(1):45-56.
233. Borradaile NM, *et al.* Disruption of endoplasmic reticulum structure and integrity in lipotoxic cell death. Journal of Lipid Research 2006;***47***(12):2726-2737.
234. Law BA, *et al.* Lipotoxic very-long-chain ceramides cause mitochondrial dysfunction, oxidative stress, and cell death in cardiomyocytes. The FASEB Journal 2018;***32***(3):1403-1416.
235. Park T-S, *et al.* Ceramide is a cardiotoxin in lipotoxic cardiomyopathy★s. Journal of Lipid Research 2008;***49***(10):2101-2112.
236. Holland WL, *et al.* Receptor-mediated activation of ceramidase activity initiates the pleiotropic actions of adiponectin. Nature medicine 2011;***17***(1):55-63.
237. Son N-H, *et al.* PPAR γ -induced cardiolipotoxicity in mice is ameliorated by PPAR α deficiency despite increases in fatty acid oxidation. The Journal of Clinical Investigation 2010;***120***(10):3443-3454.
238. Jun M, *et al.* Effects of fibrates on cardiovascular outcomes: a systematic review and meta-analysis. The Lancet 2010;***375***(9729):1875-1884.
239. Haemmerle G, *et al.* ATGL-mediated fat catabolism regulates cardiac mitochondrial function via PPAR- α and PGC-1. Nature medicine 2011;***17***(9):1076-1085.
240. Finck BN, *et al.* A critical role for PPAR α -mediated lipotoxicity in the pathogenesis of diabetic cardiomyopathy: modulation by dietary fat content. Proceedings of the National Academy of Sciences 2003;***100***(3):1226-1231.

241. Mudaliar S, Henry R. New Oral Therapies for Type 2 Diabetes Mellitus: The Glitazones or Insulin Sensitizers. Annual Review of Medicine 2001;***52***(1):239-257.
242. Niemeyer NV, Janney LM. Thiazolidinedione-induced edema. Pharmacotherapy: The Journal of Human Pharmacology and Drug Therapy 2002;***22***(7):924-929.
243. Bełtowski J*, et al.* Thiazolidinedione-Induced Fluid Retention: Recent Insights into the Molecular Mechanisms. PPAR Research 2013;***2013***:628628.
244. Yue T-l*, et al.* In vivo myocardial protection from ischemia/reperfusion injury by the peroxisome proliferator–activated receptor-γ agonist rosiglitazone. Circulation 2001;***104***(21):2588-2594.
245. van der Meer RW*, et al.* Pioglitazone Improves Cardiac Function and Alters Myocardial Substrate Metabolism Without Affecting Cardiac Triglyceride Accumulation and High-Energy Phosphate Metabolism in Patients With Well-Controlled Type 2 Diabetes Mellitus. Circulation 2009;***119***(15):2069-2077.
246. Palomer X*, et al.* PPAR β / δ and lipid metabolism in the heart. Biochimica et Biophysica Acta (BBA)-Molecular and Cell Biology of Lipids 2016;***1861***(10):1569-1578.
247. Liu J*, et al.* Peroxisome proliferator-activated receptor β / δ activation in adult hearts facilitates mitochondrial function and cardiac performance under pressure-overload condition. Hypertension 2011;***57***(2):223-230.
248. Weinberg Guy L*, et al.* Pretreatment or Resuscitation with a Lipid Infusion Shifts the Dose-Response to Bupivacaine-induced Asystole in Rats Anesthesiology 1998;***88***(4):1071-1075.
249. Rosenblatt MA*, et al.* Successful use of a 20% lipid emulsion to resuscitate a patient after a presumed bupivacaine-related cardiac arrest. Anesthesiology 2006;***105***(1):217-8.
250. Jamaty C*, et al.* Lipid emulsions in the treatment of acute poisoning: a systematic review of human and animal studies. Clin Toxicol (Phila) 2010;***48***(1):1-27.
251. Weinberg GL. Lipid emulsion infusion: resuscitation for local anesthetic and other drug overdose. Anesthesiology 2012;***117***(1):180-187.
252. Litonius E*, et al.* Effect of intravenous lipid emulsion on bupivacaine plasma concentration in humans. Anaesthesia 2012;***67***(6):600-5.
253. Partownavid P*, et al.* Fatty-acid oxidation and calcium homeostasis are involved in the rescue of bupivacaine-induced cardiotoxicity by lipid emulsion in rats. Critical care medicine 2012;***40***(8):2431-2437.
254. Udelsmann A, Melo Mde S. Hemodynamic changes with high infusion rates of lipid emulsion. Experimental study in swine. Acta Cir Bras 2015;***30***(11):720-6.
255. Kearney MT*, et al.* Acute haemodynamic effects of lipolysis-induced increase of free fatty acids in healthy men. Clin Sci (Lond) 2002;***102***(5):495-500.
256. Riksen NP*, et al.* Acute elevation of plasma non-esterified fatty acids increases pulse wave velocity and induces peripheral vasodilation in humans in vivo. Clin Sci (Lond) 2007;***113***(1):33-40.
257. Stojiljkovic MP*, et al.* Hemodynamic effects of lipids in humans. American Journal of Physiology-Regulatory, Integrative and Comparative Physiology 2001;***280***(6):R1674-R1679.
258. Paolisso G*, et al.* Elevated plasma fatty acid concentrations stimulate the cardiac autonomic nervous system in healthy subjects. The American Journal of Clinical Nutrition 2000;***72***(3):723-730.
259. Park J*, et al.* Lipofundin® MCT/LCT 20% increase left ventricular systolic pressure in an ex vivo rat heart model via increase of intracellular calcium level. Korean J Anesthesiol 2016;***69***(1):57-62.

260. Umar S, *et al.* Free Fatty Acid Receptor G-protein-coupled Receptor 40 Mediates Lipid Emulsion-induced Cardioprotection. Anesthesiology 2018;***129***(1):154-162.
261. Doursout MF, *et al.* Role of propofol and its solvent, intralipid, in nitric oxide-induced peripheral vasodilatation in dogs. British journal of anaesthesia 2002;***89***(3):492-8.
262. Osanai H, *et al.* Ascorbic acid improves postischemic vasodilatation impaired by infusion of soybean oil into canine iliac artery. J Cardiovasc Pharmacol 2000;***36***(6):687-92.
263. Rothschild L, *et al.* Intravenous lipid emulsion in clinical toxicology. Scand J Trauma Resusc Emerg Med 2010;***18***:51-51.
264. Rahman S, *et al.* Phosphorylation of GSK-3 β mediates intralipid-induced cardioprotection against ischemia/reperfusion injury. Anesthesiology 2011;***115***(2):242-253.
265. Liu SL, *et al.* [Protective effect of intralipid on myocardial ischemia/reperfusion injury in isolated rat heart]. Zhongguo Wei Zhong Bing Ji Jiu Yi Xue 2008;***20***(4):227-30.
266. Rajab TK, *et al.* Intralipid improves oxygenation after orthotopic rat lung transplantation. The Journal of Heart and Lung Transplantation 2019;***38***(2):225-227.
267. Zhou RH, *et al.* Effect of intralipid postconditioning on myocardial injury in patients undergoing valve replacement surgery: a randomised controlled trial. Heart 2017;***103***(14):1122-1127.
268. Nielsen R, *et al.* Cardiovascular Effects of Treatment with the Ketone Body 3-Hydroxybutyrate in Chronic Heart Failure Patients. Circulation 2019.
269. Curry SH, *et al.* Plasma concentrations and metabolic effects of intravenous sodium dichloroacetate. Clin Pharmacol Ther 1985;***37***(1):89-93.
270. Le Page LM, *et al.* Increasing Pyruvate Dehydrogenase Flux as a Treatment for Diabetic Cardiomyopathy: A Combined 13C Hyperpolarized Magnetic Resonance and Echocardiography Study. Diabetes 2015;***64***(8):2735-43.
271. Bristow M. Etomoxir: a new approach to treatment of chronic heart failure. The Lancet 2000;***356***(9242):1621-1622.
272. Schmidt-Schweda S, Holubarsch C. First clinical trial with etomoxir in patients with chronic congestive heart failure. Clinical Science 2000;***99***(1):27-35.
273. Abozguia K, *et al.* Metabolic Modulator Perhexiline Corrects Energy Deficiency and Improves Exercise Capacity in Symptomatic Hypertrophic Cardiomyopathy. Circulation 2010;***122***(16):1562-1569.
274. Holubarsch CJ, *et al.* A double-blind randomized multicentre clinical trial to evaluate the efficacy and safety of two doses of etomoxir in comparison with placebo in patients with moderate congestive heart failure: the ERGO (etomoxir for the recovery of glucose oxidation) study. Clin Sci (Lond) 2007;***113***(4):205-12.
275. MacInnes A, *et al.* The Antianginal Agent Trimetazidine Does Not Exert Its Functional Benefit via Inhibition of Mitochondrial Long-Chain 3-Ketoacyl Coenzyme A Thiolase. Circulation Research 2003;***93***(3):e26-e32.
276. Lu C, *et al.* Effects of trimetazidine on ischemic left ventricular dysfunction in patients with coronary artery disease. Am J Cardiol 1998;***82***(7):898-901.
277. Belardinelli R, Purcaro A. Effects of trimetazidine on the contractile response of chronically dysfunctional myocardium to low-dose dobutamine in ischaemic cardiomyopathy. Eur Heart J 2001;***22***(23):2164-70.
278. Rosano GM, *et al.* Trimetazidine improves left ventricular function in diabetic patients with coronary artery disease: a double-blind placebo-controlled study. Cardiovasc Diabetol 2003;***2***:16.

279. Zhao Y, *et al.* Trimetazidine improves exercise tolerance in patients with ischemic heart disease : A meta-analysis. Herz 2016;***41***(6):514-22.
280. Fragasso G, *et al.* Effect of partial fatty acid oxidation inhibition with trimetazidine on mortality and morbidity in heart failure: results from an international multicentre retrospective cohort study. Int J Cardiol 2013;***163***(3):320-5.
281. Winter JL, *et al.* Effects of Trimetazidine in Nonischemic Heart Failure: A Randomized Study. Journal of Cardiac Failure 2014;***20***(3):149-154.
282. Gao D, *et al.* Trimetazidine: a meta-analysis of randomised controlled trials in heart failure. Heart 2011;***97***(4):278-286.
283. Murray GL, Colombo J. Ranolazine preserves and improves left ventricular ejection fraction and autonomic measures when added to guideline-driven therapy in chronic heart failure. Heart Int 2014;***9***(2):66-73.
284. Finch KT, *et al.* Ranolazine for the treatment of pulmonary hypertension associated with heart failure with preserved ejection fraction: A pilot study. J Heart Lung Transplant 2016;***35***(11):1370-1373.
285. Sokos GG, *et al.* Glucagon-like peptide-1 infusion improves left ventricular ejection fraction and functional status in patients with chronic heart failure. J Card Fail 2006;***12***(9):694-9.
286. Halbirk M, *et al.* Cardiovascular and metabolic effects of 48-h glucagon-like peptide-1 infusion in compensated chronic patients with heart failure. American Journal of Physiology-Heart and Circulatory Physiology 2010;***298***(3):H1096-H1102.
287. Jorsal A, *et al.* Effect of liraglutide, a glucagon-like peptide-1 analogue, on left ventricular function in stable chronic heart failure patients with and without diabetes (LIVE)—a multicentre, double-blind, randomised, placebo-controlled trial. European journal of heart failure 2017;***19***(1):69-77.
288. Margulies KB, *et al.* Effects of Liraglutide on Clinical Stability Among Patients With Advanced Heart Failure and Reduced Ejection Fraction: A Randomized Clinical Trial. JAMA 2016;***316***(5):500-8.
289. Packer M. Reconceptualization of the molecular mechanism by which sodium-glucose cotransporter 2 inhibitors reduce the risk of heart failure events. Circulation 2019;***140***(6):443-445.
290. Mudaliar S, *et al.* Can a Shift in Fuel Energetics Explain the Beneficial Cardiorenal Outcomes in the EMPA-REG OUTCOME Study? A Unifying Hypothesis. Diabetes care 2016;***39***(7):1115-22.
291. Lopaschuk GD, Verma S. Empagliflozin's Fuel Hypothesis: Not so Soon. Cell Metab 2016;***24***(2):200-2.
292. Abdurrachim D, *et al.* Single dose of empagliflozin increases in vivo cardiac energy status in diabetic db/db mice. Cardiovasc Res 2018;***114***(14):1843-1844.
293. Yurista SR, *et al.* Sodium–glucose co-transporter 2 inhibition with empagliflozin improves cardiac function in non-diabetic rats with left ventricular dysfunction after myocardial infarction. European Journal of Heart Failure 2019;***21***(7):862-873.
294. McMurray JJV, *et al.* Dapagliflozin in Patients with Heart Failure and Reduced Ejection Fraction. New Engl J Med 2019.
295. Folkers K, *et al.* Biochemical rationale and myocardial tissue data on the effective therapy of cardiomyopathy with coenzyme Q10. Proceedings of the National Academy of Sciences of the United States of America 1985;***82***(3):901-4.
296. Mortensen SA, *et al.* The effect of coenzyme Q10 on morbidity and mortality in chronic heart failure: results from Q-SYMBIO: a randomized double-blind trial. JACC Heart Fail 2014;***2***(6):641-9.

297. Birk AV, *et al.* The mitochondrial-targeted compound SS-31 re-energizes ischemic mitochondria by interacting with cardiolipin. Journal of the American Society of Nephrology 2013;***24***(8):1250-1261.
298. Sabbah HN, *et al.* Chronic therapy with elamipretide (MTP-131), a novel mitochondria-targeting peptide, improves left ventricular and mitochondrial function in dogs with advanced heart failure. Circulation: Heart Failure 2016;***9***(2):e002206.
299. DeFronzo RA, *et al.* Glucose clamp technique: a method for quantifying insulin secretion and resistance. Am J Physiol 1979;***237***(3):E214-23.
300. Tyler DJ, *et al.* Reproducibility of 31P cardiac magnetic resonance spectroscopy at 3 T. NMR in biomedicine 2009;***22***(4):405-413.
301. Bottomley PA, *et al.* Four-angle saturation transfer (FAST) method for measuring creatine kinase reaction rates in vivo. Magnetic resonance in medicine 2002;***47***(5):850-863.
302. Clarke WT, *et al.* Localized rest and stress human cardiac creatine kinase reaction kinetics at 3 T. NMR in biomedicine 2019:e4085.
303. Schar M, *et al.* Triple Repetition Time Saturation Transfer (TRiST) (31)P Spectroscopy for Measuring Human Creatine Kinase Reaction Kinetics. Magnetic Resonance in Medicine 2010;***63***(6):1493-1501.
304. Schär M, *et al.* Two repetition time saturation transfer (TwiST) with spill-over correction to measure creatine kinase reaction rates in human hearts. Journal of cardiovascular magnetic resonance : official journal of the Society for Cardiovascular Magnetic Resonance 2015;***17***(1):70-70.
305. Clarke WT, *et al.* Creatine kinase rate constant in the human heart measured with 3D-localization at 7 tesla. Magn Reson Med 2017;***78***(1):20-32.
306. Clarke William T. Human Cardiac Magnetic Resonance Spectroscopy PhD Thesis. University of Oxford 2016.
307. Donati A, *et al.* Anti-aging effects of anti-lipolytic drugs. Experimental Gerontology 2004;***39***(7):1061-1067.
308. Le Page LM, *et al.* Assessing the effect of hypoxia on cardiac metabolism using hyperpolarized (13) C magnetic resonance spectroscopy. NMR in biomedicine 2019;***32***(7):e4099.
309. Rodgers CT, Robson MD. Receive array magnetic resonance spectroscopy: Whitened singular value decomposition (WSVD) gives optimal Bayesian solution. Magnetic Resonance in Medicine 2010;***63***(4):881-891.
310. Veech RL. The therapeutic implications of ketone bodies: the effects of ketone bodies in pathological conditions: ketosis, ketogenic diet, redox states, insulin resistance, and mitochondrial metabolism. Prostag Leukotr Ess 2004;***70***(3):309-319.
311. Altschul R, *et al.* Influence of nicotinic acid on serum cholesterol in man. Archives of Biochemistry 1955;***54***:558-559.
312. Carlson LA. Studies on the Effect of Nicotinic Acid on Catecholamine Stimulated Lipolysis in Adipose Tissue in Vitro. Acta Medica Scandinavica 1963;***173***(6):719-722.
313. Knopp RH, *et al.* Contrasting effects of unmodified and time-release forms of niacin on lipoproteins in hyperlipidemic subjects: Clues to mechanism of action of niacin. Metabolism 1985;***34***(7):642-650.
314. Tunaru S, *et al.* PUMA-G and HM74 are receptors for nicotinic acid and mediate its anti-lipolytic effect. Nature medicine 2003;***9***(3):352-5.
315. Halbirk M, *et al.* Suppression of circulating free fatty acids with acipimox in chronic heart failure patients changes whole body metabolism but does not affect cardiac function. Am J Physiol Heart Circ Physiol 2010;***299***(4):H1220-5.

316. Wolf P, *et al.* Suppression of plasma free fatty acids reduces myocardial lipid content and systolic function in type 2 diabetes. Nutrition, metabolism, and cardiovascular diseases : NMCD 2016;***26***(5):387-92.
317. Lehto HR, *et al.* Effects of acute and one-week fatty acid lowering on cardiac function and insulin sensitivity in relation with myocardial and muscle fat and adiponectin levels. The Journal of clinical endocrinology and metabolism 2012;***97***(9):3277-84.
318. Tuunanen H, *et al.* Free fatty acid depletion acutely decreases cardiac work and efficiency in cardiomyopathic heart failure. Circulation 2006;***114***(20):2130-7.
319. Knuuti MJ, *et al.* Enhancement of myocardial [fluorine-18]fluorodeoxyglucose uptake by a nicotinic acid derivative. Journal of nuclear medicine : official publication, Society of Nuclear Medicine 1994;***35***(6):989-98.
320. Knuuti MJ, *et al.* The effect of insulin and FFA on myocardial glucose uptake. J Mol Cell Cardiol 1995;***27***(7):1359-67.
321. Rider OJ, *et al.* Determinants of left ventricular mass in obesity; a cardiovascular magnetic resonance study. Journal of cardiovascular magnetic resonance : official journal of the Society for Cardiovascular Magnetic Resonance 2009;***11***:9.
322. Chen V, *et al.* Regulation of substrate oxidation in isolated myocardial cells by beta-hydroxybutyrate. Horm Metab Res 1984;***16***(5):243-7.
323. Forsey RG, *et al.* Competition between fatty acids and carbohydrate or ketone bodies as metabolic fuels for the isolated perfused heart. Can J Physiol Pharmacol 1987;***65***(3):401-6.
324. Roden M, *et al.* Effects of free fatty acid elevation on postabsorptive endogenous glucose production and gluconeogenesis in humans. Diabetes 2000;***49***(5):701-707.
325. Boden G. Role of Fatty Acids in the Pathogenesis of Insulin Resistance and NIDDM. Diabetes 1997;***46***(1):3-10.
326. Weiss RG, *et al.* Regional Myocardial Metabolism of High-Energy Phosphates during Isometric Exercise in Patients with Coronary Artery Disease. New Engl J Med 1990;***323***(23):1593-1600.
327. Stone CK, *et al.* Effect of nicotinic acid on exogenous myocardial glucose utilization. Journal of nuclear medicine : official publication, Society of Nuclear Medicine 1995;***36***(6):996-1002.
328. Opie LH, Knuuti J. The adrenergic-fatty acid load in heart failure. J Am Coll Cardiol 2009;***54***(18):1637-46.
329. Chen L, *et al.* Niacin-induced hyperglycemia is partially mediated via niacin receptor GPR109a in pancreatic islets. Molecular and Cellular Endocrinology 2015;***404***:56-66.
330. Wang N, *et al.* Niacin receptor GPR109A inhibits insulin secretion and is down-regulated in type 2 diabetic islet beta-cells. General and Comparative Endocrinology 2016;***237***:98-108.
331. Zafrir B, Jain M. Lipid-lowering therapies, glucose control and incident diabetes: evidence, mechanisms and clinical implications. Cardiovascular drugs and therapy 2014;***28***(4):361-77.
332. Abel ED. Glucose transport in the heart. Frontiers in bioscience : a journal and virtual library 2004;***9***:201-15.
333. Huang B, *et al.* Regulation of pyruvate dehydrogenase kinase expression by peroxisome proliferator-activated receptor-alpha ligands, glucocorticoids, and insulin. Diabetes 2002;***51***(2):276-83.
334. Doenst T, *et al.* Cardiac metabolism in heart failure: implications beyond ATP production. Circulation research 2013;***113***(6):709-724.

335. Taylor M, *et al.* An evaluation of myocardial fatty acid and glucose uptake using PET with [18F]fluoro-6-thia-heptadecanoic acid and [18F]FDG in Patients with Congestive Heart Failure. J Nucl Med 2001;***42***(1):55-62.
336. Kawel-Boehm N, *et al.* Normal values for cardiovascular magnetic resonance in adults and children. Journal of Cardiovascular Magnetic Resonance 2015;***17***(1):1-33.
337. Hudsmith LE, *et al.* Normal human left and right ventricular and left atrial dimensions using steady state free precession magnetic resonance imaging. Journal of cardiovascular magnetic resonance 2005;**7**(5):775-782.
338. Honka H, *et al.* Therapeutic Manipulation of Myocardial Metabolism: JACC State-of-the-Art Review. Journal of the American College of Cardiology 2021;**77**(16):2022-2039.
339. Osorio JC, *et al.* Impaired myocardial fatty acid oxidation and reduced protein expression of retinoid X receptor-alpha in pacing-induced heart failure. Circulation 2002;***106***(5):606-12.
340. Glatz JFC, *et al.* Re-balancing cellular energy substrate metabolism to mend the failing heart. Biochimica et Biophysica Acta (BBA) - Molecular Basis of Disease 2020;***1866***(5):165579.
341. Wang X-C, *et al.* Dobutamine Therapy is Associated with Worse Clinical Outcomes Compared with Nesiritide Therapy for Acute Decompensated Heart Failure: A Systematic Review and Meta-Analysis. American Journal of Cardiovascular Drugs 2015;***15***(6):429-437.
342. Beanlands RS, *et al.* Acute effects of dobutamine on myocardial oxygen consumption and cardiac efficiency measured using carbon-11 acetate kinetics in patients with dilated cardiomyopathy. Journal of the American College of Cardiology 1993;***22***(5):1389-1398.
343. Dass S, *et al.* No evidence of myocardial oxygen deprivation in nonischemic heart failure. Circulation: Heart Failure 2015;***8***(6):1088-1093.
344. Levelt E, *et al.* Cardiac energetics, oxygenation, and perfusion during increased workload in patients with type 2 diabetes mellitus. Eur Heart J 2016;***37***(46):3461-3469.
345. Burrage M, *et al.* Energetic basis for exercise-induced pulmonary congestion in heart failure with preserved ejection fraction. Circulation 2021.
346. Akhmedov AT, *et al.* Mitochondrial oxidative metabolism and uncoupling proteins in the failing heart. Heart failure reviews 2015;***20***(2):227-249.
347. Bienengraeber M, *et al.* Stable transfection of UCP1 confers resistance to hypoxia/reoxygenation in a heart-derived cell line. Journal of molecular and cellular cardiology 2003;***35***(7):861-865.
348. Teshima Y, *et al.* Uncoupling protein-2 overexpression inhibits mitochondrial death pathway in cardiomyocytes. Circulation research 2003;***93***(3):192-200.
349. McLeod CJ, *et al.* Uncoupling proteins 2 and 3 function in concert to augment tolerance to cardiac ischemia. Journal of Biological Chemistry 2005;***280***(39):33470-33476.
350. Giordano FJ. Oxygen, oxidative stress, hypoxia, and heart failure. The Journal of clinical investigation 2005;***115***(3):500-508.
351. Turner JD, *et al.* Uncoupling protein-2 modulates myocardial excitation-contraction coupling. Circulation research 2010;***106***(4):730-738.
352. Nielsen R, *et al.* Failing heart of patients with type 2 diabetes mellitus can adapt to extreme short-term increases in circulating lipids and does not display features of acute myocardial lipotoxicity. Circulation: Heart Failure 2013;***6***(4):845-852.
353. Recchia FA, *et al.* Reduced nitric oxide production and altered myocardial metabolism during the decompensation of pacing-induced heart failure in the conscious dog. Circulation research 1998;***83***(10):969-979.
354. Young LH, *et al.* Regulation of myocardial glucose uptake and transport during ischemia and energetic stress. The American journal of cardiology 1999;***83***(12):25-30.

355. Dyck JR, Lopaschuk GD. AMPK alterations in cardiac physiology and pathology: enemy or ally? J Physiol 2006;***574***(Pt 1):95-112.
356. Bertrand L, *et al.* Insulin signalling in the heart. Cardiovascular research 2008;***79***(2):238-248.
357. Lanner JT, *et al.* Ca2+ and insulin-mediated glucose uptake. Current opinion in pharmacology 2008;***8***(3):339-345.
358. Omar MA, *et al.* Ischemia-induced activation of AMPK does not increase glucose uptake in glycogen-replete isolated working rat hearts. American Journal of Physiology-Heart and Circulatory Physiology 2008;***294***(3):H1266-H1273.
359. Williamson JR. Metabolic effects of epinephrine in the isolated, perfused rat heart I. Dissociation of the glycogenolytic from the metabolic stimulatory effect. Journal of Biological Chemistry 1964;***239***(9):2721-2729.
360. Lou Q, *et al.* Remodeling of calcium handling in human heart failure. Calcium Signaling 2012:1145-1174.
361. Hölscher M, *et al.* Unfavourable consequences of chronic cardiac HIF-1 α stabilization. Cardiovascular research 2012;***94***(1):77-86.
362. Russell III RR, *et al.* Translocation of myocardial GLUT-4 and increased glucose uptake through activation of AMPK by AICAR. American Journal of Physiology-Heart and Circulatory Physiology 1999;***277***(2):H643-H649.
363. Hopkins T, *et al.* AMP-activated protein kinase regulation of fatty acid oxidation in the ischaemic heart. Biochemical Society Transactions 2003;***31***(1):207-212.
364. Gamble J, Lopaschuk GD. Insulin inhibition of 5′ adenosine monophosphate—activated protein kinase in the heart results in activation of acetyl coenzyme A carboxylase and inhibition of fatty acid oxidation. Metabolism 1997;***46***(11):1270-1274.
365. Kudo N, *et al.* High rates of fatty acid oxidation during reperfusion of ischemic hearts are associated with a decrease in malonyl-CoA levels due to an increase in 5'-AMP-activated protein kinase inhibition of acetyl-CoA carboxylase. Journal of Biological Chemistry 1995;***270***(29):17513-17520.
366. Baar K, *et al.* Adaptations of skeletal muscle to exercise: rapid increase in the transcriptional coactivator PGC-1. The FASEB journal 2002;***16***(14):1879-1886.
367. Barger PM, *et al.* p38 mitogen-activated protein kinase activates peroxisome proliferator-activated receptor α : a potential role in the cardiac metabolic stress response. Journal of Biological Chemistry 2001;***276***(48):44495-44501.
368. Fowler MB, *et al.* Assessment of the beta-adrenergic receptor pathway in the intact failing human heart: progressive receptor down-regulation and subsensitivity to agonist response. Circulation 1986;***74***(6):1290-1302.
369. Vatner DE, *et al.* Beta-adrenoceptor desensitization during the development of canine pacing-induced heart failure. Clinical and experimental pharmacology & physiology 1996;***23***(8):688-692.
370. Nikolaidis LA, *et al.* Catecholamine stimulation is associated with impaired myocardial O2 utilization in heart failure. Cardiovascular research 2002;***53***(2):392-404.
371. Jensen CB, *et al.* Insulin secretion and cellular glucose metabolism after prolonged low-grade intralipid infusion in young men. The Journal of clinical endocrinology and metabolism 2003;***88***(6):2775-83.
372. Barth E, *et al.* Glucose metabolism and catecholamines. Critical Care Medicine 2007;***35***(9):S508-S518.

373. Cohn JN, *et al.* Effect of vasodilator therapy on mortality in chronic congestive heart failure. New Engl J Med 1986;***314***(24):1547-1552.
374. Haber HL, *et al.* Bolus intravenous nitroglycerin predominantly reduces afterload in patients with excessive arterial elastance. J Am Coll Cardiol 1993;***22***(1):251-7.
375. Brachfeld N, *et al.* Action of Nitroglycerin on the Coronary Circulation in Normal and in Mild Cardiac Subjects. Circulation 1959;***19***(5):697-704.
376. Westerhof N. Cardiac work and efficiency. In: Elsevier Science; 2000.
377. Somani P, *et al.* Nutritional circulation in the heart. II. A reappraisal of the effect of nitroglycerin on myocardial hemodynamics, oxygen consumption and nutritional blood flow in the isolated supported heart preparation. Eur J Pharmacol 1969;***8***(1):1-13.
378. Gross GJ, Hardman HF. Alteration in oxyhemoglobin equilibrium (P-50) and myocardial oxygen consumption (MVO2) by nitroglycerin (GTN). J Pharmacol Exp Ther 1975;***193***(2):346-55.
379. Boime I, Edmund Hunter F. Effects of glycerol trinitrate, mannitol hexanitrate and erythritol tetranitrate on electron transport and phosphorylation in liver mitochondria. Biochemical Pharmacology 1971;***20***(3):535-545.
380. Brown GC, Cooper CE. Nanomolar concentrations of nitric oxide reversibly inhibit synaptosomal respiration by competing with oxygen at cytochrome oxidase. FEBS Lett 1994;***356***(2-3):295-8.
381. Peterzan Mark A. DPhil thesis: ATP delivery rates in myocardial hypertrophy. University of Oxford 2019.
382. Neubauer S. The failing heart - an engine out of fuel. N Engl J Med 2007;***356***(11):1140-51.
383. Peterzan MA, *et al.* Cardiac Energetics in Patients With Aortic Stenosis and Preserved Versus Reduced Ejection Fraction. Circulation 2020;***141***(24):1971-1985.
384. Richards DA, *et al.* Distinct phenotypes induced by three degrees of transverse aortic constriction in mice. Scientific reports 2019;***9***(1):1-15.
385. Chow E, *et al.* Rapid ventricular pacing in pigs: an experimental model of congestive heart failure. American Journal of Physiology-Heart and Circulatory Physiology 1990;***258***(5):H1603-H1605.
386. Gupta S, Figueredo VM. Tachycardia mediated cardiomyopathy: Pathophysiology, mechanisms, clinical features and management. International Journal of Cardiology 2014;***172***(1):40-46.
387. Merchant FM, Mittal S. Pacing induced cardiomyopathy. Journal of cardiovascular electrophysiology 2020;***31***(1):286-292.
388. Liu Y-C, *et al.* Sepsis-Induced Cardiomyopathy: Mechanisms and Treatments. Frontiers in immunology 2017;***8***:1021-1021.
389. Moe GW, *et al.* Left ventricular myocardial blood flow, metabolism, and effects of treatment with enalapril: further insights into the mechanisms of canine experimental pacing-induced heart failure. The Journal of laboratory and clinical medicine 1993;***121***(2):294-301.
390. Spinale FG, *et al.* Myocardial Na+, K+-ATPase in tachycardia induced cardiomyopathy. Journal of molecular and cellular cardiology 1992;***24***(3):277-294.
391. Marín-García J, *et al.* Selective endothelin receptor blockade reverses mitochondrial dysfunction in canine heart failure. Journal of cardiac failure 2002;***8***(5):326-332.
392. Casadei B, Paterson DJ. Should we still use nitrovasodilators to test baroreflex sensitivity? Journal of hypertension 2000;***18***(1):3-6.

393. Herring N, Paterson DJ. Neuromodulators of peripheral cardiac sympatho-vagal balance. Experimental physiology 2009;***94***(1):46-53.